African Journal of
Biotechnology
Volume 13 Number 30, 23 July, 2014
ISSN 1684-5315

Academic Journals

ABOUT AJB

The **African Journal of Biotechnology (AJB)** (ISSN 1684-5315) is published weekly (one volume per year) by Academic Journals.

African Journal of Biotechnology (AJB), a new broad-based journal, is an open access journal that was founded on two key tenets: To publish the most exciting research in all areas of applied biochemistry, industrial microbiology, molecular biology, genomics and proteomics, food and agricultural technologies, and metabolic engineering. Secondly, to provide the most rapid turn-around time possible for reviewing and publishing, and to disseminate the articles freely for teaching and reference purposes. All articles published in AJB are peer-reviewed.

Submission of Manuscript

Please read the **Instructions for Authors** before submitting your manuscript. The manuscript files should be given the last name of the first author

Click here to Submit manuscripts online

If you have any difficulty using the online submission system, kindly submit via this email ajb@academicjournals.org.

With questions or concerns, please contact the Editorial Office at ajb@academicjournals.org.

Editorial Board

Instructions for Author

Electronic submission of manuscripts is strongly encouraged, provided that the text, tables, and figures are included in a single Microsoft Word file (preferably in Arial font).

The **cover letter** should include the corresponding author's full address and telephone/fax numbers and should be in an e-mail message sent to the Editor, with the file, whose name should begin with the first author's surname, as an attachment.

Article Types
Three types of manuscripts may be submitted:

Regular articles: These should describe new and carefully confirmed findings, and experimental procedures should be given in sufficient detail for others to verify the work. The length of a full paper should be the minimum required to describe and interpret the work clearly.
Short Communications: A Short Communication is suitable for recording the results of complete small investigations or giving details of new models or hypotheses, innovative methods, techniques or apparatus. The style of main sections need not conform to that of full-length papers. Short communications are 2 to 4 printed pages (about 6 to 12 manuscript pages) in length.

Reviews: Submissions of reviews and perspectives covering topics of current interest are welcome and encouraged. Reviews should be concise and no longer than 4-6 printed pages (about 12 to 18 manuscript pages). Reviews are also peer-reviewed.

Review Process

All manuscripts are reviewed by an editor and members of the Editorial Board or qualified outside reviewers. Authors cannot nominate reviewers. Only reviewers randomly selected from our database with specialization in the subject area will be contacted to evaluate the manuscripts. The process will be blind review.
Decisions will be made as rapidly as possible, and the journal strives to return reviewers' comments to authors as fast as possible. The editorial board will re-review manuscripts that are accepted pending revision. It is the goal of the AJFS to publish manuscripts within weeks after submission.

Regular articles

All portions of the manuscript must be typed double-spaced and all pages numbered starting from the title page.

The Title should be a brief phrase describing the contents of the paper. The Title Page should include the authors' full names and affiliations, the name of the corresponding author along with phone, fax and E-mail information. Present addresses of authors should appear as a footnote.

The Abstract should be informative and completely self-explanatory, briefly present the topic, state the scope of the experiments, indicate significant data, and point out major findings and conclusions. The Abstract should be 100 to 200 words in length.. Complete sentences, active verbs, and the third person should be used, and the abstract should be written in the past tense. Standard nomenclature should be used and abbreviations should be avoided. No literature should be cited.
Following the abstract, about 3 to 10 key words that will provide indexing references should be listed.

A list of non-standard **Abbreviations** should be added. In general, non-standard abbreviations should be used only when the full term is very long and used often. Each abbreviation should be spelled out and introduced in parentheses the first time it is used in the text. Only recommended SI units should be used. Authors should use the solidus presentation (mg/ml). Standard abbreviations (such as ATP and DNA) need not be defined.

The Introduction should provide a clear statement of the problem, the relevant literature on the subject, and the proposed approach or solution. It should be understandable to colleagues from a broad range of scientific disciplines.

Materials and methods should be complete enough to allow experiments to be reproduced. However, only truly new procedures should be described in detail; previously published procedures should be cited, and important modifications of published procedures should be mentioned briefly. Capitalize trade names and include the manufacturer's name and address. Subheadings should be used. Methods in general use need not be described in detail.

Results should be presented with clarity and precision. The results should be written in the past tense when describing findings in the authors' experiments. Previously published findings should be written in the present tense. Results should be explained, but largely without referring to the literature. Discussion, speculation and detailed interpretation of data should not be included in the Results but should be put into the Discussion section.

The Discussion should interpret the findings in view of the results obtained in this and in past studies on this topic. State the conclusions in a few sentences at the end of the paper. The Results and Discussion sections can include subheadings, and when appropriate, both sections can be combined.

The Acknowledgments of people, grants, funds, etc should be brief.

Tables should be kept to a minimum and be designed to be as simple as possible. Tables are to be typed double-spaced throughout, including headings and footnotes. Each table should be on a separate page, numbered consecutively in Arabic numerals and supplied with a heading and a legend. Tables should be self-explanatory without reference to the text. The details of the methods used in the experiments should preferably be described in the legend instead of in the text. The same data should not be presented in both table and graph form or repeated in the text.

Figure legends should be typed in numerical order on a separate sheet. Graphics should be prepared using applications capable of generating high resolution GIF, TIFF, JPEG or Powerpoint before pasting in the Microsoft Word manuscript file. Tables should be prepared in Microsoft Word. Use Arabic numerals to designate figures and upper case letters for their parts (Figure 1). Begin each legend with a title and include sufficient description so that the figure is understandable without reading the text of the manuscript. Information given in legends should not be repeated in the text.

References: In the text, a reference identified by means of an author‘s name should be followed by the date of the reference in parentheses. When there are more than two authors, only the first author‘s name should be mentioned, followed by ’et al‘. In the event that an author cited has had two or more works published during the same year, the reference, both in the text and in the reference list, should be identified by a lower case letter like ’a‘ and ’b‘ after the date to distinguish the works.

Examples:

Abayomi (2000), Agindotan et al. (2003), (Kelebeni, 1983), (Usman and Smith, 1992), (Chege, 1998; 1987a,b; Tijani, 1993,1995), (Kumasi et al., 2001)
References should be listed at the end of the paper in alphabetical order. Articles in preparation or articles submitted for publication, unpublished observations, personal communications, etc. should not be included in the reference list but should only be mentioned in the article text (e.g., A. Kingori, University of Nairobi, Kenya, personal communication). Journal names are abbreviated according to Chemical Abstracts. Authors are fully responsible for the accuracy of the references.

Examples:

Chikere CB, Omoni VT and Chikere BO (2008). Distribution of potential nosocomial pathogens in a hospital environment. Afr. J. Biotechnol. 7: 3535-3539.

Moran GJ, Amii RN, Abrahamian FM, Talan DA (2005). Methicillinresistant Staphylococcus aureus in community-acquired skin infections. Emerg. Infect. Dis. 11: 928-930.

Pitout JDD, Church DL, Gregson DB, Chow BL, McCracken M, Mulvey M, Laupland KB (2007). Molecular epidemiology of CTXM-producing Escherichia coli in the Calgary Health Region: emergence of CTX-M-15-producing isolates. Antimicrob. Agents Chemother. 51: 1281-1286.

Pelczar JR, Harley JP, Klein DA (1993). Microbiology: Concepts and Applications. McGraw-Hill Inc., New York, pp. 591-603.

Short Communications

Short Communications are limited to a maximum of two figures and one table. They should present a complete study that is more limited in scope than is found in full-length papers. The items of manuscript preparation listed above apply to Short Communications with the following differences: (1) Abstracts are limited to 100 words; (2) instead of a separate Materials and Methods section, experimental procedures may be incorporated into Figure Legends and Table footnotes; (3) Results and Discussion should be combined into a single section.
Proofs and Reprints: Electronic proofs will be sent (e-mail attachment) to the corresponding author as a PDF file. Page proofs are considered to be the final version of the manuscript. With the exception of typographical or minor clerical errors, no changes will be made in the manuscript at the proof stage.

Fees and Charges: Authors are required to pay a $650 handling fee. Publication of an article in the African Journal of Biotechnology is not contingent upon the author's ability to pay the charges. Neither is acceptance to pay the handling fee a guarantee that the paper will be accepted for publication. Authors may still request (in advance) that the editorial office waive some of the handling fee under special circumstances

Submission of a manuscript implies: that the work described has not been published before (except in the form of an abstract or as part of a published lecture, or thesis) that it is not under consideration for publication elsewhere; that if and when the manuscript is accepted for publication, the authors agree to automatic transfer of the copyright to the publisher.

African Journal of Biotechnology

Table of Contents: Volume 13 Number 30, 23 July, 2014

ARTICLES

Molecular characterization of Doom pigs using microsatellite markers
Zaman, G., Laskar, S., Ferdoci, A. M., Chandra Shekar M. and Chetri, A. J.

Analysis of phosphoric ore bacterial and eucaryal microbial diversity by single strand conformation polymorphism (SSCP) and small-subunit (SSU) sequencing
Ilhem Omri, Imen Manaii, Zied Tlili, Jean-Jacques Godon and Moktar Hamdi

Evidence of salicylic acid regulatory mechanisms of disease resistance against banana vascular wilt *Fusarium oxysporium* f.sp. cubense in *Arabidopsis thaliana*
Raju Radhajeyalakshmi , Yiji Xia and Dhilip Shah

Crop growth rate differs in warm season C4-grasses grown in pure and mixed stands
Amanullah Khan

Optimization of alkaline protease production and its fibrinolytic activity from the bacterium *Pseudomonas fluorescens* isolated from fish waste discharged soil
Jothiprakasam Vinoth, Sambantham Murugan and Chinnathambi Stalin

Drying of carrots in slices with osmotic dehydration
Araújo, P. M., Fonseca, J. R. L., Magalhães, M. M. A. and Medeiros, M. F. D.

Antiparasitic activity of the microalgae *Cladophora crispata* against the Protoscolices of hydatid cysts compared with albendazole drug
A. M. Athbi, S. H. Al- Mayah and A. K. Khalaf

Binding properties of beetal recombinant caprine growth hormone to Bovidae liver microsomal membranes
Roquyya Gul, Rabail Alam, Mahjabeen Saleem, Mohammad Ali, Sumble Mehmood and Muhammed Waheed Akhtar

Table of Contents: Volume 13 Number 30, 23 July, 2014

Structural optimization and docking studies of anatoxin-a: A potent neurotoxin
Naresh Kumar and Archit Garg

The role of adrenergic receptors in nicotine-induced hyperglycemia in the common African toad (*Bufo regularis*)
Isehunwa, G. O., Adewunmi, G. O., Alada, A. R. A and Olaniyan, O. T

Composition and antioxidant and antifungal activities of the essential oil from *Lippia gracilis* Schauer
Caroline da S. Franco, Alcy F. Ribeiro, Natale C. C. Carvalho, Odair S. Monteiro, Joyce Kelly R. da Silva, Eloisa Helena A. Andrade and José Guilherme S. Maia

Thermodynamics, thermoeconomic and economic analysis of sugarcane biomass use for electricity production: A case study
Rafael Delapria Dias dos Santos, Samuel Nelson Melegari de Souza, Willian Cézar Nadaletti, Reinaldo Aparecido Bariccatti and Paulo Belli Filho

academicJournals

Vol. 13(30), pp. 3017-3022, 23 July, 2014
DOI: 10.5897/AJB2014.13729
Article Number: 6760D6D46216
ISSN 1684-5315

http://www.academicjournals.org/AJB

African Journal of Biotechnology

Full Length Research Paper

Molecular characterization of Doom pigs using microsatellite markers

Zaman, G.*, Laskar, S., Ferdoci, A. M., Chandra Shekar M. and Chetri, A. J.

Department of Animal Genetics and Breeding, College of Veterinary Science, Assam Agricultural University, Khanapara, Guwahati-781022, Assam, India.

Received 15 February, 2014; Accepted 10 June, 2014

Assessment of genetic diversity was carried out in Doom pig using 22 microsatellite markers, recommended by Food and Agriculture Organization (FAO). All the studied loci were highly polymorphic and a total of 120 alleles were observed across the investigated loci. The range of alleles was found to be 4 to 10 with a mean of 5.4±1.65. The frequency distribution of microsatellite alleles in the population was from 0.02 to 0.6667. The observed and expected heterozygosity values were 0.62±0.287 and 0.67±0.142, respectively. The polymorphic information content (PIC) was 0.63±0.143. Microsatellite analysis revealed moderate to less genetic diversity in the Doom pig population. The overall mean of within-population inbreeding estimate (F_{IS}) was 0.089. The Shannon's information index (I) was sufficiently high with a mean of 1.36. The bottleneck analysis revealed that population has not undergone any recent reduction.

Key words: Heterozygosity, microsatellites, polymorphic information content (PIC), bottleneck, doom pig.

INTRODUCTION

Pig rearing is an integral part of the tribal population of North-East India, which accommodates 28% of the country's pig population. Assam possesses two distinct varieties of indigenous pigs namely Doom and Assam Local pig.

The Doom variety of pig is found in Dhubri, Goalpara and Bongaigaon districts of Assam and they are comparatively larger than the Assam Local pigs. Their coat colour is black with thick line of hair on the crest extending up to the lumbar region (Figure 1).

Due to the large body size, high prolificacy and ability to be sustained in low input system, Doom pigs enjoy greater popularity amongst the pig farmers in the state of Assam. These pigs can also be considered as a potential source of new allelic combinations. To date, no molecular level studies are reported on this valuable pig germplasm of North-East region. Considering the importance and utility, the present study has been planned to investigate genetic diversity and structure within Doom pig population using 22 polymorphic microsatellite markers.

MATERIALS AND METHODS

Sample collection

A total of 40 blood samples of Doom pig were randomly collected

*Corresponding author. E-mail: gzaman60@gmail.com.

Figure 1. Typical Doom pigs (A) sow and (b) boar.

in an EDTA (10.8 mg) coated BD vacutainers (6 ml) from Dhubri, Goalpara and Bongaigaon districts of Assam (Figure 2) and immediately samples were placed on ice and transported to the laboratory and stored at 4°C until use.

Genomic DNA isolation and quantification

Genomic DNA was isolated from whole blood samples of swine by using standard phenol-chloroform method (Sambrook et al., 1989) with minor modifications. The quantity and quality of isolated DNA were confirmed. The concentrated samples were diluted to reach appropriate concentrations for the purpose of PCR amplification.

Microsatellite selection and analysis

A total of 22 microsatellite markers were selected for the present investigation based on their level of polymorphism, allele size range and reliability of allele calling to evaluate genetic diversity and structure in Doom pig of Assam. The forward primer of each marker was fluorescently labeled with either FAM, NED, PET or VIC dye. All microsatellite markers were first checked under single locus amplification conditions to evaluate their performance in the multiplex.

Multiplex PCR has been used for multicolor fluorescence genotyping Wallin et al., 2002. Based on the guidelines of Henegariu et al. (1997) and Loffert et al. (1999), the initial parameters of multiplex PCR were set up. The basic PCR reaction mixture (15 µl) containing 20-50 ng of template DNA; 1.5 mM $MgCl_2$; 5 picomoles each of forward and reverse primers; 1 unit of taq DNA polymerase and 200 mM dNTPs was prepared. Amplification was carried out with initial denaturation at 95°C for 2 min followed by 30 cycles of denaturation (95°C for 30 s), annealing (48 to 62°C for 30 s) and extension (72°C for 45 s) using Applied Biosystems (Model #: 9902) Veriti^{TM} 96- well thermal cycler.

Genotyping and data analysis

The genotyping was carried out on an automated DNA sequencer

Figure 2. Figure showing the breeding tract of Doom pig (kindness to Google earth map).

(ABI PRISM 3130XL). The resulting data were analyzed using standard software Gene Mapper™ version 4.0 (Applied Biosystems Inc., California, USA) to generate genotype calls for each locus by using GS 500 (- 250) LIZ as size standard.

Genetic diversity was determined as allele frequencies, effective number of alleles (N_e), test of Hardy-Weinberg equilibrium (HWE), observed (H_o) and expected (H_e) heterozygosity, F-statistics and Shanon information index (I) using POPGENE version 1.32 (Yeh et al., 1999). Polymorphic information content (PIC) was calculated according to Nei (1978). The BOTTLENECK (version 1.2.03) (Cornuet and Luikart, 1996) analysis was performed to know whether this pig population exhibits a significant number of loci with excess of heterozygosity.

RESULTS

The results of genetic diversity in Doom pig are presented in Table 1. All the 22 loci investigated were polymorphic in nature. The number of observed alleles (N_a) ranged from 4 (TNFB, SO107, SW72, SO008, SO225, SO90, SO226 and SO386) to 10 (SW936), with an overall mean of 5.4±1.65 and the total number of alleles in this population was found to be 120. However, the effective number of alleles (N_e) ranged from 1.383 (SO226) to 7.014 (SW96) with a mean of 3.51±1.504. Overall allele frequency ranged from 0.020 (at locus SO086) to 0.666 (at loci SW957 and SO218). The PIC value ranged from 0.262 (SO226) to 0.842 (SW936) with a mean of 0.63±0.143. The overall means for observed (H_O) and expected (H_e) heterozygosities were 0.62±0.287 and 0.67±0.142, respectively which ranged from 0 (SO226) to 0.947 (SO010) and 0.277 (SO226) to 0.857 (SW936), respectively. The chi-square (χ^2) test for Hardy-Weinberg equilibrium revealed that 13 out of 22 loci deviated from equilibrium. Shannon's information index (I) value ranged from 0.581 (SO226) to 2.093 (SW936) with a mean value of 1.3611.

The within population inbreeding (F_{IS}) estimates revealed deficiency of heterozygosity at 10 loci which ranged from 0.108 (SO335) to 0.848 (SW911). Only 12 loci revealed negative F_{IS} values indicating the absence of inbreeding in these loci. The mean F_{IS} value observed was 0.089. Though positive F_{IS} values were observed at 10 loci, only 8.9% of inbreeding was recorded in Doom pig.

Three mutation models namely, infinite allele model (IAM), two phase model (TPM), stepwise mutation model

Table 1. Microsatellite analysis in Doom pig population.

Panel	Locus	Size range (bp)	Parameter							
			Na	Ne	PIC	Ho	He	I	F_{IS}	HWE
Panel 1	SW936	91-113	10	7.0145	0.8422	0.8636	0.8574	2.0933	-0.0072	73.94**
	SW353	143-173	6	3.5000	0.6713	0.9286	0.7143	1.4439	-0.3000	18.93^{NS}
Panel 2	TNFB	167-181	4	3.5556	0.6674	0.7500	0.7188	1.3209	-0.0435	4.75^{NS}
	SW24	94-110	5	3.5714	0.6756	0.8000	0.7200	1.4185	-0.1111	11.5^{NS}
	SO355	243-265	6	4.6512	0.7516	0.7000	0.7850	1.6264	0.1083	27.20*
	SO107	145-161	4	2.5641	0.6422	0.7000	0.6100	1.1097	-0.1475	3.3^{NS}
Panel 3	SO218	193-201	5	2.0769	0.4850	0.5556	0.5185	1.0507	-0.0714	5.51^{NS}
	SW72	223-245	4	3.2667	0.6413	0.2857	0.6939	1.277	0.5882	26.8**
Panel 4	SO228	100-116	6	3.8647	0.7089	0.9000	0.7412	1.5558	-0.2142	34.77^{NS}
	SW122	173-185	7	5.1429	0.7784	0.9167	0.8056	1.7553	-0.1379	24.47^{NS}
Panel 5	SO008	100-130	4	2.4590	0.5362	0.4667	0.5933	1.0851	0.2135	9.03^{NS}
	SW957	236-242	5	2.0836	0.4877	0.4444	0.5201	1.0487	0.1454	24**
	SO225	273-293	4	3.1934	0.6295	0.8235	0.6869	1.2508	-0.1990	16.69*
	SO010	112-156	5	2.6350	0.5527	0.9474	0.6205	1.1420	-0.5268	15.37^{NS}
Panel 6	SO070	169-185	5	3.3333	0.6555	0.5000	0.7000	1.3705	0.2857	20.08*
	SW911	108-128	5	3.7674	0.6933	0.1111	0.7346	1.4555	0.8487	56.57**
	SO086	153-177	7	3.9683	0.7133	0.9200	0.7480	1.5830	-0.2299	93.31**
Panel 7	SO90	162-184	4	1.7131	0.3920	0.25	0.4163	0.8346	0.3994	22.12**
	IGFI	244-251	8	6.3297	0.8226	0.4167	0.842	1.9355	0.5052	138.75**
Panel 8	SO386	250-320	4	2.6309	0.5457	0.9286	0.6199	1.1003	-0.4979	40**
Panel 9	CGA	181-105	8	6.2439	0.8194	0.5312	0.8398	1.9051	0.3674	118.86**
Panel 10	SO226	197-209	4	1.3838	0.2620	0	0.2773	0.5819	1	163.89**
Mean overall loci			5.45 ± 1.654	3.588 ± 1.504	0.635 ± 0.143	0.624 ± 0.287	0.671 ± 0.142	1.361 ± 0.368	0.0898	

*Significant ($P \leq 0.05$); **Highly significant ($P \leq 0.01$); NS, Not significant ($P \geq 0.05$). N_a, Number of alleles; N_e, effective number of alleles; PIC, Polymorphic information content; H_o, observed Heterozygosity; H_e, expected Heterozygosity; F_{IS}, Deficit or excess of heterozygotes, HWE, Hardy-Weinberg equilibrium; I, Shannon's Information Index.

Table 2. Bottleneck analysis in Doom pig population.

Model	Sign rank test - Number of loci with heterozygosity excess			Standardized differences test - T2 values (probability)	Wilcoxon test - probability of heterozygosity excess
	Expected	Observed	Probability		
IAM	9.39	14	0.01382	2.416 (0.00785)	0.00759
TPM	9.33	12	0.13391	1.071 (0.14201)	0.04672
SMM	9.59	7	0.14331	-0.781(0.21726)	0.56987

IAM, Infinite allele model; TPM , Two phase model; SMM , Stepwise mutation model.

(SMM) were used for Bottleneck analysis (Table 2). In Doom pig population, under Sign test, the expected number of loci with heterozygosity excess was 9.59 (SMM) which is higher than the observed number of loci 7 (SMM) with heterozygosity excess. The expected number of loci (10.64 and 9.33) with heterozygosity excess was significantly (P>0.05) higher than the observed number of loci (8 and 12) with heterozygosity excess under IAM and TPM, respectively. Standard difference test (T2 statistics) in this population provided the significant gene diversity deficit under the one mutation model SMM (-0.781). Under Wilcoxon rank test,

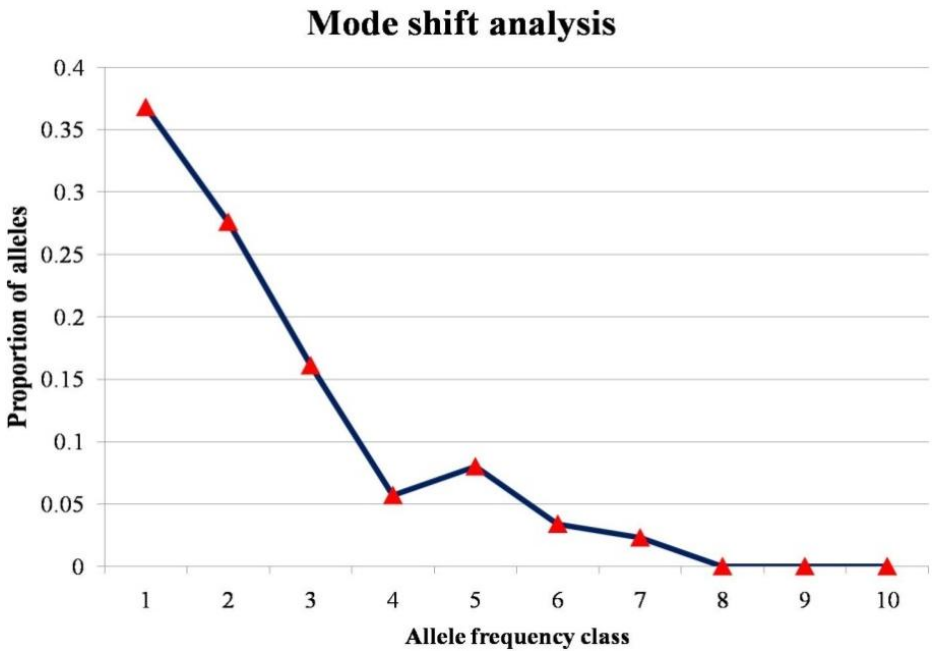

Figure 3. Graphical representation of allele proportions and their contribution in Doom pig population.

probability values of 0.00759 (IAM), 0.04672 (TPM) and 0.56987 (SMM) were found to be non-significant. The mode shift analysis (Luikart et al., 1998) revealed L-shaped curve (Figure 3) indicating no mode-shift in the frequency distribution of alleles revealing that the population has not undergone any recent and/or sudden reduction in the effective population size and remained at mutation-drift equilibrium.

DISCUSSION

The number and sizes of microsatellite alleles observed in this study fall within the range mentioned in the Secondary Guidelines for Development of National Farm Animal Genetic Resources Management Plans of FAO (FAO, 1998). The mean number of alleles observed (5.40) in the study is less than the mean number reported for Suwo pigs (6.40) (Zaman et al., 2013d), North Indian (7.92) and Northeast Indian pig (7.84) types (Rajeev et al., 2001), Brazilian (8.96) pig breeds (Sollero et al., 2010) and higher than the mean number reported for Ghungroo pigs (4.90) (Zaman et al., 2013a), Niang Megha pigs (3.9) (Zaman et al., 2013b). Moreover, the mean number of observed alleles in Mali pigs (5.63) (Zaman et al., 2013c) and Zovawk pigs (5.54) (Zaman et al., 2014) were corroborates with the present findings. However, the mean number of effective alleles (3.58) is higher than the mean number reported in Brazilian pig (Sollero et al., 2010) breeds viz., Landrace (2.70); Monterio (2.34); Moura (2.32); MS60 (2.56) and Piau (2.94). The pig population under study showed lower effective number of alleles than the observed number of alleles which might be due to very low frequency of most of the alleles at each locus and few alleles might have contributed to the major part of the allelic frequency at each locus.

The range of PIC between 0.137 and 0.874 with the mean of 0.655, reported in Brazilian pig breeds (Sollero et al., 2010) using 28 different microsatellite markers, is in close agreement with the present results which ranged from 0.262 to 0.842 with a mean of 0.635. Most of the loci possessed high PIC values (above 0.05) signifying that these markers are highly informative for characterization of Doom pig. The mean observed and expected heterozygosity (0.62 and 0.67) in the present study is in agreement with the mean number of observed (0.584) and expected (0.685) heterozygosity in Brazilian pig breeds (Sollero et al., 2010). The present findings of observed heterozygosity is higher than the reported value (Swart et al., 2010) in Southern African domestic pigs namly, Landrace (0.522), Large White (0.584), Duroc (0.504), Namibia (0.518), Mozambique (0.609), Kolbroek (0.537) and Kune-Kune (0.508).

The mean within population inbreeding estimate (F_{IS}) was 0.089. The deficiency of heterozygotes (8.9%) in Doom pig population is comparable to heterozygote shortfall observed in Duroc pig 5.1%; Landrace pig 3.8%; Large White pig 6.5%; Pietrain pig 6.1% (Vicente et al., 2008) and not significant as compared to heterozygote shortfall reported in Bae pig 22.6%; Canastra pig 23% UDB pig 22.8%; Duroc pig 25.0% (Silva et al., 2011). The

present findings of F_{IS} value support random mating in the studied population. The deviation of 13 out of 22 loci from equilibrium may be due to consequences of small population size.

The Doom pig population is non-bottlenecked as evident from the quantitative graphical method (Cornuet and Luikart, 1996). The population has not undergone any recent and/or sudden reduction in the effective population size and remained at mutation-drift equilibrium. In the present study, no mode-shift was detected in the frequency distribution of alleles and a normal L-shaped curve was observed.

In conclusion, the investigation stands first in genetic characterization of Doom pig populations in North-East India using microsatellite markers and the PIC values observed in the present study is indicative of the fact that the markers used are highly informative for characterization of diversity in Doom pigs. The population has not undergone any reduction at least in the recent past. The significant level of variability in this population is indicative of valuable genetic diversity. The needful strategy has to be taken to maintain the existing genetic variation and its sustainable utilization.

Conflict of Interest

The author(s) have not declared any conflict of interest.

ACKNOWLEDGEMENTS

The authors wish to extend their gratitude to Indian Council of Agricultural Research, New Delhi, India for the financial assistance for molecular characterization work through Network Project on Animal Genetic Resources under National Bureau of Animal Genetic Resources, Karnal, India.

REFERENCES

Cornuet JM, Luikart G (1996). Description and power analysis of two tests for detecting recent population bottlenecks from allele frequency data. Genetics 144:2001-2014.

Da Silva EC, Junior WMD, Ianella P, Filho MAG, De Ollveira CJP, De Moura Ferreira DN, Caetano AR, Paiva SR (2011). Patterns of genetic diversity of local pig populations in the State of Pernambuco. Brazil. R. Bras. Zootec. 40(8):1691-1699.

Food and Agriculture Organization (FAO) (1998) Swine. In Guidelines for development of national farm animal genetic resources management plans. Measurement of domestic animal diversity (MoDAD) recommended microsatellite markers: 19-24. Food and Agriculture Organization of the United Nations, Rome.

Henegariu O, Heerema NA, Dlouhy SR, Vance GH, Vogt PH (1997). Multiplex PCR: critical parameters and step-by-step protocol. Biotechniques 23:504-511.

Loffert D, Karger S, Twieling G, Ulber V, Kang J (1999). Optimization of multiplex PCR, Qiagen News Issue 2:5-8.

Luikart GL, Allendrof FW, Cornuet JM, Sherwin WB (1998). Distortion of allele frequency distributions provides a test for recent population bottlenecks. J. Hered. 89:238-247.

Nei M (1978). Estimation of average heterozygosity and genetic distance from a small number of individuals. Genetics 89: 583-590.

Rajeev K, Atar Singh RK, Vijh MS, Tantia, Rahul B (2001). Evaluation of the genetic variability of 13 microsatellite markers in native Indian pigs. J. Genet. 80(3):149-153.

Sambrook J, Fristisch EF, Maniatis T (1989). Molecular Cloning: A Laboratory Manual, 2nd edn. Cold Spring Harbor Laboratory Press, Cold Spring Harbor, NY, USA.

Sollero BP, Paiva SR, Faria DA, Guimaraes SEF, Castro STR, Egito AA, Albuquerque MSM, Piovezan U, Bertani GR, Mariante AS (2010). Genetic diversity of Brazilian pig breeds evidenced by microsatellite markers. Livest. Sci. doi:10.1016/j.livsci.2008.09.025.

Swart H, Kortze A, Olivier PAS, Grobler JP (2010). Microsatellite-based characterization of Southern African domestic pigs (*Sus scrofa domestica*). South African Jr. of Anim. Sci. 40(2): 121-132.

Vicente AA, Carolino MI, Sousa MCO, Ginja C, Silva FS, Martinez AM, Vega-Pla JL, Carolino N, Gama LT (2008). Genetic diversity in native and commercial breeds of pigs in Portugal assessed by microsatellites. J. Anim. Sci. 86:2496-2507.

Wallin JM, Holt CL, Lazaruk KD, Nguyen TH, Walsh PS (2002). Constructing universal multiplex PCR systems for comparative genotyping. J. Forensic Sci. 47:52-65.

Yeh FC, Boyle T, Rongcai Y, Ye Z, Xian JM (1999). Popgene, Version 1.31. A Microsoft Windows based freeware for population genetic analysis. University of Alberta, Edmonton.

Zaman G, Chandra Shekar M, Aziz A (2013b). Molecular Characterization of Meghalaya Local Pigs (Niang Megha) using Microsatellite Markers. Indian J. Sci. Technol. 6(10):5302-5306

Zaman G, Chandra Shekar M, Ferdoci AM, Laskar S (2013a). Molecular Characterization of Ghungroo pig. Int. J. Anim. Biotechnol. 3: 1-4.

Zaman G, Chandra Shekar M, Kharghoria G, Ahmed FA (2014). Molecular characterization of Mizoram local pigs (Zovawk) using microsatellite markers. Biotechnol. Indian J. 10(1): 24-28.

Zaman G, Chandra Shekar M, Nath MK, Islam N (2013c). Molecular Characterization of Mali Pigs of Tripura Using Microsatellite Markers. Glob. Vet. 11(6):742-746.

Zaman G, Kharghoria G, Nath MK (2013d). Molecular characterization of Nagaland local Pig (suwo) using micro satellite markers. Tamil Nadu J. Vet. Anim. Sci. 9(5):325-331.

academicJournals

Vol. 13(30), pp. 3023-3029, 23 July, 2014
DOI: 10.5897/AJB2013.13090
Article Number: 1FCAB9546217
ISSN 1684-5315

http://www.academicjournals.org/AJB

African Journal of Biotechnology

Full Length Research Paper

Analysis of phosphoric ore bacterial and eucaryal microbial diversity by single strand conformation polymorphism (SSCP) and small-subunit (SSU) sequencing

Ilhem Omri[1], Imen Manaii[1], Zied Tlili[2], Jean-Jacques Godon[3] and Moktar Hamdi[1]

[1]Laboratoire d'Ecologie et de Technologie Microbienne. Department de Génie Chimique et Biologique. Institut Nationale des Sciences Appliquées et de Technologie (INSAT). B. P 676, 1080.University of Carthage, Tunis, Tunisia.
[2]Higher Institute of Business Administration of Gafsa, Tunisia.
[3]INRA UR50, Laboratoire de Biotechnologie de l'Environnement, Avenue des Étangs, F-11100, Narbonne, France.

Received 30 July, 2013; Accepted 4 July, 2014

The aim of this study was to investigate the phosphoric ore bacterial and eucaryal microbial diversity by using the single strand conformation polymorphism (SSCP) technique and small-subunit (SSU) sequencing. PCR-SSCP patterns showed a remarkably simple microbial community, mainly for bacterial community, but also for the eukaryotic community. According to the highly bacterial variable V3 region of 16S rRNA sequences, five bacterial species were identified: an unidentified species belonged to proteo gamma phylum, an unidentified species belonging to proteo delta phylum, one belonged to *Moraxellaceae* and two closed to *Pseudomonadaceae* as predominant bacteria in the mining residue. The study showed for the first time that phosphoric ore harbors major bacterial groups related to organisms having a wide range of environmentally significant functional attributes. These findings provided new opportunities into phosphoric ore microbiology that could be useful in biological system removing waste gases generated from the phosphoric industry.

Key words: Microbial community, bacteria, archaea, eucarya, mining residue.

INTRODUCTION

Phosphoric industry generates a considerable quantity of waste gas with high concentrations of fluoride and sulfurous compounds such as methyl mercaptan and hydrogen sulfide. Also, air emissions may contain

*Corresponding author. E-mail: ilhemelomrii@yahoo.fr. Tel: +216 98 911 002. Fax: +216 71 704 329.

Abbreviations: H_2S, Hydrogen sulfide; **PCR,** polymerase chain reaction; **SSCP,** single strand conformation polymorphism; **SSU,** small subunit; **VOC,** volatile organic compound.

particulates containing heavy metals such as uranium, cadmium, mercury, and lead (Connett, 2003; Godson et al., 2005). The fluoride and hydrogen sulfide gases are frequently emitted in large volumes into surrounding communities, causing serious environmental damage. As a pollutant, fluoride is an extremely toxic ion. Near the sources of fluoride air pollution, the vegetation is destroyed, animals get sick and die, and people suffer eye irritation, respiratory problems, or more serious symptoms of fluoride poisoning (Othman and AlMasri, 2007). Hydrogen sulfide (H_2S) is a colorless, flammable and highly toxic gas. Toxic to living organisms and plants (Syed et al., 2006), it causes very serious consequences on human health and the environment. In spite of its serious nature, fluoride and H_2S pollution has received very little attention in the mass media and scientific research (Connet, 2003; Syed et al., 2006). In fact, emission of these gases from industrial process can be a major obstacle to its daily operations and potential. Scrubbing process have been proposed for the treatment of waste gases (Chung, 2007). Thus, scrubbers plant constitute habitats where fluoride and sulfurous compounds are present. Some extremophiles micro-organisms are able to survive and thrive in such habitats, due to their superior tolerance to extreme conditions.

The living communities that exist in extreme conditions have always attracted much interest from taxonomists, microbiologists, and ecologists alike. But the most interest has come from commercial industrial entities looking for biocatalysis that is stable under extreme conditions (Podar and Louise, 2006). The microbial community from such areas and samples from such sites are often rich in microorganisms with desired characteristics for both *in situ* and *ex situ* bioremediation processes (Berlemont and Gerady, 2011). Little data was found about the microbial structure of mining residue from phosphoric ore processing and the level of cultivable microorganisms reported on these habitats is extremely low. Some bacteria were previously detected in Acide Mine Drainage such as *Caulobacter crescentus*, *Pseudomonas* sp., *Leptothrix* sp., *Aquabacterium* sp. and *Ralstonia pickettii*. *Pseudomonas* sp., *Leptothrix* sp., *Aquabacterium* sp. and *Ralstonia pickettii*. These bacteria are known for their distinctive ability to live in low-nutrient environments, a characteristic of most heavily metal-contaminated sites (Yang et al., 2008).

In order to better understand the functions of the microbial community, a full description of the microbial ecosystem previously unknown is required. Classically, this has been addressed by enumerating members of certain microbial groups by using various culture media, followed by identification of a number of dominant isolates by phenotypic tests or molecular techniques such as ribotyping, randomly amplified polymorphic DNA analyses, and sequencing. Molecular biological tools, such as fluorescence *in situ* hybridization (FISH), and polymerase chain reaction coupled to either denaturing gradient gel electrophoresis or temperature gradient gel electrophoresis (PCR-DGGE/TGGE), have provided important information about the diversity of microorganisms in natural and engineered habitats, including those microbial species previously unknown due to the restrictions of cultivation-based approaches (Calderón et al., 2012; Chamkha et al., 2008). Acquisition of DNA sequences is a fundamental component of most phylogenetic, phylogeographic, and molecular ecological studies. Single-stranded conformation polymorphism (SSCP) offers a simple, inexpensive and sensitive method for detecting whether or not DNA fragments are identical in sequence, and so can greatly reduce the amount of sequencing necessary. It can give a more objective picture of the bacterial community from several ecosystems (Bouallagui et al., 2004). SSCP can be applied without any a priority information on the species and then can give a more objective view of the microbial community. From this microbial community, the result is a pattern in which each peak can be correlated with the V3 16S rRNA sequence of one microorganism.

The aim of this paper was to study the diversity of the microbial community, including bacteria, archaea and eucarya, of a mining residue collected from scrubbing plant of waste gas generated from phosphoric acid process and to identify the most dominant bacteria involved in this ecosystem.

MATERIALS AND METHODS

Sampling and analysis

The Tunisian phosphoric acid industry generates considerable amounts of waste gas with high concentrations of hydrogen sulfide (99000 µg/m^3), methyl mercaptan (1590 µg/m^3) and fluor trace. A scrubbing system was used in phosphoric acid plants for removing these compounds. Such scrubbing process removed pollutants from waste gas with efficiencies between 20 to 60% and outlet waste gas may contain fluor trace, hydrogen sulfide and methyl mercaptan with concentration of 39600 and 635 µg/m^3, respectively. As shown in Figure 1a, the waste gas generated from the reactor tank is aspired by a venture and passed through two semi-cross flow scrubbers before being discharged in the atmosphere through the chimney. Its worth to note that the further away we move from the reactor, the concentration of gaseous pollutants decreases. Samples were collected from five points (Figure 1a and 1b): (1) outlet of reactor tank, (2) venture, (3) first semi-cross flow, (4) second semi-cross flow and (5) waste gas outlet. Samples were collected in a glass vial and stored at 4°C during 4 days.

Extraction and purification of total genomic DNA

DNA extractions were performed on samples collected from scrubbing spray plant of phosphoric industry. Samples were suspended in 2 ml of 4 mol.L^{-1} guanidine thiocyanate, 0.1 mol.L^{-1}, Tris pH 7.5 and 600 µl of N-lauroyl sarcosine 10% (Sigma, Taufkirchen, Germany). 250 µl of treated samples were transferred in micro-centrifuge tubes (2 ml) and stored frozen at -20°C. Extraction and purification of total genomic DNA was implemented according to the protocol developed by Bouallagui et al. (2004). This protocol consists of mechanical cell perturbation by heat

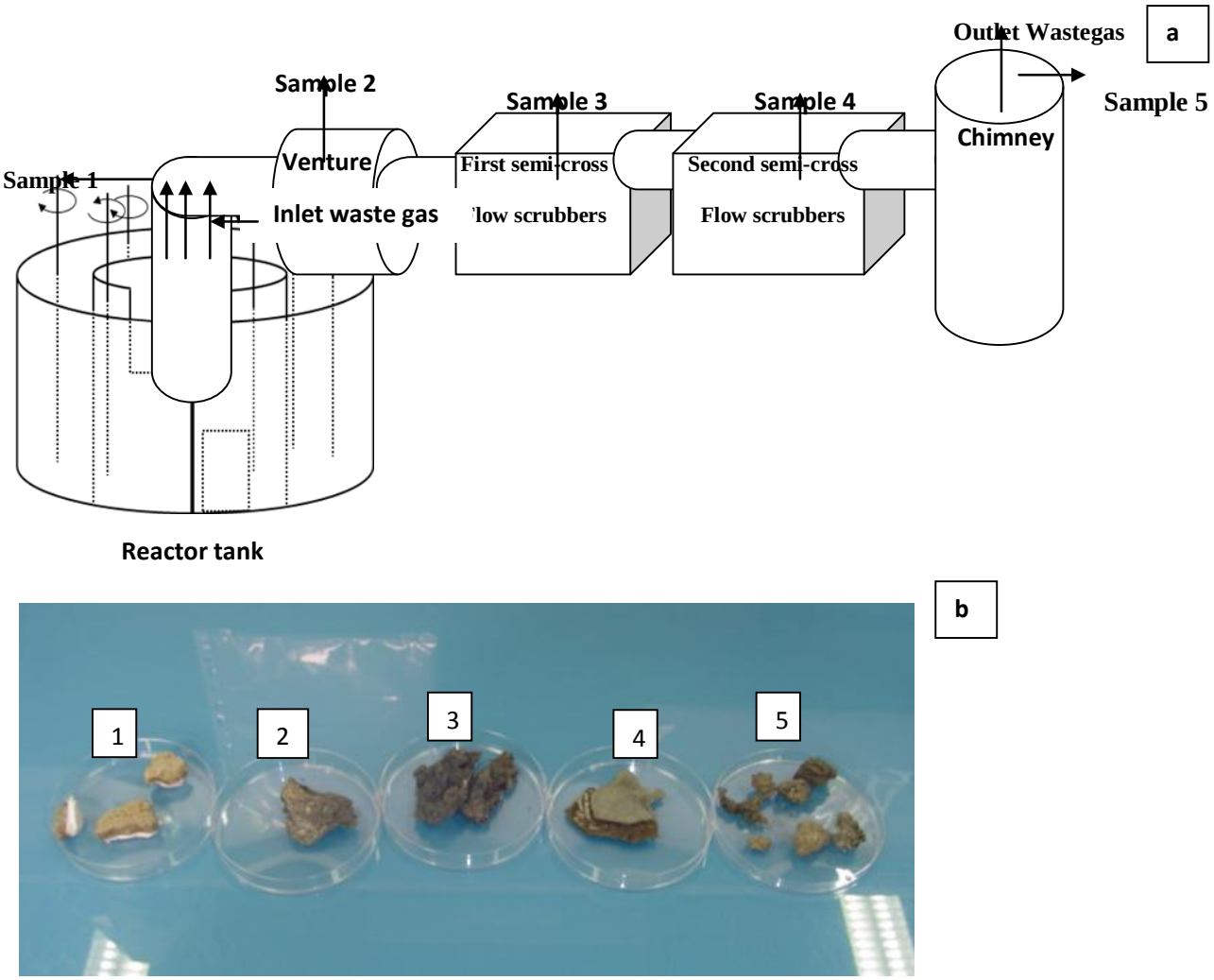

Figure 1. Schematic description of Scrubbing system (a) and mining residue (b) collected from 5 points: (1) vaccum, (2) venture, (3) first semi-cross flow, (4) second semi-cross flow and (5) waste gas outlet (chimney).

treatment (70°C for 1 h) and cells being shaken in the presence of zirconia beads. Nucleic acids were recovered after several washes with polyvinylpolypirolidone to remove PCR inhibitors, followed by alcohol precipitation. Concentration and size of DNA were estimated by electrophoresis on a 0.7% agarose gel (Figure 2).

Amplification for SSCP analysis

The amplification of the V3 region of 16S rRNA and the small subunit (SSU) 18S rRNA region was carried out, from the total DNA, with specific primers w49-w104 for Bacteria, W16-W131 for Eucarya and w116-w104 for Archaea (Omri et al., 2011). Each PCR reaction tube contained: 1x Pfu Turbo DNA polymerase buffer (Stratagene, California, USA), 200 $\mu mol.L^{-1}$ of each deoxynucleotide triphosphate (Promega, Madison, USA), 0.13 µg of each primer, 1.25 U of Pfu Turbo DNA polymerase (Stratagene, California, USA), 1 µl of total DNA previously diluted in water, adjusted to a total volume of 50 µl with Milli-Q water. PCR conditions were as follows: an initial denaturation step at 94°C for 2 min, followed by 25 cycles of a three-stage program with 1 min at 94°C, 1 min at 61°C for bacteria and 51°C for archaea, then 1 min at 72°C and a final elongation step run for 10 min at 72°C. PCR-SSCP products providing bands of the proper size [approximately 200 bp for Bacteria (Figure 3a), and 300 bp for Eucarya (Figure 3b)] were confirmed on a 2% (w/v) agarose gel-electrophoresis and purified by means of a QIA quick PCR purification kit (Quiagen, Hilden, Germany).

SSCP analysis

For SSCP electrophoresis, each reaction tube contained 1 µl of diluted PCR-SSCP product, 18.80 µl of formamide (Genescan-Applied Biosystems, Foster City, USA) and 0.20 µl of internal standard (400 Rox, Genescan-Applied Biosystems, Foster City, USA) according to the protocol of SSCP (Rochex et al., 2008). Prior to analysis, the reaction mixture was denaturated by heating at 95°C for 5 min and cooled in ice water for 10 min. Single strands of DNA molecules make stable secondary conformation which were separated by capillary electrophoresis. SSCP analyses were performed on an automatic DNA sequencer (ABI 310 Genetic Analyzer, Applied Biosystems, Foster City, USA). Using fluorescent

Table 1. Phylogenetic affiliation of the 16S rRNA bacteria sequences.

Phylogeny	Closest	Relatives Similarity (%)	Accession Number	Abundance	Sources
Gamma Proteobacteria	*Clone US263M*	100	HM641011.1	16/42	Geothermal environment
Proteobacteria	*Moraxellaceae culture clone*	100	FJ985732.1	11/42	Uranium rock
Pseudomonadacea	*Pseudomonas putida*	97	GU396283.1	9/42	soil
Pseudomonadace	*Pseudomonas sp. YKS1*	98	AB504894	5/42	Seawater, soil polluted by oil
Delta Proteobacteria	*Benzene mineralizing consortium clone SB-22*	97	AF029046	2/42	Environmental sample

dye-labelled PCR primers, the strands of each different DNA fragment were detected by laser. The obtained results were analyzed by GeneScan (Applied Biosystems, Foster City, USA).

Amplification, cloning and sequencing for bacterial identification

The highly bacterial variable V3 region of 16S rRNA was amplified by PCR using bacterial (W49-W31) primers (Chamkha et al., 2008). For PCR reaction, the solution contained: 1x Red Taq DNA polymerase buffer (Sigma, Saint Louis - Missouri, USA), 200 µ mol.L^{-1} of each deoxynucleotide triphosphate (Promega, Madison, USA), 0.2 µg of each primer, 1 U Red Taq DNA polymerase (Sigma, Saint Louis - Missouri, USA), 1 µl of total DNA previously diluted in water. The total volume of 50 µl was adjusted with Milli-Q water. PCR conditions were as follows: an initial denaturation step at 94°C for 2 min, followed by 25 temperature cycles of a three stage program: 1 min at 94°C, 1 min at 61°C for Bacteria, then 1 min at 72°C; and by a final elongation step run for 10 min at 72°C. PCR products providing bands of the proper size were purified with the QIA quick PCR purification kit (Quiagen, Hilden, Germany). Cloning was performed with the TOPO TA cloning kit (Invitrogen, Groningen, the Netherlands) following the manufacturer's instructions. Plasmid inserts were amplified by PCR with pGEMt primers T7 and P13 (Rochex et al., 2008). Clones to be sequenced were chosen as described by Godon et al. (1997). Bacterial inserts from selected clones were sequenced using the “dye-terminator cycle sequencing reaction” kit (Applied Biosystems, Forster City, USA) with AmpliTaq DNA polymerase FS kit (Applied Biosystems, Forster City, USA) and the T7 primer. Reaction sequences were separated and analyzed using the ABI model 373A sequencer (Applied Biosystems, Perkin Elmer, Forster City, CA, USA).

Sequence analysis and nucleotide sequence accession numbers

Each cloned DNA sequence was compared with sequences available in databases, using BLAST from the National Center for Biotechnology Information and the Ribosomal Database Project (RDP-II). The nucleotide sequence data reported in this work will appear in the GenBank nucleotide database under accession numbers are presented in Table 1.

RESULTS AND DISCUSSION

In this study, SSCP technique was used to monitor the structure and the intensity of the microbial community of a mining residue collected from scrubbing spray plants of phosphoric industry. The obtained profiles are shown in Figure 4a for bacteria and Figure 4b for eucarya. SSCP techniques enable DNA fragments with similar size to be separated according to their configuration, which is primarily determined by their sequence. Thus, targeting the 16S rRNA V3 region and 16S rRNA, allows phylogenetic discrimination of bacterial and eucaryotic species making it possible to assess mining residue microbial community by one profile of peaks where each peak theoretically corresponds to a different sequence of 16S rRNAV3 region (Chamkha et al., 2008). The obtained result showed that DNA was detected only in the outlet waste gas residue (chimney) (sample 5) (Figure 3). This sample has the lowest pollutant concentration of the 5 samples. The SSCP pattern of the microbial communities of this sample revealed a simple profile, with higher bacterial than eukaryotic diversity. The SSCP bacterial profile (Figure 4a) revealed 18 distinguishable peak and about 7 prominent ones [peaks (S1, S2, S5, S6, S10, S11 and S18)]. The SSCP eukaryotic profile (Figure 4b) revealed 7 distinguishable peak and about 4 prominent ones [peaks (E3, E4, E6 and E7)]. In this work, archaeal populations were not detected despite many amplifications of the specific total archaeal 16S rRNA and the archaeal 16S rRNAV3 region.

SSCP results indicated a low microbial diversity for bacteria and eukaryotic community. It was reported that the pollutants concentration could affect noticeably the bacterial diversity in different samples. In addition, the highest polluants concentration induced a decrease of the diversity and allowed the growth of few bacterial species. Therefore, few bacterial populations were selected, in relation with the toxicity of the accumulated polluants. The low microbial diversity according to SSCP analysis was consistent with the results of previous work in a similar environment. Yang et al. (2008) have used ARDRA (amplified ribosomal DNA restriction analysis) analysis to characterize the diversity and community structure of Acide Mine drainage. They showed that pH and polluant concentrations exert a considerable

Figure 2. Agarose gel electrophoresis of DNA extracted from mining residue [DNA was detected only in the sample 5 (the outlet waste gas residue: chimney)].

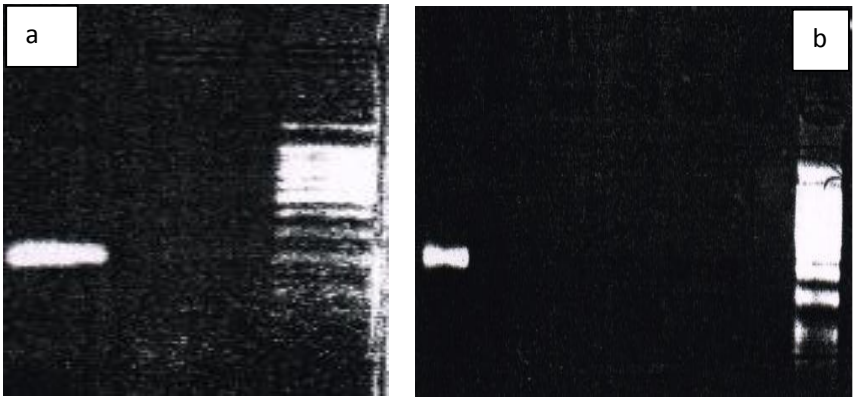

Figure 3. Agarose gel-electrophoresis of PCR products amplified from DNA extracted from sample 5 providing bands of the proper size [approximately 200 bp for Bacteria (a), and 300 bp for Eucarya (b)].

influence on the phylogenetic diversity of microbial communities in mining sites. Furthermore, zones subjected to highest pollutants concentrations (near the reactor tank: sample N° 1, 2, 3 and 4) provide unfavorable environment for microbial growth. But zone subjected to the lowest pollutants concentration (sample N°5) provide a favorable environment for the microbial growth. This phenomenon could well be the case for waste gas toxicity and inhibition to even the bacteria. This was found to be in agreement with the findings of Omri et al. (2011) which focused on the study of microbial diversity of the peat used as a packed bed in H_2S biofiltration system. They demonstrated that the diversity and relative abundance of microbial species present in ecosystem may be influenced by availability of the influent waste gas (substrate), environmental conditions (pH, temperature), and pollutant concentrations. The obtained results showed that there were bacteria that could survive in scrubbing plants of phosphoric ore processing and tolerate the toxicity of reduced sulfur compounds, fluoride and uranium traces. These bacteria were able to inhabit environments characterized by properties harsh enough to hinder the survival of common cells. They notably produce enzymes that are adapted to work in unusual conditions often required in biotechnological processes (Podar and Louise, 2006).

In order to better understand the differences in bacterial diversity among samples, 42 clones were sequenced, and the closest relative was identified by comparison with the Genebank database (Table 1). Five bacterial phylotypes were identified. The presence of these bacteria in mining residue had not been previously reported. It was important to note that *Pseudomonas putida, Pseudomonas sp* and *Moraxellacea* have a wide range of environmentally significant functional attributes. They were common bacterial species involved in the volatile organic compounds and sulfur odor treatment system (Xie et al., 2009; Tang et al., 2009). Since waste gas generated from phosphoric acid industry contained high concentration of sulfurous compounds (H_2S and methyl mercaptan), the dominance of these bacteria in mining residue is not surprising.

Islam and Sar (2011) have studied the bacterial community structure of heavy metal rich- uranium ores

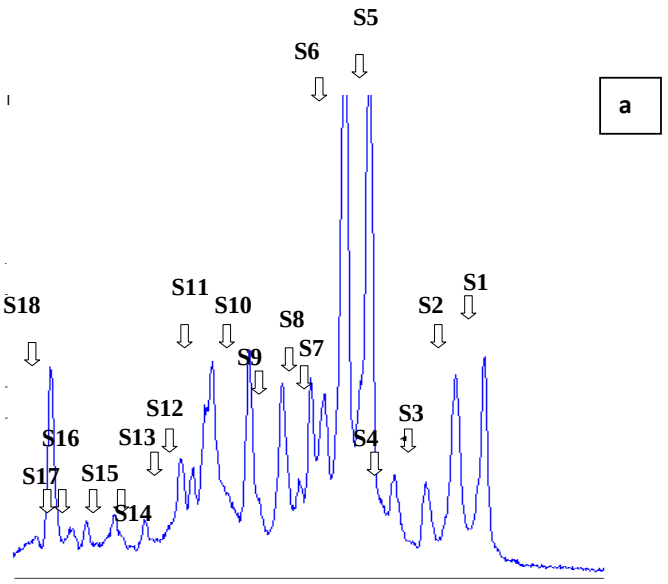

Figure 4a. Single strand conformation polymorphism (SSCP) patterns of bacterial 16S rDNA region amplification products in mining residue collected from the chimney (outlet waste gas, sample N°5).

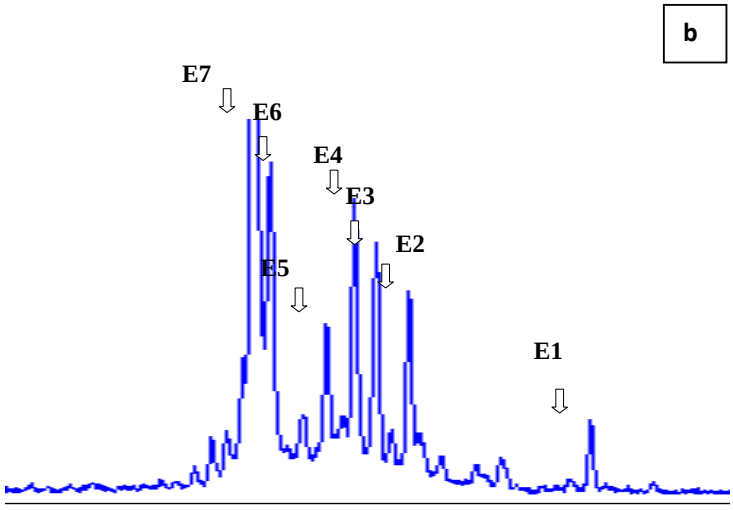

Figure 4b. Single strand conformation polymorphism (SSCP) patterns of eukaryotic 18S rDNA region amplification products in mining residue collected chimney (outlet waste gas, sample N°5).

using 16S rRNA gene based clone library analysis and denaturing gradient gel electrophoresis (DGGE). Sequence analysis of major DGGE bands revealed that *Moraxellaceae* was abundant in uranium rock samples. The presence of this bacterium in the mining residue could be explained by the fact that the waste gas generated by phosphoric industry may contain dust with uranium traces (Connett, 2003). In a recently published work, Goh et al. (2011) have identified the *clone US263M!* from geothermal environment. The sampling site temperature was about 95°C with the pH value as high as 9.3. Under such state, the heated water should be anoxic. The described condition were the same of the sampling site of mining residue which was characterized by high temperatures and alkaline pH as the scrubbing of waste gas generated from phosphoric industry was done by spraying seawater.

This is the first time that SSCP analysis has been applied to the description of the microbial community of mining residue. The SSCP analysis provided a picture of

dominant 16S and 18S rRNA sequences of the different microorganisms which could be present in the phosphoric industry. The inventory of the diversity based on molecular biological techniques, eliminated the dependence on isolation of pure cultures. These methods provide a rapid fingerprint of a complex microbial community without cultivation. In contrast, cultivation-dependent approaches do not necessarily provide reliable information on the composition of entire microbial communities because of the disparity between cultivable and *in situ* biodiversity (Bouallagui et al., 2004; Calderón et al., 2012). However, there are biases closely linked to the use of the PCR-SSCP method including preferential lysis during nucleic acid extraction, preferential amplification of certain sequences during PCR amplification of a mixture of templates, formation of chimeric products during the amplification process, and the high degree of dilution of template DNA causing the disproportionate representation of particular sequence types in the clone library (Chamkha et al., 2008; Rochex et al., 2008). Also, just 42 clones were sequenced and analyzed during this work. It seemed that the amount of clones was not sufficient to have an idea about the diversity in the mining residue. In addition, the bacterial strains detected in this study, have not been isolated. Their physiological role in the ecology will remain uncertain, so further investigation should be concentrated on isolating these bacteria.

The obtained results indicated that environmental conditions of the phosphoric industry were used to select a interseting microflora able to survive in extreme conditions. This confers upon these bacteria is a very important potential. *P. putida* and *Moraxellacea* are the target of a steadily increasing interest and are nowadays largely used in various industrial applications (Xie et al., 2009; Tang et al., 2009; Syed et al., 2006). The use of these bacteria for treatment of waste gas generated from phosphoric industry could be an attractive alternative.

Conclusion

Molecular tools have made a considerable contribution to a better understanding of the microbial diversity of mining residue collected from phosphoric industry. SSCP profiles demonstrated a simple microbial community. It also demonstrated that *Pseudomonas* and *Morxcellacea* were the dominant bacteria in the mining residue. The identification of these microorganisms has scientific and practical interest due to their important role in the treatment of reduced sulfurs compounds, VOC and uranium. This could be viewed as a benefit of operating biological system removing waste gas generated from phosphoric industry.

Conflict of Interest

The author(s) have not declared any conflict of interest.

ACKNOWLEDGMENTS

The authors gratefully acknowledged the financial support provided by the Ministry of Higher Education, Scientific Research and Technology. They express their sincere appreciation to Mr. Chaker CHTARA for his help and technical support.

REFERENCES

Berlemont R, Gerday C (2011). Extremophiles. Compr. Biotechnol. 1:229-242.

Bouallagui H, Torrijos M, Godon JJ, Moletta R, Ben Cheikh R, Touhami Y, Delgenes JP, Hamdi M (2004). Microbial monitoring by molecular tools of two-phase anaerobic bioreactor treating fruit and vegetable wastes. Biotechnol. Lett. 26:857-862.

Calderón K, González-Martínez A, Montero-Puente C, Reboleiro-Rivas P, Poyatos J, Juárez-Jiménez B, Martínez-Toledo MV, Rodelas B (2012). Bacterial community structure and enzyme activities in a membrane bioreactor (MBR) using pure oxygen as an aeration source. Bioresour.Technol. 103(1):87-94.

Chamkha M, Sayadi S, Bru V, Godon JJ (2008). Microbial diversity in Tunisian olive fermentation brine as evaluated by small subunit rRNA - Single strand conformation polymorphism analysis. Int. J. Food Microbiol. 122:211-215.

Chung YC (2007). Evaluation of gas removal and bacterial community diversity in a biofilter eveloped to treat composting exhaust gases. J. Hazard. Mater.144:377-385.

Connett M (2003). The Phosphate fertilizer Industry: An Environmental overview. A Report by Fluoride Action Network, U.S.A.

Godon JJ, Zumstein E, Darbert P, Habouzit F, Moletta R (1997). Molecular bacterial diversity of an anaerobic digester as determined by small-subunit rDNA sequence analysis. Appl. Environ. Microbiol. 63: 2802-2813.

Godson A, Mynepalli S, Olawuyi J (2005). Air Pollution in a Chemical Fertilizer Complex in Nigeria: The Impact on the Health of the Workers. J. Environ. Health Res. 4(2): 57.

Goh KM, Chua YS, Zaliha RN, Rahman RA, Chan R, Illias AR (2011). A comparison of conventional and miniprimer PCR to elucidate bacteria diversity in Malaysia Ulu Slim hot spring using 16S rDNA clone library. Rom. Biotechnol. Lett. 16(3): 6247- 6255.

Islam E, Sar P (2011). Culture-dependent and -independent molecular analysis of the bacterial community within uranium ore. J. Basic Microbiol. 51(4):372-384

Omri I, Bouallagui H, Aouidi F, Godon JJ, Hamdi M (2011). H_2S gas biological removal efficiency and bacterial community diversity in biofilter treating wastewater odor. Bioresour.Technol. 102 : 10202-10209.

Othman I, AlMasri MS (2007). Impact of phosphate industry on the environment: A case study. Appl. Radiat. Isot. 65(1): 131-14.

Podar M, Louise A (2006). New opportunities revealed by biotechnological explorations of extremophiles. Curr. Opin. Biotechnol. 17:250-255.

Rochex A, Godon JJ, Bernet N, Escudie R (2008). Role of shear stress on composition, diversity and dynamics of biofilm bacterial communities. Water Res. 42: 4915 - 4922.

Syed M, Soreanu G, Falletta P, Beland M, (2006) Removal of hydrogen sulphide from gaz streams using biological processes - A review. Can. Biosyst. Eng. 48: 21-30.

Tang K, Baskaran V, Nemati M (2009). Bacteria of the sulphur cycle: An overview of microbiology, biokinetics and their role in petroleum and mining industries. Biochem. Eng. J. 44: 73-94.

Xie B, Liang SB, Tang Y, Mi WX, Xu Y (2009). Petrochemical wastewater odor treatment by biofiltration. Bioresour. Technol. 100: 2204-2209.

Yang Y, Shi W, Wan M, Zhang Y, Zou L, Huang J, Qiu G, Liu X (2008). Diversity of bacterial communities in acid mine drainage from the Shen-bu copper mine, Gansu province, China. Electron. J. Biotechnol.11(1):107-118.

academicJournals

Vol. 13(30), pp. 3030-3035, 23 July, 2014
DOI: 10.5897/AJB2013.13362
Article Number: 7B7A13046218
ISSN 1684-5315

http://www.academicjournals.org/AJB

African Journal of Biotechnology

Full Length Research Paper

Evidence of salicylic acid regulatory mechanisms of disease resistance against banana vascular wilt *Fusarium oxysporium* f.sp. cubense in *Arabidopsis thaliana*

Raju Radhajeyalakshmi [1,2]*, Yiji Xia[1] and Dhilip Shah[1]

[1]Donald Danforth Plant Science Center 975 N. Warson Road.St. Louis, MO 63132, USA.
[2]Department of Plant Pathology Center for Plant Protection Studies Tamil Nadu Agricultural University Coimbatore-641 003, TN, India.

Received 9 October, 2013; Accepted 4 July, 2014

Symptomatological studies on Arabidopsis- *Fusarium oxysporium f.sp. cubense* (*Foc*) interaction has led to the identification of signaling pathways required for plant resistance to *Foc*, as well as key regulators of innate immunity against this type of vascular wilt pathogens. From the *in planta* symptom expressions of *Foc* on Arabidopsis, there is a clear indication of involvement of salicylic acid (SA) and jasmonic acid (JA) for disease resistance. Mutations occur in synthesis of salicylic acid and Jasmonic acid, which modulate disease resistance with the evident of severe veinal necrosis on leaves and petiole. The typical symptom of leaf rosetting was the clear indication of the active participation of SA biosynthesis for *Foc* resistance in nahG, npr-1 plants. This analysis revealed that salicylic acid, ethylene (ET) and jasmonic acid (JA) pathways influence the *Foc* disease outcome in Arabidopsis. All the three signaling pathways interact in a positive way in the activation of Arabidopsis resistance to *Foc*. Hence, there must be co-ordinate regulation of both SA and JA for *Foc* resistance in Arabidopsis. Constitutive expressions of some transcriptional regulators of these pathways are sufficient to confer enhanced resistance to *Foc* and it might be an oligogenic trait.

Key words: *Fusarium oxysporium f.sp.cubense, Arabidopsis thaliana,* disease resistance.

INTRODUCTION

Fusarium wilt of banana, commonly referred to as Panama Disease, is caused by *Fusarium oxysporum* Schlechtend.: Fr. *f. sp. Cubense* (E.F. Sm.) W.C. Snyder and H.N. Hans. *Fusarium* wilt is the preferred name for what was first called Panama disease because it became prominent in that Central American country early last century. Cavendish plantations has been affected with annual losses over 75 millions USD with effects on family income of thousands of workers and farmers (Masdek et al., 2003; Nasdir, 2003). The global distribution of the disease has an important anthropogenic component; as the infected rhizomes are frequently free of symptoms, is

*Corresponding author. E-mail: radhajeyalakshmi@hotmail.com.

not unusual that *Foc* were introduced into new areas with conventional plantation material (Ploetz and Pegg, 2000). *Foc* is thought to have originated in Asia, and then spread during the 20th century to become a major problem throughout most banana production regions of the world. An important exception is the South Pacific, where *Fusarium* wilt is a new disease and not yet widespread (Davis et al., 2000; Smith et al., 2002). The fungus infects banana plants through the roots and invades the plant's water conducting tissues. Once *Foc* is introduced into banana gardens, it remains in the soil making it impossible to grow susceptible bananas in the same location for up to several decades.

As *Foc* disrupts the plants' water conducting vessels, leaves become yellow (progressing from older to younger leaves) and wilted. This is also a sign of drought stress that is reduced when water supply is good. Distinctive symptoms appear inside the pseudo stem: brown, red or yellow lines are visible in vertical section which appears as rings in cross-section. These are the infected water conducting vessels. Smaller brown streaks or flecks appear in the corm, at ground level. Later, all leaves turn yellow and die and internal rotting becomes extensive. Splits may also appear in the pseudo stem. Infected plants usually do not produce fruit.

Foc grows better in warmer condition, global warming might positively influence its incidence. *Foc* can persist in affected fields for an extended period of time on plant stubbles as macro conidia or even survive on soils as dormant chlamydospores in the absence of a suitable host plant. Therefore, there is much interest in determining the molecular and genetic basis of plant innate immunity against this type of pathogens.

Foc can invade the weed roots in banana plantations as saprophyte or as a weak parasite of the tissues of senescent roots in decomposition remaining in soil by long periods. There are reports of the isolations of *Foc* from roots of the weeds *Euphorbia heterophylla* L. (Euphorbiaceae), *Tridax procumbens* L. (Poaceae), *Chloris inflata* (Link.) and *Cyanthillium cinereum* L. (Asteraceae) (Waite y Dunlap, 1953); *Cyperus iria* L., *Cyperus rotundus* L., *Gnaphalium purpureum* L., *Fimbristylis koidzuminana* Ohwi (Su et al., 1986) and from decolorated roots without wilting of the species *Paspalum fasciculatum* Sw., *Panicum purpurascens* (Roddi.), *Ixophorus unisetus* Schl., and *Commelina* spp (Podovan, 2003). Persistance of *Foc* disease can be attributed to two principal factors: resistance appears to be genetically complex and thus is a difficult trait to confer by breeding. The role of the signaling pathways mediated by salicylic acid (SA), jasmonic acid (JA) and ethylene (ET) in the Arabidopsis innate immune response is well established (Glazebrook, 2005).

Hence, in this study, we investigate the underlying molecular mechanisms of plant resistance to *Foc*, when infect the dicot *Arabidopsis thaliana*. The report is pertaining to the pathogenicity of the various *Foc* strains and corresponding response of Arabidopsis mutants to *Foc*.

MATERIALS AND METHODS

Inoculation of *Fusarium oxysporium f.sp.cubense* and disease scoring

We maintained a frozen stock of each *Fusarium oxysporium f.sp.cubense* isolate in 50% glycerol at -80°C. *Fusarium* was thawed and grown on Czapek-Dox (CzD) plates (CzD broth with 1.5% Bacto agar, Becton Dickinson, Sparks, MD) at 22-28°C. Liquid cultures were inoculated from plates. The following are the *Foc* isolates:

FGSC # 8359
Genotype:*F.oxysporium f.sp.cubense*
Alleles : Australia
Stock Number : 01219
Ref : Phytopathology : 87:915-923

FGSC # 8361
Genotype:*F.oxysporium f.sp.cubense*
Alleles : Australia
Stock Number : 8611
Ref : Phytopathology : 87:915-923

FGSC # 8363
Genotype:*F.oxysporium f.sp.cubense*
Alleles : Malawi
Stock Number : MAL 11
Ref : Phytopathology : 87:915-923

FGSC # 8368
Genotype:*F.oxysporium f.sp.cubense*
Alleles : Taiwan
Stock Number : F9130
Ref : Phytopathology : 87:915-923

Arabidopsis lines, growth conditions

Seeds of Arabidopsis ecotypes, including Col1 and Salk insertion lines, eds5, npr1, jin1, C-24, nahg, ler were provided by Arabidopsis Biological Resource Center (ABRC, Ohio State University, Columbus, OH). Seeds were disinfected in 10% household bleach for 15 min and subsequently washed three times with excess sterile water. Plants were kept at 22°C in a greenhouse with supplemental fluorescent lighting to maintain a 12 h day length. Four plants for each mutant were maintained for *foc* infection.

Fusarium bud cells were cultured in 700 ml CzD broth in a 2 L Erlenmeyer flask by shaking at 250 rpm at 22-28°C for 5 days. To harvest bud cells, the culture was filtered with Steri-Pad gauze pads (Johnson and Johnson Medical, Arlington, TX), settled by centrifugation at 8000 rpm for 15 min, washed with water, and finally resuspended in water. The soft bud-cell pellet was washed by resuspending bud cells in water and settling by centrifugation three consecutive times. Bud-cell culture density was measured using a hemocytometer, and bud cells were diluted with sterile water. Unless stated otherwise, the inoculum density was 13106 bud cells ml^{-1}. For soil inoculation, 5 ml of bud-cell suspension was applied below the surface of the soil with a pipette. Infested plantings were incubated in a growth chamber (Percival Scientific, Perry, IA) with a 12 h day, under a light density of 120 mEm^{-2} sec^{-1} and at 26°C and 70% relative humidity. Czapek Dox (CzD) broth without bud cells

has been used as mock for inoculation.

Disease was evaluated using the disease index (DI). To measure stunting, we determined the distance from the stem to the distal end of the midrib (leaf length). The three longest leaves of each rosette were included in each measurement. Disease symptoms of *Fusarium* wilt DI score, a representative plant exhibits the symptoms of that score: 0, the plant is dead; 1, older leaves are dead and younger leaves are severely stunted; 2, older leaves are chlorotic, yellow, or dead and younger leaves are stunted; 3, older leaves have vascular chlorosis and the rosette appears compact because leaves are stunted; 4, leaf petioles are stunted; and 5, plants are indistinguishable from mock inoculated plants (Diener and Ausubel, 2005).

RESULTS

Symptoms of *Foc* on Arabidopsis have led to the identification of signaling pathways, as well as key regulators of innate immunity against this type of vascular wilt pathogens. The investigations have been initiated with isolates of *Foc* from the culture collections of FGSC # 8359 (Australian isolate), FGSC # 8361 (Australia), FGSC # 8363 (MALI), FGSC # 8368 (Taiwan) and their disease producing ability in Arabidopsis mutants and ecotypes, Col1 and Salk insertion lines, eds5, npr1, jin1, c-24, nahg, ler Arabidopsis Biological Resource Center (ABRC, Ohio State University, Columbus, OH). According to Diener and Ausubel (2005), the disease ratings was measured (0 = dead, 1 = severe stunting of young leaves and senescence of older leaves, 2 = chlorosis and premature senescence, 3 = more stunting and mild chlorosis in older leaves, 4 = rosette leaf stunting, 5 = unaffected).

The strains FOC#8359, FOC#8361 exhibited slow growth after 12 h with less branching and minimum number of spores. The mycelium is ceonocytic, septate with micro as well macro conidia. Whereas strains FOC#8363 and FOC#8368 was able to produce well grown ceonocytic, separate branched hyphae with micro and macro conidia. Excessive branching was noticed as typical growth patterns in the above said strains under *in vitro* conditions. The signal transduction network controlling Arabidopsis resistance to *Foc* has been explored by analyzing the pathogen susceptibility in different defective mutants *viz.,* ET (eds-5)-enhanced disease susceptibility 5, which is a salicylic acid induction deficient mutant and a negative regulator of defense response involved in ethylene biosynthesis, JA (jin-1)-jasmonate insensitive 1, which is response to wounding, ABA, chitin, JA signaling pathways, NahG-bacterial Salicylic Acid hydrolase gene suppressing Salicyic Acid (SA) accumulation in plants and npr1-Inactivation of PR-1 gene expression mutant.

Some of the Arabidopsis ecotypes ler and C-24 have also been tested for the resistance to *Foc.* Among the strains, FGSC#8359 (Australia) producing typical symptoms viz. petiole, stem necrosis, resetting of young leaves and chlorosis on all the mutants of Arabidopsis (Table 1). The symptoms indicate that *Foc* was shown to induce acquired resistance (SAR) and pathogenesis-related proteins (PRs) in Arabidopsis.

DISCUSSION

From the *in planta* symptom expressions of *Foc* on Arabidopsis, there is a clear indication of involvement of salicylic acid (SA) and Jasmonic acid (JA) for disease resistance (Figure 1). When the mutations occur in synthesis of salicylic acid and Jasmonic acid, it modulates disease resistance with the evident of severe veinal necrosis on leaves and petiole. The typical symptom of leaf rosetting was the clear indication of the active participation of salicylic acid biosynthesis for *Foc* resistance in nahG and npr-1 plants. Leaf resetting is a phenomenon by which pathogen-induced senescence allow cells to dedifferentiate and subsequently trans-differentiate to switch function (Grafi et al., 2011).This analysis revealed that salicylic acid (SA), ethylene (ET) and Jasmonic acid (JA) pathways influence the *Foc* disease outcome in Arabidopsis with respect to pathogen-induced structural modifications. All the three signaling pathways interact in a positive way in the activation of Arabidopsis resistance to *Foc*. Hence, there must be co-ordinate regulation of both SA and JA for *Foc* resistance in Arabidopsis.

Constitutive expressions of some transcriptional regulators of these pathways are sufficient to confer enhanced resistance to *Foc* and it might be an oligogenic trait (Marta Berrocal-Lobo and Antonio Molina, 2007). Moreover, the C-24 ecotype is having a single dominant locus (VET1); specific to root pathogen resistant mechanism located in xylem and may be identified for disease resistance QTL mapping against *Foc.* Typical aboveground symptoms of *Verticillium* infection on *Brassica napus* and *Arabidopsis thaliana* are stunted growth, vein clearing, and leaf chlorosis as observed by Michaele Reusche et al. (2012). Vein clearing is caused by pathogen-induced trans-differentiation of chloroplast, containing bundle sheath cells to functional xylem elements. Re-initiation of cambial activity and trans-differentiation of xylem parenchyma cells results in xylem hyperplasia within the vasculature of Arabidopsis leaves, hypocotyls and roots. Hyperplasia is generally defined as an induced increase in cell number and has been reported as a symptom of host plant infection by fungal plant pathogens (Malinowski et al., 2012). Salicylic acid-dependent and Jasmonic acid -ethylene dependent pathways induce the expression of different PR genes and also confer resistance to different pathogens (Lorenzo and Solano, 2005). Pieterse et al. (1998) identified a convergence point between different pathways in NPR1, which is required for both Salicylic Acid (SA)-dependent systemic acquired resistance (SAR) and jasmonic acid (JA)-Ethylene (ET) dependent induced systemic resistance (ISR).

Table 1. Variability in symptom expressions by Arabidopsis mutants and ecotypes against *FOC* strains under *in vitro* conditions.

Arabidopsis Mutants	Description	*FOC* (FGSC#8359)	*FOC* (FGSC#8361)	*FOC* (FGSC#8363)	*FOC* (FGSC#8368)
Col-1-	Wild type	Chlorosis and rosetting of younger leaves	Chlorosis	Chlorosis	Chlorosis
eds-5	Enhanced disease susceptibility-5,salicylic acid induction deficient mutant and a negative regulator of defense response involved in ethylene biosynthesis	Veinal necrosis, collapsed petiole and stem, chlorosis on older leaves	Mild chlorosis on leaves	Not producing any symptoms	Not producing any symptoms
Npr-1	Inactivation of PR-1 gene expression mutant	Severe veinal necrosis, complete necrotization of petiole and stem, blocks in nutrient flow	Mild chlorosis on leaves	Not producing any symptoms	Not producing any symptoms
Jin-1	JA- jasmonate insensitive 1, which is response to wounding, ABA, Chitin, JA signaling pathways	Veinal necrosis, mild rosette leaf stunting	Not producing any symptoms	Not producing any symptoms	Not producing any symptoms
Nah g	Bacterial SA hydrolase gene suppressing SA accumulation in plants	Rosette leaf stunting of young leaves, veinal necrosis, complete collapse of petiole and stem	Not producing any symptoms	Not producing any symptoms	Not producing any symptoms
C-24	Ecotype	Veinal necrosis, complete necrotization of petiole	Not producing any symptoms	Not producing any symptoms	Not producing any symptoms
Ler	Ecotype	Veinal necrosis, complete necrotization of petiole	Not producing any symptoms	Not producing any symptoms	Not producing any symptoms

From the disease ratings, we would like to conclude that the strain FGSC#8359 (Australia) might be able to produce typical symptoms of panama wilt with vascular browning and necrotization of tissues in Arabidopsis lines (Figure 2) and furthering research activities in potentiating the Salicylic Acid (SA) regulatory mechanisms for developing disease resistance strategies in banana cultivars (Edgar et al., 2006). Zhu et al. (2012) revealed from the time-course RNA-seq analysis results upon *F. oxysporum* infection, the biogenesis and signaling signaling pathways of ET, SA and JA were coordinately activated with the ET-mediated signaling pathway activated earlier than the JA and SA mediated signaling pathways. A number of genes responsive to *F. oxysporum* infection identified have been previously shown to be part of the defense network in various plant-pathogen interactions, for instance, genes involved in jasmonic acid (JA), indole-3-ylmethy-glucosinolate (I3G) and camalexin biosynthesis pathways (Bednarek et al., 2009; Clay et al., 2009; Kidd et al., 2011; Pfalz et al., 2009)

The symptoms produced by FOC strain FGSC#8359 have coincidences with the findings of Batlle and Pérez (2003) who found that Cuban *Foc* isolates of race 1 and 2 indistinctly can or not produce volatiles aldehyde in direct relationship with pathogenesity (Moore et al., 1991). From these findings, we wish to conclude that the defense response of Arabidopsis lines against *Foc* strains is under the control of minor resistance genes, rather than a single dominant “R” gene (Hwang and Ko, 2004). Different climatic zones can determine the disease development and can classify the strains into “Tropical” and “Subtropical” strains (Ploetz et al., 1990).

Conflict of Interest

The author(s) have not declared any conflict of interest.

ACKNOWLEDGEMENTS

The author is thankful to the Department of Science and Technology, GOI, New Delhi for funding through BOYSCAST programme and Donald Danforth Plant Science Center, MO, USA-63132 for providing laboratory facilities and technical guidance to perform research programme.

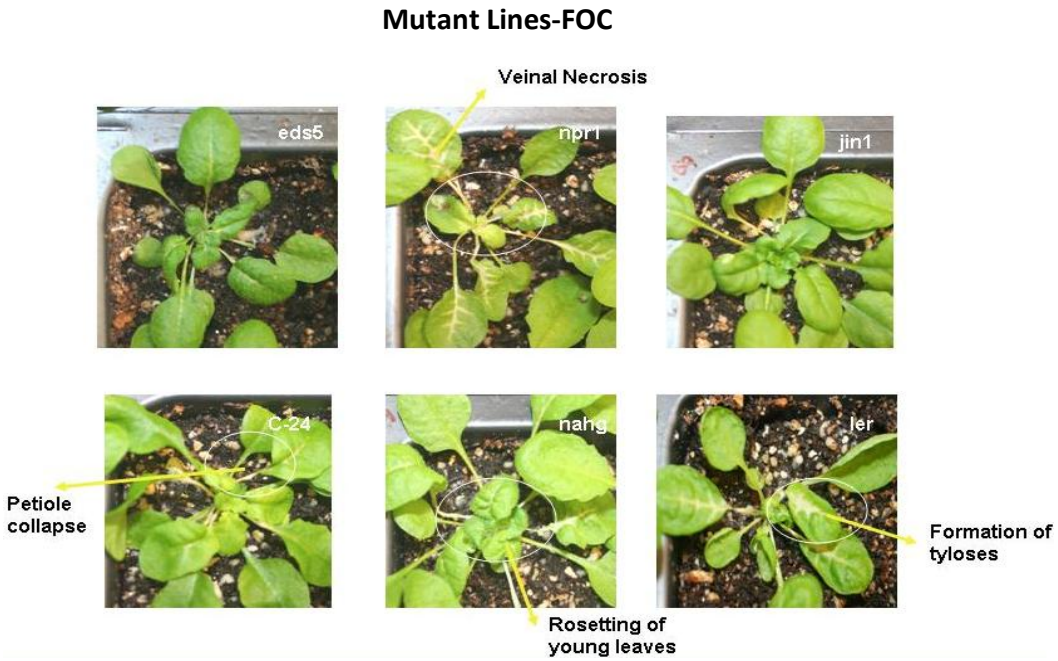

Figure 1. Arabidopsis lines expressing symptoms in response to *F. oxysporum f.sp.cubense* (*Foc*) strain FGSC#8359. Top: Left to right: eds5, npr1, jin1; Bottom: Left to right: C 24, nahg, ler.

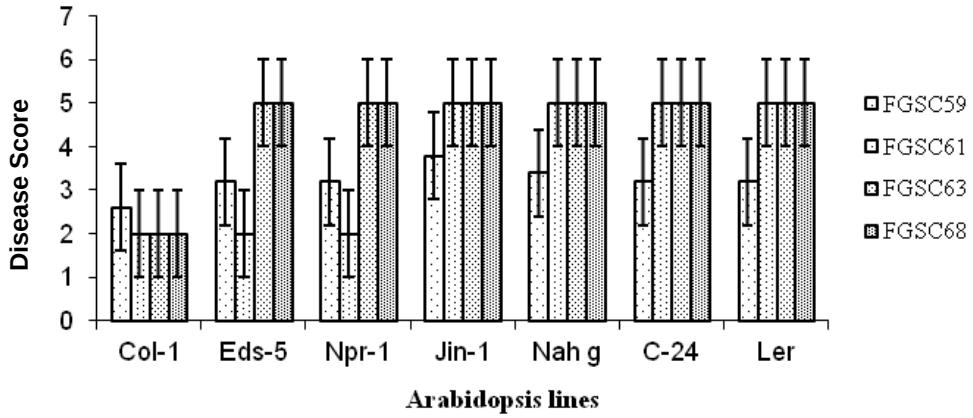

Figure 2. Measurement of Disease Index (DI) in Arabidopsis lines in response to *F.oxysporum f.sp.cubense* (*Foc*).

REFERENCES

Batlle A, Pérez L (2003). Population Biology of *Fusarium oxysporum f.sp. cubense* in Cuba. In: 2nd. International Symposium on *Fusarium* wilt on banana. PROMUSA-INIBAP/EMBRAPA. Salvador de Bahía, Brazil. pp. 22-26 .

Bednarek P et al (2009). A glucosinolate metabolism pathway in living plant cells mediates broad-spectrum antifungal defense. Science. 323:101-106.

Clay NK, Adio AM, Denoux C, Jander G, Ausubel FM (2009). Glucosinolate metabolites required for an Arabidopsis innate immune response. Science 323:95-101.

Davis RI, Moore NY, Bently S, Gunua TG, Rahamma S (2000). Further records of *Fusarium oxysporum f.sp. cubense* from New Guinea. Australas. Plant Pathol. 29:224.

Diener AC, Ausubel FM (2005). Resistance to *Fusarium oxysporum* 1, a dominant Arabidopsis resistance gene, is not race specific. Genetics.171:305-321.

Edgar CI et al (2006). Salicylic acid mediates resistance to the vascular wilt pathogen *Fusarium oxysporum* in the model host *Arabidopsis thaliana*. Australas. Plant Pathol. 35:581-591.

Glazebrook J (2005). Contrasting mechanisms of defense against biotrophic and necrotrophic pathogens. Annu. Rev. Phytopathol. 43:205-227.

Grafi G, Chalifa-Caspi V, Nagar T, Plaschkes I, Barak S, Ransbotyn V (2011). Plant response to stress meets dedifferentiation. Planta. 233:433-438.

Hwang S, Ko W (2004). Cavendish banana cultivars resistant to *Fusarium* wilt acquired through somaclonal variation in Taiwan. Plant Dis. 88:580-588.

Kidd BN et al (2011). Auxin signaling and transport promote susceptibility to the root-infecting fungal pathogen Fusarium oxysporum in Arabidopsis. Mol. Plant Microbe Interact. 24:733-748.

Lorenzo O, Solano R (2005). Molecular players regulating the jasmonate signaling network. Current Opinion in Plant Pathol. 8:532-540.

Malinowski R, Smith JA, Fleming AJ, Scholes JD, Rolfe SA (2012). Gall formation in clubroot-infected Arabidopsis results from an increase in existing meristematic activities of the host but is not essential for the completion of the pathogen life cycle. Plant J. 71:226-238.

Marta B-L, Antonio M (2007). Arabidopsis defense response against *Fusarium oxysporum*. Trends Plant Sci. 13(3):145-150

Masdek N, Mahmood M, Molina A, Hwang SC, Dimyati A, Tangaveli R, Omar I (2003). Global significance of *Fusarium* wilt: Asia. Abstracts of Papers 2nd. International Symposium on *Fusarium* wilt on banana. PROMUSA-INIBAP/EMBRAPA. Salvador de Bahía, Brazil. pp. 22-26.

Moore NY, Hargreaves PA, Pegg K, Irwin JAG (1991). Characterization of strains of *Fusarium oxysporum f. sp. cubense* by production of volatiles, Aust. J. Bot. 39:161-166.

Nasdir N (2003). *Fusarium* wilt race 4 in Indonesia. Research Institute for Fruits west Sumatra, Indonesia. Abstracts of Papers 2nd. International Symposium on *Fusarium* wilt on banana. PROMUSA-INIBAP/EMBRAPA.Salvador de Bahía, Brazil. pp. 22-26.

Pfalz M, Vogel H, Kroymann J (2009). The gene controlling the indole glucosinolate modifier1 quantitative trait locus alters indole glucosinolate structures and aphid resistance in Arabidopsis. Plant Cell. 21:985-999.

Pieterse CM, Van Wees SC, VanPelt JA, Knoester M, Laan R, Gerrits H, Weisbee PJ, Van Loon LC (1998). A novel signaling pathway controlling induced systemic resistance in Arabidopsis. Plant Cell 10:1571-1580.

Ploetz RC (1990). Population biology of *Fusarium oxysporum f. sp. cubense*. In: Fusarium wilt of banana. Ploetz, R.C. (Ed.) APS Press St Paul. pp. 63-76.

Ploetz RC, Pegg K (2000). *Fusarium* wilt. In: Diseases of Banana, Abaca and Enset. Jones, D.R. (Ed), CABI Publishing, Wallingford, UK. 143-159.

Podovan A, Henessey C, Walduck G (2003). Alternative hosts of *Fusarium oxysporum f.sp. cubense* tropical race 4 in northern Australia. In: 2nd. International Symposium on *Fusarium* wilt on banana. PROMUSAINIBAP/EMBRAPA. Salvador de Bahía, Brazil, pp. 22-26.

Smith LJ, Moore NY, Tree DJ, Bently S, Pattemore J (2002). Firs record of *Fusarium oxysporum f.sp cubense* from Yap, Federated States o Micronesia, Australas. Plan Pathol. pp. 31:101

Su HJ, Hwang SC, Ko WH (1986). Fusarial wilt of bananas in Taiwan. Plant Dis. 70:813-818.

Waite BH, Dunlap VC (1953). Preliminary host range studies with *Fusarium oxysporum f. cubense*. Plant. Dis. Rptr. 37:79-80.

Zhu QH et al (2012). Characterization of the defense transcriptome responsive to *Fusarium oxysporum*-infection in Arabidopsis using RNA-seq, Gene, http://dx.doi.org/10.1016/j.gene.2012.10.036.

academicJournals

Vol. 13(30), pp. 3036-3051, 23 July, 2014
DOI: 10.5897/AJB12.264
Article Number: F3A12BF46219
ISSN 1684-5315

http://www.academicjournals.org/AJB

African Journal of Biotechnology

Full Length Research Paper

Crop growth rate differs in warm season C_4-grasses grown in pure and mixed stands

Amanullah Khan

Department of Agronomy, Faculty of Crop Production Sciences, The University of Agriculture Peshawar-Pakistan-25130.

Received 14 January, 2012; Accepted 16 May, 2014

Crop growth rate (CGR) response of three warm season C_4-grasses (cereals) namely: corn (*Zea mays* L., cv. Hybrid-5393 VT3), grain sorghum (*Sorghum bicolor* L. Moench, cv. Hybrid-84G62 PAT), and foxtail millets (*Setaria italica*, cv. German Strain R) grown in pure and mixed stands under low and high water levels was investigated at one month interval namely: 30, 60 and 90 days after emergence (DAE), in pot experiment at Dryland Agriculture Institute, West Texas A&M University, Canyon, Texas, USA during spring 2010. The corn CGR in the mixed stands was 22, 11 and 9% higher than in pure stand at 30, 60 and 90 days after emergence (DAE), respectively. The corn plants in pure stand had 91, 66 and 84% higher CGR than the average CGR of both sorghum and millets at 30, 60 and 90 DAE, respectively. Grain sorghum in pure stand had 72, 30 and 40% higher CGR than that of millets in pure stand at 30, 60 and 90 DAE, respectively. The CGR of the three crops in mixed stand was 10 and 12% higher than the average of two crops mixed stand at the two early stages; but the CGR was reduced by 42% in the three crops mixed stand than the average of two crops mixed stand at 90 DAE. Corn mixed stand in two crops (average of corn + sorghum and corn + millets) had 78, 75 and 74% higher CGR than the mixed stand of sorghum and millets at 30, 60 and 90 DAE, respectively. Corn and millets mixed stand had 16, 9 and 38% higher CGR than the corn and sorghum mixed stand at 30, 60 and 90 DAE, respectively. Corn had higher CGR under high water at 30 DAE. There was no difference in the CGR of sorghum under low and high water levels at different growth stages. Millets had higher CGR under high water level at 30 DAE, but had lower CGR under high water level at 90 DAE. Among the three crops, corn plants had the higher CGR due to the highest total dry matter accumulation in both shoots and roots and was considered the best competitor in all the mixed stands. Grain sorghum ranked second, while foxtail millets ranked in the bottom in terms of competitiveness in the mixed stands.

Key words: *Zea mays*, *Sorghum bicolor*, *Setaria italica*, competition, water levels, crop growth rate.

INTRODUCTION

Crop growth rate [the total dry matter accumulation (shoot plus root dry weights) per unit ground area per unit time]

E-mail: amanullah@aup.edu.pk.

is used to measure the primary productivity of crop plants (Youshida, 1981). Crop growth rate can be affected by competition among crop plants, because the crops are the members of community and each individual interact with its neighbors (Sadras and Calderini, 2009); and that the competition may have an impact on both above- and below-ground total biomass (Rubio et al., 2001). Crop growth requires a limited number of resources, which are light, nutrients and water. Several studies have shown that below-ground competition for water and nutrients can be stronger and can involve more neighbors than above-ground competition for light (Casper and Jackson, 1997). The degree of competition below and above the ground may vary among different species. Dubbs (1971) reported that Russian wild rye (*Elymus junceus* Fisch.) was the most competitive species in terms of total dry matter accumulation and sainfoin (*Onobrychis viciaefolia* Scop.) the least. Wild rye yielded more when competing with legumes than with each other's (intra-specific competition). Competition between alfalfa plants was more intense than between other species. In another study, Hannay et al. (1977) found that total yield of the legume component in mixed stand was consistently higher for the alfalfa-grass association than for the sainfoin-grass. Competition for nutrients among neighbouring roots occurs when their individual nutrient depleted volumes overlap, causing a reduction in nutrient uptake.

Plants with contrasting root architecture (root length and numbers) may reduce the extent of competition among neighbouring root systems. Competition among roots of the same plant was three- to five-times greater than competition among roots of neighbouring plants (Rubio et al., 2001). The yield of medic (*Medicago trunculata*) in both pure and mixed stand increased with the increase of P rate up to 160 ppm P and then decreased with further increase in P levels; but ryegrass plants benefited individually from growing in mixed stand with legume, producing as much shoot dry matter from three plants in mixture as from six in monoculture (Dahmane and Graham, 1981). It is generally believed that crop plants do not compete for space (Aldrich, 1984). This issue was recently investigated by Wilson (2007) and suggested that competition for space may occur, but the effect is so small it can be ignored within plants communities. Whenever two plants grow near each other, they will interact by altering the environment in which they grow, which will influence their acquisition of resources (light, water and nutrients) and their growth rate (Sadras and Calderini, 2009). Plants can sense the presence of neighbors through changes in the ratio of red: far light even before the onset of competition for water and nutrients. There is some evidence that roots can respond to the presence of neighbouring roots and can distinguish roots from the same plant of neighbouring plants (Sadras and Calderini, 2009). There is lack of research on competition among warm season grasses in pure and mixed stand under different water regimes. The objective of this experiment was to investigate the differences in crop growth rate of warm season grasses (maize, sorghum and millets) in pure and mixed stands in various combinations under low and high water levels.

MATERIALS AND METHODS

Experimental site

Crop growth rate [the total dry matter accumulation (shoot plus root dry weights) per unit ground area per unit time] response (g m^{-2} day^{-1}) of three warm season grasses (cereals) namely corn (*Zea mays* L., cv. Hybrid-5393 VT3), grain sorghum (*Sorghum bicolor* L. Moench, cv. Hybrid-84G62 PAT), and foxtail millets (*Setaria italica*, cv. German Strain R) was investigated in pure and mixed stands under low water level (50 % less water was applied that required for the high water level) and high water level (maintained at field capacity, water was applied whenever reached to field capacity) in pot experiment at Dryland Agriculture Institute, West Texas A&M University, Canyon, Texas, USA during spring 2010. The potting soil known as *Miracle Grow* was used in the pots. Miracle Grow is formulated from 50-60% sphagnum peat moss, coconut husk fibers (coir pith), composted bark fines, pertile, wetting agent, and fertilizer. The nitrogen, phosphorus and potassium sources have been coated to provide 0.10% slow-release nitrogen (N), 0.10% slow-release phosphate (P_2O_5), and 0.10% potash (K_2O). The ACGIH threshold Limit Values (TLV) for nuisance (inert) dust containing less than 1% crystalline silica and no abestas are: 10 mg/m^3 inhalable particulates and 3 mg m^{-3} respirable particulate.

Experimental design

The experiment was performed in completely randomized design with three replicates. There were seven grasses combinations [T_1 = corn in pure stand; 18 corn plants per pot, T_2 = grain sorghum in pure stand; 18 grain sorghum plants per pot, T_3 = foxtail millets in pure stand; 18 millets plants per pot, T_4 = corn and sorghum mixed stand; 9 plants each of corn and sorghum per pot, T_5 = corn and millets mixed stand; 9 plants each of corn and millets per pot, T_6 = sorghum and millets mixed stand; 9 plants each of sorghum and millets per pot, and T_7 = corn, sorghum, and millets mixed stand; 6 plants each of corn, sorghum and millet per pot] and two water levels [(high (the pots maintained at field capacity) and low (used 50% less water than applied for the high water level)]. Nitrogen (urea) at the rate of 100 ppm was applied to each pot in two equal applications that is 50 ppm each at 7 and 60 DAE.

Data recording and handling

A total of six plants were uprooted at 30, 60 and 90 DAE from each treatment (pot). In case of T_1, T_2 and T_3, six plants of the same crop were uprooted, while in the case of T_4, T_5 and T_6, three plants of each crop were uprooted. But in the case of T_7, two plants of each species were uprooted. The roots of each crop were washed with tap water, and the plants were then divided into three parts that is roots, leaves and stems. The materials was put in paper bags and then put in an oven at 80°C for about 20-24 h. The samples were weighed by electronic scale (*Sartorius Basic, BA2105*) and the average data on dry weight of root, leaf, and stem per plant was

Table 1. Analysis of variance for crop growth rate of summer cereals grown alone in pure and mixed stands under low and high water levels at 30, 60 and 90 days after emergence.

Source of variance	Degree of freedom	Level of Significance		
		30 DAE	60 DAE	90 DAE
Replications	[2]	ns	ns	ns
Treatments	[13]	***	**	***
Water levels	{1}	***	ns	ns
Crops combinations	{6}	***	**	***
Corn versus sorghum +millets	(1)	***	***	***
Sorghum versus millets	(1)	***	ns	ns
2 crops versus 3 crops	(1)	***	ns	*
Corn in 2 crops versus number corn in 2 crops	(1)	***	**	***
Corn + sorghum versus corn + millets	(1)	***	ns	*
Water levels x crops combination	{6}	***	ns	ns
Error	[26]			
Total	[41]			

*Significant at 5%, **significant at 1%, and ***significant at 0.1% level of probability, and ns means non significant.

Table 2. Crop growth rate means and significance of differences for the pre-planned comparisons at first cut (30 DAE).

Comparison	Mean 1	Mean 2	Difference	Significance
Sole corn versus corn in combination	1.782	2.295	0.514	***
Corn versus Sorghum + millets	4.566	0.390	-4.176	***
Sorghum versus millets	0.610	0.169	-0.441	***
2 Crops versus 3 crops	2.230	2.492	0.262	***
Corn in 2 crops versus number corn in 2 crops	3.017	0.655	-2.362	***
Corn + sorghum versus corn + millets	2.749	3.286	0.537	***

*Significant at 5%, **significant at 1%, and *** significant at 0.1% level of probability, and ns means non significant.

calculated. Shoot dry weight per plant was obtained by adding up leaf dry weight to stem dry weight per plant. The sum of the shoot and root dry weight was calculated as the total dry weight per plant, and then crop growth rate (CGR) at each growth stage was calculated on the basis of total dry weight (shoot + root) using the following formula:

$$CGR = W_2 - W_1 / (GA) (t_2 - t_1)$$

Where, W_1 = dry weight per plant at the beginning of interval (gram), W_2 = dry weight per plant at the end of interval (gram), $t_2 - t_1$ = the time interval between the two consecutive samplings (days), GA = ground area occupied by plants at each sampling (m^2), and CGR is in g m^{-2} day^{-1}.

Statistical analysis

Data on CGR at each sampling period were subjected (maybe another word) to analysis of variance (ANOVA) according to the methods described in Steel and Torrie (1980) and treatment means were compared using the least significant difference (LSD) at $P \leq 0.05$. The complete ANOVA is presented in Table 1. Mean comparisons of various treatments at 30, 60 and 90 DAE is given in Tables 2, 3 and 4, respectively.

RESULTS

Corn

Crop growth rate (CGR) of corn was higher with high (5.9 g m^{-2} day^{-1}) than with low water level (5.0 g m^{-2} day^{-1}) at 30 DAE (Table 5). The CGR reached to maximum (6.4 g m^{-2} day^{-1}) each when corn was grown together in mixed stand with millets or with both sorghum + millets, and the higher increase was noticed at high than at low water level. The CGR declined to 4.5 g m^{-2} day^{-1} when corn was grown mixed with sorghum, followed by 4.6 g m^{-2} day^{-1} when corn was grown alone in pure stand. At second cut (60 DAE), corn produced higher CGR at low (38.1 g m^{-2} day^{-1}) than at high water level (29.4 g m^{-2} day^{-1}). The CGR ranked first (43.8 g m^{-2} day^{-1}) when corn was grown mixed with both sorghum + millets, and the higher increase was noticed at high (44.8 g m^{-2} day^{-1}) than at low water level (42.8 g m^{-2} day^{-1}). The CGR reduced to minimum (22.1 g m^{-2} day^{-1}) when corn was grown alone in pure stand, and the higher reduction was observed at

Table 3. Crop growth rate means and significance of differences for the pre-planned comparisons at second cut (60 DAE).

Comparison	Mean 1	Mean 2	Difference	Significance
Sole Corn vs. Corn in combination	12.238	13.807	1.568	ns
Corn versus sorghum + millets	22.106	7.305	-14.801	***
Sorghum versus millets	8.580	6.029	-2.551	ns
2 crops versus 3 crops	13.342	15.201	1.859	ns
Corn in 2 crops versus number corn in 2 crops	17.785	4.455	-13.331	**
Corn + sorghum versus corn + millets	16.909	18.662	1.753	ns

*Significant at 5%, **significant at 1%, and ***significant at 0.1% level of probability, and ns means non significant.

Table 4. Crop growth rate means and significance of differences for the pre-planned comparisons at third cut (90 DAE).

Comparison	Mean 1	Mean 2	Difference	Significance
Sole Corn versus corn in combination	44.9	40.8	-4.1	ns
Corn versus sorghum + millets	101.9	16.5	-85.4	***
Sorghum versus millets	21.1	11.8	-9.2	ns
2 crops versus 3 crops	45.7	26.3	-19.3	*
Corn in 2 crops versus number corn in 2 crops	60.6	15.9	-44.7	***
Corn + sorghum versus corn + millets	46.4	74.8	28.4	*

*Significant at 5%, ** significant at 1%, and *** significant at 0.1% level of probability, and ns means non significant.

Table 5. Crop growth rate (g m^{-2} day^{-1}) response of corn when grown alone in pure and mixed stands with sorghum and millets under low and high water levels.

Crops combination	30 days after emergence			60 days after emergence			90 days after emergence		
	HWL	LWL	Mean	HWL	LWL	Mean	HWL	LWL	Mean
Corn (C) alone	4.7	4.5	4.6	14.8	29.4	22.1	86.0	117.8	101.9
Corn in sorghum (S)	4.7	4.2	4.5	27.4	37.6	32.5	65.1	114.2	89.6
Corn in millets (M)	7.3	5.4	6.4	30.6	42.7	36.6	177.0	115.8	146.4
Corn in S + M	6.8	6.0	6.4	44.8	42.8	43.8	38.2	117.0	77.6
Mean	5.9	5.0	5.4	29.4	38.1	33.8	91.6	116.2	103.9
$LSD_{0.05}$									
Water Levels	0.1			ns			ns		
Crops combination	0.3			ns			48.3		
Interaction	0.4			ns			68.3		

HWL stands for high water level (maintained at field capacity) and LWL stands for low water level (maintained at 50% less water than at HWL).

high (14.8 g m^{-2} day^{-1}) than at low water level (29.4 g m^{-2} day^{-1}). At third cut (90 DAE), corn had high CGR (116.2 g m^{-2} day^{-1}) at low than at high water level (91.6 g m^{-2} day^{-1}). The CGR reached maximum (146.4 g $plant^{-1}$ day^{-1}) when corn was grown mixed with millets, and the higher increase was noticed at high (177.0 g m^{-2} day^{-1}) than at low water level (115.8 g m^{-2} day^{-1}). The CGR was reduced significantly (77.6 g m^{-2} day^{-1}) when corn was grown in mixed stand with both sorghum + millets, and the higher reduction was observed at high (38.2 g m^{-2} day^{-1}) than at low water level (117.0 g m^{-2} day^{-1}).

Grain sorghum

There was no interaction in the CGR of sorghum under high and low water levels at 30 DAE (Table 6). The CGR reached to maximum (1.1 g m^{-2} day^{-1}) when sorghum was grown along with millets, followed by 1.0 g m^{-2} day^{-1} when sorghum was grown together with corn. The CGR of

Table 6. Crop growth rate (g m^{-2} day^{-1}) response of grain sorghum when grown alone in pure and mixed stands with corn and millets under low and high water levels.

Crops combination	30 days after emergence			60 days after emergence			90 days after emergence		
	HWL	LWL	Mean	HWL	LWL	Mean	HWL	LWL	Mean
Sorghum (S) alone	0.7	0.5	0.6	8.77	8.39	8.58	20.2	21.9	21.1
Sorghum in Corn (C)	1.0	1.1	1.0	0.75	1.92	1.34	1.2	5.0	3.1
Sorghum in Millets (S)	1.3	0.8	1.1	2.19	10.75	6.47	25.1	27.8	26.5
Sorghum in C + M	0.8	1.1	0.9	2.07	1.18	1.63	0.1	1.3	0.7
Mean	0.9	0.9	0.9	3.45	5.56	4.50	11.7	14.0	12.8
$LSD_{0.05}$									
Water Levels	ns			ns			ns		
Crops Combination	0.09			3.45			11.6		
Interaction	0.13			4.88			16.4		

HWL stands for high water level (maintained at field capacity) and LWL stands for low water level (maintained at 50% less water than at HWL).

Table 7. Crop growth rate (g m^{-2} day^{-1}) response of millets when grown alone in pure and mixed stands with corn and sorghum under low and high water levels.

Crops combination	30 days after emergence			60 days after emergence			90 days after emergence		
	HWL	LWL	Mean	HWL	LWL	Mean	HWL	LWL	Mean
Millets (M) alone	0.18	0.16	0.17	6.28	5.78	6.03	5.8	17.9	11.8
Millets in Corn (C)	0.19	0.23	0.21	0.46	0.90	0.68	1.9	4.4	3.1
Millets in Sorghum (S)	0.28	0.22	0.25	3.34	1.53	2.44	3.8	6.7	5.2
Millets in C + S	0.18	0.14	0.16	0.26	0.27	0.27	0.6	0.8	0.7
Mean	0.21	0.19	0.20	2.59	2.12	2.35	3.0	7.5	5.2
$LSD_{0.05}$									
Water Levels	0.01			ns			1.0		
Crops Combination	0.02			0.97			2.7		
Interaction	0.02			1.38			3.9		

HWL stands for high water level (maintained at field capacity) and LWL stands for low water level (maintained at 50% less water than at HWL).

sorghum declined to minimum (0.6 g m^{-2} day^{-1}) when sorghum was grown alone in pure stand. At second cut (60 DAE), sorghum produced higher CGR (5.56 g m^{-2} day^{-1}) at low than at high water level (3.45 g m^{-2} day^{-1}). The CGR ranked first (8.58 g m^{-2} day^{-1}) when sorghum was grown alone in pure stand, followed by sorghum + millets mixed stand (6.47 g m^{-2} day^{-1}). The CGR reduced significantly (1.34 g m^{-2} day^{-1}) when sorghum was grown mixed with corn, and the higher reduction was observed at high (0.75 g m^{-2} day^{-1}) than at low water level (1.92 g m^{-2} day^{-1}). At third cut (90 DAE), sorghum had high CGR (14.0 g m^{-2} day^{-1}) at low than high water level (11.7 g m^{-2} day^{-1}). The CGR reached maximum (26.5 g $plant^{-1}$ day^{-1}) when sorghum was grown mixed with millets, and the higher increase was noticed at low (27.8 g m^{-2} day^{-1}) than at high water level (25.1 g m^{-2} day^{-1}). The CGR reduced significantly to 0.7 g m^{-2} day^{-1} when sorghum was grown with both corn + millets mixed stand, and the higher reduction was observed at high (0.1 g m^{-2} day^{-1}) than at low water level (1.3 g m^{-2} day^{-1}).

Foxtail millets

Crop growth rate of millets was relatively higher (0.21 g m^{-2} day^{-1}) under high than low water level (0.19 g m^{-2} day^{-1}) at 30 DAE (Table 7). The CGR reached maximum to 0.25 g m^{-2} day^{-1} when millets was grown together with sorghum, followed by 0.21 g m^{-2} day^{-1} when millets was grown together with corn. The CGR declined to 0.16 g m^{-}

Table 8. Average crop growth rate (g m^{-2} day^{-1}) response of summer cereals when grown alone in pure and mixed stands under low and high water levels.

Crops combination	30 days after emergence			60 days after emergence			90 days after emergence		
	HWL	LWL	Mean	HWL	LWL	Mean	HWL	LWL	Mean
Corn (C) alone	4.65	4.47	4.56	14.83	29.38	22.10	86.0	117.8	101.9
Sorghum (S) alone	0.69	0.52	0.61	8.76	8.39	8.58	20.2	21.9	21.1
Millets (M) alone	0.18	0.15	0.16	6.28	5.77	6.02	5.8	17.9	11.8
Average of C + S	2.83	2.66	2.74	14.08	19.73	16.90	33.1	59.6	46.4
Average of C + M	3.73	2.83	3.28	15.54	21.77	18.66	89.5	60.1	74.8
Average of S + M	0.78	0.52	0.65	2.76	6.14	4.45	14.5	17.2	15.9
Average of C + S + M	2.59	2.38	2.49	15.72	14.67	15.20	13.0	39.7	26.3
Mean	2.21	1.93	2.07	11.14	15.125	13.13	37.4	47.7	42.6
$LSD_{0.05}$									
Water levels	0.07			ns			ns		
Crops combination	0.13			8.69			22.0		
Interaction	0.18			12.30			31.2		

HWL stands for high water level (maintained at field capacity) and LWL stands for low water level (maintained at 50% less water than at HWL).

^{2} day^{-1} when millets was grown mixed with both corn and sorghum mixed stand (corn + sorghum + millets). At second cut (60 DAE), millets had higher CGR at high (2.59 g m^{-2} day^{-1}) than at low water level (2.12 g m^{-2} day^{-1}). The CGR ranked first (6.03 g m^{-2} day^{-1}) when millets was grown alone in pure stand, and the higher increase was noticed at high (6.28 g m^{-2} day^{-1}) than at low water level (5.78 g m^{-2} day^{-1}). The CGR reduced significantly (0.27 g m^{-2} day^{-1}) when millets was grown mixed with corn + sorghum, and there was no difference in CGR at high (0.26 g m^{-2} day^{-1}) and low water level (0.27 g m^{-2} day^{-1}). At third cut (90 DAE), millets had high CGR (7.5 g m^{-2} day^{-1}) at low than high water level (3.0 g m^{-2} day^{-1}). The CGR reached maximum (11.8 g $plant^{-1}$ day^{-1}) when millets was grown alone in pure stand, and the higher increase was noticed at low (17.9 g m^{-2} day^{-1}) than at high water level (5.8 g m^{-2} day^{-1}). The CGR reduced significantly to 0.7 g m^{-2} day^{-1} when millets was grown mixed with corn, and the higher reduction was observed at high (0.6 g m^{-2} day^{-1}) than at low water level (0.8 g m^{-2} day^{-1}).

Crops average

The average CGR of the three summer grasses was higher (2.21 g m^{-2} day^{-1}) at high than low water level (1.93 g m^{-2} day^{-1}) at 30 DAE (Table 8). The CGR ranked first (4.56 g m^{-2} day^{-1}) when corn was grown alone in pure stand, followed by the average of corn + millets mixed stand (3.28 g m^{-2} day^{-1}). The CGR reduced to minimum (0.16 g m^{-2} day^{-1}), when millets was grown alone in pure stand. At second cut (60 DAE), there were no significant difference in the CGR at low and high water levels. However, the CGR was higher (15.12 g m^{-2} day^{-1}) at low than high water level (11.14 g m^{-2} day^{-1}). The CGR reached to maximum (22.10 g m^{-2} day^{-1}) when corn was grown alone in pure stand, followed by the average of corn + millets mixed stand (18.66 g m^{-2} day^{-1}); while CGR reduced to minimum (4.45 g m^{-2} day^{-1}) when sorghum + millets mixed stand was averaged, being at par with each sorghum and millets in the pure stands. At third cut (90 DAE); there were no significant difference in the CGR at low and high water levels. However, the average CGR was higher (47.7 g m^{-2} day^{-1}) at high than low water level (37.4 g m^{-2} day^{-1}). The CGR reached to maximum (101.9 g m^{-2} day^{-1}) when corn was grown alone in pure stand, followed by the average of corn + millets mixed stand (74.8 g m^{-2} day^{-1}). The CGR reduced to minimum (11.8 g m^{-2} day^{-1}), when millets was grown alone in pure stand.

DISCUSSION

Corn

The higher CGR of corn at high than at low water level at early stage was explained by the delay in emergence of corn at low than at high water level. The increase in corn CGR was due to its taller plants, higher leaf area and highest shoot and root dry weights in mixed stand with millets (corn + millets) or both sorghum and millets mixed stand (corn + sorghum + millets) because of the very well developed canopy and root architecture of corn at the early growth stage (Figures 1 and 2) had negative impacts on the growth and total dry matter accumulation

Figure 1. Corn (Left), grain sorghum (middle) and foxtail millets (right) shoot and root lengths 30 days after emergence.

of millets and sorghum adversely reduced the CGR of sorghum and millets in the mixed stand with corn. According to Bazzaz (1998), plants parts in space and their mode of display (plant architecture) are very important in plant-plant interactions. The intra plants completion among corn plants was observed when corn was grown alone in pure stand that reduced both shoots and roots dry weights and so the CGR of corn declined in pure stand. This indicates that corn plants in pure stand were quite competitive among themselves. Dubbs (1971) reported that alfalfa plants received more competition from other alfalfa plants than from plants of other species. The lower CGR of corn plants was noticed when corn was grown mixed with sorghum (corn + sorghum) indicating that the sorghum plants competed very well against corn that reduced the shoots and roots dry weights (Amanullah and Stewart, 2013) and CGR of corn plants (Figures 1 and 3). As compared to millets, that do not have negative impacts on the corn CGR, sorghum on the other hand with well developed canopy had more adverse effects on corn plants (Figures 1 and 4). According to Sorrenson et al. (1993), measurement of canopy architecture is very important in crop-crop competition. The lower CGR of corn plants at high than at low water level at 60 DAE was due to the negative effects of high water level on plant heights, root length, leaf area, shoots and roots dry weights of corn plants (Amanullah and Stewart, 2013). The increase in the CGR of corn

Figure 2. Corn root system (very strong) 30 days after emergence.

plants when it was grown in mixed stand with both sorghum and millets (corn + sorghum + millets) was probably due to the reduction in the growth and total dry weights of millets and sorghum and also there was no strong intra plants competition among the corn plants in the mixed stand.

The strong intra plants completion among the corn plants in the pure stand reduced the shoots and roots dry weights that resulted in the lower corn CGR. According to Rubio et al. (2001), competition among roots of the same plant was three- to five-times greater than competition among roots of neighboring plants. Dubbs (1971) reported that alfalfa plants received more competition from other alfalfa plants than from plants of other species. The lower CGR of corn plants at high than at low water level at 90 DAE was due to the negative effects of high water level on plant heights, root length, leaf area, shoot, root and total plant dry weights of corn (data not shown). Rubio et al. (2001) reported that competition among plants occurs for both above- and below-ground. The above-ground competition involves one principal resource (light); below-ground competition encompasses a broader spectrum of resources, including water and all the essential mineral nutrients. Root architecture of corn

Figure 3. Grain sorghum root system (strong) 30 days after emergence.

plants in the mixed stand was better established than that of sorghum and millets, and therefore, corn plants probably may have took more nutrients and water than the two crops. According to Casper and Jackson (1997) the below-ground competition for water and nutrients can be stronger and can involve more neighbors than above-ground competition.

The increase in the CGR of corn plants when grown mixed with millets (corn + millets) was due to the reduction in the growth of millets (Figure 8) and also the reduction in intra plants competition among the corn plants. On the other hand, mixing sorghum with corn (corn + sorghum or corn + sorghum + millets) had negative impacts on the root length and root dry weight of corn plants that resulted in the lower corn CGR (Figure 7).

Rubio et al. (2001) reported that plants with contrasting root architecture may reduce the extent of competition among neighboring root systems.

Grain sorghum

When sorghum was grown mixed with other crops, its plant heights, stem and leaf dry weights increased that resulted in the higher CGR of sorghum at 30 DAE. At the early growth stage, sorghum reduced its plant heights; leaf area and shoot dry weight that declined its CGR in the pure stand because of delay in emergence as compared to the early emergence in mixed stand. According to Sadras and Calderini (2009), there has been emerging evidence of the importance of early crop

Figure 4. Foxtail millets root system (weak) 30 days after emergence.

vigor for competitive ability of crop plants. Likewise corn plants, the lower CGR of sorghum at high than at low water level was attributed to the negative effects of high water level on plant height, root length, leaf area, shoot and root dry weights of sorghum (Amanullah and Stewart, 2013) at 60 DAE. According to Sadras and Calderini (2009), plant height tend to be the most common shoot trait implicated in competitive ability of different crops. The increase in the CGR of sorghum when it was grown alone in pure or mixed stand with millets (sorghum + millets) was due to the increase in shoot and root dry weights of sorghum (Figures 3 and 4). But including corn in the mixtures with sorghum (corn + sorghum or corn + sorghum + millets) had negative impacts on both shoot and root growth of sorghum that declined sorghum CGR. The higher leaf area and root dry weights of corn plants had negative influence on the root and shoot and root dry weights and CGR of sorghum (Figures 5 and 6). According to Caldwell et al. (1983), the species with higher root density may be more competitive than the species with lower root density. Moreover, different species demand different quantities of resources from their environment, and so different species will have different impacts on their neighborhoods (Bazzaz, 1998). The lower CGR of sorghum plants (90 DAE) at high than at low water level was attributed to the negative effects of high water level on plant height, root length, leaf area, shoot and root dry weights of sorghum ((Amanullah and

Figure 5. Millets (Left), corn (Middle) and grain sorghum (Right) shoot and root growth 60 days after emergence under low water level.

Stewart, 2013)). The increase in the CGR of sorghum when it was grown alone in pure or mixed stand with millets (Figure 9) was due to the increase in shoot and root dry weights of sorghum. But the higher leaf area and root dry weights of corn plants in the mixed stand with sorghum (corn + sorghum or corn + sorghum + millets) had negative influence on the shoot and root dry weights of sorghum (Figures 7 and 10) which resulted in the lower CGR of sorghum plans. Rubio et al. (2001) reported that competition among plants occur both above- and below-ground. According to Casper and Jackson (1997) the below-ground competition for water and nutrients can be stronger and can involve more neighbors than above-ground competition.

Foxtail millets

The higher CGR of millets plants at high than at low water level at 30 DAE was because of the delay in

Figure 6. Millets (Left), corn (Middle) and grain sorghum (Right) shoot and root growth 60 days after emergence under high water level.

emergence at low than at high water level. According to Sadras and Calderini (2009), there has been emerging evidence of the importance of early crop vigor for competitive ability of crop plants. At the early growth stage, millets reduced its plant heights; leaf area and shoot dry weight when it was grown in mixed stand with both crops (Figure 1) that declined the CGR in millets plants. The higher leaf, stem and root dry weight of millets when it was grown mixed with sorghum (sorghum + millets) under high water level resulted in the higher CGR of millets at 60 DAE. The increase in the CGR of millets when it was grown alone in pure stand was due to the increase in shoot and root dry weights of millets indicating less intraspecific plants competition among the millets plants than in the inter plants competition in the mixed stands. Including corn in the mixtures with millets (Figures 8 and 10) (corn + millets or corn + sorghum + millets) had negative impacts on the shoot and root dry

Figure 7. Corn and grain sorghum grown together in mixed stand under low (Left) and high (Right) water level 90 days after emergence

Figure 8. Corn and foxtail millets grown together in mixed stand under low (left) and high (right) water level 90 days after emergence.

Figure 9. Grain sorghum and foxtail millets grown together in mixed stand under low (Left) and high (Right) water level 90 days after emergence.

Figure 10. Corn, grain sorghum and foxtail millets grown together in mixed stand under low (Left) and high (Right) water level 90 days after emergence.

weights of millets that resulted in the minimum CGR. The higher leaf area and taller plants (canopy architecture); deeper roots, more number of roots and higher root dry weight of corn plants (root architecture) had negative influence on the shoot and root dry weights of millets plants and so the CGR of millets was reduced. Competition among crop plants occur both above- and below-ground (Rubio et al., 2001), and therefore, measurement of canopy architecture is very important in crop-crop competition (Sorrenson et al., 1993). As compared to corn, that declined the CGR of millets to minimum, sorghum plants had little influence on the shoot and root dry weights as well as the CGR of millets. The lower CGR of millets (90 DAE) at high than at low water level was attributed to the negative effects of high water level on plant height, root length, leaf area, shoot and root dry weights of millets (Amanullah and Stewart, 2013).

The increase in the CGR of millets when grown alone in pure stand was due to the increase in shoot and root dry weights of millets. The leaf area, plant height, shoot and root dry weights of millets plants increased significantly when grown alone in pure stand indicating less intra plants competition among the millets. When corn was included in the mixtures with millets (corn + millets or corn + sorghum + millets) had negative impacts on the shoot and root development of millets that declined the total plant dry weights of millets and so the CGR was reduced. The higher leaf area, root and shoot dry weight of corn in the mixture had negative influence on the root and shoot dry weights of millets that had negative influence on the total plant dry weight and CGR of millets (Figure 8). On the other hand, sorghum plants had little negative influence on the shoot and root dry weights as well as the CGR of millets. Competition among plants occur both above- and below-ground (Rubio et al., 2001), but the below-ground competition for water and nutrients can be stronger and can involve more neighbors than above-ground competition Casper and Jackson (1997).

Crops average

The higher average CGR of summer grasses at high than at low water level at 30 DAE was because of the delay in emergence at low than at high water level. The CGR of corn in pure stand was the highest than all other treatments due the highest shoot and root dry weights of corn. The corn plants were considered the most competitive, followed by sorghum, while the millets plants were least competitive in different mixed stand. The corn plants developed very faster when it was grown mixed with millets; therefore the combination of corn + millets had the second highest CGR. According to Moony (1976), among the plants, which normally use the same set of resources, the individual that captures the most resources over time is assumed to be the most successful competitor and potentially the most fertile producer. The contribution of millets in the corn + millets mixture was very less because the corn plants suppressed adversely the shoot and root growth of millets. Because of the less root and shoot dry weights of millets in the pure stand (30 DAE) resulted in the minimum CGR. The highest CGR of corn in the pure stand was attributed to the highest shoot and root dry weights of corn. Similarly, corn had the highest shoot and root dry weights when it was grown mixed with millets (corn + millets) that resulted in the second highest CGR. The lowest shoot and root dry weights produced by the mixed stand of sorghum and millets (sorghum + millets) or pure stands of sorghum and millets had the lowest CGR at 60 DAE.

The CGR of corn in pure stand was the highest than all other treatments due the highest shoot and root dry weights of corn. The corn plants also had the highest shoot and root dry weights (Amanullah and Stewart, 2013) when it was grown mixed with millets; therefore the combination of corn + millets mixed stand also had the second highest CGR at 90 DAE. Although, the contribution of millets in the corn + millets mixed stand was very less because the corn plants suppressed the shoot and root dry development of millets adversely. The corn plants were considered the most competitive, followed by sorghum, while the millets plants were least competitive in different mixed stands. Dubbs (1971) reported that Russian wild rye (*Elymus junceus* Fisch.) was the most competitive species and sainfoin (*Onobrychis viciaefolia* Scop.) the least competitive. In general, all species were quite competitive to themselves in pure stands due to intra plant competition.

Conclusions

The three warm season grasses (corn, sorghum and millets) responded differently in terms of crop growth rate when grown in pure and mixed stands under low and high water levels at different growth stages. Among the three crops, corn plants had the higher CGR due to the highest dry matter accumulation in both shoots and roots (Amanullah and Stewart, 2013) and was considered the best competitor in all the mixed stands. This indicated that corn plants captured the most resources above (light) and below (water and nutrients) ground over time because of its well developed shoot and root canopy architectures. Measurement of canopy and root architecture is considered very important in crop-crop competition. The intra-plant competition among the crop plants in pure stands was also observed and had negative impacts on the CGR. Better understanding of root architecture of different crop species in pure and mixed stands was suggested to maximize water and

nutrients uptake, and adaptation to diverse agro climatic conditions.

Conflict of Interest

The author(s) have not declared any conflict of interest.

REFERENCES

Aldrich RJ (1984). Nature of weed competition. In: Weed-Crop Ecology. Principles in Weed Management. Breton Publishers. Belton. CA. pp. 189-213.

Amanullah, Stewart BA (2013). Shoot: root differs in warm season C4-cereals when grown alone in pure and mixed stands under low and high water levels. Pak. J. Bot. 45:83-90.

Bazzaz FA (1998). Plants in changing environments. Cambridge University Press, UK.

Caldwell MM, Dean TJ, Nowak RS, Dzurec RS, Richards JH (1983). Bunchgrass architecture, light interception, and water use efficiency: assessment by fiber optic point quadrats and gas exchange. Oecologia. 59:178-184.

Casper BD, Jackson RB (1997). Plant competition underground. Ann. Rev. Ecol. Syst. 28:545-570.

Dahmane ABK, Graham RD (1981). Effect of phosphate supply and competition from grasses on growth and nitrogen fixation of *Medicago trunculata.* Aust. J. Agric. Res. 32:761-772.

Dubbs AL (1971). Competition between Grass and Legume Species on Dryland. Agron. J. 63:359-362.

Hannay MR, Kozub GC, Smoliak S (1977). Forage production of sainfoin and alfalfa on dryland in mixed- and alternate-row seedlings with three grasses. Canadian J. Plant Sci. 57:61-70.

Moony HA (1976). Some contributions of physiological ecology to plant population biology. Syst. Bot. 1:260-283.

Rubio G, Walk T, Ge Z, Yank S, Liaok H, Lynch JP (2001). Root gravitropism and below-ground competition among neighboring plants: A modelling approach. Ann. Bot. 88:929-940.

Sadras VO, Calderini DF (2009). Crop Physiology: Applications for Genetic Improvement and Agronomy. Academic Press. New York, USA.

Sorrenson CKA, Ford ED, Sprugel DG (1993). A model of competition incorporating plasticity through modular foliage and crown development. Ecol. Monog. 63:277-304.

Steel RGD, Torrie JH (1980). Principles and Procedures of Statistics. McGraw-Hill, NY, United States.

Wilson, JB, Steel JB, Steel SLK (2007). Do plants ever compete for space? Folia Geobot. 42:431-436.

Yoshida S (1981). Fundamentals of rice crop science. Los Banos, Philippines: IRRI.

academicJournals

Vol. 13(30), pp. 3052-3060, 23 July, 2014
DOI: 10.5897/AJB2014.13863
Article Number: 6D1846946220
ISSN 1684-5315

http://www.academicjournals.org/AJB

African Journal of Biotechnology

Full Length Research Paper

Optimization of alkaline protease production and its fibrinolytic activity from the bacterium *Pseudomonas fluorescens* isolated from fish waste discharged soil

Jothiprakasam Vinoth*, Sambantham Murugan and Chinnathambi Stalin

CAS in Marine Biology, Annamalai University, Parangipettai-608 502, Tamil Nadu, India.

Received 16 April, 2014; Accepted 4 July, 2014

Pseudomonas fluorescens **AU_{17} was isolated from the fish waste discharged soil and it was tested for its ability to produce the protease enzyme. The effect of different production parameters such as temperature, pH, carbon and nitrogen sources and sodium chloride concentration for protease production by the isolated bacterial strain were studied. The optimum conditions observed for protease production were temperature (37°C) and pH 9, 1% wheat bran for carbon source, 0.5% peptone for nitrogen source; magnesium sulphate has less inhibitory effect among the metal ions tested. Under optimized parameters, maximum protease activity was 0.9343 U/ml/min. The bacterial isolate has potential that could be commercially exploited to assist in protein degradation in various industrial processes.**

Key words: Alkaline protease, casein agar, fish contaminated soil, *Pseudomonas fluorescens,* fibrinolytic activity.

INTRODUCTION

Pseudomonas fluorescens is well known as a major psychrotrophic contaminant of raw milk stored in refrigerated tanks (Law et al., 1977). *P. fluorescens* is a ubiquitous soil microorganism that inhabits the surfaces of seeds and roots. Some strains of *P. fluorescens*, when growing in association with plants, can protect them from infection by plant pathogens (Thomashow and Weller, 1995). One such strain, *P. fluorescens* Pf-5, produces a number of antibiotics, including pyoluteorin (Plt) (Howell and Stipanovic, 1980), pyrrolnitrin (Prn) (Howell and Stipanovic, 1979), and 2,4-diacetylphloroglucinol (Phl) (Nowak-Thompson et al., 1994). Of the three antibiotics, Plt is most toxic to the oomycete *Pythium ultimum* (Maurhofer et al., 1994), which can infect seeds and roots of many plant hosts and cause seedling death and root rot (Martin and Loper, 1999).

Proteases or proteinases are proteolytic enzymes which catalyze the hydrolysis of proteins. Based on their structures or properties of the active site, there are several kinds of proteases such as metallo, serine, acidic, carboxyl, alkaline and neutral proteases. Proteases are industrially important enzymes constituting a quarter of the total global enzyme production (Kalaiarasi and Sunitha, 2009). Proteases are industrially important due

*Corresponding author. E-mail: vinodbio89@gmail.com. Tel: +91-9894686625.

to their wide applications in leather processing, detergent industry, food industries, pharmaceutical, textile industry etc., (Jellouli et al., 2009; Deng et al., 2010). The Industrially important proteases are obtained from plants, animal organs and microorganisms, with the majority obtained from microbial sources. Microorganisms are the most important sources for enzyme production. For manufacture of enzymes for industrial use, isolation and characterization of new promising strains using low-priced carbon and nitrogen source is a continuous process. Habitats that contain protein are the best sources to isolate the proteolytic microorganism (Dalev, 1994). Waste products of meat, poultry and fish processing industries can supply a large amount of protein rich material for bioconversion to recoverable products (Gaustevora et al., 2005). This present study aims to isolate protease-producing bacteria from fish shop waste discharged soil. The optimization of the extracellular protease production is influenced by several physical parameters. This study presents effect of different cultural conditions on production of protease from *P. fluorescens* isolated from fish discharged soil.

MATERIALS AND METHODS

Screening and isolation of proteolytic bacteria

Fish waste discharged soils were collected from Chidambaram fish market. One gram of the contaminated soil sample was weighed aseptically into 100 ml of sterile distilled water, agitated for 45 min on a shaker. 0.2 ml was cultured in 1% casein with nutrient agar plates and incubated at 37°C for 24 h. A total of 23 bacterial isolates from enriched sample was plated over nutrient agar medium containing 0.4% gelatin (Harrigan and Cance, 1966). After 24 h of incubation, plates were flooded with 1% tannic acid. Isolates having a higher ratio of clearing zone to colony size were grown in liquid broth and the amount of protease production was determined from culture filtrate. The isolate which showed higher protease activity was selected and maintained on nutrient agar slants selected isolate was identified based on morphological and biochemical characteristics following the method described by Kannan (2002).

Production of protease enzyme

Yeast extract casein medium was the excellent medium for the production of protease enzyme. In this basal medium contains, glucose 10 g, casein 5 g, yeast extract 5 g, KH_2PO_4 2 g, Na_2CO_3 10 g (Naidu and Devi, 2005). The test bacteria were inoculated into yeast extract casein medium and incubated at 37ºC overnight in shaking incubator. At the end of the fermentation period, the culture medium was centrifuged at 5000 rpm at 4°C for 15 min to obtain the crude extract, which served as enzyme source.

Protease assay

The protease activity was estimated by the method described by Beg et al. (2003). Following incubation, the bacterial broth was centrifuged at 5000 rpm for 20 min at 4°C to obtain the cell free supernatant (CFS). 1 mL of CFS was added to 1 mL of 1% (w/v) casein solution in glycine-NaOH buffer of pH 10.5 and incubated for 10 min at 60°C. The reaction was stopped by the addition of 4 mL of 5% trichloroacetic acid. The reaction mixture was centrifuged at 3000 rpm for 10 min and to 1 mL of the supernatant, 5 mL of 0.4 M Na_2CO_3 was added, followed by 0.5 mL Folins-Ciocalteu reagent. The amount of tyrosine released was determined using a UV-VIS spectrophotometer (SANYO Gallenkamp, Germany) at 660 nm against the enzyme blank. One unit of protease activity was defined as the amount of enzyme required to release 1 µg of tyrosine per mL per min under standard assay conditions.

Process optimization for maximum protease production

Effect of Inoculum concentration

The concentration effect of the inoculums on protease production was determined by inoculating the production medium with different concentration ranging from 2 to 7% of overnight grown selected bacterial culture. The inoculated medium was incubated for 24 h. The culture medium was centrifuged at 5000 rpm at 4°C for 15 min. Protease activity was determined in the cell free supernatant.

Effect of Incubation time

The incubation time effect on protease production was determined by incubating the culture medium at different time intervals (24 - 168 h) with an interval of 24 h.

Effect of pH

The pH effect of the protease production was carried out by adjusting the pH of the production medium in the range of 5 to 11 using 1 N HCl and 1 N NaOH as found appropriate. After the incubation time, the culture medium was centrifuged at 5000 rpm for 15 min in a refrigerated centrifuge at 4°C. Protease activity was determined in the supernatant.

Effect of temperature

The yeast extract casein medium at pH 9 was inoculated with 2% overnight grown selected bacterial strain. The broth was incubated at different temperatures ranging from 27 - 67°C at 10°C interval for 24 h. Protease activity was determined after 24 h.

Effect of carbon sources

The effect of various carbon sources such as starch, wheat bran, rice bran, maltose and sucrose at a concentration of 1% was examined by replacing glucose in the production medium.

Effect of nitrogen sources

Various nitrogen sources like beef extract, tryptone, glycine, peptone and casein were examined for their effect on protease production by replacing 0.5% of yeast extract in the production medium.

Effect of metal ions

Influence of various metal ions on protease production was determined by incubating the yeast extract casein medium with different metal ions such as $BaCl_2$, $CaCl_2$, $MgSO_4$, K_2HPO_4 and $CuSO_4$ at a con-

Figure 1. Protease production of *P. fluorescens* in Skim Milk Agar.

centration of 0.2%. All the experiments were carried out in triplicates and results presented are the mean of three values.

Determination of fibrinolytic activity

Four pieces of cotton fabric were individually impregnated with 500 µL of blood and the blood stains were allowed to dry. Then the fabrics were soaked in 2% (v/v) formaldehyde for 30 min and rinsed with water to remove excess formaldehyde (Adinarayana et al., 2003). Upon drying, the fabric pieces were separately incubated with 1 mL of the partially purified protease, 1 mL of the partially purified protease with detergent, 1 mL of sterile distilled water with detergent and 1 mL of sterile distilled water at 37°C for 1 h. Following incubation, the fabric pieces were rinsed with water, dried and checked for the extent of blood removal.

Statistical analysis

Data obtained were analyzed by statistical method described by Steel et al. (1997). MS Excel software was used to draw graphs.

RESULTS

Isolation and screening of proteolytic bacteria

A total of 23 bacteria were isolated from the dairy sludge examined. When tested for their proteolytic potential, 8 isolates (AU_5, AU_9, AU_{11}, AU_{14}, AU_{17}, AU_{19}, AU_{21}, and AU_{23}) demonstrated clear zones around the streak on the skimmed milk agar (an indication of protease production) (Figure 1). Among these isolates, AU_{17} demonstrated the highest zone of proteolysis (24 mm) as compared to the other isolates and therefore it was selected for further studies (Table 1).

Table1. Protease activity of isolated bacteria.

Bacterial colonies	Protease activity (U/ml/min)
AU_5	0.3245
AU_9	0.1798
AU_{11}	0.5709
AU_{14}	0.4212
AU_{17}	0.9343
AU_{19}	0.2312
AU_{21}	0.3112
AU_{23}	0.1699

Identification of the selected bacterial isolate

Based on the morphological characters, the isolate AU_{17} was found to be gram negative short rod showing motility. Biochemical characterization revealed the identity of the isolate as *P. fluorescens*. The morphological and biochemical characterization are presented in Table 2.

Process optimization for maximum protease production

The protease production was carried out in 1-7% inoculums and the results are 0.1-0.25 respectively. In 2%, inoculums showed the higher activity of protease production likes 0.25%. The enzyme activity was gradually decreased in 3-7% (Figure 2).

The pH of the culture strongly affects many enzymatic processes and transport of compounds across the cell membrane. Maximum protease production was achieved at pH 9.0 by *P. fluorescens*. The production of protease enzyme increased as pH of the medium increases and reaches maximum at pH 9.0. After pH 9.0, there was a decrease in enzyme production (Figure 3).

P. fluorescens was capable of producing protease in the range of 7 - 67°C with production maximum at 37°C. However, increase in temperature beyond 37°C led to decline in production of enzyme proving that temperature plays a major role in protease production (Figure 4).

Protease production was found to be maximum at 24 h. The enzyme activity gradually decreased from 24 to 168 h. This finding is in partial agreement with findings of Kumar et al. (2002) who reported that *Pseudomonas* sp. S22 showed a peak for protease production at 24 h of incubation and again peaks at 108 h which contradicts the finding of this present study (Figure 5).

The addition of carbon source in the form of either monosaccharide or polysaccharides could influence the production of enzyme (Sudharshan et al., 2007). Among the carbon sources, wheat bran and maltose were found to support protease production. The isolated strain showed high enzyme yield (0.389 U/ml/min), when wheat bran was used as carbon source (Figure 6).

Table 2. Biochemical tests of the selected bacterium.

Biochemical character	Bacterial colony AU_{17}
Gram staining	Gram negative
Motility test	Motile
Indole production test	Negative
Methyl red test	Negative
Voges Proskaurer test	Negative
Citrate utilization test	Positive
Catalase test	Positive
Oxidase test	Positive
Urea hydrolysis	Positive
Nitrate reduction	Positive
Starch hydrolysis	Negative
Gelatin hydrolysis	Positive
Fluorescence on King's B medium	Positive
Growth at 4°C and 41°C	Good
Levan formation	Positive

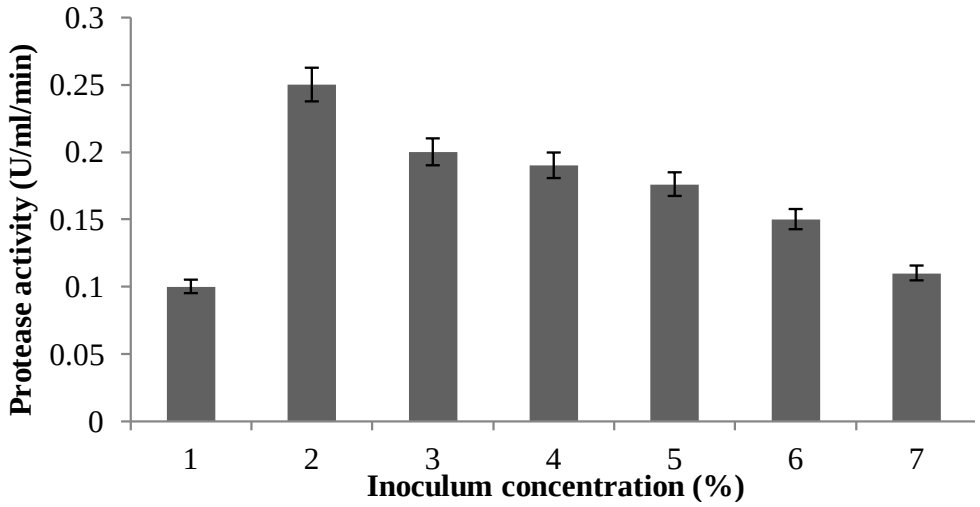

Figure 2. Effect of inoculum concentration on protease production by *Pseudomonas fluorescens.*

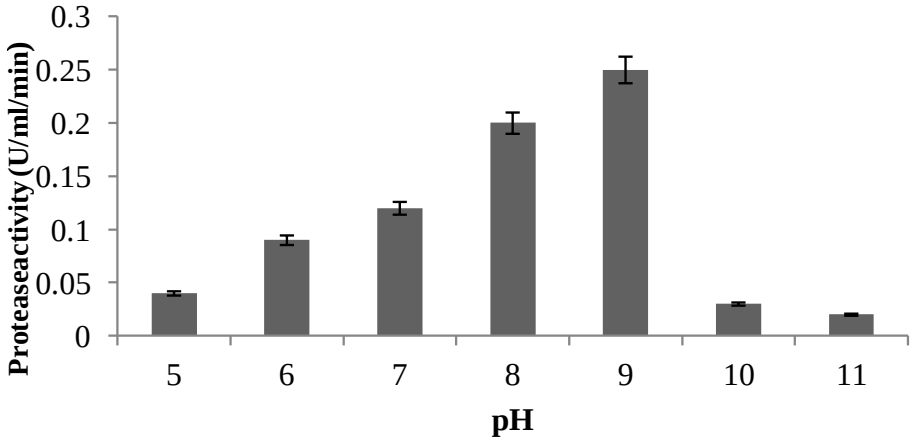

Figure 3. Effect of pH on protease production by *Pseudomonas fluorescens.*

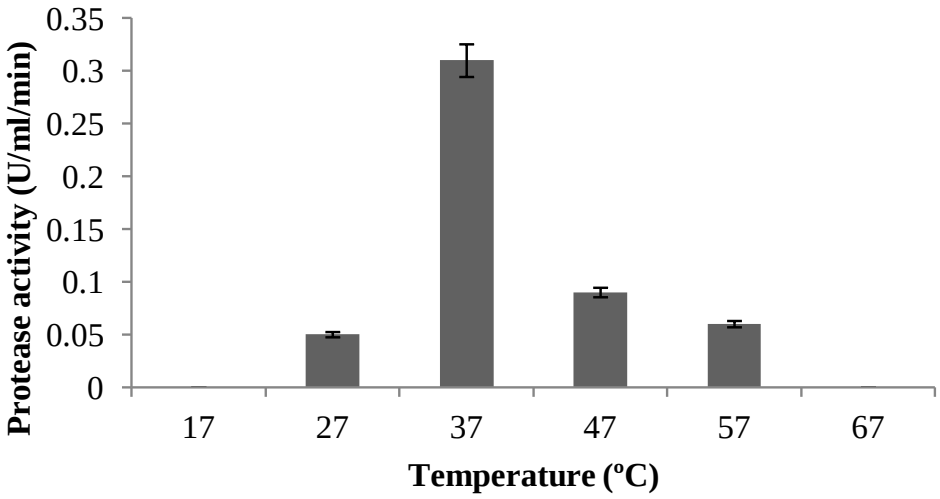

Figure 4. Effect of temperature on protease production by *P. fluorescens.*

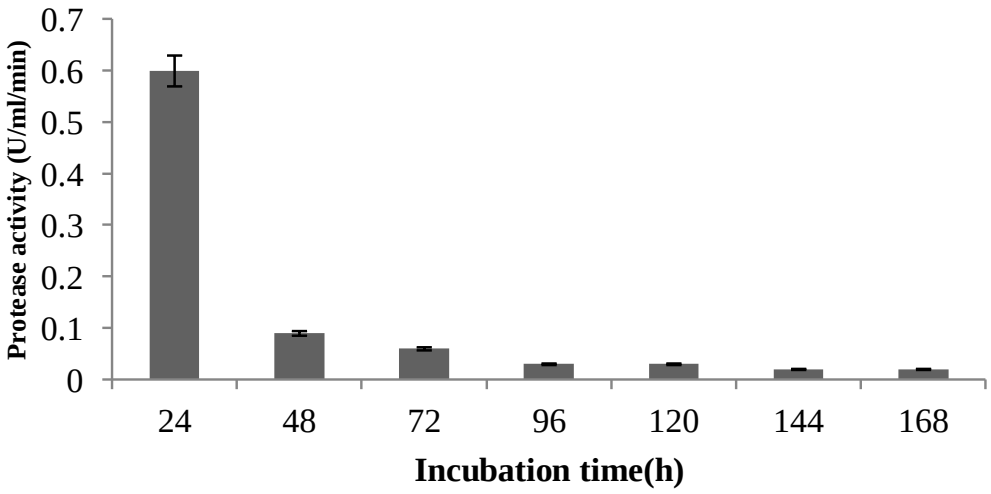

Figure 5. Effect of incubation time on protease production by *P. fluorescens.*

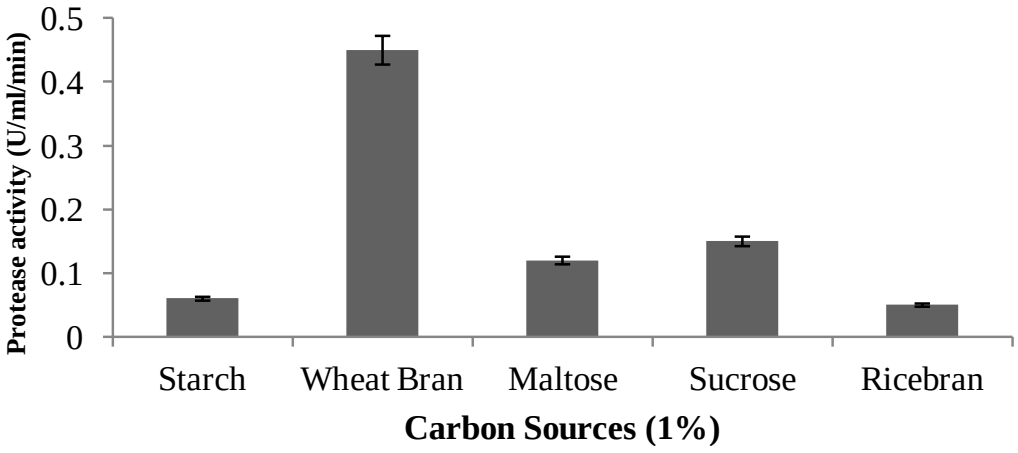

Figure 6. Effect of carbon source on protease production by *P. fluorescens.*

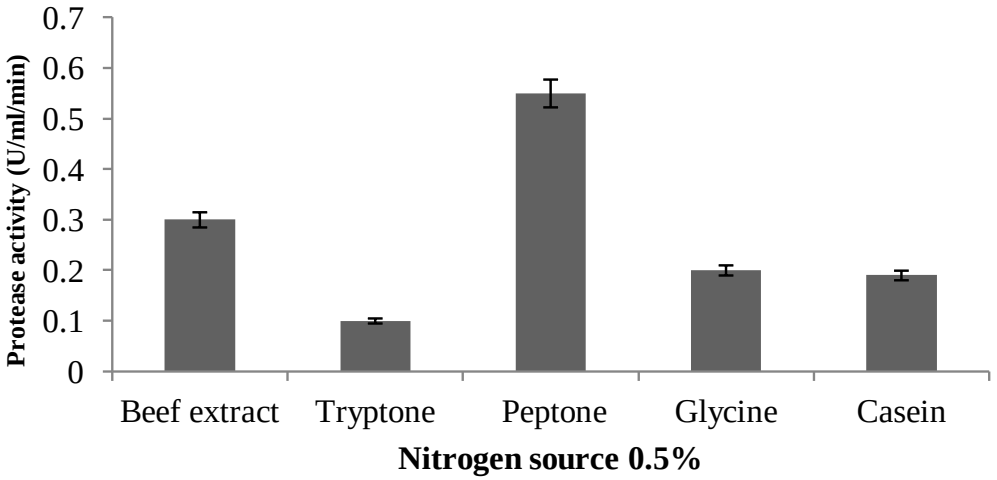

Figure 7. Effect of nitrogen for protease production by *P. fluorescens.*

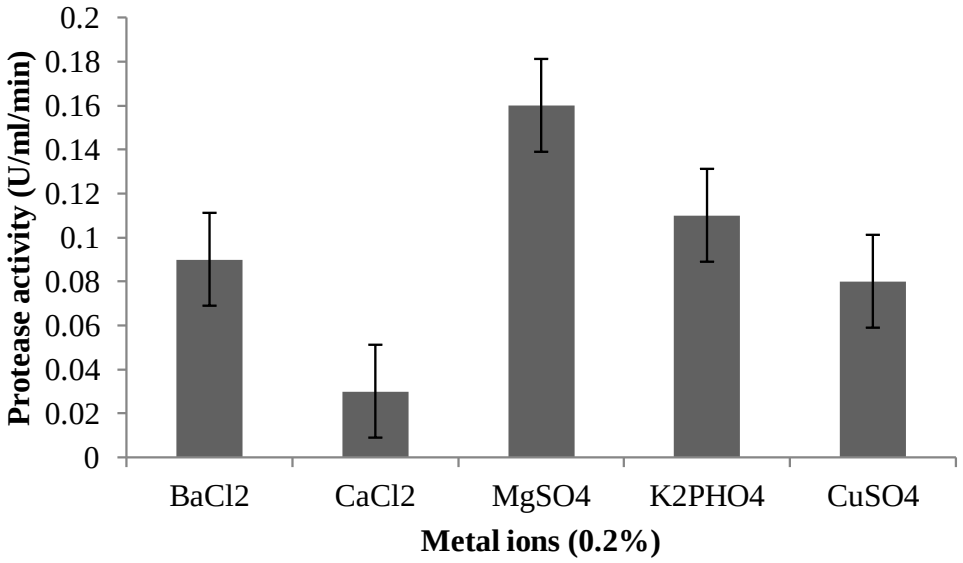

Figure 8. Impact of metal ions on protease production by *P. fluorescens.*

Nitrogen is metabolized to produce primarily amino acid, nucleic acid and protein and cell wall components. These nitrogen sources have regulatory effect on the enzyme synthesis. Production of protease is highly dependent on both carbon and nitrogen sources available in the medium (Shanthakumari et al., 2010). Testing the effect of various nitrogen sources on protease production, it was found that peptone gave the highest enzyme activity of 0.55 U/ml/min while. The inorganic nitrogen sources appeared to be less preferred when compared to the organic nitrogen sources in protease production observed after 48 hours of incubation (Figure 7).

A metal ion in media is an important factor that affects enzyme production. $CaCl_2$ at a concentration of 0.2% inhibits protease production followed by $CuSO_4$ and $BaCl_2$. Magnesium sulphate has less inhibitory effect on the production of protease. These results are in accordance with Wang et al., (2008), they reported that the optimized metal ion for protease production by *Chryseo* bacterium was 0.05% $MgSO_4$ (Figure 8).

Fibrinolytic potential of the protease

The degree of blood removal from the cotton fabric was found in the order of: partially purified protease with detergent > partially purified protease > sterile distilled water with detergent> sterile distilled water.

DISCUSSION

Proteases (EC 3.4.21-24 and 99; peptidyl-peptide hydrolases) are enzymes that hydrolyze proteins via the addition of water across peptide bonds and catalyze peptide synthesis in organic solvents and in solvents with low water content. In all living organisms, proteolytic enzymes are widely found and are essential for cell growth and differentiation (Vadlamani and Parcha, 2011). Maximum protease productions were achieved at 2% inoculum concentration. The enzyme activity gradually decreased from 3 to7%. Elibol et al. (2005) noticed the higher protease production in that 2.5% inoculum level.

The microbial cells are significantly affected by the environmental pH because they in fact have no mechanism for adjusting their pH. Different organisms have different pH optima and decrease or increase in pH on either side of the optimum value results in poor microbial growth (Bhattacharya et al., 2011). The pH of the culture strongly affects many enzymatic processes and transport compounds across the cell membrane. Maximum protease production was achieved at pH 9.0 by *P. fluorescens*. The production of protease increased as pH of the medium increases and reaches maximum at pH 9.0. After pH 9.0 there was a decrease in enzyme production. This suggests that there is a stimulation of enzyme production at alkaline pH. The results coincide with those of Kumar et al. (2002) which found out that protease production was maximum at pH 7 and 9 for *Bacillus* sp. strain S4 and *Pseudomonas* sp. strains S22 respectively. Similarly, Borriss (1987) found maximum alkaline protease production at pH 9 -13.

The highest enzyme yield was observed at pH 7.0 of the production of organic solvent protease by *P. aeruginosa* strain K. Neutral media increased the protease production as compared to acidic or alkaline media (Rahman et al., 2005). Likewise, when the protease production medium for *B. subtilis* was adjusted at different pH values with different buffers, results indicated that the best buffer was phosphate buffer and the optimum pH for production of protease was recorded at 7.0. A decline in the enzyme productivity occurred at both higher and lower pH values (Qadar et al., 2009). Certain *Bacillus* species produced protease over the entire range of pH investigated (pH 5 - 10). The optimum pH for maximum protease production from *Bacillus* SNR01 was at pH 7.0 (Josephine et al., 2012). Radha et al. (2011) studied the production and optimization of acid protease by *Aspergillus* sp. from soil. A gradual increase in protease at pH from 3.0 to 5.0 was reported (Radha et al., 2011), whereas, it declined at neutral and alkaline pH. Fungal acid proteases have an optimal pH range from 4 - 4.5 and they can be stable at pH values from 2.5 - 6.0. Maximum production of enzyme and fungal dry mass were observed at pH of 5. Similarly, Kumar et al. (2002) reported that the optimum pH was in the acidic range of 5.5 - 6.5 for acid protease production from solid tannery waste by Synergists species.

Temperature significantly regulates the synthesis and secretion of bacterial extracellular proteinase by changing the physical properties of the cell membrane (Balaji et al., 2012), therefore, temperature is a critical parameter that should be controlled in order to obtain an optimum proteinase production. In concurrence of the present study with previous findings, where the bacterial isolates like *P. aeruginosa* MTCC 7926, *Serratia liquefaciens* preferred 37°C for maximum production of protease (Patil and Chaudhari, 2011; Smita, 2012). The production of alkaline protease by *Bacillus halodurans* was investigated, wherein the maximal cell growth was seen at 50°C and maximum enzyme production was found at 37°C (Ibrahim and Al-Salamah, 2009). It is very essential to detect the optimum incubation time at which an organism exhibits highest enzyme activity since organisms show considerable variation at different incubation periods (Kumar et al., 2008). *P. fluorescens* was capable of producing protease in the range of 17 - 67°C inconsistent with what you have in the result however there was no production of enzyme at 17 and 67°C (Figure 3) so I suggest your range should be from 27- 57°C, with production of maximum at 37°C (Figure 3). However, increase in temperature beyond 37°C led to decline in enzyme production proving that temperature plays a major role in protease production. Fujiwara and Yamamoto (1987) also noticed that protease activity was high at 30°C for *Bacillus* sp.

The addition of carbon source in the form of either monosaccharide or polysaccharides could influence the production of enzyme (Sudharshan et al., 2007). Among the carbon sources, wheat bran and maltose were found to support protease production. The isolated strain showed high enzyme yield (0.389 U/ml/min), when wheat bran was used as carbon source (Figure 5). These results are in agreement with those of Naidu and Devi (2005) as wheat bran supported the maximum production of protease in *Bacillus* sp. Uyar and Baysal (2004) examined wheat bran and lentil husk, in that wheat bran showed highest protease production in *Bacillus* sp. Among the nitrogen sources, peptone produced maximum protease. Wang and Hsu (2005) found that casein and peptone were better nitrogen sources for protease production by *Prevotella ruminicolo* 23. However, production medium enriched with soybean meal has been reported as best nitrogen source for protease production as stated by Sinha and Satyanarayana (1999). A metal ion in media is an important factor that affects enzyme production. $CaCl_2$ at a concentration of 0.2% inhibits protease production followed by $CuSO_4$ and $BaCl_2$. Magnesium sulphate has less inhibitory effect on the production of protease. Wang et al. (2008) reported that the optimized metal ion for protease production by *Chryseo* bacterium was 0.05% $MgSO_4$.

It is very essential to detect the optimum incubation time at which an organism exhibits highest enzyme activity since organism show considerable variation at different

incubation periods (Kumar et al., 2012). This present study is in agreement with those of previous workers, who reported high proteolytic activity by *Bacillus* sp. Using beef extract for an incubation time of 48 h (Shivakumar, 2012). *P. aeruginosa* showed maximum protease activity at pH 9.5, temperature 37°C and 48 h of incubation time (Samanta et al., 2012). Protease production from *P. fluorescens* was found to be maximum at 24 h beyond which the enzyme activity gradually decreased from 48 to 168 h, which is in contrast to the present finding (Kalaiarasi and Sunitha. 2009). When applied alone, this protease removed blood stain from the fabric significantly.

The washing efficiency of the detergent was also remarkably increased with addition of the enzyme. Similar result of the usage of this enzyme as formulation in detergent preparation, was obtained earlier (Mala and Srividya, 2010).

The results of this present study elucidated that fish contaminated soil can be a very good source for isolating proteolytic bacteria. This study gains its importance since there is scarcity in terms of proteolytic enzymes from *P. fluorescens*. Considering the fact that enzyme production by microorganisms is under the influence of various growth conditions, the present investigation determined the optimum environmental and nutritional parameters for maximum production of protease from the isolate. The fibrinolytic nature of the enzyme alone and in synergy with the detergent evokes the idea that this particular organism may be exploited in the pharmaceutical and detergent industries in future.

Conflict of Interests

The author(s) have not declared any conflict of interests.

Acknowledgements

The authors are grateful thanks Prof. K. Kathiresan, Dean and Director, CAS in Marine biology, Faculty of Marine Sciences, Annamalai University for giving facilities and encouragement and also thank to the Ministry of Human Resource and Development (MHRD), Government of India, New Delhi for providing financial support during the study period.

REFERENCES

Adinarayana K, Ellaiah P, Prasad DS (2003). Purification and partial characterization of thermo stable serine alkaline protease from a newly isolated *Bacillus subtilis* PE-11. AAPS Pharm. Sci. Technol. 4(4): 440-448.

Balaji N, Rajasekaran KM, Kanipandian N, Vignesh V, Thirumurugan R (2012). Isolation and screening of proteolytic bacteria from freshwater fish *Cyprinus carpio*. Int. Multidiscip. Res. J. 2(6): 56-59.

Beg QK, Sahai V, Gupta R (2003). Statistical media optimization and alkaline protease production from *Bacillus mojavensis* in a bioreactor. Process. Biochem. 39(2): 203-209.

Bhattacharya S, Bhardwaj S, Das A, Anand S (2011). Utilization of sugarcane bagasse for solid- state fermentation and characterization of α- amylase From *Aspergillus flavus* isolated from Muthupettai Mangrove, Tamil Nadu, India. Aust. J. Basic. Appl. Sci. 5(12): 1012-1022.

Borriss R (1987). Biology of enzymes. In: Biotechnology (Rehm H and Reed G. Ed). Weinheim, Verlag Chemie 35-62.

Dalev PG (1994). Utilization of waste feather from poultry slaughter for production of protein concentrate. Bioresour. Technol. 48: 265-267.

Deng A, WU J, Zhang Y, Zhang G, Wen T (2010). Purification and characterization of a surfactant-stable high-alkaline protease from *Bacillus* sp. B001. Bioresour. Technol. 101(18): 7100-7116.

Elibol M, Antouio R, Moreira (2005). Optimizing some factors affecting alkaline protease production b a marine bacterium *Terclinobacter turbirae* under solid substrate fermentation. Process. Biochem. 40: 1951-1956.

Fujiwara N, Yamamoto K (1987). Production of alkaline protease in a low cost medium by alkalophutlic *Bacillus* sp. and properties of the enzymes. J. Ferment. Technol. 65: 345-348.

Gaustevora A, Braikova D, Christov P, Tishinov K, Vasileva Tonkova E, Haertle T, Nedkov P (2005). Degradation of keratin and collagen containing wastes by newly isolated. *Thermnoactivomycetes* or by alkaline hydrolysis. Lett. Appl. Microbiol. 40: 335-340.

Harrigan WF, Mc-Cance ME (1966). Laboratory methods in Microbiology, Academic Press, New York. pp. 55-68.

Howell CR, Stipanovic RD (1979). Control of *Rhizoctonia solani* in cotton seedlings with *Pseudomonas fluorescens* and with an antibiotic produced by the bacterium. Phytopathology 69:480–482.

Howell CR, Stipanovic RD (1980). Suppression of *Pythium ultimum* induced damping-off of cotton seedlings by *Pseudomonas fluorescens* and its antibiotic pyoluteorin. Phytopathology 70:712–715.

Ibrahim ASS, Al-Salamah AA (2009). Optimization of media and cultivation conditions for alkaline protease production by alkaliphilic *Bacillus halodurans*. Res. J. Microbiol. 4(7): 251-259.

Jellouli K, Bougatef A, Manni L, Agrebi R, Siala R, Younes I, Nasri M (2009). Molecular and biochemical characterization of an extracellular serine-protease from *Vibrio etschnikovii* J1. J. Ind. Microbiol. Biotechnol. 36:939-948.

Josephine FS, Ramya VS, Devi N, Ganapa SB, Siddalingeshwara KG, Venugopal N, Vishwanatha T (2102). Isolation, production and characterization of protease from Bacillus sp. isolated from soil sample. J. Microbiol. Biotechnol. Res. 2:163-168.

Kalaiarasi K, Sunitha PU (2009). Optimization of alkaline protease production from Pseudomonas fluorescens isolated from meat waste contaminated soil. Afr. J. Biotechnol. 8:7035-7041.

Kannan N (2002). Hand book of laboratory culture media, reagents, stains and buffers, Pahima Publishing Corporation, Bangalore, p. 101.

Kumar A, Sachdev A, Balasubramanyam SD, Saxena AK, Lata A (2002). Optimization of conditions for production of neutral and alkaline protease from species of *Bacillus* and *Pseudomonas*. Ind. J. Microbiol. 42: 233-236.

Kumar DJM, Venkatachalam P, Govindarajan N, Balakumaran MD, Kalaichelvan PT (2012). Production and purification of alkaline protease from *Bacillus* sp. MPTK 712 isolated from dairy sludge. Glob. Vet. 8: 433-439.

Kumar GA, Nagesh N, Prabhakar TG, Sekharan G (2008). Purification of extracellular acid protease and analysis of fermentation metabolites by *Synergistes* sp. utilizing proteinaceous solid waste from tanneries. Bioresour. Technol. 99: 2364-2372.

Law BA, Andrews AT, Sharpe ME (1977). Gelation of UHT sterilized milk by proteases from a strain of Pseudomonas fluorescens isolated from raw milk. J. Dairy Res. 44:145-178.

Mala M, Srividya S (2010). Partial purification and properties of a laundry detergent compatible alkaline protease from a newly isolated *Bacillus* species Y. Ind. J. Microbiol. 50: 309-317.

Martin FN, Loper JE (1999). Soilborne plant diseases caused by *Pythium* spp.: ecology, epidemiology, and prospects for biological control. Crit. Rev. Plant Sci. 18:111–181.

Maurhofer M, Keel C, Haas D, De´fago G(1994). Pyoluteorin production by *Pseudomonas fluorescens* strain CHA0 is involved in the sup-

pression of Pythium damping-off of cress but not of cucumber. Eur. J. Plant Pathol. 100:221–232.
Naidu KSB, Devi KL (2005). Optimization of thermo stable alkaline protease production from species of *Bacillus* using rice bran. J. Biotechnol. 4: 724-726.
Nowak-Thompson B, Gould SJ, Kraus J, Loper JE (1994). Production of 2,4-diacetylphloroglucinol by the biocontrol agent *Pseudomonas fluorescens* Pf-5. Can. J. Microbiol. 40:1064–1066.
Patil U, Chaudhari A (2011). Optimal production of alkaline protease from solvent- tolerant alkalophilic *Pseudomonas aeruginosa* MTCC 7926. Ind. J. Biotechnol 10: 329-339.
Qadar SAU, Shireen E, Iqbal S, Anwar A (2009). Optimization of protease production from newly isolated strain of *Bacillus* sp. PCSIR EA-3. Ind. J. Biotechnol. 8: 286-290.
Radha S, Nithya VJ, Himakiran R Babu, Sridevi A, Prasad NBL, Narasimha B (2011). Production and optimization of acid protease by *Aspergillus* sp under submerged fermentation. Arch. Appl. Sci. Res. 3: 155-163.
Rahman RN, Geok LP, Basri M, Salleh AB (2005). Physical factors affecting the production of organic solvent-tolerant protease by *Pseudomonas aeruginosa* strain K. Bioresour. Technol. 96: 429-436.
Samanta A, Pal P, Mandal A, Sinha C, Lalee A, Das M, Kaity S, Mitra D (2012). Estimation of biosurfactant activity of an alkaline protease producing bacteria isolated from municipal solid waste. Cent. Eur. J. Exp. Biol. 1: 26-35.
Shanthakumari AR, Nagalakshmi R, Ramesh S (2010). Scale-up and media optimization of protease by *Vibrio alginolyticus*. J. Ecobiotechnol. 2: 17-25.
Shivakumar S (2012). Co-production of alkaline protease and amylase of *Bacillus* sp Y in solid state cultivations. Res. J. Biotechnol. 7: 32-38.
Sinha N, Satyanarayana T (1999). Alkaline protease production by thermopile *Bacillus licheniformis*. Enzyme Microbiol. Technol 8: 370-372.
Smita GS, Ray P, Mohapatra S (2012). Quantification and optimization of bacterial isolates for production of alkaline protease. Asian. J. Exp. Biol. Sci. 3:180-186.
Steel, RGD, Torrie JH, Dickey DA (1997). Principles and Procedures of Statistics - a Biometrical Approach. 3rd Ed. McGraw-Hill, New York.
Sudharshan RK, Dutt L, Nayyar R (2007). A highly thermo stable and alkaline amylase from a *Bacillus*. sp. PN5. Bioresour. Technol. 21: 25-29.
Thomashow L, Weller D (1995). Current concepts in the use of introduced bacteria for biological control: mechanisms and antifungal metabolites, In. G. Stacey and N. T. Keen (ed.), Plant-microbe interactions. Chapman and Hall, New York, N.Y. 187–235.
Uyar F, Baysal Z (2004). Production and optimization of process parameters for alkaline protease production by a newly isolated. Process. Biochem. 39: 1893-1898.
Vadlamani S, Parcha SR (2011). Studies on industrially important alkaline protease production from locally isolated superior microbial strain from soil microorganisms. Int. J. Biotechnol. Appl. 3: 102-105.
Wang HT, Hsu J (2005). Optimal protease production condition for *Prevotella ruminicola 23* and characterization of its extra cellular crude protease. Anaerobe 11: 155-162.
Wang SL, Yang CH, Liang TW, Yen YH (2008). Optimization of conditions for protease production by *Chryseobacterium taeanense* Thu001. Bioresour. Technol. 99: 3700-3707.

academicJournals

Vol. 13(30), pp. 3061-3067, 23 July, 2014
DOI: 10.5897/AJB12.1676
Article Number: 26D765246221
ISSN 1684-5315

http://www.academicjournals.org/AJB

African Journal of Biotechnology

Full Length Research Paper

Drying of carrots in slices with osmotic dehydration

Araújo, P. M.*, Fonseca, J. R. L., Magalhães, M. M. A. and Medeiros, M. F. D.

Laboratory of Food Technology, Federal University of Rio Grande do Norte, 59072-970, Natal/RN, Brazil.

Received 26 April, 2012; Accepted 27 October, 2012

Carrot is dried for consumption in the form of slices and cubes. The objective of this work was to find alternative ways for the conservation of carrot slices by osmotic dehydration with additional drying in heat. Pre-osmotic dehydration (temperature, immersion time and type of osmotic solution) based on the results of humidity loss, solid gain, weight reduction and efficiency ratio of pre-dehydrated carrot slices were initially defined as the best conditions for this study. The osmotic solutions used were composed of NaCl (10%) and sucrose (50° Brix) named OD1 and sucrose (50° Brix) called OD2. The experiment of pre-osmotic dehydration of carrot slices in two temperature levels with complementary drying in heat with air circulation at 70°C was used. The best results were obtained with the solution OD1 at 60°C with immersion time of 60 min. The osmotic pre-treatment reduced the initial humidity of carrot slices, reducing the time for the product to reach the same humidity content.

Key words: Carrot, conservation, osmotic solution, pre-osmotic dehydration.

INTRODUCTION

Carrot *Daucus carota, L.*, is rich in β-carotene, a precursor of vitamin A. The daily requirement of vitamin A can be met almost entirely by consuming only 100 g of this vegetable. This vitamin contributes to good vision, skin and mucous membranes. It is also a significant source of calcium, potassium and phosphorus, and contain B vitamins, which help regulate the nervous system and digestive function. Among vegetables, carrot has higher sugar content and therefore is a good source of energy.

Most fruits and vegetables have a definite harvesting time and a limited shelf-life. Most harvested fruits quickly deteriorate due to microbial and biochemical activity. However, different preservation methods are used to extend the shelf-life by a few weeks, one year or more. The methods include canning, bottling, freezing, drying, fermentation, pasteurisation, chemical additives, packaging and irradiation (Burrows, 1996).

The technique of food dehydration is probably the oldest method of food preservation. The main purpose of drying is to allow longer periods of storage, minimize packaging requirement and reduce shipping weight (Amiryousefi and Mohebbi, 2009).

In recent years, some pre-treatments including osmotic dehydration, blanching, and microwave have been used for improving the quality of fruit products and reducing energy consumption (Levent and Ferit, 2011).

Dehydration techniques are based on the fact that the main causes of deterioration of fresh and processed foods is the amount of free water contained in the aliment. The water activity in vegetables and fruits can be reduced through dehydration techniques, consequently

*Corresponding author. E-mail: paulymedeiros@msn.com.

there are reducing weight, greater stability and lower cost storage products (Lopes, 2007). Water activity (a_w) is the most important factor that affects the stability of dehydrated and dry products during storage. It is determinant for microbial growth and can be associated with most degradation reactions of a chemical, enzymatic and physical nature (Levent and Ferit, 2011).

The drying of food using heated air is based on the product temperature increasing to evaporate water and if not properly controlled can cause undesirable changes in the appearance, color and texture, as well as in the nutrient content of the final product (Rastogi et al., 2004). As it is a process of simultaneous transfer of heat and mass, the drying usually requires heat to evaporate moisture from the product and to remove water vapor formed in the product surface to be dried. The process involves three modes of heat transfer: Convection, conduction and radiation. During the drying process, moisture migrates from the interior to the surface of the product, where it evaporates into the environment (Meloni, 2005).

Ponting et al. (1966) are among the first to suggest dehydration process based on the osmotic exchange. Osmotic dehydration (OD) is also known as a technique of removing water by impregnation or saturation. As a technique of removing water, applying the principle of osmosis, the OD generates foods with intermediate water activity (a_w).

OD is used as pre-treatment, it is also used as a stage previous to the freezing process, microwave, lyophilization, vacuum drying or drying by hot air in order to improve product quality, lower energy costs, or even make new products (Gomes et al., 2007).

According to Torreggiani (1993), osmotic dehydration is a special method of drying which is based on the principle that when cellular material are immersed in a hypertonic aqueous solution, a driving force for water removal sets up because of the higher osmotic pressure of the hypertonic solution. There are two major countcurrent flows during osmotic dehydration, that is, water flows out of the food into the solution and likewise solute is transferred from the solution into the food. The osmotic dehydration of fruits and vegetables there is a reduction of water content and consequently the water activity too, but these values are not sufficient to generate stable intermediate moisture products. Therefore, exists the necessity of an additional drying process, the most common is dried with hot air or vacuum. The pre-drying by osmosis, followed by a hot air drying has been widely used in producing dried fruits and partially dried for minimizing the adverse effects that usually appear when the product is subjected to drying with hot air (Neto et al., 2005). This combination of drying methods has been identified as a safe and economical alternative for the conservation of dehydrated products with a better quality when compared to conventional dehydrated products (Brandão et al., 2003). A complex issue in the osmotic dehydration is the choice of the type and concentration of osmotic substance, which is directly related to the sensory properties of the final product and the cost of the processing.

The influences of concentration and composition of osmotic solution, temperature, immersion time, pretreatments, agitation, nature of food and its geometry, and solution to sample ratio on the process have been studied extensively (Singh and Gupta, 2007). The osmotic agent type affects the kinetics of water removal and the incorporation of solids. As one increases, the molecular weight of the solutes observed a solids reduction incorporated and increased water loss. Osmotic agents commonly used are sucrose and sodium chloride, but any water-miscible solution may be used (dextrose 1996).

Considering the importance of researching alternative technologies that enable low cost production of dehydrated carrots, this work studied the drying of carrot with pre-osmotic dehydration.

MATERIALS AND METHODS

The Brasilia variety of carrot used in this study was purchased from a local market. The carrots were selected in order to standardize the maturation stage, picking up, and without any perforations in the skin or other physical damage. They were then washed in water, peeled manually and cut into slices, approximately 3.8 mm thick.

The osmotic solution was prepared using distilled water, commercial sucrose and sodium chloride, purchased from the local market, in pre-defined proportions. The pH of the solution was adjusted in the range of 4 to 5 by adding citric acid. The addition of sodium metabisulfite and calcium chloride at concentrations of 200 ppm was also required. The carrots were blanched in boiling water for approximately 3 min.

The carrot slices were placed in a solution with osmotic concentration, temperature and immersion time defined. The solution was kept under stirring and the temperature controlled by a heating plate. The osmotic proportion between the solution and carrot was 5:1.

Processing conditions

Preliminary tests were performed in six trials with three replicates for each parameter, using two types of osmotic solution. During the preliminary tests, the immersion time of the carrot slices was 3 h at a controlled temperature of 60°C. The following conditions were based on the preliminary tests chosen:

•Composition of the osmotic solution:

a. Sucrose 50° Brix solution + 10% NaCl.
b. Sucrose 50° Brix solution.

•Osmotic solution temperature: 50 and 60°C.
• Immersion Time: 1, 2, 3 and 4 h.

Each processing condition of osmotic dehydration were calculated as water loss (PU), soluble solid gain (SG), weight loss (RP), according to the study of Levi et al. (1983), and dehydration efficiency index (Pr).

$$PU = \frac{Mo.Xo - Mf.Xf}{Mo}$$

Table 1. Results of water loss (PU), solid gain (GS), weight loss (RP), dehydration efficiency (Pr) and water activity (a_w) in OD1 and OD2 solution to carrot slices with 60ºC, in preliminary tests.

Condition	t (min)	PU (%)	GS (%)	RP (%)	P_r	a_w
OD1	180	60.98	29.18	35.03	2.09	0.840
OD2	180	50.99	30.57	18.76	1.67	0.935

$$GS = \frac{Mf.Yf - Mo.Yo}{Mo}$$

$$RP = \frac{Mo - Mf}{Mo} .100$$

$$\Pr = \frac{PU}{GS} .100$$

Where, Mo is the initial weight; Xo is the initial water content; Mf is the final weight; Xf is the final water content; Yf is the final soluble solids and Yo is the initial soluble solids.

The osmotic solution temperature was controlled at 60°C in preliminary tests. Table 1 presents the results of loss of moisture (PU), solid gain (SG), weight reduction (RP), efficiency (Pr) and water activity (a_w) for osmotic agents: OD1 (solution 10% NaCl and 50° Brix sucrose) and OD2 (50° Brix sucrose solution).

The results presented in Table 1 show that moisture loss was higher and solid gain lower when the combination of sucrose (50° Brix) and 10% NaCl with a dehydration efficiency index of 2.09 was used. Similar results were observed in the study of Borin et al. (2008) for squash, and Singh and Mehta (2008) for carrot cubes. The cited authors found that the best solutions were composed of sucrose-NaCl.

Dehydration OD2 with the solution obtained results consistent with the literature for cubes of carrot treated with sucrose solution (Singh et al., 2007b).

Oven drying

After osmotic dehydration, carrot slices were distributed within a single layer of perforated trays and taken to an oven with air circulation of 70°C for 3 h for the completion of drying.

Physical-chemical

Samples were taken at each stage of processing (fresh carrots, bleached, after the osmotic dehydration - OD1 and OD2 - and after final drying), to perform the following analysis according to the method of the Institute of Adolfo Lutz (1985).:

a) pH - measured directly in pot Digimed - DMPH - 2
b) Total titratable acidity, expressed in mg citric acid/100mg per sample.
c) Soluble solids (° Brix) - RL2 refractometer directly measured in the NR 2720-25°C
d) Moisture - determined in an oven with air circulation, until constant weight at 70°C.
e) Weight Loss - obtained directly using balance semi-analytical model BEL MARK 35545.
f) Water activity (aw) - measured directly on the analyzer activity, model AQUALAB series 3TE.

RESULTS AND DISCUSSION

Tests with the osmotic agents

To define the type of osmotic agent, tests were performed with two different solutions. Six trials were performed for solutions OD1 and OD2, with immersion time of 180 min.

Definition of solution temperature on osmotic dehydration of carrot slices for osmotic agents OD1 and OD2

Table 2 shows the results for the dehydration of carrot slices in four differents immersion times, provided OD1 (10% NaCl and 50° Brix sucrose) at 50 and 60°C. It was observed that the best efficiency ratio (Pr) was obtained at a temperature of 50°C and immersion time of 60 min. The greatest loss of moisture (PU) was the measured slices dried for 60 min at 50°C. When dried at a temperature of 60°C, slices began to lose moisture during further drying, where the PU rates increased with the immersion time of slices, reaching a maximum of 67.94% at 180 min (Table 2). For the immersion time of 240 min, there was a decrease due to increased Pr, GS by carrot slices.

Table 3 shows the results for the dehydration of carrot slices in four differents immersion times, provided OD2 (50° Brix sucrose) at 50 and 60°C. It also appears that with sucrose solution; only the best efficiency ratio was obtained at a temperature of 50°C and immersion time of 60 min. Singh et al. (2007) observed similar behavior in dehydrated carrot cube, where the dehydration in shorter time and lower temperature showed better efficiency with better value for PU/GS. With increasing time of immersion, PU tends to increase, but due to the increased rate gain solid efficiency tends to decrease (Table 3). Manivannan and Rajasimman (2009) also observed this behavior for pre-dehydrated beets with sucrose solution at a temperature of 45°C.

From the results in Tables 2 and 3, it can be seen that the immersion time of 60 min was the most efficient in osmotic dehydration. Dehydration with the osmotic agent OD1 (10% NaCl and 50° Brix sucrose) gave better results in the same condition as compared to the osmotic agent OD2 (50° Brix sucrose).

It is important to use solutions combined to improve efficiency of the osmotic dehydration.

Table 2. Performance of water loss (PU), solid gain (GS), weight loss (RP), dehydration efficiency (Pr) and water activity (a_w) in OD1 solution to carrot slices with 50 to 60ºC.

Condition	T (ºC)	t (min)	PU (%)	GS (%)	RP (%)	P_r
OD1 (10% NaCl + 50°Brix Sucrose)	50	60	65.60	15.74	50.10	4.16
	60		62.65	18.32	45.51	3.42
	50	120	59.43	23.37	48.20	3.26
	60		64.29	18.53	48.25	3.47
	50	180	60.19	25.28	47.25	3.09
	60		67.94	23.80	44.31	2.85
	50	240	61.09	29.99	46.34	2.85
	60		63.91	29.00	45.62	2.20

Table 3. Performance of water loss (PU), solid gain (GS), weight loss (RP), dehydration efficiency (Pr) and water activity (a_w) in OD2 solution to carrot slices with 50 to 60ºC.

Condition	T (ºC)	t (min)	PU (%)	GS (%)	RP (%)	P_r
OD2 (50° Brix Sucrose)	50	60	59.53	14.94	43.54	3.98
	60		46.29	20.83	32.23	2.22
	50	120	64.12	16.82	46.16	3.81
	60		53.76	21.42	36.00	2.51
	50	180	65.08	19.25	45.24	3.38
	60		56.37	25.16	33.36	2.24
	50	240	62.95	22.13	39.23	2.84
	60		54.15	28.49	27.58	1.90

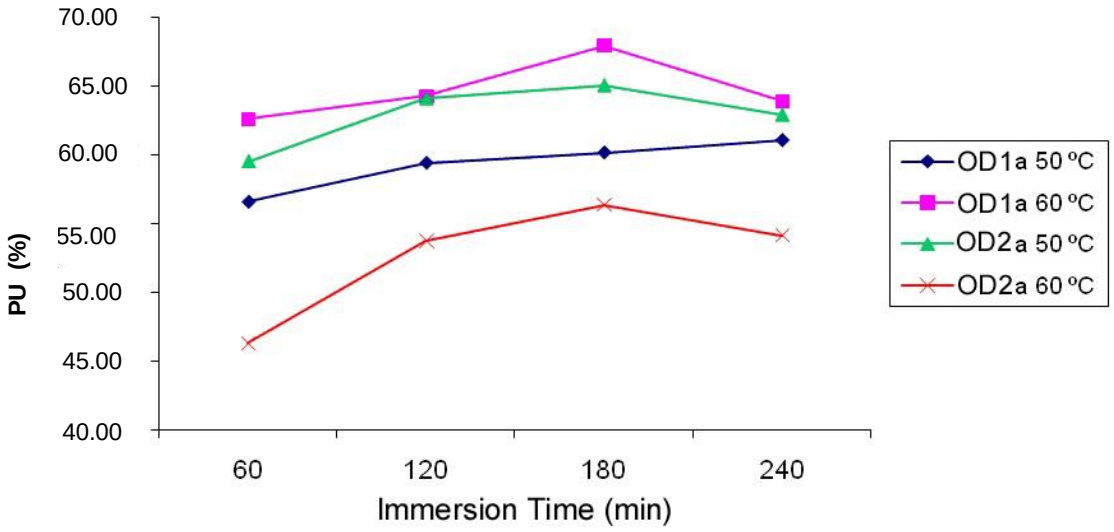

Figure 1. Effect of immersion time (60, 120, 180, 240 min) on water loss (PU) during osmotic dehydration of carrots slices at OD1 and OD2 solution.

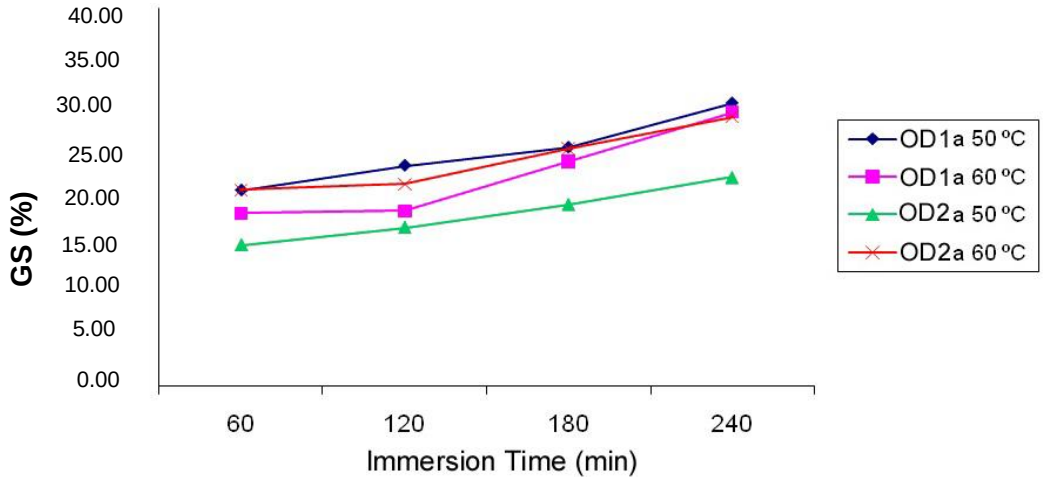

Figure 2. Effect of immersion time (60, 120, 180, 240 min) on solid gain (GS) during osmotic dehydration of carrots slices at OD1 and OD2 solution.

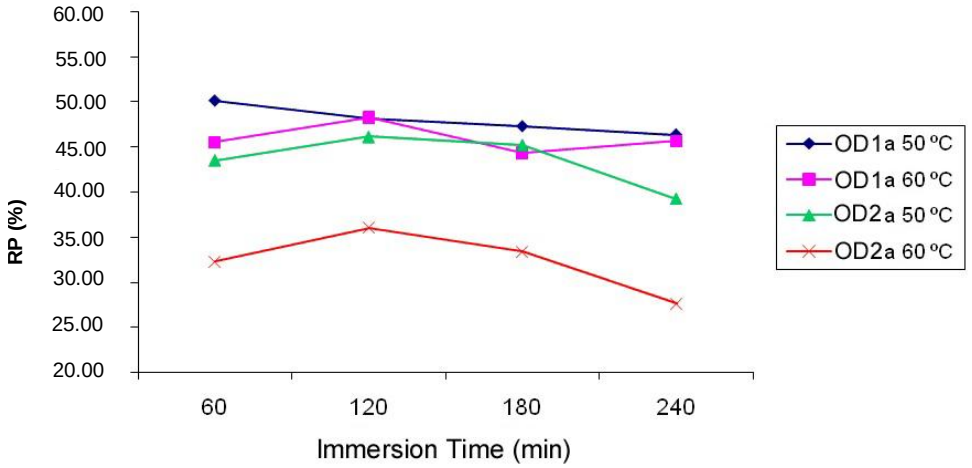

Figure 3. Effect of immersion time (60, 120, 180, 240 min) on weight reduction (RP) during osmotic dehydration of carrots slices at OD1 and OD2 solution.

Several authors use a combination of solutions to achieve better value for PU/GS (Borin et al., 2008; Ayşe and İnci, 2008; Singh and Mehta, 2008).

Comparison between osmotic agents

Figures 1, 2, 3 and 4 show the variation of moisture loss (PU), solid gain (GS), weight reduction (RP) and efficiency (Pr) in dehydrated carrot slices in different immersion times with osmotic agents OD1 and OD2 at 50 and 60°C, using the data from Tables 2 and 3.

Figure 1 shows that the greatest loss of moisture (PU) occurs in slices of carrots treated with the osmotic agent OD1 at 60°C. There is an increase in PU with increasing immersion time, which is consistent with the literature studied (Borin et al., 2008; Rastogi et al., 1997; Amami et al., 2007). The highest rates of PU are located in time of 180 min. Result in Figure 2 was observed in all treatments that was a solid gain increase with the immersion time increment. Carrots immersed in OD1 solution showed the highest solids gain (GS) at 50°C and immersion time of 240 min. In the first hour of drying the dehydrated slices in a solution at 50°C OD1 and OD2 dehydrated with a solution at 60°C showed similar GS; with increasing immersion time these values differ. Sodium chloride for presenting a low molecular weight increases outflow of water from the slices to the solution, and the input solid solution for the carrot slices. This is explained by the fact that low molecular weight substances such as salt can easily penetrate into the food, favoring the solid gain (Borin et al., 2008; Singh et al., 2007a). Figure 3 shows that the solution OD2 in tem-

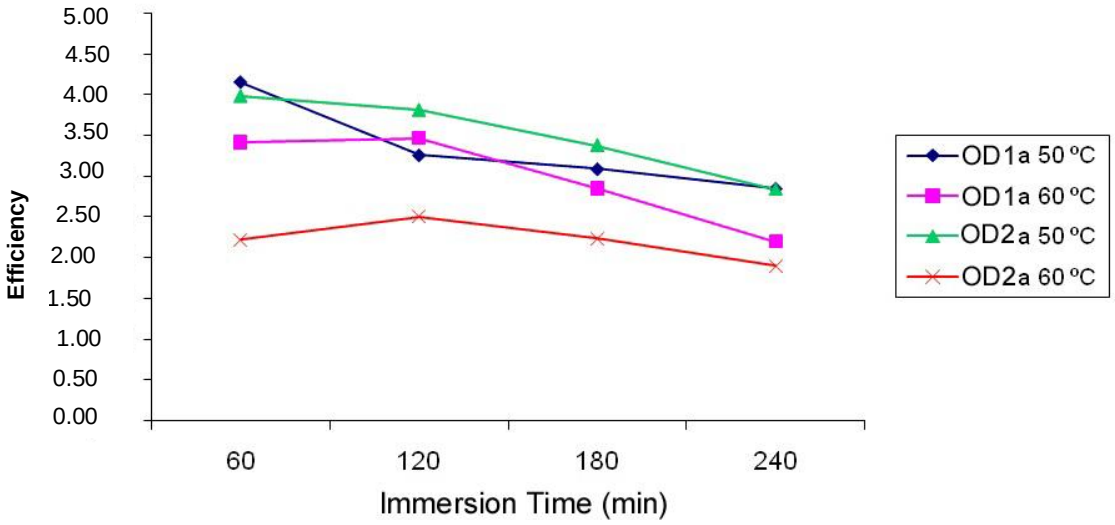

Figure 4. Effect of immersion time (60, 120, 180, 240 min) on rate of efficiency during osmotic dehydration of carrots slices at OD1 and OD2 solution.

perature of 60°C resulted in less weight reduction (RP), while the solution OD1 promoted the highest levels of RP at both temperatures. This is due to be favored by impregnating solution consisting of low molecular weight substances, and the removal of water facilitated by compounds of high molecular weight. Low molecular weight substances can easily penetrate into the food, they are small, and thus favor the solid gain. In contrast, solutions containing high molecular weight, provide favorable conditions for weight reduction. OD1 solution is formed by two compounds, sucrose, high molecular weight and low molecular weight NaCl, favoring the solid gain (GS) and weight reduction (RP). Figures 3 and 4 shows that OD1 immersion in the solution at 50°C provided the best results in 60 min immersion, being the more efficient dehydration.

Conclusion

The pre-dehydration of carrot slices in 10% solution of NaCl and sucrose, for the immersion time of 60 min and 50°C showed the best results. The decrease of the initial water promoted by osmotic dehydration favored the production of carrot slices with intermediate levels of water, requiring additional drying.

Conflict of Interest

The author(s) have not declared any conflict of interest.

ACKNOWLEDGEMENTS

The authors would like to thank the PPGEQ/DEQ/CT-UFRN-NATAL, RN. CAPES (Coordination of Superior Level Staff Improvement) and CNPq (National Council for the Scientific and Technological Development) for the financial support for carrying out the present work.

REFERENCES

Amami E, Fersi A, Vorobiev E, Kechaou N (2007).Osmotic dehydration of carrot tissue enhanced by pulsed electric field, salt and centrifugal force. Food Eng. J. 83:605-613.

Amiryousefi MR, Mohebbi M (2009). Neural network approach for modeling the masstransfer of potato slices during osmotic dehydration using genetic algorithm. Afr. J. Biotechnol. 5(1):070-077.

Ayşe İspir, İnci Türk Toğrul (2008). The influence of application of pretreatment on the osmotic dehydration of apricots. Food Process. Preserv. J. 33:58-74.

Borin I, Frascareli EC, Mauro MA, Kimura M (2008).Efeito do pré-tratamento osmótico com sacarose e cloreto de sódio sobre a secagem convectiva da abóbora. Ciênc. Tecnol. Aliment. 28:39-50.

Brandão MCC, Maia GA, Lima DP, Parente EJS, Campello CC, Nassu RT, Feitosa T, Sousa PHM (2003). Análise físico-química, microbiológica e sensorial de frutos de manga submetidos à desidratação osmótica-solar. Rev. Bras. Fruticult. 25(1):38-41

Burrows G (1996). Production of thermally processed and frozen fruit. In: Fruit processing. Artley D, Ashurst PR (Eds.). Blackie Academic and Professional, London, UK. pp.135-164.

Ertekin FK, Cakaloz T (1996). Osmotic dehydration of peas: influence of process variables on mass transfer. Food Process. Preserv. J. 20:87-104.

Gomes AT, Cereda MP, Vilpouxo O (2007). Desidratação osmótica: uma tecnologia de baixo custo para o desenvolvimento da agricultura familiar. Rev. Bras. Gestão e Desenv. Regional. 3(3):212-226.

Levent IA, Ferit AK (2011). Partial removal of water from red pepper by immersion in an osmotic solution before drying. Afr. J. Biotechnol. 11(6):1449-1459.

Lopes RLT (2007). Conservação de alimentos- Fundação centro tecnológico de Minas Gerais, CETEC.

Manivannan P, Rajasimman M (2009). Optimization of process parameters for the osmotic dehydration of beetroot in sugar solution. Food Process Eng J. Early View: 1-22.

Meloni PLS (2005). Curso - Desidratação de frutas e hortaliças. UFRN. Escola Agrícola de Jundiaí.

Ponting JD, Watters GG, Forrey RR, Jackson R, Stanley WL (1966). Osmotic dehydration of fruits. Food Technol. J. 20:125-128.

Rastogi NK, Nayak CA, Raghavarao KSMS (2004). Influence of osmotic pre-treatments on rehydration characteristics of carrots. . Food Eng. J. 65:287-292.

Rastogi NK, Raghavarao KSMS (1997). Water and solute diffusion coefficients of carrots as a function of temperature and concentration during osmotic dehydration. Food Eng. J. 34: 429-440.

Singh B, Gupta AK (2007). Mass transfer kinetics and determination of effective diffusivity during convective dehydration of pre-osmosis carrot cubes. J. Food Eng. 79:459-470.

Singh B, Mehta S (2008). Effect of osmotic pretreatment on equilibrium moisture content of dehydrated carrot cubes. Int. J. Food Sci. Technol. 43:535-537.

Singh B, Panesar PS, Gupta AK, Kennedy JF (2006). Sorption isotherm behavior of osmoconvectively dehydrated carrot cubes. Food Process. Preserv. J. 30: 684-698.

Singh B, Panesar PS, Nanda V (2007a). Osmotic dehydration kinetics of carrot cubes in sodium chloride solution. Int. J. Food Sci. Technol. April. 43: 1361-1370**.**

Singh B, Panesar PS, Nanda V (2007b). Optimization of osmotic dehydration process of carrot cubes in sucrose solution. Food Process Eng. J. 31:1-20.

Torreggiani D (1993). Osmotic dehydration in fruit and vegetable processing. Food Res. Int. J. 26: 59-68.

academicJournals

Vol. 13(30), pp. 3068-3080, 23 July, 2014
DOI: 10.5897/AJB2013.13550
Article Number: 2387B8B46223
ISSN 1684-5315

http://www.academicjournals.org/AJB

African Journal of Biotechnology

Full Length Research Paper

Antiparasitic activity of the microalgae *Cladophora crispata* against the Protoscolices of hydatid cysts compared with albendazole drug

A. M. Athbi[1]*, S. H. Al- Mayah[1] and A. K. Khalaf[2]

[1]Biology Department, College of Education for Pure Sciences, University of Basrah, Basrah, Iraq.
[2]Microbiology Department, College of Medicine, Thi-Qar University, Al-Nasiriyah, Iraq.

Received 10 December, 2013; Accepted 20 June, 2014

Antiparasitic activity of the microalgae *Cladophora crispata* isolated from Garmat-Ali River in southern Iraq was studied. Water samples were collected from river in the northern of Basrah, and cultured in chu-10 medium. Supernatants, alkaloidic and ethylacecate extracts from biomass were extracted and screened against the hydatidosis compared with albendazole drug. The present study reveal that 2- (N, N-dimethyl hydrazine) cyclohexanecarbointrile and pyridine 2,3,4,5 - tetrahyro compounds have activity against the protoscolices of hydatid cysts accordingly to the activity of albendazole based on the mean of weight of mice, mean of hydatid cysts number, mean of diameters and weights of hydatid cysts. The current study concludes that the alkaloidal and ethylacetate extracts of *Cladophora crispata* have a positive effect on the protoscolices of hydatid cyst in comparison with albendazole activity, related to reduction in the number and weight of hydatid cyst as well as the obstruction of germinated layer which is responsible for proliferation of protoscolices.

Key words: Algae, *Cladophora crispata*, bioactive chemical compounds, antiparasitic activity, hydatid cysts.

INTRODUCTION

Microalgae are a diverse group of photosynthetic microorganisms found in the soil, fresh water and marine environments (Metting and Pyne, 1986). They are able to produce a range of biochemical active compounds such as antibacterial, antifungal, antiviral, enzyme inhibitors, immunostimulants, cytotoxic, atiplasmodial activities (Ghasemi et al., 2004) and antitrypanosomal activities (Lorena et al., 2009). Most of the isolated chemical substances belong to groups of alkaloids, peptides, tannins, saponins, triterpenes and phenols (Molera and Semesi, 1996) as well as proteins (Athbi, 2011).

Diseases such as hydatid disease, hydatidosis, cystic echinococcosis, unilocularhydatid disease and echinococcosis, are referred to as the infections which are caused by cestodes of the genus *Echinococcus* and mainly by *E. granulosus* (Dar et al., 1977; Akhan et

*Corresponding author. E-mail: athbi62@yahoo.com.

al., 2002; Georgopoulos et al., 2007). Hydatid cysts remains a significant public health problem in the endemic areas such as Turkey, the Middle East, South America, New Zealand, Mediterranean region, Africa, China, northern Kenya, Australia, and other sheep-raising areas (Morar and Feldman, 2005; McMnus et al., 2003). As an endemic disease, it causes social and economic losses for countries. WHO reports that approximately 100 000 people in the world are infected with these diseases every year which is more common in rural population of underdeveloped countries because of their close association with domestic and wild animals (Parija and Sheeladevi, 1999). Until recently, surgery was the only option for treatment of echinococcal cysts, however, chemotherapy with benzimidazole compounds and, cyst puncture, percutaneous aspiration, injection of chemicals, and reaspiration (PAIR) are increasingly used to as an alternative to replace a surgical method (Morar and Feldman, 2005).

The undesirable side effects associated with this classical drug, as well as the development of resistance, has encouraged researchers to use alternative synthetic or natural compounds for treatment of hydatid disease. In this regard, studies have focused on the bioactivity of natural substances derived from algae, mainly due to their accessibility and use in traditional medicine (Smit, 2004; Kladietal, 2008; Lorena et al., 2009); although many researches have been focused on the extracts from algae as a source of antiparasitic compounds. Early studies on bioactive chemical compounds isolated from chlorophyta have led to the discovery of several compounds, including the diterpenoids, udoteal and halimedatrial isolated from *U. flabellum* and *Halimeda sp*. respectively, and the sesquiterpenoids hipocephanal isolated from *Rhipocephalus phoenix* that inhibited cell division in sea urchin eggs (Fenical and Paul, 1984). Anuomrthine, Pronueiferine, Glaucine, Nuciferine, Yeserpin, Evodianin, Caulerpine, Leptoclinidamin-A, and Halimedin are alkaloidal chemical compounds isolated from the species of chlorophyta and act as antioxidant, antiviral, antibacterial, antifungal, and anticancer (Calixto et al., 2000; Radwan et al., 2007; Carrol et al., 2007; Everton et al., 2009). Al-Nasiri (2010) isolated an alkaloid chemical compound from *C. crispata* which was similar in structure to calothrixin and had *in vitro* antibacterial activity.

Recent studies have shown promising antimalarial activity by the alga *Laurencia sp.* (Topcu et al., 2003) and trypanocidal and leishmanicidal activity by *Fucuse vanescens, pelvetiaba bingtonil*, *Ulva lactuca* and *Sargassum natans* (Naraetal, 2000; Orhan et al., 2006). A study of Leon - Deniz et al. (2009) revealed that the activity of the organic extracts of green algae *U. conglutinata* and *U. flabellum* cause a total inhibition of the trypanosomes parasite at 24 h; 48 h and even seven days after growth. The present study was designed to examine the *in vivo* activity of bioactive chemical compounds (alkaloids and ethylaacetale) extracted from *Cladophora crispata* (Chlorophyta) against the proto-scolices of hydatid cyst of *E. granulosus* compared with a commercial drug albendazole.

MATERIALS AND METHODS

Isolation of microalga

C. crispata was isolated from Garmat - Ali River in Basra city, southern Iraq, from January to April 2012. Primary culturing was done in Chu - 10 medium. After incubation, pure cultures of the living specimens were prepared by sub culturing with agar plate method in Chu -10 medium (Stein,1975). Preserved specimens were prepared and the living specimens were inoculated in 100 ml conical flasks. Constant illumination was used at 60 µE m^{-2} Sec^{-1} intensity using white fluorescent lamps and incubated at 25 ± 2°C. Algal cultures were identified based on thier morphological characteristic following the taxonomy schemes of Prescott (1975) and Sant 'Anna (2004).

Prepration of algal extracts

Preparation of extracts was made according to Reichelt and Borowitazka (1984) using ethylacetate extract. 1 g of *C. crispata* biomass were extracted by soxhlet continuously with 250 ml of ethylacetate as solvent for 24 h. The alkaloidal extract was prepared using 0.5 g of dried culture extracted with acidic ethanol (ethanol absolute with 2% acetic acid) for 24 h in a continuous extraction by soxhlet apparatus. The extracts were filtered, and ethanol was evaporated on a rotary evaporator under vacuum at a temperature of 45°C to a small volume (about a quarter), then a small amount of NH_3 (25%) was added to make pH of 9. Subsequently, 100 ml of chloroform was added and slowly shacked for 10 min. until the alkaloidal compounds were separated from water and enter to the chloroform phase. This process was repeated three times, then total chloroform phase was evaporated, yielding a total alkaloid extract and dried under a reduced pressure and stored in -20°C for further studies.

Identification of biochemical active compounds

Ultra-violet (UV) spectrum (LKB-Sweden UV), Infra-red spectrum (IR) (Pye- Unicam Sp3- 3005 UK), and gas Chromatography Mass (GC-mass) (Agilent Technologies GC-mass 7890 AGC System) methods were applied for the identification and determination of the molecular weights and chemical structure of the isolated biochemical active compounds.

Parasite materials

E. granulosus hydatid cysts containing protoscolices were removed under aseptic conditions from livers and lungs of naturally infected sheep (The outer surfaces of the cysts were sterilized with70% ethanol before being dissected). Protoscolices were extracted according to Smyth (1980) (Figure 1).

Estimation of viable protoscolics

200 µL of hydatid fluid and 200 µL of 0.1% eosin staining solution

Figure 1. Hydatid sand containing the daughter cyst, brood capsule and protoscolex aspired from the hydatid cyst.

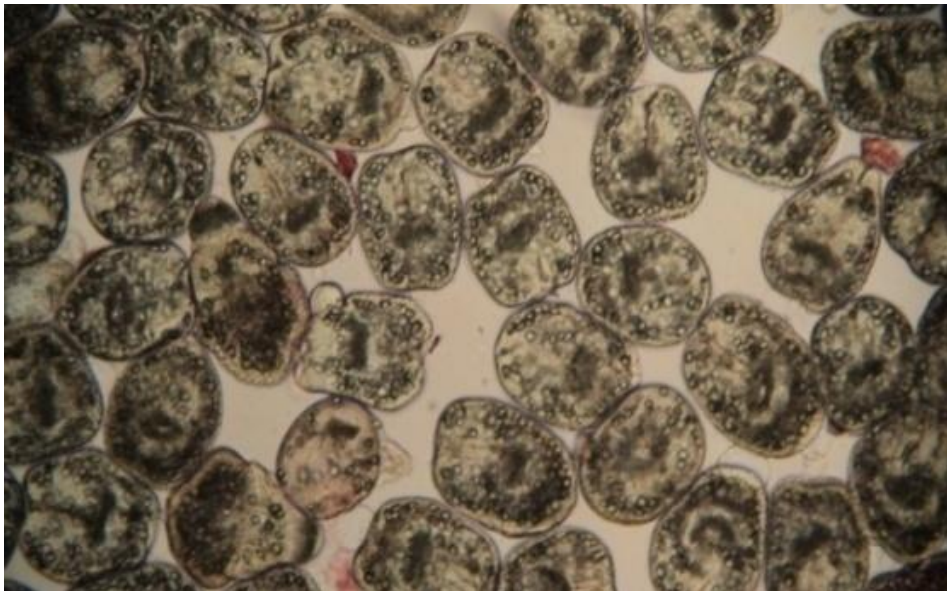

Figure 2. Viable protoscolices.

were combined in a microtube. After 20 min of incubation, the viability of protoscolices was assessed by microscopic observation. Stained protoscolices were considered as nonviable (Figure 3) and the protoscolices which have been stained with eosin were considered as viable (Figure 2) according to conventional (Taran et al., 2009).

The counting of viable protoscolices

Protoscolices were counted according to the method of Rounno et al. (1974) cited by Al- Humairy (2010). After estimating the viability of protoscolices, 10 µL of the hydatid fluid was taken by a micropipette, the count was done under dissecting microscope, and

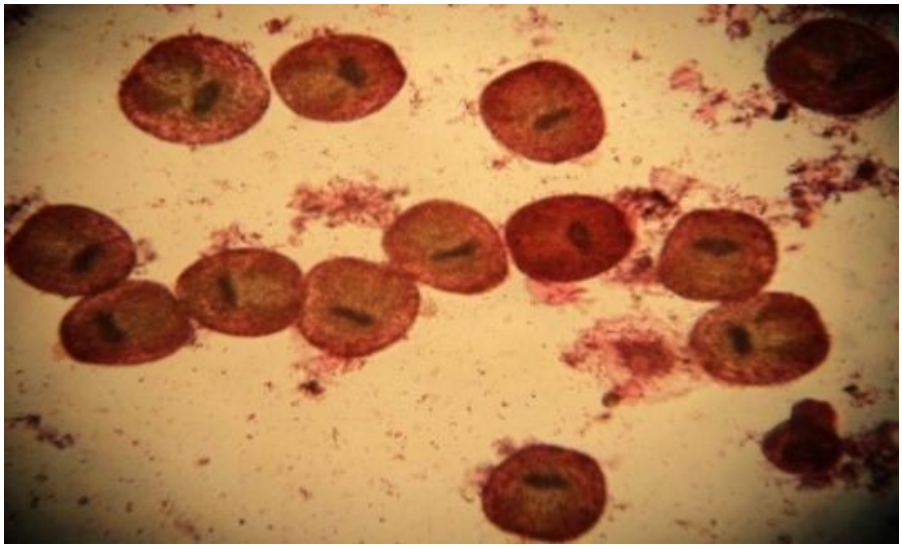

Figure 3. Non viable protoscolices.

Table 1. Experimental albino mice model.

Treatment	Number	Mice group
Alkaloids of *C. crispata*	24	T1 group
Ethylacelate extract of *C. crispata*	24	T2 group
Treated with Albendazole	8	Albendazole group
Infected without treatment	8	Positive control group
Without infection and treatment	8	Negative control group
- - - -	73	Total

repeated three times. The viable protoscolices were counted in 1 ml based on the formula:

Viability in 1 ml = number of protoscolices in 10 µL × 100

Injection of mice with protoscolices

Male Mus musculus mice Balb/C strain was injected with 0.2 ml 480/ L (2400/5 ml rate of viability) of protoscolices intraperitoneally (I.P) using 1 ml volume syringes. The region of injection was sterilized with 70% of ethyl acohol.

Determination of lethal dose (LD50)

Males of the *M. musculus* Balb/C strain were dosed orally to determine the LD_{50} using a stomach tube with bioactive chemical compounds extracted from *C. crispata* (ethylacetate and alkaloid extracts). The animals were monitored for 72 h and weakness, unstable walking, loss of balance and death was checked during this period. Injection started with low dose then continued to high dosages based on Litchfield and Wilcoxon (1949) equation:

$$LD_{50} = \text{highest dosage} - \frac{\sum ab}{n}$$

Where, LD_{50} is the lethal dose 50, highest dosage is the dose with 100% mortality of mice, a is the value of difference between the previous and next dose, b is the summation of dead animal for each dose (previous dose + next dose / 2) and n is the number of animals used for each dose .

Experimental design

Male mice of *M. musculus* Balb/c albino strain aged 6 to 8 weeks were used in this study. They were injected interperitoneal (IP) with viable protoscolices of the *E. granulosis* and left for six months before treatment.

A positive control group was infected without treatment and the negative control group was left without infection and treatment. The *in vivo* study included two parts (Table 1).

Treatment

The treatment included two groups of 24 infected male albino mice which were treated with bioactive chemical compounds. Eight infected mice were treated with albendazole and 8 more left as a positive control. Eight intact male mices were used as a negative control. More details as follows:

Treated 1 (T1) group

In this group, 24 infected male mice were dosed orally daily for one month with concentrations (280, 300, 330 µg/ml) of the alkaloidal bioactive compound extracted from *C. crispata* with 8 mices for each concentration.

Treated 2 (T2) group

This group consists of 24 infected male mice which were treated orally daily for one month with (100, 110, 120 µg/ml) concentration of ethyl acetate extracted from *C. crispata* with four pairs for each concentration.

Albendazole group

In this group, 8 of infected male mice were daily treated orally with 500 µg/ml of albendazole for 30 days.

The weight of mices and their organs were checked before and after treatment. Diameters of cysts were measured by the ruler and the number of hydatid cysts was counted based on the following formula to calculate the effective dose:

$$\text{Effective dose group} = \frac{\text{Number of cysts in positive control group - Number of cysts in treated}}{\text{Number of cysts in positive control group}}$$

Statistical analysis

The statistical analysis was conducted in SPSS 9.0; T-test at 0.05 level was used to analyze variation of the mean of viable protoscolices treated with bioactive chemical compounds and albendazole *in vitro* and *in vivo* experiments.

RESULTS

GC- mass spectrum

Alkaloid extract

In the present study, two peaks were detected by the GC-Mass analysis as a results of alkaloidal component analysis (Figure 4): Pyridine, 2, 3, 4, 5 - tetrahydro with R.T. 26.187 min and molecular weight 83 killo Dalton (kd), and the other compound was N-methyl- propylamine with R.T 26.289 min and amolecular weight of 73 kd (Figure 5).

Ethylacetate extract of *C. crispata*

The GC-mass spectrum of ethylacetate extract revealed the presence of 17 peaks as shown in Figure 6. The results indicate that the compounds were arranged as 2-(N, N- dimethylhydrazino) cyclohexanecarbonitrile which consist of 8.77% (R.T. 20.59 min) of the total extract followed by Triazolo [1, 5-a] pyrimidine carboxylic acid (7.25%) (Figure 7).

Experimental infection with hydatid cysts

The examination of experimentally infected males Balb/C mice with protoscolices, 1,2,3,4, and 6 months-post infection revealed the presence of hydatid cysts in liver, spleen, mesenteries, kidneys and lungs (Plates 1 and 2).

In vivo effects of the extracts on the weight of infected and treated mice:

Weight of the negative control group, positive group, and the treated groups of mice were checked. Results show that the weight of the positive control group weighted about 40.2 g, while the weight of the negative control group was 32.64 g and the weight of treated group with albendazole was 31.4 g. The T1 group showed 34 g of weight compared with T2 (33.8g) groups. Table 2 shows the weight of organs for each group.

In vivo activity of extracts on the number of hydatid cysts compared with albendazole

The number of hydatid cysts was decreased after the treatment with extracts of C*. crispata.* The number of hydatid cysts in spleen, lung and kidney was decreased to zero; this result is similar to those of other groups of mice treated with albendazole. Mesenteries and liver had a higher number of hydatid cysts than other organs for the positive control group (6 and 7.1 hydatid cysts) and they decreased after treatment with bioactive chemical compounds from *C. crispata* and albendazole (Table 3 and Plate 3A, B and C).

The results of the *in vivo* activity of the extract on the number of hydatid cysts of infected mice showed significant differences between groups treated with extracts and the positive control group compared with the group treated with albendazole. In T2 group, the percent number of hydatid cysts recorded 59.86% while the T1 group it was 48.6%, since the number of hydatid cysts reduced from 15.2 in the positive control group to 6.1 and 7.8 respectively in T2 and T1 groups. These results almost corresponded with the effective dose of albendazole (61.18%) compared with the T2 group and are slightly different from T1 group (Table 3).

In vivo activity of extracts on dimiter and weight of hydatid cysts compared with albendazole

The mean of hydatid cysts diameters was 8.2 mm for

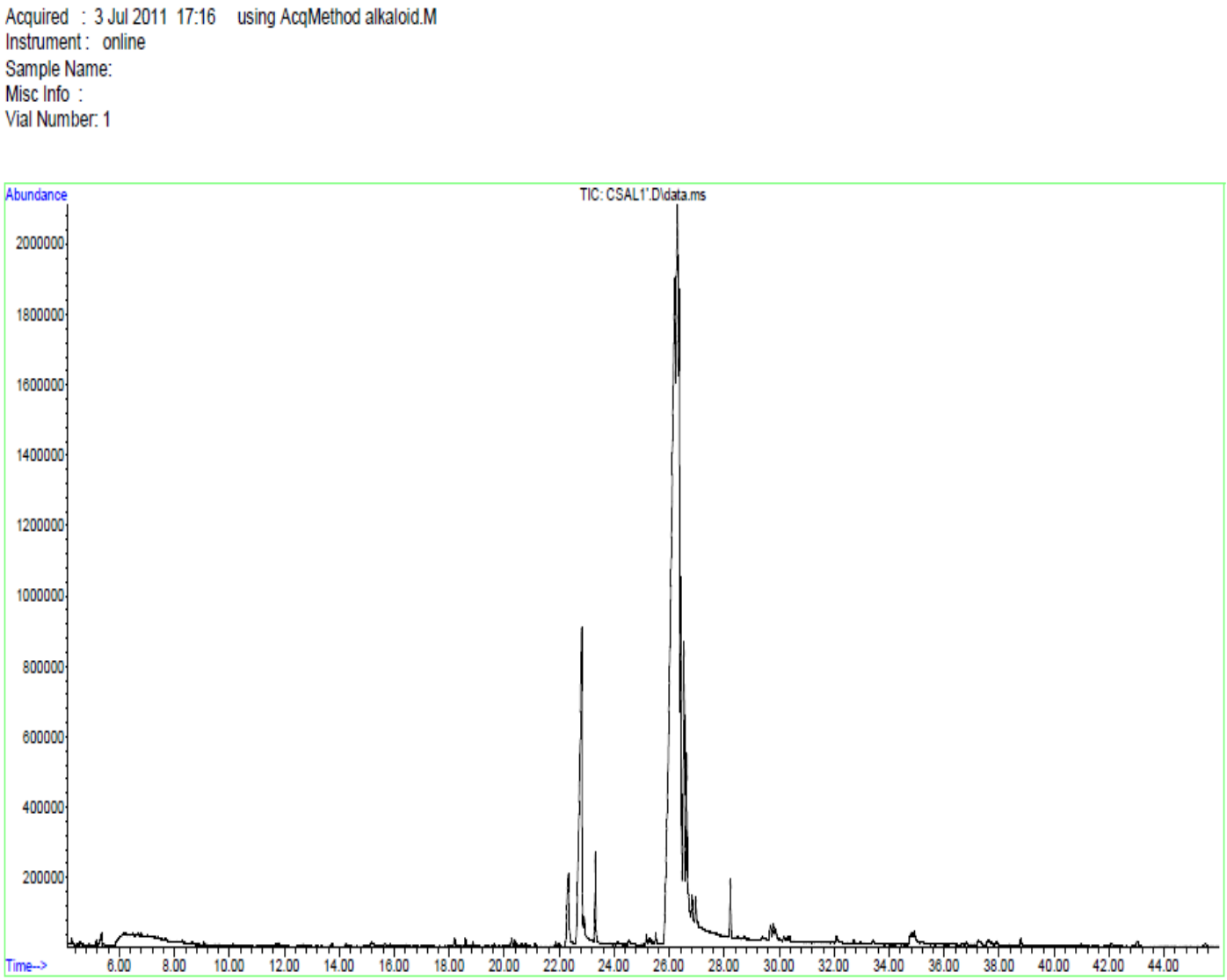

Figure 4. GC-Mass spectrum of alkaloid components of *C. crispata.*

the positive control group and was reduced to 4.2 mm in the group treated with albendazole, 4.6 mm in the T2 group, and 6.1 mm for the T1 group (Table 4, Plates 4A, B, C and 5). The weight of hydatid cysts was also studied for each group treated with the bioactive chemical compounds extracted from *C. crispata* as well as the group treated with albendazole. These results show a decrease in weight of hydatid cysts of the T2 group (0.55 g) and (0.63 g) in the T1 group compared with the group treated with albendazole recording 0.53 g where positive control group was 1.22 g in mean.

DISCUSSION

The current study demonstrated that the weights of infected experimental mice examined at 6th months - post infection, were increased compared with the negative control group. The weights of liver and spleen were also increased. On the other hand, there were slight increases in the weight of kidneys and lungs (Table 2). These results agree with those of other studies (Al-Nasiri, 2006; Al-Mobarek, 2006; Barzanjietal, 2009 and Al-Humairy, 2010). There was a significant difference of weights and diameters among the hydatid cysts of organs (livers, spleens, kidneys, lungs and mesenteries). Hepato-spleenomegaly caused by the parasite lead to an increase in weights of the experimental animals and their organs. However, many studies have explained the reasons of the increase in the weight of the organs infected with the hydatid cyst. Lightowlers et al. (2003)

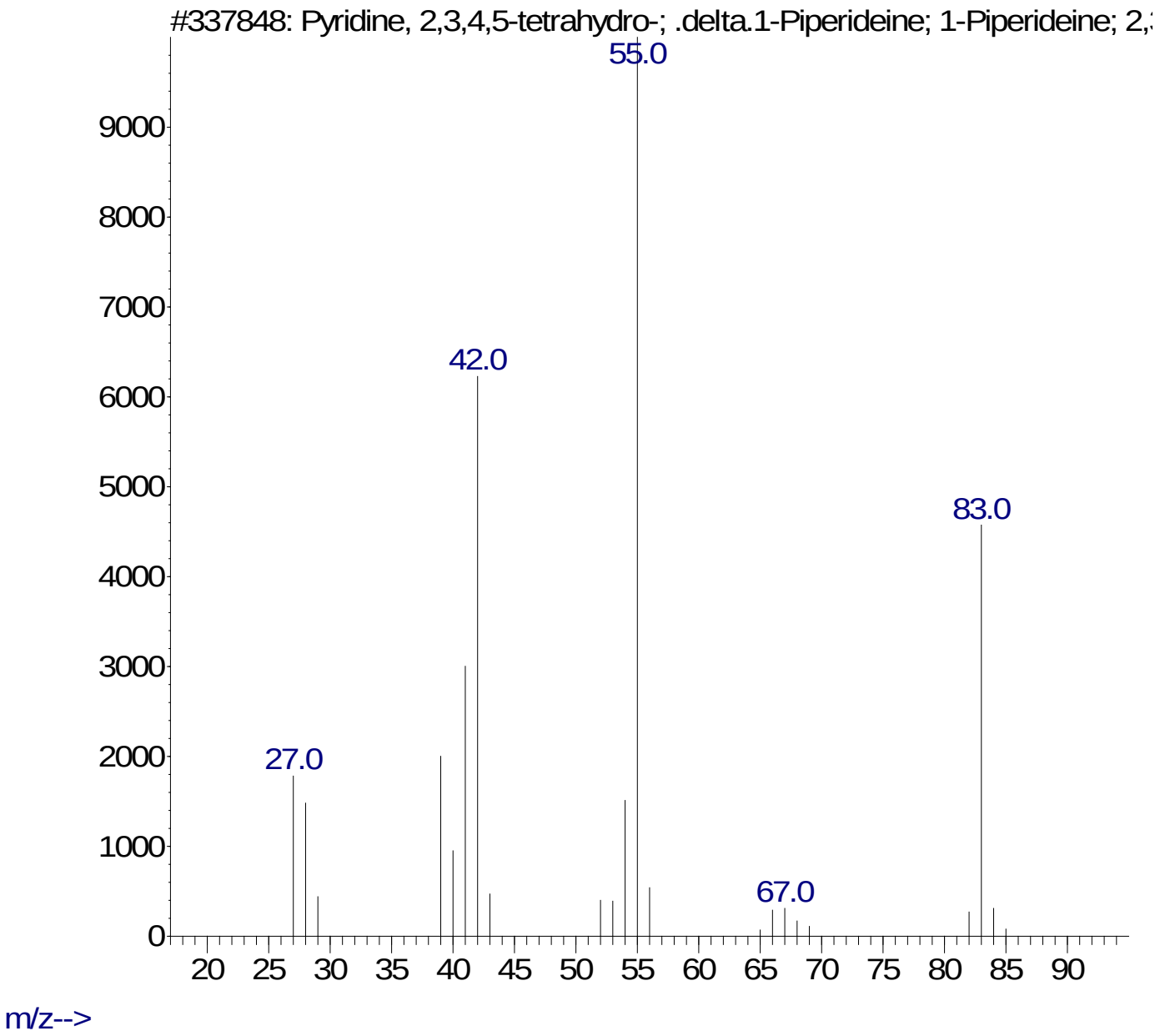

Figure 5. Mass spectrum of pyridine, 2,3,4,5 - tetrahydro.

concluded that the increase in liver and lungs weight was due to the formation of granuloma the increase in the immune cell and its migration to the target organ, so the ability of spleen to produce lymphocyte to secrete specific antibody had led to the increase of the spleen weights. The weights and diameters of hydatid cysts reported in the present study were affected by parasite infection because the weight decreased and approached the values of the negative control group especially in T2 group. The decrease in weight can be explained in relation to the decrease of number of hydatid cysts and calcification with the sloughing of the germinal layer and the disintegration of laminated layer (Maizeles and Yazdanbakhsh, 2003). However the complex layer of cyst

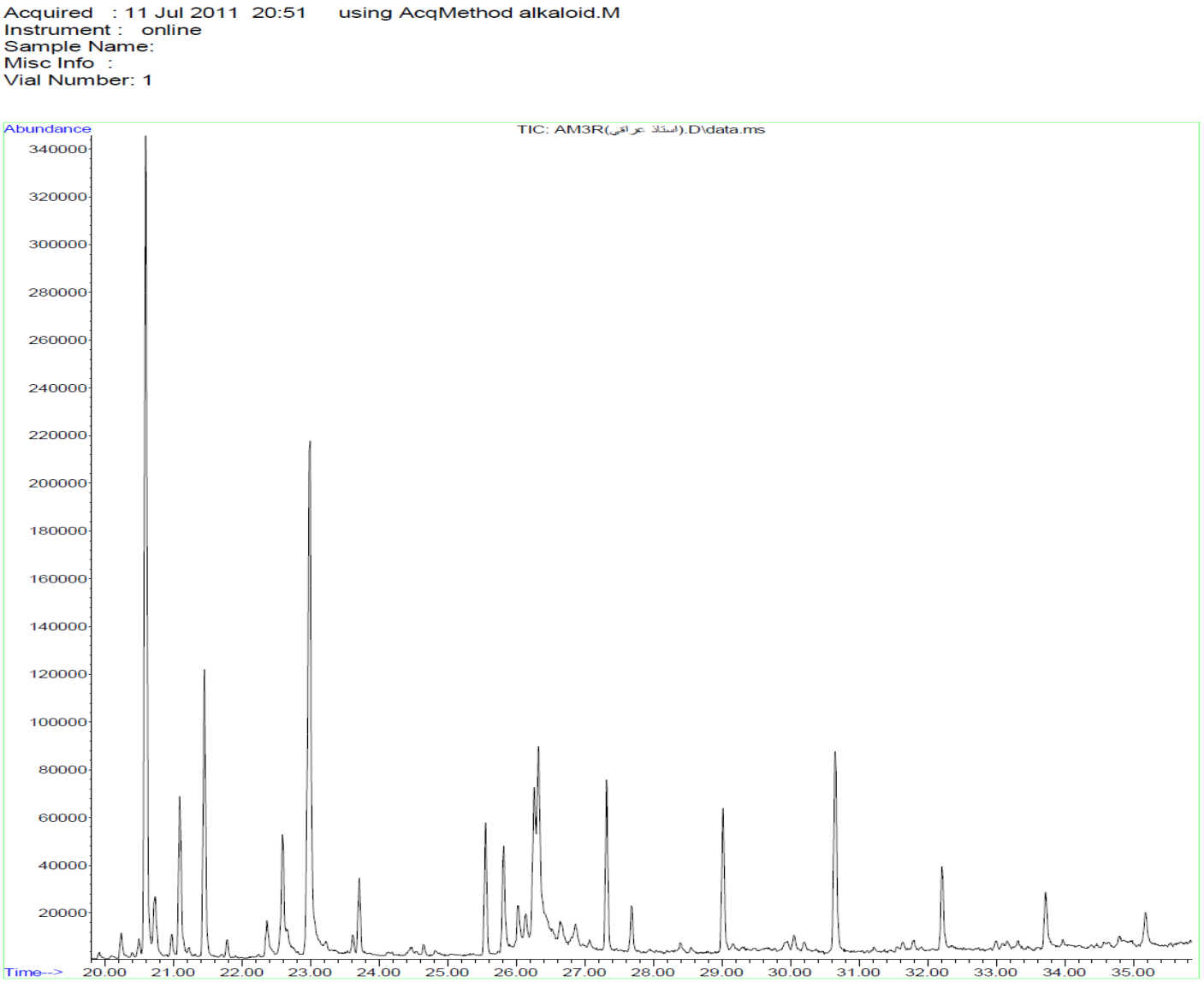

Figure 6. GC spectrum of ethylacetate extract of *C. crispata*.

has an important role in the transformation of nutritional material from serum to cyst. The knowledge of the parasite nutrition behavior can help for a drug treatment of the inoperative cyst via the selection of the effective drug and adhere them to biological material that promote distribution of drug to the cyst (Rahda et al., 2008). Compared to the bioactive chemical compounds, albendazole decreases the weights of infected testes animals more than those of the negative control group.

It is difficult to speculate the mechanism by which these bioactive compounds act as parasitic agents. In this regard, Sepulveda-Boza and Cassels (1996) suggested that many bioactive chemical compounds exhibited their parasitecidal activity by virtue of their interference with the redox balance of the parasites, acting either on the respiratory chain or the cellular defenses against oxidative stress.

It is also known that some bioactive compounds act by binding with the DNA of the parasite. For example, dihydroorotate dehy-drogenase (DHOD), the fourth enzyme in the *de novo* pyrimidine biosynthetic pathway, is essential to parasites, including the electron acceptor capacity and cellular localization (Nara et al., 2000). In this way, it has been recently demonstrated that the methanol extracts of brown algae *Ishige okamurae*, *F. evanescens* and *P. bingtonil* contain potent noncompetitive inhibitors against *Trypanosoma cruzi* DHOD (Takeaki et al., 2003; Nara et al., 2000).

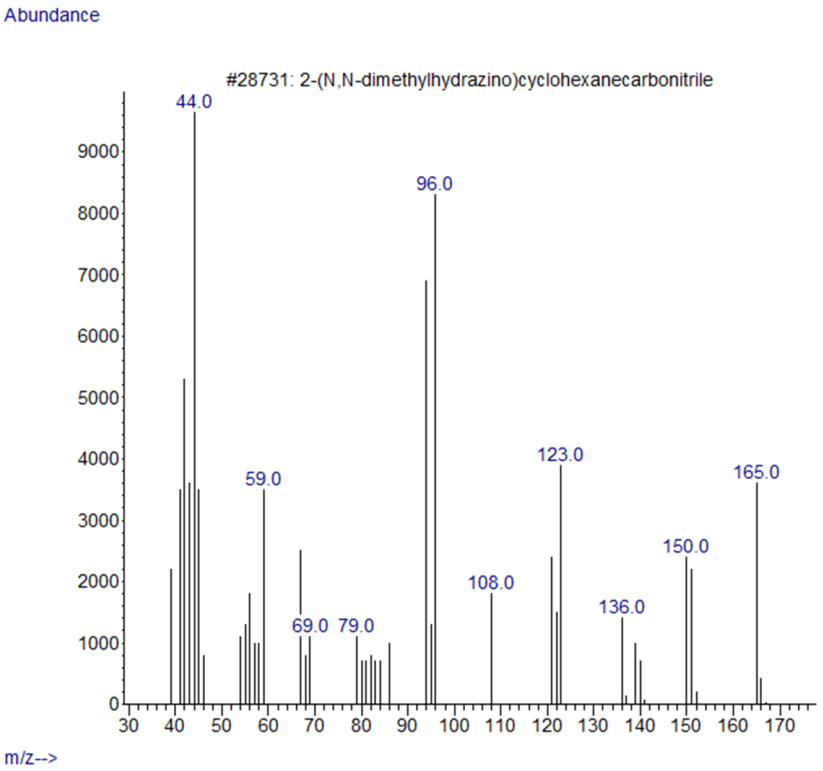

Figure 7. Mass spectrum of 2-(N,N-didimethylhydrazino) cyclohexanecarbonitrile.

Plate 1. Pictures of experimentally infected mice. (A) mice with 4 months. (B, C, D) mice with 6 months after infection.

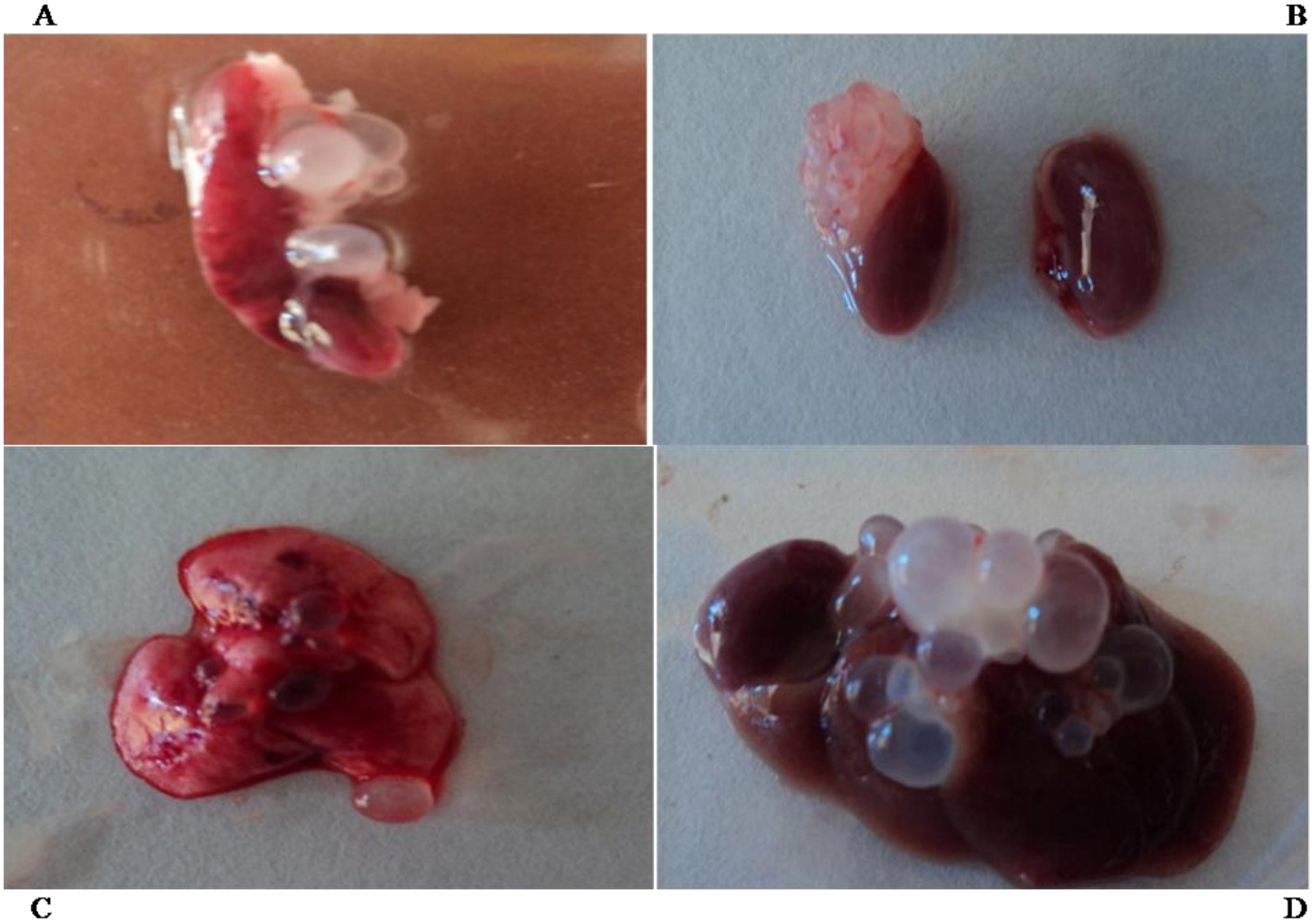

Plate 2. Pictures of infected mice organs at 6-months-post infection. A. Spleen. B. Kidney. C. Lung. D. Liver.

Table 2. Mean of weight of mice and organs treated with extracts compared with albendazole.

Group	Dose	Mean of weight/g				
		Liver	Mice	Spleen	Kidney	Lung
	280	34.8±1.527*	4.3± 0.1152	0.45 ±0.057	0.22 ±0.100	0.26 ±0.07
T1 group (alkaloid of C. crispata)	300	34.2 ±1.527	4.3± 0.100	0.45 ±0.035	0.22 ±0.100	0.26 ±0.021
	330	34.0± 1.509	4.3±0.100	0.45 ±0.051	0.23 ±0.015	0.24 ±0.007
	100	33.8 ±0.453	3.7± 0.112	0.40± 0.034	0.23± 0.030	0.25± 0.005
T2 group Ethylacetate of C. crispata	110	33.8 ±1.915	3.2 ±0.091	0.37 ±0.032	0.22 ±0.024	0.25±0.004
	120	33.8 ±0.627	3.2 ±0.092	0.37 ±0.42	0. 22 ±0.0 20	0.24 ±0.008
Albendazole	500	31.4± 1.152	3.11 ±0.404	0.30 ±0.062	0. 22 ±0.005	0.23 ±0.007
Negative control		32.64 ±1.352	2.93 ±0.264	0.36 ±0.045	0.23 ±1.566	0.24 ±0.010
Positive control		40.24 ±0.956	6.7 ±0.529	0.58 ±0.450	0.27±0.251	0.28 ±0.100
LSD		1.017	0.42	0.47	0.6	0.01

Significant differences, $P \leq 0.05$, n=8 Standard deviations*.

Table 3. Mean of hydatid cysts number in treated mice and the effective dose.

Group	Dose µg/ml	Mean of hydatid cyst number in treated mice						Effective dose (%)
		Liver	kidney	Spleen	Lung	Mesenteric	Total	
T1 group	280	4.5 ± 1.000*	0 ± 0.000	0 ± 0.000	0 ± 0.000	4 ± 0.577	8.5	44.07
(alkaloid of C. crispata	300	4.5 ± 1.000	0 ± 0.000	0 ± 0.000	0 ± 0.000	4 ± 0.577	8.5	44.07
	330	4.1 ± 1.000	0 ± 0.000	0 ± 0.000	0 ± 0.000	3.8 ± 0.577	7.8	48.68
T2 group	100	4.1 ± 1.527	0 ± 0.000	0 ± 0.000	0 ± 0.000	3.12 ± 1.000	7.22	52.63
Ethylacetate of C. crispata)	110	4.1 ± 0.577	0 ± 0.000	0 ± 0.000	0 ± 0.000	2.8 ± 1.000	6.9	54.6
	120	3.6 ± 1.000	0 ± 0.000	0 ± 0.000	0 ± 0.000	2.5 ± 0.577	6.1	59.86
Albendazole	500	3.3 ± 1.000	0 ± 0.000	0.01 ± 0.000	0 ± 0.000	2.6 ± 1.000	5.91	61.18
Negative control		0 ± 0.000	0 ± 0.000	0 ± 0.000	0 ± 0.000	0 ± 0.000	0	0
positive control		6 ± 2.000	0.7 ± 0.000	1.1 ± 1.000	0.3 ± 0.000	0.7 ± 0.003	15.2	0
L.S.D.		0.89	0.39	0.95		1.63		

Significant differences, P ≤ 0.05, n=8, Standard deviations*.

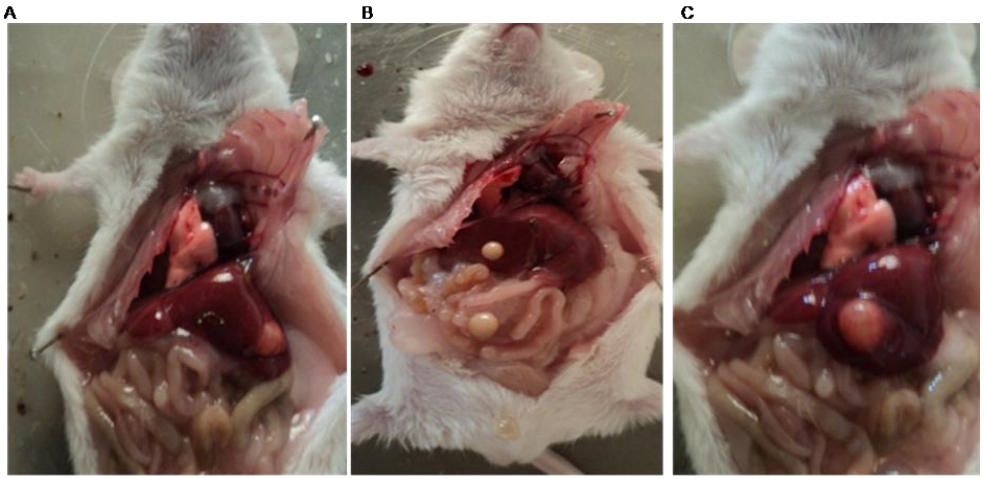

Plate 3. Pictures of treated mice. (A) T2 treated group. (B) Treated with albendazole. (C) T1 treated group in which the numbers, diameters, cysts fluids of hydatid cysts were reduced.

Table 4. Mean of diameter and weight of hydatid cysts of treated mice with bioactive chemical compound.

Group	Dose µg/ml	Mean of diameter/mm	Mean of weight/g
	280	7.4 ± 0.534*	0.75 ±0.055
T1 group (alkaloid of C. crispata	300	7.0 ± 0.64	0.66 ± 0.61
	330	6.1 ± 0.64	0.63 ± 0.069
	100	5.32 ± 0.517	0.67 ± 0.034
T2 group (Ethylacetate of C. crispata)	110	5.1 ± 1.06	0.61 ± 0.045
	120	4.6 ± 0.925	0.55 ± 0.016
Albendazole	500	4.2 ± 0.744	0.53 ± 0.034
Positive control		8.2 ± 1.724	1.22 ± 1.02
L.S.D.		0.908	0.55

Significant differences, P ≤ 0.05, n=8, *rd Standard deviation

Plate 4. Pictures of treated organs of infected mice with hydatid cysts. (A) Liver from mice treated with 500 µg/ml of albendazole. (B) Liver from mice treated with 120 µg/ml of T4 group.

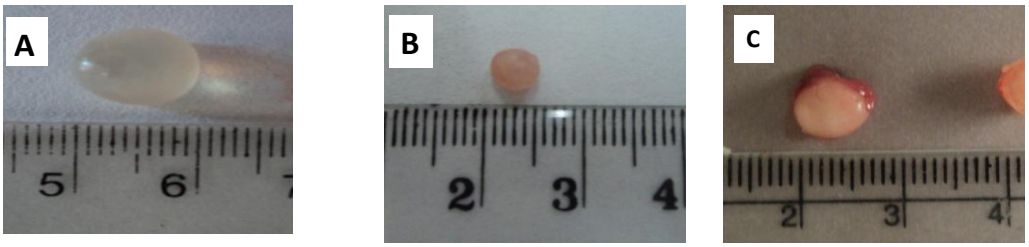

Plate 5. Pictures of hydatid cysts. (A) Positive control. (B) Hydatid cyst treated with albendazole. (C) Hydatid cyst of T2 group.

Conclusions

Overall results of the present study concluded that ethyl acetate extract is more active than alkaloid extract. The bioactive chemical compounds and albendazol decreased the weight of infected animals, and further the weight of organs (liver, spleen, kidney, lung, mesentery), and weight, number and diameter of hydatid cysts more than that of the negative control groups.

Conflict of Interest

The author(s) have not declared any conflict of interest.

REFERENCES

Akhan O, Ensari S, Ozmen M (2002). Precutaneous treatment of a period gland hydatidcyst . Eur. Radial. 12:597-599.

Al- Humairy A (2010). Evaluation of the activity *Daturastramonium* seeds extracts on growth and development of hydatid cysts for

echinococcusgranulosus in white mice Balb/c (Therapeutic, Histologic and Immunologic Study) PhD Thesis. College of Science, Kufa University.
Al-Mobarek ZA (2006). Effect of peel extracts of *Punica* fruits on onechinococcosis of *Echinococcus granulosus*. MSc. Thesis, College of Education, Kufa University.
Al-Nasiri AA (2010). Isolation and Identification of some active compounds from the green alga *Cladophoracrispata* with their bioactivity test. MSc. Thesis, College of Education, University of Basrah.
Al-Nasiri FS (2006). Biological and immunological study of hydatid cyst formation in albino mice. PhD Thesis, College of Education, University of Baghdad.
Aslan M, Saribas S, polat, E, Cakan H, Yuksel P, Zengin K, Arikan S, Alioner Y, Torun M, Kocazeybek B (2009). Can cystic echinococcosis trigger autoimmunity. Afr. J. Microbiol. Res. 3:787-790.
Athbi A, Ali D, Salman Al-Lafta, Noory A (2011). Determination of total proteins and some amino acids in green alga *Chlorella vulgaris*. J. Thi-Qar. Edu. 5(1):224-234.
Barzinji AK, Mothana R, Nasher A (2009). Effect of leaf extracts of *Dendrosicyos socotranaand Jatropha unicostataon* the viability of *Echinococcus granulosusprotoscolices*. Eur. Asia .J. Bio.Sci. 3:122-129.
Calixto JB, Beirith A, Ferreir J, Santos A, Cechenial V, Yunes R (2000). Naturally occurring antinociceptive substance from plants. Phytother. Res. 14:401-418.
Carrol A, Veiry C, Vick M (2007). Leptoclinidamines A indol alkaloid from the Australian ascidian Leptoclinide drug. 15:498-505
Dar FK, Alkarmi T (1997). Public health aspects of cystic echinococcosis in the Arab countries Acta. Tropica. 67:125-132.
Everton T, Paysianne P, Aline G, Diogo J, Anansa B, Elian A, Vitor P, George E, Joao A, Maria C, Oliveira C, Magna S (2009). The Antinociceptive and anti-inflammatory activites of caulerpin a BisindoleAlkaloid. Isolated from seaweeds of the Genus *Caulerpa* sp. Mar. Drugs. 7:689-704.
Fenical W, Paul V (1984). Antimicrobial and cytotoxic terpenoids from tropical green algae of the family Udoteaceae Hydrobiologia. 116-117:135-140
Georgopoulos S, Korres S, Riga M, Ferekidis E (2007). Hydatid cyst in the bile duct of the submandibular gland. Int. J. Oral. Surg. 36:177-179.
Ghasemi Y, Tabatabei Yazdi, Shafiee A, Amini M, Shokravi Sh, Zarini G (2004). Parsiguine, A novel antimicrobial substance from *Fischerella ambigua*. Pharm. Biol. 2:318-322.
Kladi M, Vagias C, Stavri M, Rahman M, Gibbons S, Roussis V (2008). C15 acetogenins with antistaphylococcal activity from the red alga *Laurencia glandulifera Phytochem.* Lett. 1, 31-36.
Leon-Deniz A, Eric D, Moo-Puc R, Freile-Pelegrin Y (2009). Antitrypanosomal*in vitro* activity of tropical marine algae extracts. Pharmaceutical Biology 47(9):864-871.
Lightowlers MW, Colebrook A, Gauci C, Gauci S, Kyngdon C, Monkhouse J, Rodriquez C, Read A, Rolfe R, Sato C (2003). Vaccination against cestode parasites: anti-helminth vaccines that work and why. Veter. Parasitol. 115:83-123.
Litchfield JT, Wilcoxon F (1949). A simplified method of evaluating dose effect experiments. J. Pharmacol. Exp. Therap. 96:94-113.
Lorena V. León-Deniz, Eric Dumonteil, Rosa Moo-Puc and Yolanda Freile-Pelegrin (2009). Antitrypanosomal *in vitro* activity of tropical marine algae extracts. Pharmaceut. Biol. 47(9):864-871.
Maizeles RM, Yazdanbakhsh M (2003). Immune regulation by Helminth parasites: Cellular and molecular mechanisms. Nature Rev. Immunolo. 3:733-744.
McManus DP, Zhang L, Castrodale L, Pearson M, Blair D (2002). Short report: molecular genetics characterization of an unusually severe case of hydatid disease in Alaska caused by the cervid strain of *Echinococcus granulosus*. Am. J. Tro. Med. Hyg. 67:296-298.
Metting B, Pyne J (1986). Biologically active compounds from microalgae. Enzyme Microb. Tech. 8:386-394.
Molera M, Semesi A (1996). Antimicrobial activity of extracts from six green algae from Tanzania. Curr. Trends. Mar. Bot. Res. East Afr. Reg. 211-217.
Moraitaki P, Roussi P, Emmanouil Y, Pechlivanidou R, Bitsakou C, Konstantinou M, Marosis K (2010). Pulmonary echinococcosis presenting as a pulmonary mass with fever and haemoptysis, a case report. Pneumon. J. 23(2):180-183.
Morar R, Feldman C (2005). Pulmonary echinococcosis. Eur. Resp. J. 21:1069-1077.
Nara T, Kamei Y, Tsubouchi A, Annoura T, Hirota K, Lizumi K, Dohmoto Y, Aoki T .(2000). Inhibitory action of marine algae extracts on the *Trypanosoma cruzidihydroorotate* dehydrogenase activity and on the protozoan growth in mammalian cells. Parasitol. Int. 54:59-64.
Orhan I, Sener B, Atici T, Brun R, Perozzo R, Tasdemir D (2006). Turkish freshwater and marine macrophyte extracts show *in vitro* antiprotozoal activity and inhibit FabI, a key enzyme of *Plasmodium falciparum* fatty acid biosynthesis. Phytomedicine 13:388-393.
Parija SC, Sheela D (1999). Current concepts in the diagnosis of cystic echinococcosis in humans and livestocks and intestinal echinococcosis in canine hosts. J. vet. Parasit. 13:93-102.
Prescott G, (1975). Algae of the Western Great lake aria 6th ed. William, C. Brown Co. Publisher Dubugue Towa, 977 pp.
Radwan M, Ragab E, Sabry N, El-Shenawy S (2007). Synthesis and biological evalution of new 3-substituted indole derivatives as potential anti-inflammatory and analgesic agents Biol. Med. Chem. 15:3832-3841.
Rahdar M, Maraghi S, Rafei M, Razijalali M (2008). Comparison of some electrolytes in hydatid cyst fluid and serum of liver hydatidosis of sheep. Jundishapur J. Micro. 1(1):10-14
Reichelt JL, Borowitzka MA (1984). Antimicrobial activity from marine algae: Results of a large-scale screening programme. Hydrobiology 116/117:158-168.
Sant Anna CL, Azevedo De, Senna P, Komarek J, Komarkova J (2004). Planktic cyanobacteria from Sao Paulo State, Brazil: Chlorococcales. Revista Brasil Bot. 27:31-327.
Sepulveda-Boza S, Cassels BK (1996): Plant metabolites active against *Trypanosoma cruzi*. Planta Med. 62:98-105.
Smith AJ (2004). Medicinal and pharmaceutical uses of seaweed natural products: A review. J. Appl. Phycol. 16:245-262.
Smyth JD, Barrett N (1980). Procedure for testing the viability of human hydatid cysts following surgical removal, especially after chemotherapy. Trans. Roy. Soci. Trop. Med. Hyg. 74(5):649-652.
Stein JR (1975). Handbook of phycological methods. Cambridge University. Press, Cambridge, UK. 448 pp.
Takeaki O, Ryuta T, Takeshi N, Takashi A, Yuto K (2003). Screening for anti- *Trypanosoma cruzi* dihydroorotate dehygrogenase from marine algae collected from Japanese coasts. Coast Bioenviron 2:67-76.
Taran M, Azizi E, Shikhvaisi A, Asadi N (2009). The Anthelmintic Effect of *Pistacia khinjuk Against* Against Protoscoleces of *Echinococcus granulosus.* World J. Zoo. 4:291-295.
Topcu G, Anydoqmus Z, Imre S, Goren A, Pezzuto J, Clement J, and Kingston D, (2003). Brominated sesquiterpenes from the red alga *Laurencia obtusa*. J. Nat. Prod. 66:1505-1508.

academicJournals

Vol. 13(30), pp. 3081-3091, 23 July, 2014
DOI: 10.5897/AJB2014.13796
Article Number: C042BBA46224
ISSN 1684-5315

http://www.academicjournals.org/AJB

African Journal of Biotechnology

Full Length Research Paper

Binding properties of beetal recombinant caprine growth hormone to Bovidae liver microsomal membranes

Roquyya Gul[1,5]*, Rabail Alam[2], Mahjabeen Saleem[3], Mohammad Ali[1], Sumble Mehmood[4] and Muhammed Waheed Akhtar[1]

[1]School of Biological Sciences, University of the Punjab, Lahore, Pakistan.
[2]Institute of Molecular Biology and Biotechnology, the University of Lahore, Lahore, Pakistan.
[3]Institute of Biochemistry and Biotechnology, University of the Punjab, Lahore, Pakistan.
[4]INMOL Hospital, Lahore, Pakistan.
[5]The University of Lahore, Defense Road, Lahore, Pakistan.

Received 15 March, 2014; Accepted 20 June, 2014

The aim of the study was to illustrate the radio-receptor assay of beetal recombinant caprine growth hormone (rcGH). Tracer (^{125}I-rcGH) was prepared by iodinating beetal rcGH with iodine-125 and its biological activity was analyzed by rabbit anti-rcGH antibodies. Liver microsomal membranes of the Bovidae species (caprine, ovine and bovine) were prepared to study the binding properties of beetal rcGH. The tracer binding was dependent on receptor protein concentration, tracer counts, temperature, time of incubation and assay pH. The maximum percentage specific binding of the tracer to the microsomal membrane was 45% in 32 h at 4°C. In cross-reactive study, human GH competed and displaced the ^{125}I-rcGH by binding effectively to the cGH receptor. Scatchard analysis of the rcGH binding suggested a single class of binding site to the caprine microsomal membrane with an affinity of 337.1 ± 82.94 × 10^9 M^{-1} and capacity of 57.61 ± 4.23 fmol mg^{-1} while rcGH binding affinity and capacity to the ovine and bovine receptor protein showed 365.4 ± 66.82 × 10^9 M^{-1}, 57.69 ± 3.23 (fmol mg^{-1}) and 392.6 ± 56.25 × 10^9 M^{-1}, 56.8 ± 2.56 (fmol mg^{-1}) respectively. This study provides data for beetal rcGH interaction with microsomal membrane that shall be beneficial to study hormone receptor interactions of other Bovidae species.

Key words: Beetal recombinant caprine growth hormone, Bovidae, iodine-125, microsomal membrane, receptor protein.

INTRODUCTION

Growth hormone (GH) a 22 kDa polypeptide is produced by somatotroph cells of the anterior pituitary gland and its mode of action is widespread (Edmondson et al., 2003). It is accepted that receptors for the GH are widely occurring on the cell membrane and crude membrane preparations of various tissues (Posner et al., 1974). But the most specific binding site for the GH is the liver, where it acts and ultimately produces insulin-like growth

factors (IGF-I and II), which targets other tissues of the body (adipose tissues, bones, muscles) thus leading to cell proliferation and increases the protein, lipid and carbohydrate metabolism (Leung and Ho, 2001).

The initial step in studying the mechanism of signal transduction of a hormone (Piwien-Pilipuk et al., 2002) and its receptor protein (Alves dos Santos et al., 2001) is to explore the hormone-receptor characteristics. Several works have been done on the characterization of human GH (Herington et al., 1976; Cadman and Wallis, 1981), Bovidae GHs (Wingfield et al., 1987; Sami et al., 2008) and on GH receptors (Waters and Friesen, 1979; Jiang et al., 1999; Connor et al., 2002). Bovidae, a family of artiodactyla contains 140 species (Grubb, 1993) and has 10 known subfamilies (Allard et al., 1992; Grubb, 2005). Out of these subfamilies, two are extensively documented that is, bovinae (for example, cattle, bison, and buffalos) and caprinae (for example, sheep, goat) (Maj and Zwierzchowski, 2006). One of the breed of caprinae is beetal; which is widely present in South Asian countries including Pakistan. It has a great potential of milk production and may play the leading role in enhancing the economy of the country by producing milk and meat. It is reported that milk and meat production of the livestock can be improved by exogenous administration of the GH (Bauman, 1999). By the use of genetic engineering, recombinant growth hormone (rGH) has shown its importance in cattle to increase their milk and meat production (Machin, 1973). In the family Bovidae, the percentage homology of caprine GH with the mammalian GHs is high that is, ovine (100%), bovine and *Bubalus bubalis* (99%), porcine (92%), rat (87%) and human (66%).

The current study shares the possible of understanding the receptor binding characteristics of recombinant beetal caprine GH. These findings would eventually contribute the valuable information regarding the Bovidae GH system and ultimately lead to explore and comprehend the hormone-receptor interaction.

MATERIALS AND METHODS

Liver samples of Bovidae species (bovine, caprine and ovine) were freshly collected from a local abattoir (Lahore, Pakistan). The liver samples were sliced into 10 × 20 mm pieces, immediately frozen in liquid nitrogen and stored at -80°C till further analysis. Chemicals / reagents used in this study were of the highest purity grade commercially available from Sigma-Aldrich. Free ^{125}I-sodium iodide-37MBq was purchased from Amersham, GE Healthcare (1mCi, carrier free). Recombinant beetal cGH was produced in the laboratory (School of Biological Sciences, University of the Punjab, Lahore, Pakistan) and human GH (hGH) used for the cross reactive study was a gift from NETRIA, UK. Rabbit anti-rcGH antibodies were raised against beetal rcGH in a local animal house.

Iodination of rcGH

Iodination of rcGH was done by chloramine-T method (Edwards, 1999). For the purification of the iodinated rcGH or tracer (^{125}I-rcGH), 0.05 M phosphate buffer pH 7.4 (1% BSA and 1% potassium iodide) was used as a carrier (Herington et al., 1976; Edwards, 1999). Gel exclusion chromatography was done to remove the unchanged I^- from the conjugated rcGH (^{125}I-rcGH). Chromatographic column (30 × 0.9 cm) was packed with Sephacryl S300 and equilibrated with elution (0.05 M phosphate buffer pH 7.4 containing 0.01% NaN_3) at a flow rate of 6 ml h^{-1}. Tracer was loaded on the column and 1 ml fractions were collected at flow rate of 3 ml h^{-1} adjusted by peristaltic pump (Amersham, GE Healthcare, Pump-P1). Radioactivity of each fraction was checked by gamma counter (LB2111, Berthold Technologies GmbH & Co. KG) and chromatogram was plotted between the number of fractions and counts per 30 s.

Analysis of the tracer (^{125}I-rcGH)

The binding of the ^{125}I-rcGH was analyzed by using rabbit anti-rcGH antibodies. Total number of counts of ^{125}I-rcGH (200 c.p.m. μl^{-1}) was made in an assay buffer (0.05 M phosphate buffer, pH 7.4). Rabbit anti-rcGH antibodies were diluted (1: 100, 1: 1K & 1: 10K) and 100 µl of each antibody dilution, 200 µl assay buffer and 100 µl tracer (200 c.p.m. μl^{-1}) were added in the tubes (duplicates), and incubated for 4 h at room temperature. Reaction was stopped by adding 1 ml of ice cold assay buffer, followed by 1 ml of 25% (w/v) PEG 6000.

Suspension was mixed and centrifuged at 3,000×*g* at 4°C for 30 min. Supernatant was decanted and radioactivity of the pellet as total binding (TB) of the tracer was checked by gamma counter. Non-specific binding (NSB) or control was determined by adding 200 µl of assay buffer and 100 µl tracer. Specific binding was calculated by subtracting non-specific binding (NSB) from total binding (TB) (Cadman and Wallis, 1981). 1% BSA (20 $\mu g ml^{-1}$) was added in the purified tracer and aliquots were stored at -20°C.

Preparation of microsomal membrane (receptor protein)

The crude microsomal membranes were prepared from the livers of slaughtered Bovidae species (caprine, ovine and bovine) according to the method described by Rad cliff (Rad cliff et al., 2003). Approximately 2.0 g of liver pieces (10 × 20 mm) were homogenized in ice cold 0.025 M Tris-HCl buffer pH 7.8 containing 0.3 M sucrose, 0.01M EDTA, 0.01M EGTA (ethylene glyco-bis [β-aminoethyl ether]-N,N,N′,N′-tetraacetic acid) and 0.001 M PMSF (phenylmethyl sulfonyl fluoride) by using Polytron tissue homogenizer (Brinkmann Instruments, Westbury, NY). The homogenate was centrifuged at 11,000 x *g*, 4°C for 20 min to remove the tissue fragments. The supernatant was transferred to clean tube and volume was adjusted to 30 ml and was further centrifuged at 100,000 x *g*, 4°C for 120 min. The supernatant was discarded and pellet was homogenized in 0.025 M Tris-HCl buffer pH 7.8 containing 0.01 M calcium chloride. Aliquots were made and

*Corresponding author. E-mail: roquyya@yahoo.com, ruqayya.gul@imbb.uol.edu.pk. Tel: 0092 423004177639.

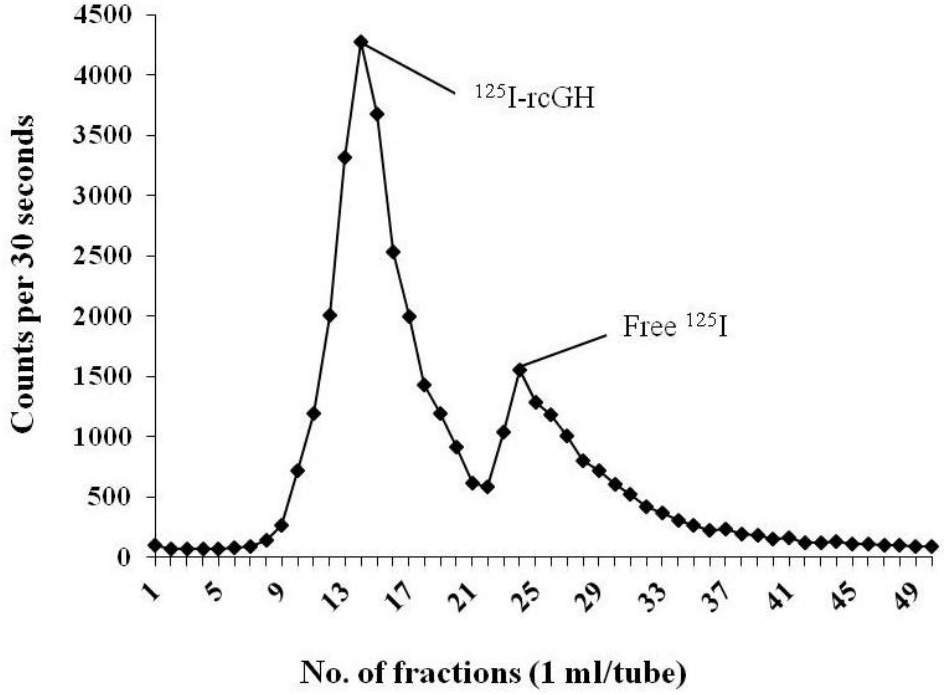

Figure 1. Chromatographic profile of the tracer (^{125}I-rcGH). Purification of the tracer by gel exclusion chromatography (Sephacryl S-300 packed column 30 × 0.9 cm). Two peaks were obtained; big and small peak showing the purified tracer and free ^{125}I, respectively.

stored at -80°C up till analysis. The protein estimation of the microsomal membranes (also known as membrane bound receptors) was measured by Bradford method (Bradford, 1976).

Factors affecting the binding of the tracer to receptor protein

The radio-receptor assay of the rcGH was set in triplicates and the method was based on previously described protocol by Cadman and Wallis, (1981). Factors affecting the binding of the tracer to receptor protein such as effect of receptor protein concentrations, tracer counts, temperature, time of incubation, assay pH and binding to different Bovidae receptor proteins (caprine, ovine and bovine) were studied. Cross reactivity of the tracer was investigated in the presence of unlabeled rcGH and human GH. Scatchard analysis of rcGH binding to Bovidae receptors was analyzed by Prism statistical program provided by Graph Pad I (Manson, 1990).

RESULTS AND DISCUSSION

Preparation of ^{125}I-rcGH

Preparation of the tracer is a primary step for the characterization of beetal rcGH by radio-receptor assay. There are number of methods by which iodination of a protein is done (Edwards, 1999). In the current study, rcGH was iodinated by chloramine-T method (Herington et al., 1976); previously GH has been iodinated by iodogen method (Cadman and Wallis, 1981) and by lactoperoxidase method (Tsushima and Friesen, 1973). Gel exclusion chromatography was carried out to remove the free iodine (I^-) from the labeled rcGH (^{125}I-rcGH). Total 50 fractions were collected and radioactivity of each fraction was checked by gamma counter. Chromatographic profile is shown in Figure 1. Two peaks were obtained; big and small peak represented the purified ^{125}I-rcGH and free ^{125}I, respectively. From total of 50 fractions, fraction no. 11-19 were pooled and their binding activity was analyzed by using different dilutions of rabbit anti-rcGH antibodies. The maximum binding was obtained at 1: 100 dilution of the antibody, however, the binding was decreased with the increase in the dilution of the antibody (Table 1). This gave the idea that the tracer was in working condition or rcGH was not damaged during the iodination process (Edwards, 1999).

Preparation of microsomal membrane (receptor protein)

For the receptor assay, another important step is the preparation of the microsomal membrane or receptor protein. These membranes play significant role in learning protein-protein and lipid-protein interactions and understanding their functional properties for membrane bound enzymes. It is commonly accepted that polypeptide hormone receptors are associated with the cell or

Table 1. Analysis of the tracer (^{125}I-rcGH): total binding (TB), non-specific binding (NSB) and specific binding of the tracer at different rabbit anti-rcGH antibody dilutions.

Antibody dilution	TB	NSB	Specific binding = TB - NSB
1: 100	13,904	180	13724
1: 1K	7712	183	7529
1: 10K	3320	180	3140

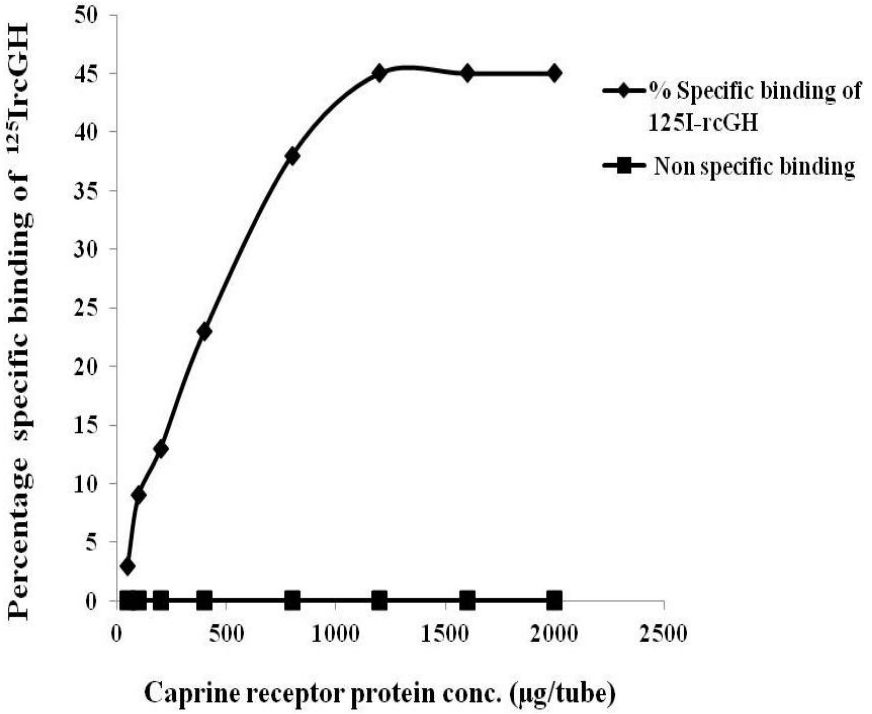

Figure 2. Effect of binding of the tracer (^{125}I-rcGH) to caprine receptor protein. Tracer (50,000 c.p.m.) and different receptor protein concentrations used per assay tube and maximum 45% specific binding (◆) of the tracer is shown at 1200 µg of the receptor protein and non-specific binding (■) is shown at 0% at all protein concentrations.

plasma membranes of various tissues like liver, lungs, mammary glands etc. (Labbe et al., 1992), however liver microsomal membrane fraction exhibit highest binding affinity for the GH (Herington et al., 1976). Therefore, crude microsomal membranes were prepared from fresh liver tissues of the Bovidae species (caprine, ovine and bovine) to investigate the rcGH biological activity that is, whether the recombinantly produced caprine GH is functionally active.

Effect of different factors on ^{125}I-rcGH binding

Effect of receptor protein concentration

To study the effect of binding of ^{125}I-rcGH to the caprine receptor protein concentrations (50, 100, 200, 400, 800, 1200, 1600 and 2000 µg), assay was set. The receptor proteins were incubated with 50,000 c.p.m. of ^{125}I-rcGH for 24 h at 4°C and then centrifuged to separate the bound and unbound ^{125}I-rcGH.

The maximum binding of ^{125}I-rcGH occurred at the concentration of 1200 µg receptor protein, however, further increase or decrease in protein concentration had no significant effect on the specific binding of the ^{125}I-rcGH to the caprine receptor protein as shown in Figure 2. Since maximal binding was observed at 1200 µg, this receptor protein concentration was therefore selected to perform subsequent experiments. Contrary to this, specific binding of the ^{125}I-rbGH (iodinated recombinant bovine GH) was shown to be 48% with the crude receptor membrane (Haro et al., 1984).

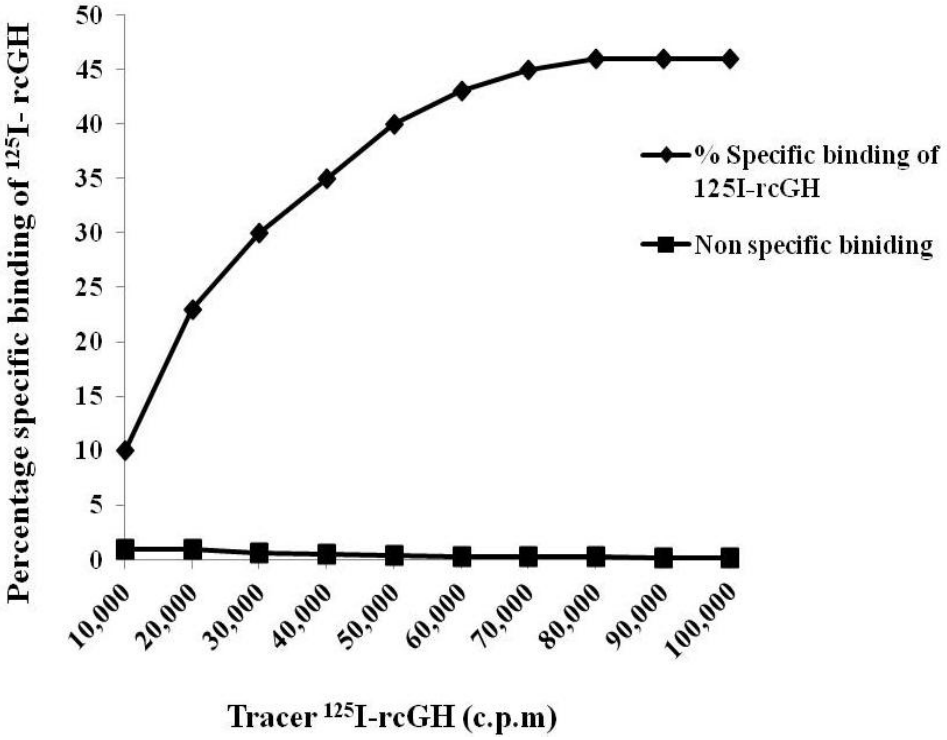

Figure 3. Effect of binding of different tracer (^{125}I-rcGH) counts. Maximum percentage specific binding (◆) is shown at 70,000 c.p.m. Non-specific binding (■) is shown at 0% at all tracer counts.

Effect of tracer counts

The effect of different tracer counts (10,000-100,000 c.p.m.) on ^{125}I-rcGH binding was analyzed for 24 h at 4°C with selected caprine receptor protein concentration that is, 1200 µg. Maximum 45% specific binding was observed at 70,000 c.p.m. and saturation of the tracer binding was seen above 80,000 c.p.m. as shown in Figure 3. Hence, tracer 70,000 c.p.m. was selected for subsequent experiments. Although, non-specific binding was negligible in all the ^{125}I-rcGH counts.

Effect of temperature

Effect of binding of the tracer was studied at two different temperatures that is, 4 and 37°C for 24 h (Figure 4). At 37°C, the tracer binding was fast at the beginning of the assay as compared to 4°C. Although, the specific binding was too low that is, 5%, this could be due to the degradation of the receptor protein or tracer after 24 h of incubation. These results are in agreement with the previous work done in which ^{125}I-human GH was observed to be degraded when incubated with rat microsomal membrane (Posner et al., 1974; Herington et al., 1976). Whereas, at 4°C, the percentage specific binding showed to be 45% in contrast to 37°C. This might be the reason of non-degradation of the tracer and the receptor protein or tracer remained bound to the receptor protein which ultimately led to the prolonged equilibrium time of hormone-receptor complex and thus %age binding of the hormone with its receptor was increased (Posner et al., 1974; Haro et al., 1984). Thus, 4°C was selected as an appropriate temperature for further assay. While, non-specific binding at both the temperatures was found to be insignificant. The effect of temperature was in consensus with the findings of Kelly et al. (1973) who observed that hGH had a very long equilibration time at 4°C due to non-degradation.

Effect of assay pH

The influence of assay buffer pH on ^{125}I-rcGH binding to receptor protein was studied over the pH range 6-9 (Figure 5). Tracer (70,000 c.p.m.) and caprine receptor protein (1200 µg) were used in the assay as optimized from the earlier experiments. Maximal specific binding (45%) of the tracer was attained at pH 7.0, however, below and above pH 7.0 binding of the tracer to receptor

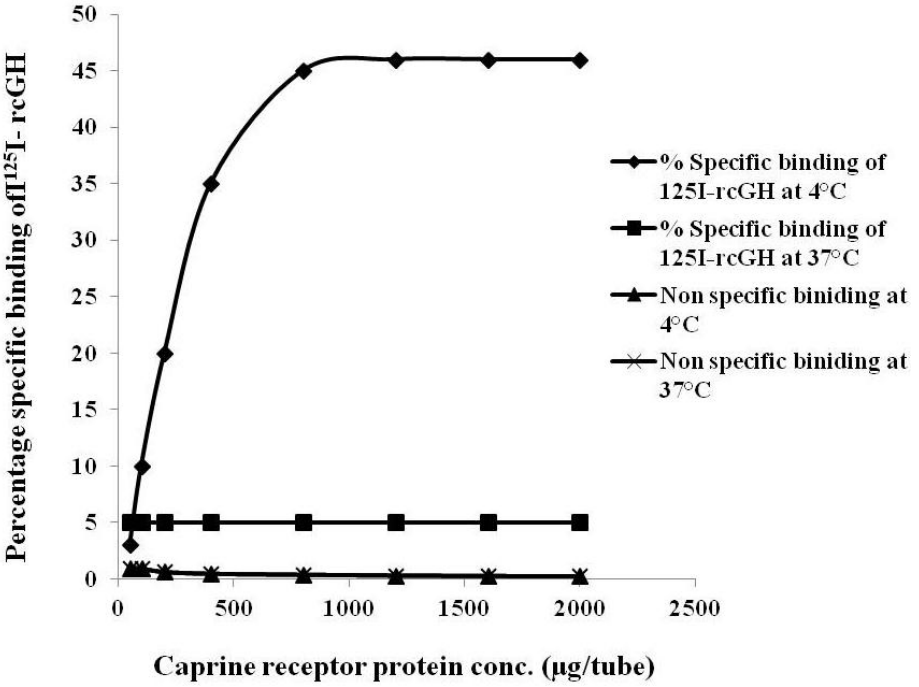

Figure 4. Effect of temperature. Tracer (70,000 c.p.m.) and different caprine receptor protein concentrations (µg per assay tube) used. Maximum percentage specific binding was seen at 4°C (◆) while at 37°C (■) percentage specific binding was low. Non-specific binding at 4°C (▲) and 37°C (×) was negligible.

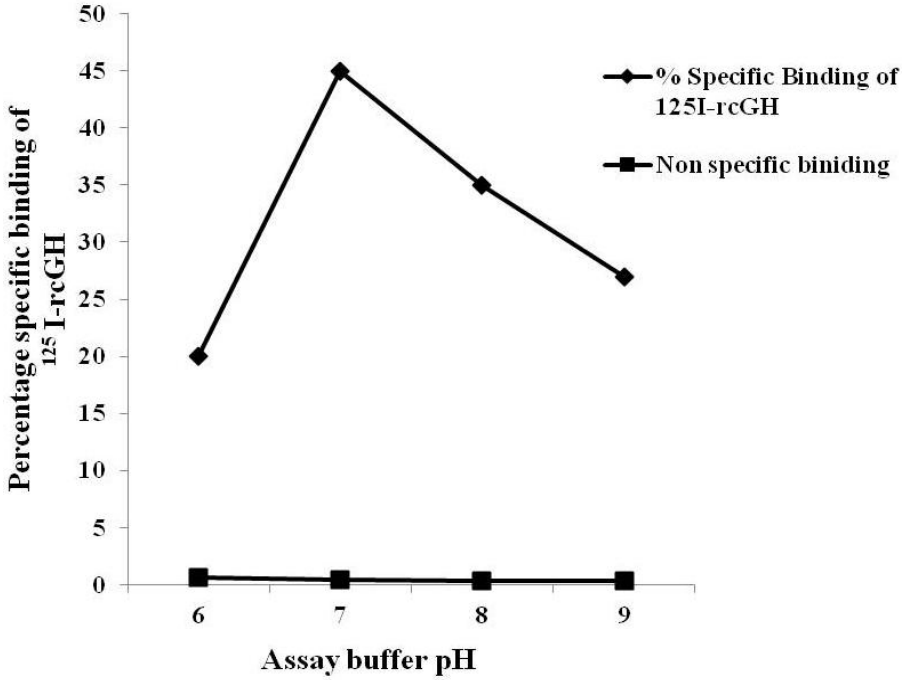

Figure 5. Effect of pH. Tracer (70,000 c.p.m.) and receptor protein concentration (1200 µg) per assay tube used. Maximum of 45% age specific binding (◆) was seen at pH 7. Non-specific binding (■) was shown to be insignificant.

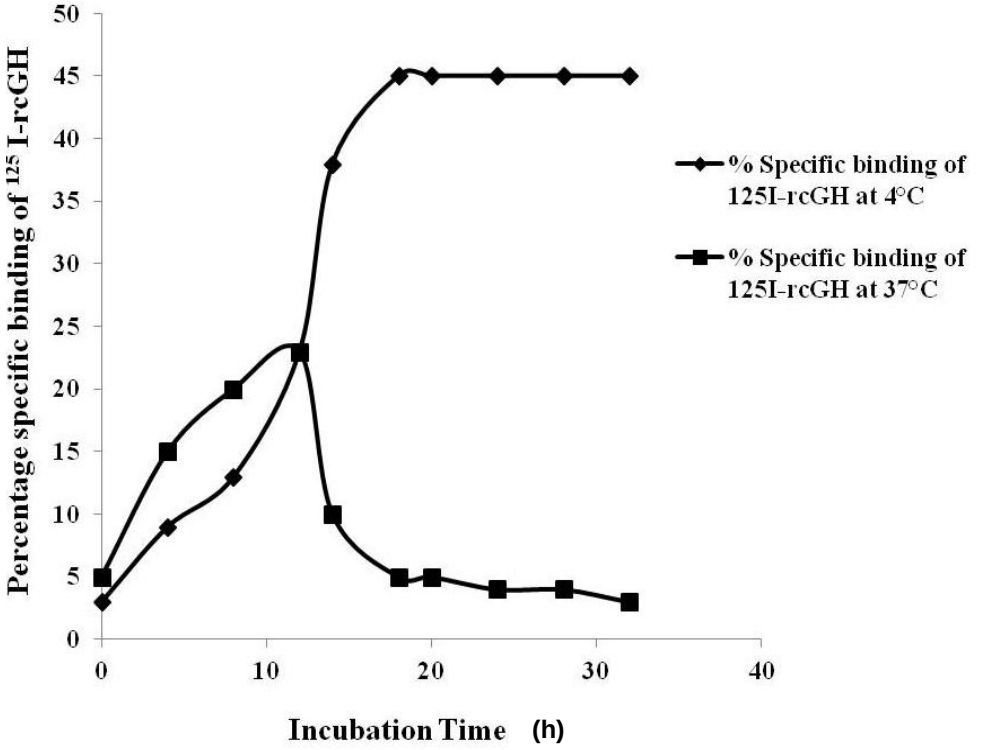

Figure 6. Effect of time. Tracer (70,000 c.p.m.) and receptor protein concentration (1200 µg) per assay tube used. Incubation was given at different durations (0-32 h) at 4 and 37°C respectively. Maximum percentage specific binding (◆) was seen at 45% at 18h incubation for 4°C. At 37°C, maximum %age specific binding (■) reached 23% at 12 h incubation time.

protein was significantly lost. The results reveal that pH 7 was favorable for binding of the tracer to its receptor protein. The optimum pH for binding of Bovidae GH to receptor protein was reported as 7.8 (Haro et al., 1984).

Effect of incubation time

The binding of the ^{125}I-rcGH to the caprine receptor protein was analyzed at different incubation time at two respective temperatures that is, 4 and 37°C under the optimized conditions of incubation time (32 h), receptor protein (1200 µg) and tracer counts (70,000 c.p.m.). After every 4 h, specific and non-specific binding of the ^{125}I-rcGH was checked by taking the counts on gamma counter (Figure 6). Maximum specific binding i.e. 45% was observed at 4°C. The binding of the ^{125}I-rcGH showed to be slow at the start of the assay, however it reached at its maximum levels after 18 h of incubation. After 18 h binding of the ^{125}I-rcGH remained steady, up till 32 h. While at 37°C binding of the hormone to its receptor was fast and the %age binding reached 23% at 12h of incubation. However, after 12 h binding drastically dropped to 5%. This could be due to the degradation of the hormone and its receptor protein at 37°C, as degradation of the protein is seen to be extensive at 37°C (Herington et al., 1976).

Binding of the ^{125}I-rcGH to different Bovidae receptor proteins

The effect of binding of the ^{125}I-rcGH to different microsomal membranes of Bovidae species (caprine, ovine and bovine) was studied. Different concentrations of Bovidae receptor proteins (50, 100, 200, 400, 800, 1200, 1600 and 2000 µg) were incubated with 70,000 c.p.m. of tracer for 24 h (Figure 7). It was observed that all the microsomal membranes of the Bovidae species showed 45% specific binding. Thus, showing all the receptor proteins of the Bovidae species are similar in nature. The result was in the agreement with the statement that Bovidae family has well conserved GH receptor nucleotide and amino acid sequences. However, Maj and Zwierzchowski (2006) have reported 99 and 97% amino acid sequence homology of the caprine growth hormone receptor (GHR) with ovine and bovine species, respectively. While, non-specific binding was

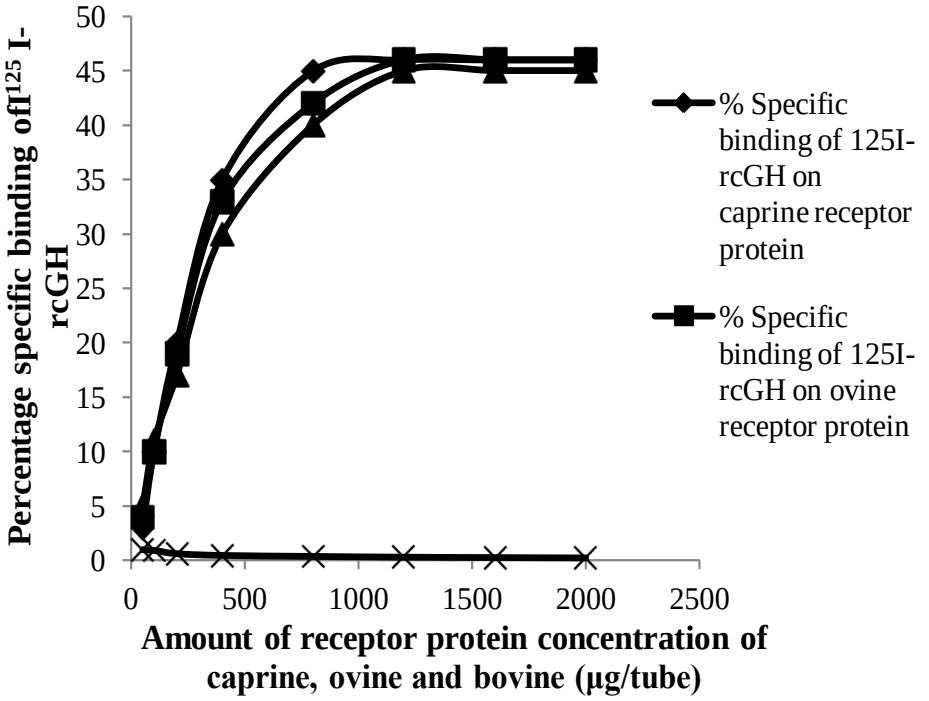

Figure 7. Binding of the tracer (^{125}I-rcGH) to different microsomal membranes of Bovidae species (caprine, ovine and bovine). Tracer 70,000 c.p.m. per assay tube was used, incubation given for 24 h at 4°C. Maximum percentage specific binding in all the Bovidae species, caprine (◆), ovine (■) and bovine (▲) seen to be 45 %. Non-specific binding (×) showed to be negligible.

observed to be negligible in all the Bovidae species.

Cross reactive study of the ^{125}I-rcGH

The cross reactive study was done by using two unlabeled GHs that is caprine and human, and competitive assay was performed in the presence of ^{125}I-rcGH (Figure 8). Different concentrations of unlabeled caprine and human GH (0, 0.1, 1, 10, 100 and 1000 µg) were used in the assay and results showed that 1000 µg concentration of both unlabeled hormones disrupted the binding of the ^{125}I-rcGH at a maximum level. These results were in consensus with that of Tech et al. (1988). The cross reactive results explained that human GH binds with high affinity to the Bovidae microsomal membrane or with non-primates GHR and similar results have also been reported by Souza et al. (1995). Whereas, non-specific binding was found to be insignificant in both cases of unlabeled rcGH and hGH.

Scatchard analysis of rcGH binding

The Scatchard analysis of rcGH binding to Bovidae receptors indicated single class of binding site. The Scatchard plot was analyzed to calculate the dissociation constant (K_d). As K_d is defined as the ratio of unbound and bound molecules at equilibrium that is,

$$K_d = \frac{[A][B]}{[AB]}$$

Thus small K_d value shows high affinity interaction while large K_d value indicates low affinity interaction. The Scatchard analysis of rcGH binding to Bovidae receptor protein that is, caprine, ovine and bovine is shown in Figure 9. The analysis showed that rcGH has 57.61 ± 4.32 fmol mg^{-1} binding capacity and 337.1 ± 82.94 × 10^{9} M^{-1} affinity for caprine receptor protein. Ovine receptor protein also exhibit high binding capacity that is, 57.69 ± 3.23 fmol mg^{-1} and slightly low affinity (365.4 ± 66.82 × 10^{9} M^{-1}) for rcGH as compared to caprine receptor protein. However, with bovine receptor protein, both the binding capacity (56.8 ± 2.56 fmol mg^{-1}) as well as affinity (392.6 ± 56.25 × 10^{9} M^{-1}) of rcGH were found to be the least when compared with other two receptor proteins as shown in Table 2. The possible reason of differences in binding affinity of rcGH with the caprine, ovine and bovine

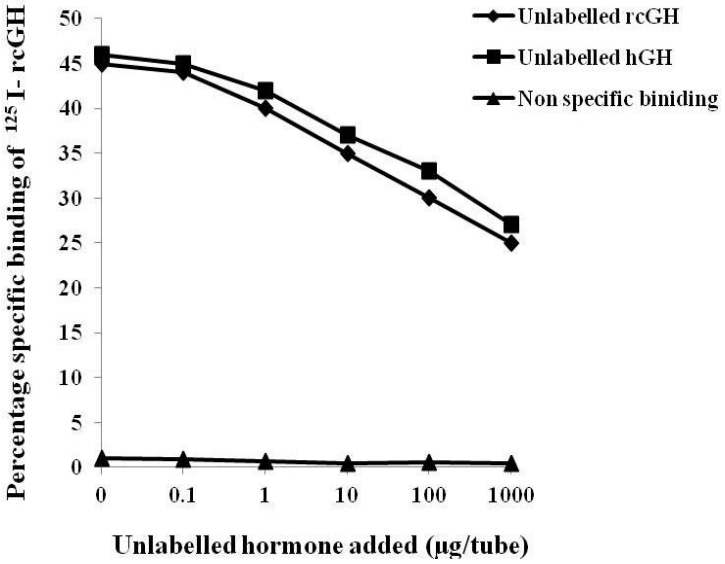

Figure 8. Cross reactive study of the tracer (^{125}I-rcGH) in the presence of unlabeled rcGH and unlabeled hGH. Tracer (70,000 c.p.m.) and 1200 µg receptor protein per assay tube was used in the presence of unlabeled rcGH and hGH. Incubation given for 24 h at 4°C and displacement of the tracer observed in the presence of unlabeled rcGH (◆) and hGH (■). Non-specific binding (▲) showed results to be insignificant.

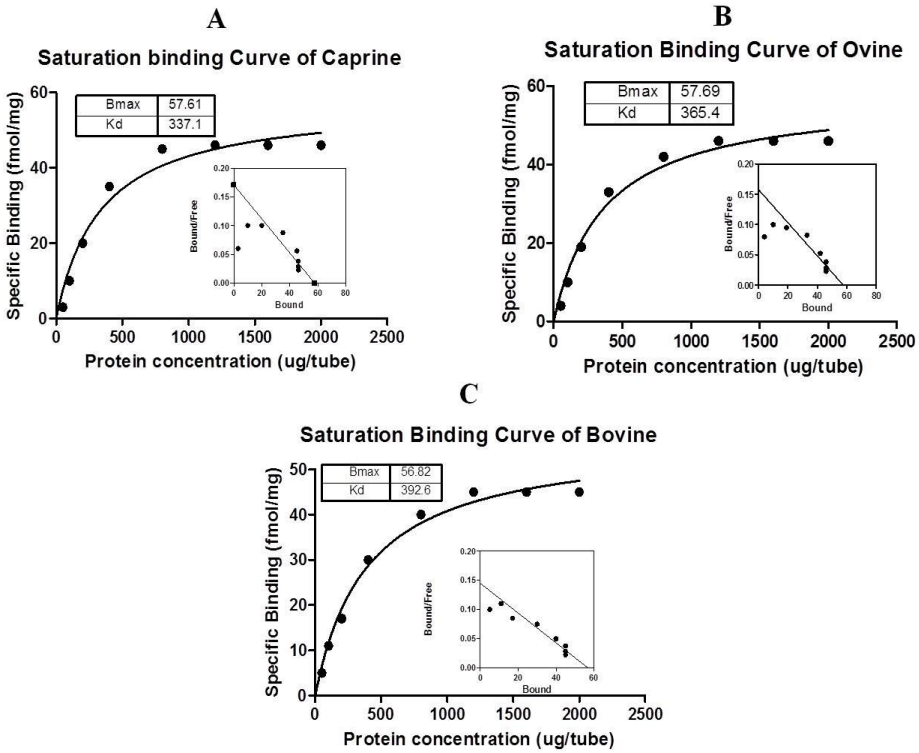

Figure 9. Scatchard analysis of rcGH binding to Bovidae receptors. **A.** rcGH binding to caprine microsomal membrane. **B,** rcGH binding to ovine microsomal membrane. **C.** rcGH binding to bovine microsomal membrane.

Table 2. Saturation binding data of rcGH with the Bovidae receptor proteins that is, caprine, ovine and bovine.

Saturation binding data		Caprine receptor protein	Ovine receptor protein	Bovine receptor protein
B_{max}	Mean	57.61	57.69	56.82
	Standard Error	4.23	3.23	2.56
	Confidence Interval (95%)	47.26-67.95	49.77-65.61	50.55-63.09
K_d	Mean	337.1	365.4	392.6
	Standard Error	82.94	66.82	56.25
	Confidence Interval (95%)	134.1-540	201.9-528	255-530

receptor protein could be due to the amino acid variations found in amino acid sequence alignment of GHR among the Bovidae species (Gul et al., 2012).

Conclusion

Our results conclude that the specific binding of the radiolabeled rcGH to the caprine liver microsomal membrane is dependent on various factors like receptor protein concentration, tracer counts, temperature, time of incubation and assay pH. Moreover, the binding of the ^{125}I-rcGH to the Bovidae (caprine, ovine and bovine,) receptor proteins was 45%. These findings would add to study further the hormone-receptor interaction of the Bovidae growth hormones.

Conflict of Interest

The author(s) have not declared any conflict of interest.

ACKNOWLEDGEMENT

The work was supported by a grant from Higher Education Commission and British Council (HEC-BC), Pakistan.

REFERENCES

Allard MW, Miyamoto MM, Jarecki L, Kraus F, Tennant MR (1992). DNA systematics and evolution of the artiodactyla family Bovidae. Proc. Natl. Acad. Sci. U.S.A. 89:3972-3976.

Alves dos Santos CM, Kerkhof PV, Strous GJ (2001). The signal transduction of the growth hormone receptor is regulated by the ubiquitin/proteasome system and continues after endocytosis. J. Biol. Chem. 276:10839-10846.

Bauman DE (1999). Bovine somatotropin and lactation: from basic science to commercial application. Domest. Anim. Endocrin. 17:101-116.

Bradford MM (1976). Rapid and sensitive method for the quantitation of microgram quantities of protein utilizing the principle of protein-dye binding. Anal. Chem. 72:248-254.

Cadman HF, Wallis M (1981). An investigation of sites that bind human somatotropin (growth hormone) in the liver of the pregnant rabbit. Biochem. J. 198:605-614.

Connor EE, Ashwell MS, Dahl GE (2002). Characterization and expression of the bovine growth hormone-releasing hormone (GHRH) receptor. Domest. Anim. Endocrin. 22:189-200.

Edmondson SR, Thuniger SP, Werther GA, Wraight CJ (2003). Epidermal Homeostasis; The role of the growth hormone and insulin like growth factor systems. Endocr. Rev. 24:737-764.

Edwards R (1999). Immunodiagnostics; A practical approach Series, Oxford University Press.

Grubb P (1993). FAMILY Bovidae. (In Wilson D. E. and Reeder D. M. eds.) Mammals Species of the World: A Taxonomic and Geographic Reference. Smithsonian Inst. Press, Washington. 393-414.

Grubb P (2005). FAMILY Bovidae. (In Wilson, D. E. and Reeder, D. M., eds.) Mammal Species of the World: A Taxonomic and Geographic Reference. 3rd ed. Baltimore: Johns Hopkins University Press. 2:2142.

Gul R, Sadaf S, Akhtar MW (2012). Expression and sequence characterization of growth hormone binding protein of Nili-Ravi buffaloes (*Bubalus bubalis*). Afr. J. Biotechnol. 57:12103-12109.

Haro LS, Collier RJ, Talamantes FJ (1984). Homologous somatotropin radioreceptor assay utilizing recombinant bovine growth hormone. Mol. Cell. Endocrinol. 28:109-116.

Herington AC, Veith N, Burger HG (1976). Characterization of the binding of human growth hormone to microsomal membrane from rat liver. Biochem. J. 158:61-69.

Jiang H, Okamura CS, Lucy MC (1999). Isolation and characterization of a novel promoter for the bovine growth hormone receptor gene. J. Biol. Chem. 274:7893-7900.

Kelly PA, Posner BI, Tsushima T, Shiu RPC, Friesen HG (1973). Advances in Human growth hormone research (Raiti, S., ed.). 567-84, (U.S. department of Health Education and Welfare, Washington, D.C.).

Labbe A, Delcros B, Dechelotte P, Novailles C, Grizard G (1992). Comparative study of the binding of prolactin and growth hormone by rabbit and human lung cell membrane fraction. Biol. Neonate. 61:179-87.

Leung KC, Ho KK (2001). Measurement of growth hormone, insulin-like growth factor I and their binding proteins: the clinical aspects. Clin. Chim. Acta. 313:119-123.

Machin LJ (1973). Effect of growth hormone on milk production and feed utilization in dairy cows. J. Dairy Sci. 56:575-80.

Maj A, Zwierzchowski L (2006). Molecular evolution of coding and non-coding sequences of the growth hormone receptor (GHR) gene in the family Bovidae. Folia Biol-Krakow. 54:31-36.

Manson PJ (1990). A user's guide to legend: Data analysis on curve fitting for ligand binding experiments, National Institute of Health: Betherda, MD, USA.

Piwien-Pilipuk G, Huo JS, Schwartz J (2002). Growth hormone signal transduction. J. Pediatr. Endocrinol. 15:771-786.

Posner BI, Kelly PA, Shiu RPC, Friesen HG (1974). Studies of insulin

growth hormone and prolactin binding: tissue distribution, species variation and characterization. Endocrinology. 95:521-531.
Rad cliff RP, McCormarck BL, Crooker BA, Lucy MC (2003). Growth hormone (GH) binding and expression of GH receptor 1A mRNA in hepatic tissue of periparturient dairy cows. J. Dairy Sci. 86:3933-40.
Sami AJ, Wallis OC, Wallis M (2008). Production, purification and characterization of two recombinant DNA-derived N-terminal ovine growth hormone variants: oGH3 and oGH5. Afr. J. Biotechnol. 7:1859-1864.
Souza SC, Frick GP, Wang X, Kopchick JJ, Lobo RB, Goodman HM (1995). A single arginine determines species specificity of human growth hormone receptor. Proc. Natl. Acad. Sci. U.S.A. 92:959-63.
Tech LC, Ormandy CJ, Surus AS, Sutherland RL, Chapman GE (1988). Human growth hormone binds to lactogenic receptors in bovine, ovine and rat adrenals. Horm. Metab. Res. 20:278-281.
Tsushima T, Friesen HG (1973). Radioreceptor assay for growth hormone. J. Clin. Endocrinol. Metab. 37:334-37.
Waters MJ, Friesen HG (1979). Purification and partial characterization of a non-primate growth hormone receptor. J. Biol. Chem. 254:6815-6825.
Wingfield PT, Graber P, Buell G, Rose K, Simona MG, Burleigh BD (1987). Preparation and characterization of bovine growth hormone produced in recombinant *Escherichia coli.* Biochem. J. 243:829-839.

academicJournals

Vol. 13(30), pp. 3092-3100, 23 July, 2014
DOI: 10.5897/AJB2014.13671
Article Number: 5A7C07F46225
ISSN 1684-5315

http://www.academicjournals.org/AJB

African Journal of Biotechnology

Full Length Research Paper

Structural optimization and docking studies of anatoxin-a: A potent neurotoxin

Naresh Kumar* and Archit Garg

Department of Biotechnology, Indian Institute of Technology Roorkee, Roorkee, 247667 India.

Received 28 January, 2014; Accepted 4 July, 2014

In this investigation, our aim was to get more insight on the geometry optimization, structural properties and molecular interaction of anatoxin-a, a naturally occurring potent neurotoxin. The geometry of the anatoxin-a was fully optimized in terms of density functional theory Gaussian 09. Calculations for structural parameters viz. total energy, dipole moment, electro-negativity, chemical hardness, chemical softness, electronic chemical potential and electrophilic index of optimized geometries has been carried out. The energy difference between HOMO-LUMO was found to be -4.89 eV. Furthermore, the molecular docking of anatoxin-a with nicotinic acetylcholine receptor (nAChR) was performed in order to find the molecular interaction involved in the inhibition process of nicotinic acetylcholine receptor by anatoxin-a by using Glide 5.9. Our results clearly indicates that anatoxin-a bind to the A-chain of nAChR with hydrophobic interactions between anatoxin-a and Phe214, Tyr277 and Thr281 residues of protein with bond length 1.97, 1.96 and 2.04 Å, respectively. The glide energy and docking score were found to be -18.242 and -4.567, respectively.

Key words: Anatoxin-a, Neurotoxin, Acetylcholine, Gaussian 09, molecular docking, glide.

INTRODUCTION

The presence of toxic cyanobacterial blooms in eutropic lakes, rivers and reservoirs has been reported during the last four decades all over the world. The continuous increment in the number of cases of animal poisoning and human illness have altered worldwide attention on one of the most potential cyanotoxin anatoxin-a, gene-rated by some strains of *Anabaena* (particularly *Anabaena flos-aquae*), *Aphanizomenon*, *Microcystis*, *Planktothrix* and *Oscillatoria* (Fawell et al., 1999; Viaggiu et al., 2004). Chemical synthesis of anatoxin-a hydrochloride and its conformational study with the crystal structure description has been done in past (Koskinen and Rapoport, 1985). Anatoxin-a has a semi - rigid bicyclic secondary amine structure and two enantiomeric forms, from which only (+)-anatoxin-a is produced in nature. The investigations on the characterization of anatoxin-a was effectively initiated in 1961 following after the death of cows that had ingested water from a lake containing an algal bloom in Saskatchewan, Canada (Carmichael et al., 1975; Carmichael and Gorham, 1978; Devlin et al., 1977; Moore, 1977). Anatoxin-a was implicated in the death of a 17-year-old boy who died 2 days after swallowing water while swimming in a pond containing an algal bloom (Behm, 2003). The toxin was termed very fast death factor (VFDF) because intraperitoneal (i.p.) injection of toxin-producing cells or cell culture filtrates into mice

*Corresponding author. E-mail: nareshkumariitr@gmail.com. Tel: 091-9528721247.

induced paralysis, tremors, mild convulsions and death within 2 to 7 min. Anatoxin-a has also been implicated in cases of animal poisoning following consumption of water containing blooms of *Anabaena flos-aquae* although no quantitative exposure data are available (Carmichael and Gorham, 1978; Edwards et al., 1992; Gunn et al., 1992; Pybus et al., 1986). The signs of anatoxin-a contact are failure of coordination, muscular fasciculations, convulsions and finally death of a person by respiratory paralysis. From the two modes of action of anatoxin-a, firstly it binds with the receptor and acts as an agonist of acetylcholine by stimulating the nerve. Upon binding of anatoxin-a with the receptor, it is not expelled due to which the nerve impulse does not fade. In its second mode of action, anatoxin-a inactivates the acetylcholine which is released by normal impulses and thus it inhibits the acetylcholinesterase enzyme. Cholinesterase, takes part in the hydrolysis of acetylcholine (a neurotransmitter), and is not capable of degrading the anatoxin-a due to which it causes permanent stimulation of the muscle cells which leads to paralysis. This result is an over stimulation of the muscle that leads to limp paralysis and death, when the muscles of the chest responsible for breathing are affected. Anatoxin-a has become a very useful agent in investigating nicotinic acetylcholine receptors (nAChRs) because it is resistant to enzymatic hydrolysis by acetylcholinesterase and 100-fold more selective for nicotinic acetylcholine receptors than for muscarinic acetylcholine receptors (Aronstam and Witkop, 1981). When acetylcholine is released at the neuromuscular junction of motor neurons, it binds to muscle cell receptor molecules consisting of a neuromuscular binding site and an ion channel. This triggers ionic currents that induce muscle cell contraction. The extracellular acetylcholinesterase acts on acetylcholine by degrading the neurotransmitter to prevent overstimulation of the muscle. After the contamination with anatoxin-a, the muscle cells keep on stimulated and causing muscle twitching, fatigue and finally, paralysis takes place. There are animal studies reports on the acute lethality of anatoxin-a resulted in the overstimulation of respiratory muscles may result in respiratory arrest and rapid death (Carmichael et al., 1975; 1977; Stevens and Krieger, 1991). The main known toxic effect of anatoxin-a is acute neurotoxicity that is manifested as progressive clinical signs.

Theoretical investigations

Quantum chemical calculations

The geometry optimization of anatoxin-a was done by means of density functional theory with a hybrid function B3LYP and because of its excellent compromise between computational time and description of electronic correlation. All the calculations were performed by Gaussian 09 suite of program at 6-311G** basis set (Becke, 1993; Frisch et al., 2009; Goel and Singh, 2013; Goel and Kumar 2014; Lee et al., 1988). The input file for the simulation of geometry optimization was a Z-matrix, generated with the help of Gaussview 5.0 that was also used in the visualization of output files. The electronic absorption spectra for the optimized structure of Anatoxin-a was calculated at TD-DFT/B3LYP/6-311G** basis set both in gas and solvent phase (water). Energy calculations for HOMO, LUMO, electronegativity (χ), chemical hardness (η), soft-ness (S) and electrophilic index (ω) were also calculated by using Koopmans theorem for closed shell molecule (Koopmans, 1934) and defined as:

Chemical hardness determines the resistance to change in the electron distribution. It is associated with the stability and reactivity of a chemical system and calculated by using Equation 1.

$$\eta = -(E_{\mathrm{HOMO}} + E_{\mathrm{LUMO}})/2 \quad (1)$$

The softness is the property of a molecule which helps in the calculation of chemical reactivity. It is the reciprocal of hardness and calculated by using the Equation 2.

$$S = \frac{1}{2\eta} \quad (2)$$

Electronic chemical potential is the negative of electronegativity of a molecule and determined by using the Equation 3.

$$\mu = (E_{\mathrm{HOMO}} + E_{\mathrm{LUMO}})/2 \quad (3)$$

Electronegativity describes the tendency of an atom or a functional group to attract electrons towards it. Higher the associated electronegativity, more an element or compound attracts electrons. Electronegativity is determined according to Equation 5.

$$\chi = (E_{\mathrm{HOMO}} - E_{\mathrm{LUMO}})/2 \quad (4)$$

Electrophilic index (capacity of a species to accept electrons) is calculated by using the electronic chemical potential and chemical hardness as given away in Equation 4. It is the measure of stabilization in energy after a system accepts extra amount of electronic charge from environment (Koskinen and Rapoport, 1985; Lee et al., 1988).

$$\omega = \frac{\chi^2}{2\eta} \quad (5)$$

Molecular docking studies

The protein-ligand docking is a well established computational technique widely applied in structure-based drug design, constantly used to predict the correct 3D conformation of a protein-ligand complex (Sergio et al., 2006). The molecular docking of anatoxin-a with nAChR (PDB ID: 2BG9) was performed using Glide version 5.9 by Maestro 9.4 software interface in Schrodinger 2013 (Friesner et al., 2006). The protein was prepared using Maestro's protein preparation wizard in which the water molecules were deleted, hydrogens were added, bond orders were assigned, and the overall structure was minimized to RMSD of 0.30 Å using OPLS2005 force field. The five active sites within the protein were predicted using SiteMap module version 2.7 (SiteMap, version 2.7, Schrodinger, LLC, New York, NY, 2013) in Maestro 9.4, which uses a novel algorithm for rapid binding site identification, from which the active site with the best site score was selected for preparing the grid. The centroids of the selected amino acid residues in the active site were taken into consideration for grid preparation. The ligand was prepared using Maestro's LigPrep module version 2.6. Further, the

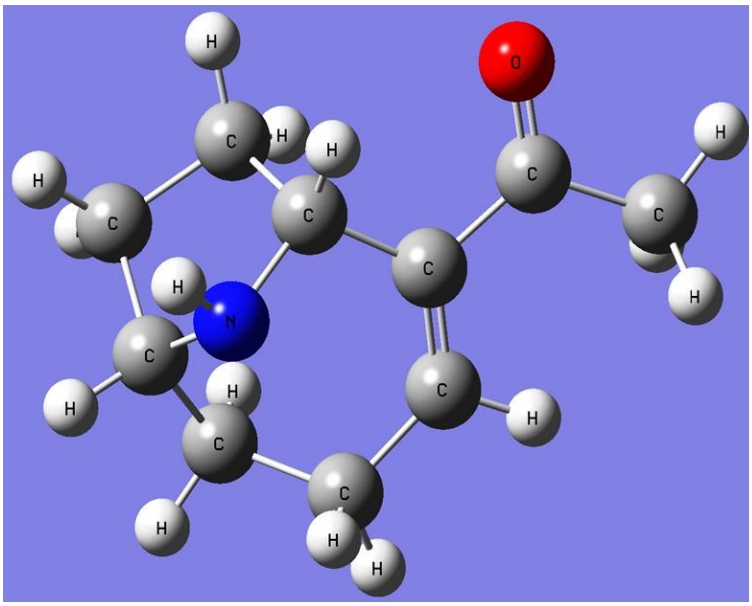

Figure 1. Optimized geometry of anatoxin-a at B3LYP/6-311G** basis set.

docking of anatoxin-a with nAChR was done by Glide using Extra Precision (XP). The best pose was selected on the basis of docking score, Glide energy and rank. The most energetically favourable conformation was selected and visualized using Maestro's XP viewer and PyMol (DeLano, 2002).

RESULTS AND DISCUSSION

Molecular geometry and ultraviolet spectra analysis

The geometry of anatoxin-a has been optimized at B3LYP/6-311G** basis set which has been shown in Figure 1. The optimized geometry showed positive vibrational frequencies indicating the global minimum on the potential energy surface was attained during optimization. The single-point energy calculations were performed, and zero-point corrected total energies recorded. In addition to the characterization of anatoxin-a, the gas phase geometries, harmonic vibrational frequencies and binding energies were also computed. Further, the structural parameters like bond angle (Table 1) and bond length (Table 2) between different atoms of anatoxin-a from optimized geometry were also calculated. The ultraviolet spectra analyses of anatoxin-a was carried out both in water and gas phase at TD-DFT/B3LYP/6-311G**. The theoretical electronic excitation energies, oscillator strengths and absorption wavelength of anatoxin-a in gas and solvent phase were computed (Table 3) which show that the calculated absorption maxima are at 423, 349 and 243 nm in gas phase, while it was observed at 392, 362 and 258 nm in water. The molecular orbital geometry illustrates that the absorption maxima of Anatoxin-a corresponds to the electron transition between frontier orbitals (HOMO and LUMO).

Frontier molecular orbitals (FMOs)

The FMO plays an important role in the computation of quantum chemistry, optical and electric properties of a molecule (Goel and Kumar, 2014). The HOMO and LUMO are known as FMOs in which, HOMO represents the ability to donate an electron and LUMO acts as an electron acceptor. The gap between the energies of HOMO and LUMO helps in the determination of chemical reactivity, kinetic stability, chemical hardness and softness and optical polarizability of a molecule. The hard molecules are not more polarizable than the soft ones because they need big excitation energy. For evaluating the energetic activities of anatoxin-a, we did the calculations in water and gas phase at B3LYP/6-311G** level. The energies of the highest and second highest occupied molecular orbital, lowest and the second lowest unoccupied molecular orbital were calculated (Table 4). The molecular orbital surfaces and energies (eV) of HOMO, HOMO-1, LUMO and LUMO+1 in gas phase for anatoxin-a are shown in Figure 2. The energy differences between the HOMO and LUMO in anatoxin-a are -5.150, -4.945 eV in water and gas phase, respectively, that shows the chemical stability of the molecule. The HOMO lies on whole molecule except the acetyl group while LUMO lies on the acetyl group and some atoms of seven membered ring within the anatoxin-a molecule.

Docking analysis

Protein-Ligand docking is a well established computational technique widely applied in structure-based drug design (Badry et al., 2003). This methodology evolved constantly to predict the correct three- dimensional

Table 1. Bond Angles in degree (˚) for optimized structure of anatoxin-a.

Bond type	Bond Angle (˚)	Bond type	Bond Angle (˚)
H5-C1-C6	107.11	H11-C7-C5	108.40
H5-C1-C3	110.25	C7-C5-C8	114.71
H5-C1-N1	109.72	C7-C5-H8	109.20
H1-C3-C4	112.06	C7-C5-H9	108.68
H2-C3-C4	111.59	H8-C5-H9	106.74
H1-C3-H2	106.91	H8-C5-C8	108.83
H3-C4-C3	110.38	H9-C5-C8	108.39
H4-C4-C3	113.07	C5-C8-H15	115.14
H3-C4-H4	107.24	C5-C8-C6	127.05
H3-C4-C2	109.40	H15- C8-C6	117.81
H4-C4-C2	113.41	C8-C6-C1	123.97
C4-C2-H6	112.02	C6-C1-H5	107.11
H6-C2-N1	108.50	C1-C6-C9	114.72
C2-N1- H7	108.41	C8-C6-C9	121.31
H7-N1-C1	108.35	C6-C9-O1	119.85
C2-N1-C1	105.01	C6-C9-C10	120.46
N1-C2-C7	110.23	O1- C9-C10	119.69
N1-C1-C6	110.59	C9-C10-H12	111.29
H6-C2-C7	109.25	C9-C10-H13	108.12
C2-C7-H10	109.16	C9-C10-H14	111.41
C2-C7-H11	109.94	H12-C10-H13	10916
C2-C7-C5	114.46	H12-C10-H14	107.51
H10-C7-H11	105.96	H13-C10-H14	109.32
H10-C7-C5	108.57		

Table 2. Bond distances in Å for optimized structure of anatoxin-a.

Bond type	Bond length(Å)	Bond type	Bond length(Å)
C1-H5	1.092	C7-H10	1.096
C1-C3	1.574	C7-H11	1.097
C1-C6	1.520	C7-C5	1.541
C3-H1	1.092	C5-H8	1.097
C3-H2	1.093	C5-H9	1.096
C3-C4	1.549	C5-C8	1.510
C4-H3	1.097	C8-C6	1.347
C4-H4	1.095	C8-H15	1.088
C4-C2	1.546	C6-C9	1.493
C2-H6	1.095	C9-O1	1.226
C2-N1	1.473	C9-C10	1.523
N1-C1	1.478	C10-H12	1.09
N1-H7	1.018	C10-H13	1.090
C2-C7	1.558	C10-H14	1.095

conformation of a protein-ligand bound complex. Anatoxin-a is a severe neurotoxin that act as mimic of acetylcholine (irreversibly binds with the nAChR) used for docking experiment. Binding of Anatoxin-a causes overstimulation of mussels, results in fatigue and then paralysis (Wonnacott et al., 1991). Docking study is planned to know the mode of binding and forces responsible for the stabilization of Anatoxin-a at the nAChR surface. The anatoxin-a was docked with nAChR using Glide in order to study the binding mode of the anatoxin-a with NAR.

Table 3. Absorption wavelength (λ in nm), excitation energies (E in eV) and oscillator strengths (*f*) of anatoxin-a calculated at TD-DFT/B3LYP/6-311G**.

Water			Gas		
E (eV)	**λ (nm)**	***f***	**E (eV)**	**λ (nm)**	***f***
3.1604	392.30	0.0003	2.9307	423.05	0.0002
3.4251	361.99	0.0127	3.5478	349.47	0.0054
4.8037	258.10	0.4538	5.0985	243.18	0.2184

Table 4. Calculated values of dipole moment, electronegativity, chemical hardness and softness, electrophilic index, and energies of anatoxin-a in water and gas phase at TD-DFT/B3LYP/6-311G** basis set.

TD-DFT/B3LYP/6-311G**	Water	Gas
Total energy (a.u.)	-520.148	-520.107
Dipole moment (Debye)	2.866	2.643
Chemical hardness (eV)	2.575	2.472
Softness $(eV)^{-1}$	0.194	0.202
Electronegativity (eV)	-2.575	-2.472
Electrophilic index (eV)	1.287	1.236
E_{HOMO} (eV)	-6.211	-6.107
E_{HOMO-1} (eV)	-6.833	-6.589
E_{LUMO} (eV)	-1.061	-1.163
E_{LUMO+1} (eV)	1.714	1.735
E_{HOMO}- E_{LUMO}	-5.150	-4.945
E_{HOMO-1}- E_{LUMO+1}	-8.547	-8.324

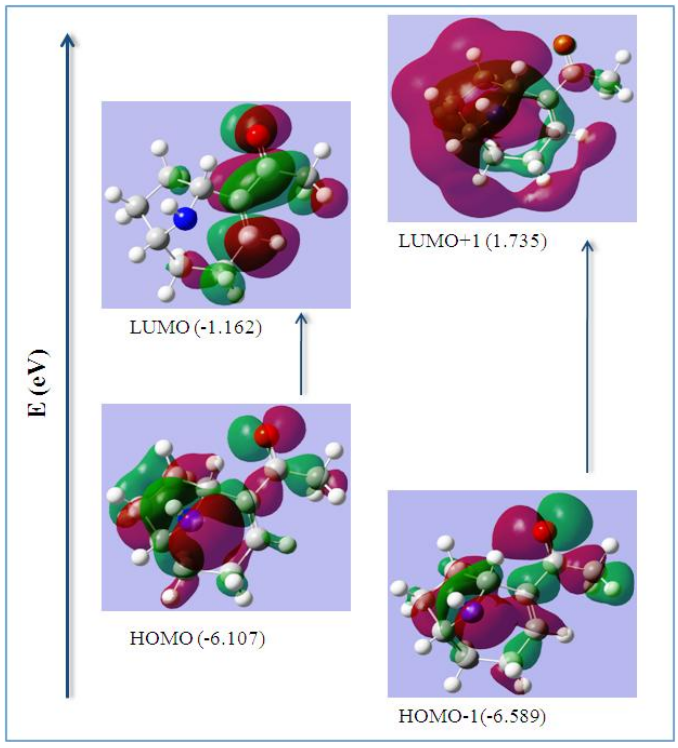

Figure 2. Molecular orbital surfaces with their corresponding energy (eV) for HOMO, HOMO-1, LUMO and LUMO+1 in gas phase in anatoxin-a computed by TD-DFT.

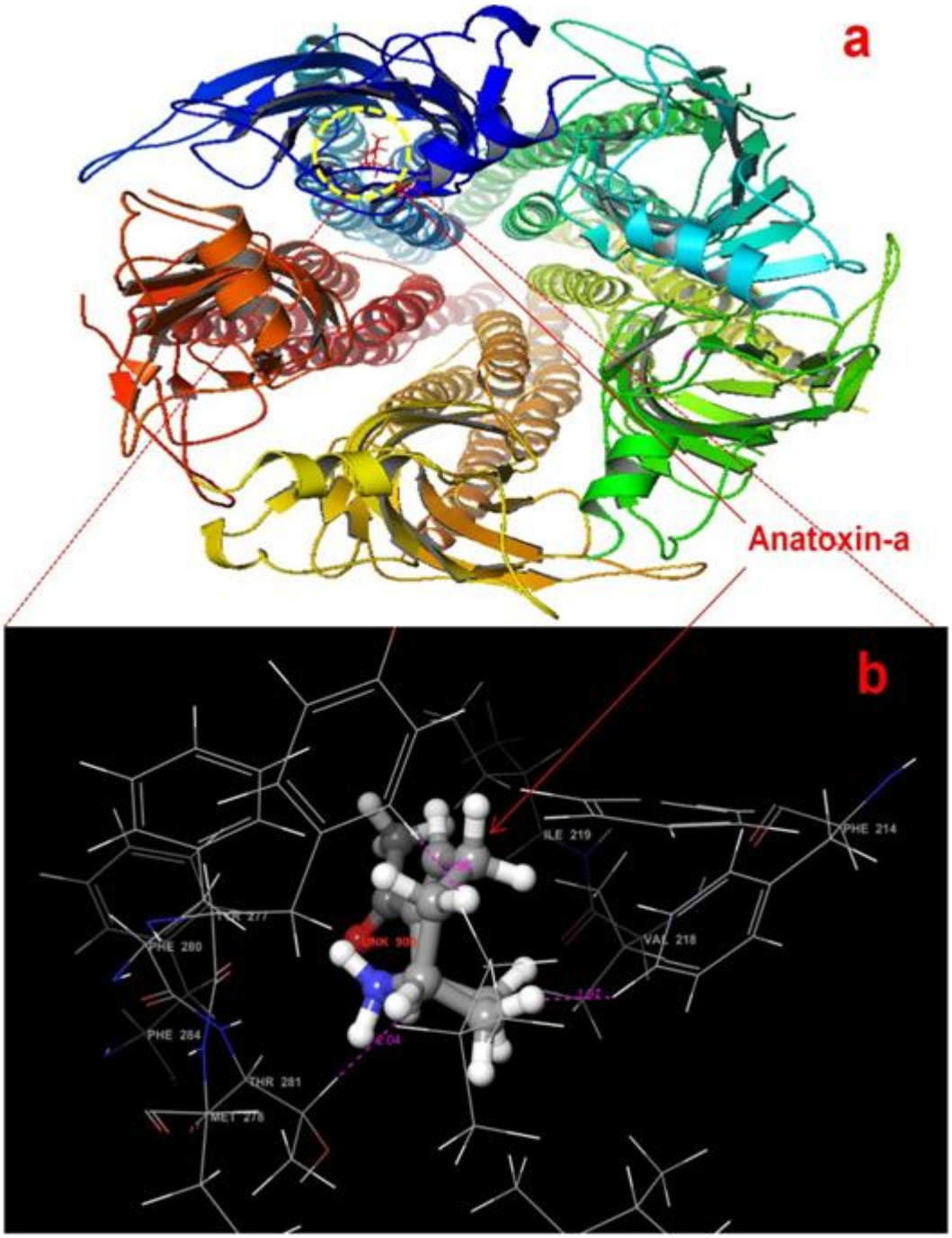

Figure 3. Anatoxin-a docked in the binding pocket of nAChR using Glide 5.9. Different views of nAChR and anatoxin-a conformation. **a)** overview in cartoon model. **b)** Residues around the 4 Å region of binding site of anatoxin-a, the anatoxin is shown in ball and stick and hydrophobic interactions are depicted in pink dotted lines. Images are generated using PyMol and Maestro's XP viewer.

The docking score and glide energy were found to be -4.567 and -18.242, respectively. The present study indicates that the anatoxin-a binds mainly to the hydrophobic pocket of chain A of the nAChR protein (Figures 3 and 4). The residues involved in polar interactions with anatoxin-a are Phe214, Val218, Ile219, Ile264, Leu273, Tyr277, Met278, Phe280, Thr281 and Phe284 (Figure 3). The complex of anatoxin-a and nAChR is stabilized by hydrophobic interactions between the ligand and Phe214, Tyr277 and Thr281 amino acid residues of the protein of bond lengths 1.97, 1.96 and 2.04 Å, respectively (Figure 3b). This study shows that anatoxin-a binds to the nAchR

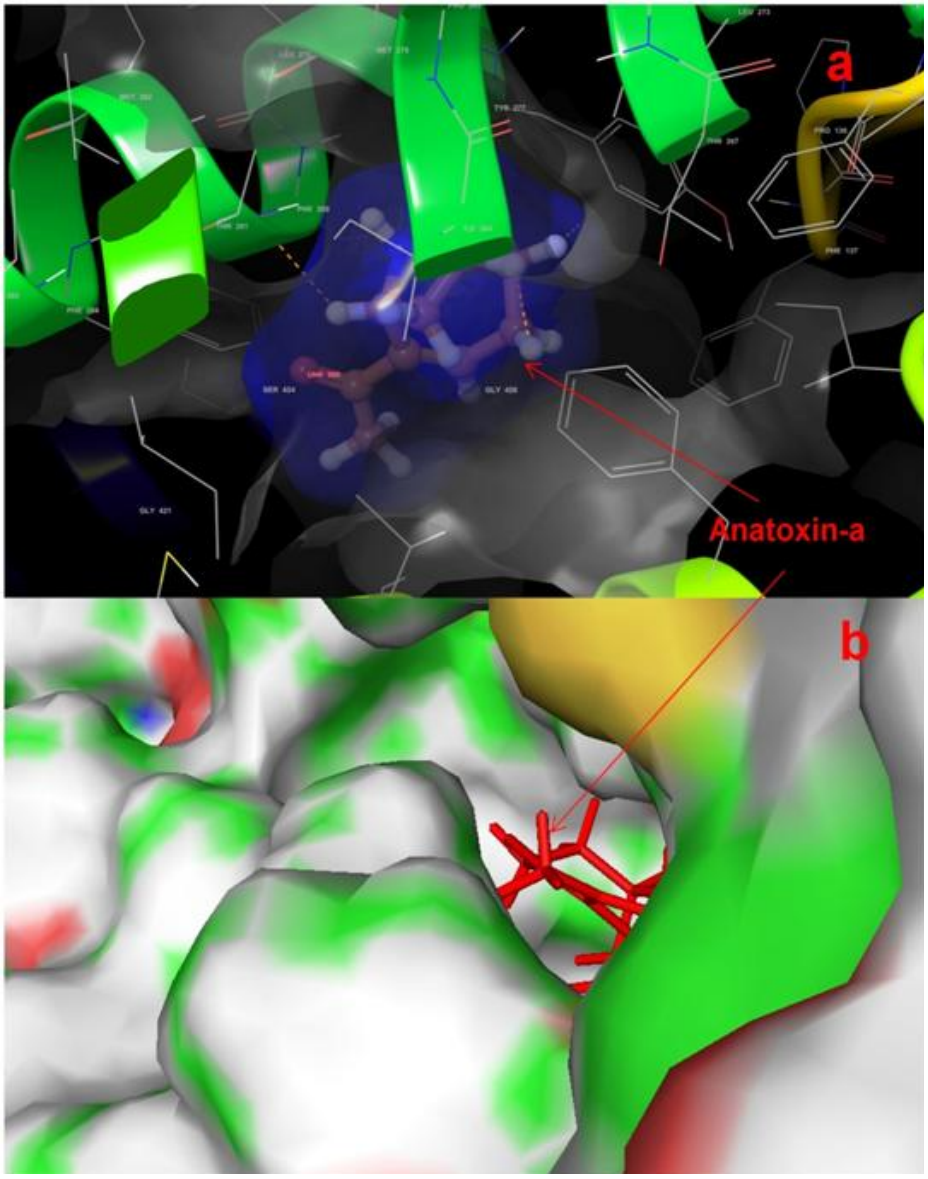

Figure 4. Surface view of anatoxin-a binding pocket. **a)** protein surface (grey colour) and ligand surface (blue colour) are shown separately which shows that ligand is embedded in the binding pocket of protein. **b)** Hydrophobic pocket of nAChR and anatoxin-a, the anatoxin-a represents in ball and stick model and the binding pockets in cyanocolor, in which the green color represents the binding pocket residues. Images are generated using PyMol and Maestro's XP viewer.

and acts as an agonist of acetylcholine and also inactivates it as reported previously.

Conclusions

The structure of anatoxin-a has been optimized by the Gaussian 09 at B3LYP/6-311G** level. At this level, the total energy, dipole moment, degrees of freedom and the energy difference between HOMO and LUMO were found to be -520.107 a.u., 2.643 Debye, 84 and -4.945 eV, respectively. As anatoxin-a is a very fast neurotoxin, it is not degraded by cholinesterase and thus causes permanent stimulation of muscle cells leading to paralysis. The present study highlighted the structural parameters of anatoxin-a, which will be a useful base for rational drug designing as well as for experimental studies. The docking studies suggest that the anatoxin-a bound to the nAChR with hydrophobic interactions and inactivates the acetylcholine. The structure and binding related scatter data will be very useful in the cure of the neurodegenerative disorder, such as Alzheimer's disease by using the modified analogues of Anatoxin to further elucidate the

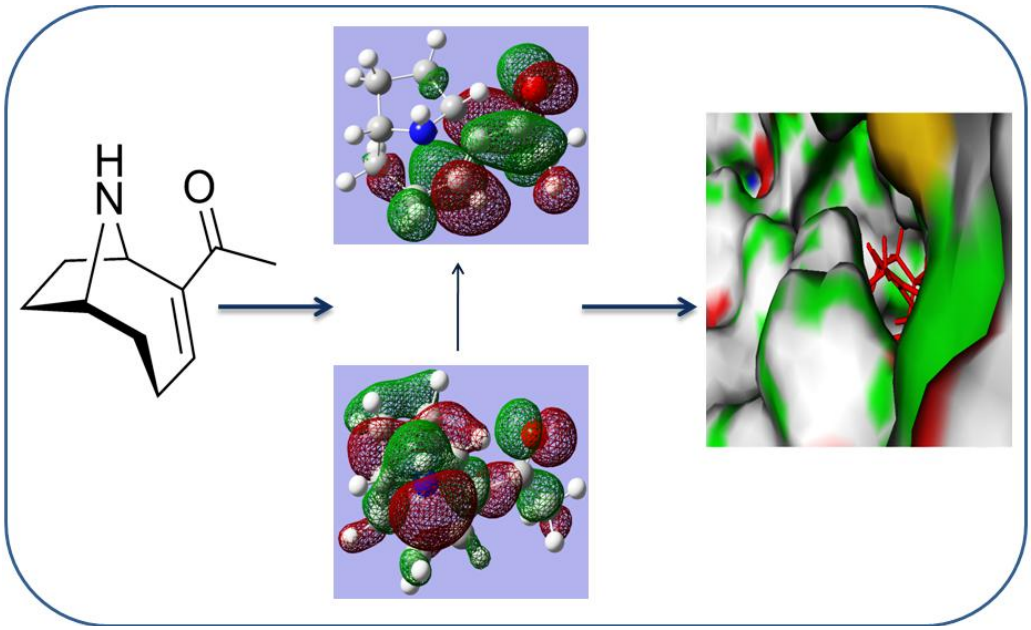

Figure 5. Graphical abstract.

receptor sub-types (Wonnacott et al., 1991; Araoz et al., 2010). This may lead to the development of new drugs which do not have the toxicity like anatoxin-a, but which act merely as acetylcholine replacement candidates.

Conflict of Interests

The author(s) have not declared any conflict of interests.

ACKNOWLEDGEMENTS

Authors gratefully acknowledge Council of Scientific and Industrial Research (CSIR), New Delhi, India, for their financial assistance to Naresh Kumar.

REFERENCES

Araoz R, Vilarino N, Botana LM, Molgo L (2010). Ligand-binding assays for cyanobacterial neurotoxins targeting cholinergic receptors. Anal. Bioanal. Chem. 397: 1695-1704.

Aronstam RS, Witkop B (1981). Anatoxin-a interactions with cholinergic synaptic molecules. Proc. Natl. Acad. Sci. 78: 4639-4643.

Badry DB, Maxim T, Abagyan R, Brooks CL (2003). Comparative study of several algorithms for flexible ligand docking. J. Comput. Aided Mol. Des. 17: 755-763.

Becke AD (1993). Density functional thermochemistry. III. The role of exact exchange. J. Chem. Phys. 98: 5648.

Behm D (2003). Coroner cites algae in Ten's death. In Milwaukee Journal Sentinel. September 6, 2003.

Carmichael WW, Biggs DF, Gorham PR (1975). Toxicology and pharmacological action of A*nabaena flos-aquae* toxin. Science 187: 542-546.

Carmichael WW, Gorham PR (1978). Anatoxins from clones of *Anabaena flos-aquae* isolated from lakes of western Canada. Mitt. Infernal. Verein. Limnol. 21: 285-295.

Carmichael WW, Gorham PR, Biggs DF (1977). Two laboratory case studies on the oral toxicity to calves of the freshwater cyanophyte (blue-green alga) *Anabaena flos-aquae* NRC-44-1. Can. Vet. J. 18: 71-75.

DeLano WL (2002). PyMOL: An Open-source Molecular Graphic Tool, DeLano Scientific, San Carlos, CA (www.pymol.org).

Devlin JP, Edwards OE, Gorham PR, Hunter NR, Pike RK, Stavric B (1977). Anatoxin-a, a toxic alkaloid from *Anabaena flos-aquae*. Can. J. Chem. 55: 1367-1371.

Edwards C, Beattie KA, Scrimgeour CM, Codd GA (1992). Identification of anatoxin-A in benthic cyanobacteria (blue-green algae) and in associated dog poisonings at Loch Insh, Scotland. Toxicon 30: 1165-1175.

Fawell JK, Mitchell RE, Hill RE, Everett DJ (1999). The toxicity of cyanobacterial toxins in the mouse: II anatoxin-a. Hum. Exp. Toxicol. 18: 168-173.

Friesner RA, Murphy RB, Repasky MP, Frye LL, Greenwood JR, Halgren TA, Sanschagrin PC, Mainz DT (2006). Extra precision glide: docking and scoring incorporating a model of hydrophobic enclosure for protein-ligand complexes. J. Med. Chem. 49: 6177-6196.

Frisch MJ, Trucks GW, Schlegel HB, Scuseria GE, Robb MA, Cheeseman JR et al (2009). Gaussian 09, Revision A.1; Gaussian: Wallingford, CT.

Goel N, Kumar N (2014). Study of supramolecular frameworks having aliphatic dicarboxylic acids, N,N′-bis(salicyl)ethylenediamine and N,N′-bis(salicyl)butylenediamine J. Mol. Struct. 1071: 60–70.

Goel N, Singh UP (2013). Syntheses, Structural, Computational, and Thermal Analysis of Acid–Base Complexes of Picric Acid with N-Heterocyclic Bases. J. Phys. Chem. A 117: 10428-10437.

Gunn GJ, Rafferty AG, Rafferty GC, Cockburn N, Edwards C, Beattie KA, Codd GA (1992). Fatal canine neurotoxicosis attributed to blue-green algae (cyanobacteria). Vet. Rec. 130: 301-302.

Koopmans T (1934). About the allocation of wave functions and eigenvalues of the individual electrons one atom. Physica 1:104-113.

Koskinen AMP, Rapoport H (1985). Synthetic and conformational studies on anatoxin-a: a potent acetylcholine agonist. J. Med. Chem. 28(9): 1301-1309.

Lee C, Yang W, Parr RG (1988). Development of the Colle-Salvetti correlation-energy formula into a functional of the electron density. Phys. Rev. B Condens. Matter. 37: 785-789.

Moore RE (1977). Toxins from blue-green algae. BioScience 27: 797-802.

Pybus MJ, Hobson DP, Onderka DK (1986). Mass mortality of bats due to probable blue-green algal toxicity. J. Wildl. Dis. 22: 449-450.
Sergio FS, Fernandes PA, Ramos MJ (2006). Protein–ligand docking: Current status and future challenges. Proteins 65: 15-26.
Stevens DK, Krieger RI (1991). Effect of route of exposure and repeated doses on the acute toxicity in mice of the cyanobacterial nicotinic alkaloid anatoxin-a. Toxicon 29: 134-142.
Viaggiu E, Melchiorre S, Volpi F, Corcia DA, Mancini R, Garibaldi L, Crichigno G, Bruno M (2004). Anatoxin-a toxin in the cyanobacterium *Planktothrix rubescens* from a fishing pond in northern Italy. Environ. Toxicol. 19: 191-197.
Wonnacott S, Jackman S, Swanson KL, Rapoport H, Albuquerque EX (1991). Nicotinic pharmacology of anatoxin analogs. II. Side chain structure-activity relationships at neuronal nicotinic ligand binding sites. J. Pharmacol. Exp. Ther. 259: 387-391.

academicJournals

Vol. 13(30), pp. 3101-3106, 23 July, 2014
DOI: 10.5897/AJB2014.13765
Article Number: A5848EF46226
ISSN 1684-5315

http://www.academicjournals.org/AJB

African Journal of Biotechnology

Full Length Research Paper

The role of adrenergic receptors in nicotine-induced hyperglycemia in the common African toad (*Bufo regularis*)

Isehunwa, G. O.[1]*, Adewunmi, G. O.[1], Alada, A. R. A[1] and Olaniyan, O. T.[2]

[1]Department of Physiology, University of Ibadan, Ibadan, Nigeria.
[2]Department of Physiology, Bingham University, Karu, Nasarawa, Nigeria.

Received 28 February, 2014; Accepted 2 June, 2014

The role of adrenergic receptors in nicotine-induced hyperglycaemia has not been well studied in amphibians. Thus, this study investigates the effects of alpha and beta adrenergic receptor blockers in nicotine-induced hyperglycaemia in the common African toad *Bufo regularis*. Toads fasted for 24 h were anaesthetized with sodium pentobarbitone (3 mg/100 g body weight) intraperitoneally (i.p) and given intravenous (i.v) injection of 0.7% amphibian saline, or nicotine (50 µg/kg), nicotine(50 µg/kg i.v) 30 min after pretreatment with prazosin (0.2 mg/kg i.v), propranolol (0.5 mg/kg i.v) or combination of both prazosin (0.2 mg/kg i.v) and propranolol (0.5 mg/kg, i.v). Thereafter, blood samples were also collected from truncus arteriosus for estimation of blood glucose level using the modified glucose oxidase method. Nicotine caused significant increase (P<0.01) in the levels of blood glucose in the common African toad. Pre-treatment of the toads with prazosin (0.2 mg/kg i.v) or propranolol (0.5 mg/kg, i.v) significantly (p < 0.01) reduced the hyperglycaemia induced by nicotine (50 µg/kg i.v). However, the combination of prazosin (0.2 mg/kg i.v) and propranolol (0.5 mg/kg, i.v) abolished the hyperglycaemic effect of nicotine (50 µg/kg i.v). The above results on glucose metabolism suggests involvement of both alpha and beta adrenoceptors in nicotine-induced hyperglycaemia in common African toad *B. regularis*.

Key words: Nicotine, hyperglycaemia, prazosin, propranolol, common African toad *Bufo regularis*.

INTRODUCTION

Nicotine, the main psychoactive and addictive compound in tobacco (Benowitz, 1988), is a low molecular weight alkaloid found in cigarettes and through insecticide inhalation (Hosseini, 2011). Its consumption alters cardiovascular, neural, and endocrine functions through its effects on the central and peripheral nervous system (Benowitz, 1988; Matta et al., 2007; Hosseini, 2011).

Another important role of nicotine is the ability to induce hyperglycaemia in animals such as dogs, rats and rabbits (Grayson and Oyebola, 1985; Oyebola and Alada, 1993; Oyebola et al., 2009). Nicotine acts indirectly on blood glucose levels by stimulating adrenaline release from the

*Corresponding author. E-mail: funmisehunwa@yahoo.com.

adrenal glands that in turns triggers the glycaemic response via acetylcholine nicotinic receptors (Tsuijimoto et al., 1965; Milton, 1966). In particular, nicotine rapidly increases blood sugar levels by mobilizing glucose release from hepatic and muscle glycogen stores through adrenergic actions (Molimard, 2013). The hyperglycaemic response to adrenaline is mediated by both alpha and beta adrenoceptors (Al-Jibouri et al, 1980).

Previous studies showed occurrence of modulation in alpha and beta adrenoceptors during nicotine-induced hyperglycaemia (Grayson and Oyebola, 1985; Oyebola et al., 2009). However, there are conflicting reports on receptor-types involved in the hyperglycaemic response to nicotine action. For instance, both alpha and beta adrenoceptors are modulated in dogs (Grayson and Oyebola, 1985) and rabbits (Oyebola et al., 2009) during nicotine-induced hyperglycaemia; whereas in rats, only beta-adrenoceptors are functional (Oyebola and Alada, 1993). Therefore, our study aimed at investigating the role of the alpha and beta adrenergic receptors in nicotine-induced hyperglycaemia in the common African toad (*Bufo regularis*).

The levels of blood glucose in the test and control groups were measured using modified glucose oxidase method (Trinder, 1969). Finally, our studies confirm the involvement of both apha and beta adrenergic receptors in nicotine-triggered glucose metabolism.

MATERIALS AND METHODS

Laboratory animals

Adult male and female toads (n=240) weighing between 70-100 g were studied. The toads were obtained from the banks of slow-moving streams, around ponds and wet bushes. The collection process, which took place at night, was done randomly to prevent bias.

Experimental procedures

Toads were fasted for 24 h before treatment. They were anaesthesized by intraperitoneal (i.p) injection of sodium pentobarbitone (3 mg/100 g body weight). Blood was collected from truncus arteriosus after careful dissection to remove connective tissues surrounding it. The anterior abdominal vein was cannulated for drug injection. Thereafter, each toad was heparinised (170 units/0.1 ml) to maintain fluidity of blood and allowed 30 min to stabilize. After stabilization period, basal blood collection (this represented 0 min) was made from the truncus arteriosus.

Control and treatment groups

The animals were randomly divided into five groups (I to V) of 48 toads per group. Toads in control group I were injected intravenously (i.v) with 0.7 % amphibian saline; whereas, those in group II (untreated) were given 50 µg/kg i.v nicotine injections. Group III, IV, and V were pre-treated with prazosin 0.2 mg/kg i.v, 0.5 mg/kg i.v propranolol or combination of both 0.2 mg/kg i.v. prazosin and 0.5mg/kg i.v propranolol, respectively. After 30 min, group 111-V were injected with a dose of nicotine (50 µg/kg i.v).

Each drug injection was in a total volume between 0.1 and 0.12 ml given intravenously through the anterior abdominal vein cannula. In each animal, blood sample (0.05 ml per sample) was drawn directly from the truncus arteriousus for blood glucose determination. Blood samples were collected after 0, 5, 10, 20, 30, 60 and 90 min post-drug injection. Blood glucose levels were determined following a modified glucose oxidase method by Trinder (1969). Owing to the small size of the toad, animals were sampled only once in each experiment and then sacrificed.

Determination of liver and muscle glycogen

In order to determine the glycogen content of *B. regularis*, six toads were analysed in each group. Following the surgical procedure and thirty minutes for the animal to stabilize, each toad was given 0.7 % amphibian saline or 50 µg/kg nicotine through anterior abdominal vein cannula. The whole liver and gastrocnemius muscle of each anaesthetized toad were quickly removed sixty minutes post injection period. These tissues were weighed using an electronic weighing balance (Coledo DT 1000 England). Thereafter, 1 g of liver and muscle were excised separately and the glycogen content determined using anthrone reagents method (Seifter et al., 1950; Jermyn, 1975).

Purification and quantitation of glycogen

One-gram each of liver and muscle were placed in individual pre-heated Erlnmeyer flasks containing 10 ml of 30% potassium hydroxide solution. The liver and muscle were digested separately by heating the flasks for 20 min in a steam bath with occasional shaking until the tissues dissolved. The solution was allowed to cool. Then, 4 ml of the aliquot from each was transferred into a sterile 15 ml centrifuge tube. Subsequently, 5 ml of 95% ethanol was added to each sample, mixed and centrifuged at 3500 rpm for 5 min; it was then decanted and drained for 5 min. Precipitated glycogen from each sample was dissolved in 0.5 ml distilled water. The tube contents were re-precipitated with 5 ml of 95% ethanol and recovered through centrifugation. Centrifugation was repeated four times until a white precipitate was obtained. The final glycogen precipitate was dissolved in 2 ml of distilled water. Then, 0.5 ml aliquot was taken from the unknown glycogen solution obtained above. The next step involved step-wise addition of 0.5ml of concentrated HCl, 0.5 ml formic acid (88%) and 4 ml of anthrone reagent. Similarly, 0.5 ml of distilled water (used as a blank) was treated following above steps.

Several dilutions of the glycogen standard (0.2 mg/ml) were prepared. The dilutions used are 0.1, 0.2, 0.3, 0.4 ml of standard glycogen solution with distilled water to make a total volume of 0.5 ml. These dilutions of glycogen standard were then treated and used to generate a standard curve.

All the tubes containing the solutions were heated in boiling water for ten minutes and allowed to cool. Content from each tube was poured into a cuvette, followed by measurement of absorbance at 630 nm against the blank. Glycogen content was calculated from the following Equation 1:

$$\text{Mg glycogen/100 g fresh liver} = \text{Mg glycogen/ml} \times \frac{10}{4} \times \frac{2}{0.5} \times \frac{100}{\text{Total fresh liver weight}} \quad (1)$$

Statistical analysis

All values provided represent mean ± standard error of mean (S.E.M) of the variables measured. Differences between two groups were compared using student t test whereas one-way analysis of variance (ANOVA) was employed in comparison between mean values in multiple groups. $P \leq 0.05$ were taken as statistically significant.

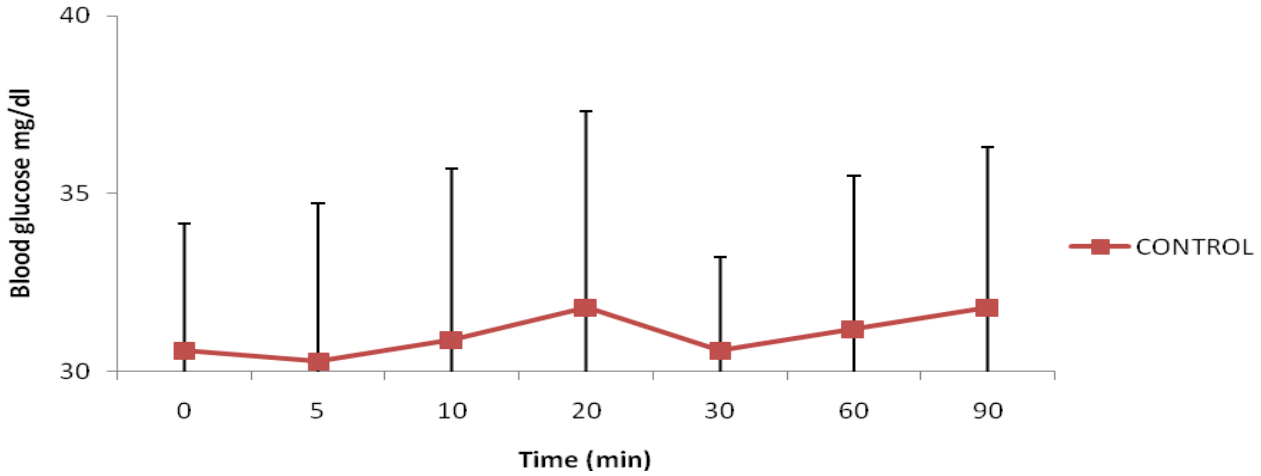

Figure 1. The effects of 0.7% amphibian saline on blood glucose levels. Amphibian saline produced no significant effect (p≥0.05) on blood glucose level. The points represent Mean ± S.E.M. N=7 toads for each timed observation.

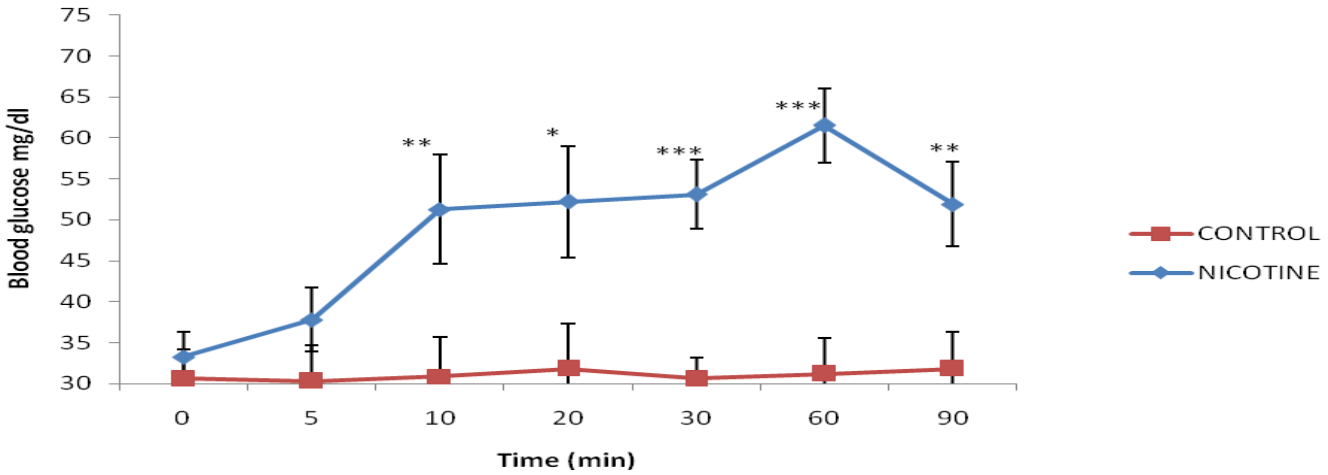

Figure 2. The effects of nicotine (50 µg/kg) on blood glucose levels (untreated toads). Note the hyperglycaemic effects of nicotine which became significant (p <0.05) 10 min post-injection period. Nicotine (50 µg/kg) caused blood glucose to increase from basal value (33.3±2.97 mg/dl) to maximal value of (61.5±4.52 mg/dl***) 60 min post-injection. The points are mean ±S.E.M. Asterisk (*) indicate values that are significantly different (*P≤ 0.05), (**p≤0.01) and (***p≤0.001) from the control. (n=7 toads for each timed observation).

RESULTS

The results are shown in Figures 1 to 6 and Table 1. All values given are mean ± S.E.M of the variables measured. Toads in group 1 were not pre-treated with any adrenoceptor blocker and are referred to as the untreated animals.

Effect of 0.7% amphibian saline and nicotine injection on blood glucose, liver and muscle glycogen levels

Infusion of 0.7% amphibian saline had no effect on blood glucose level (Figure 1). However the mean fasting glucose level in the toad *B. regularis* was 33.3±3.0 mg/dl. Injection of nicotine 50 µg/kg caused a significant increase in blood glucose level from mean basal value of 33.3±3.0 mg/dl to a maximum value of 61.5±4.5 mg/dl 60 min post injection (Figure 2). The hyperglycaemic effect of nicotine became significant 10 min post-injection and rose progressively till 60 min post-injection period. Injection of nicotine 50 µg/kg caused significant reduction in liver and muscle glycogen content compared with the control group.

Effect of nicotine during prazosin and propranolol pre-treatment

Pre-treatment with prazosin prevented the increase in

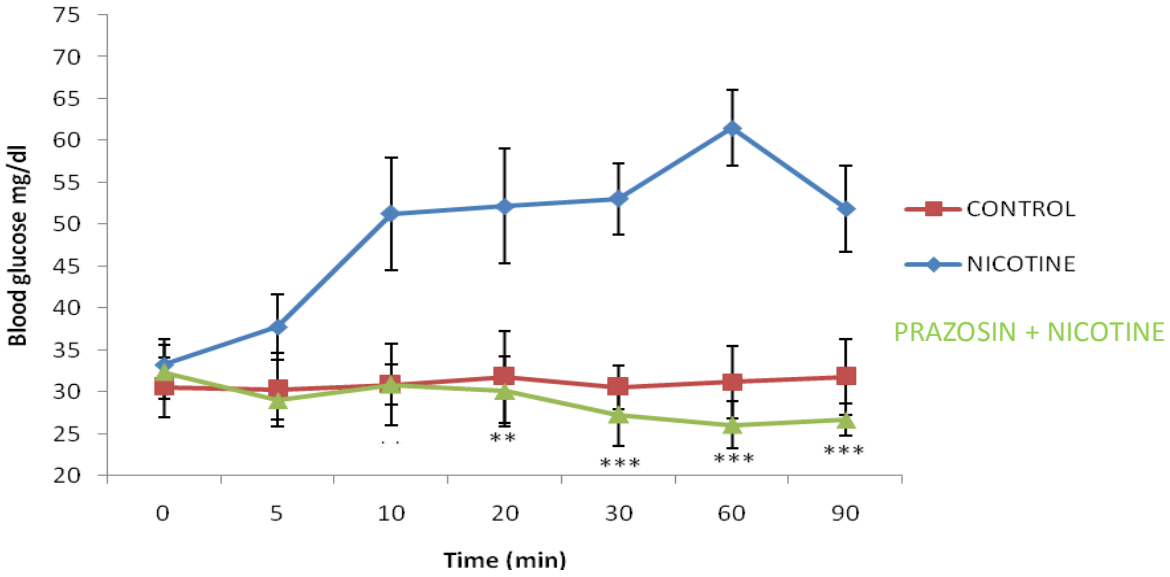

Figure 3. The effects of nicotine (50 µg/kg) on blood glucose levels in untreated and prazosin treated (0.2 mg/kg) toads. Prazosin produced a significant reduction on nicotine-induced hyperglycaemia when compared with the untreated toads. Each data points represent mean ± S.E.M.

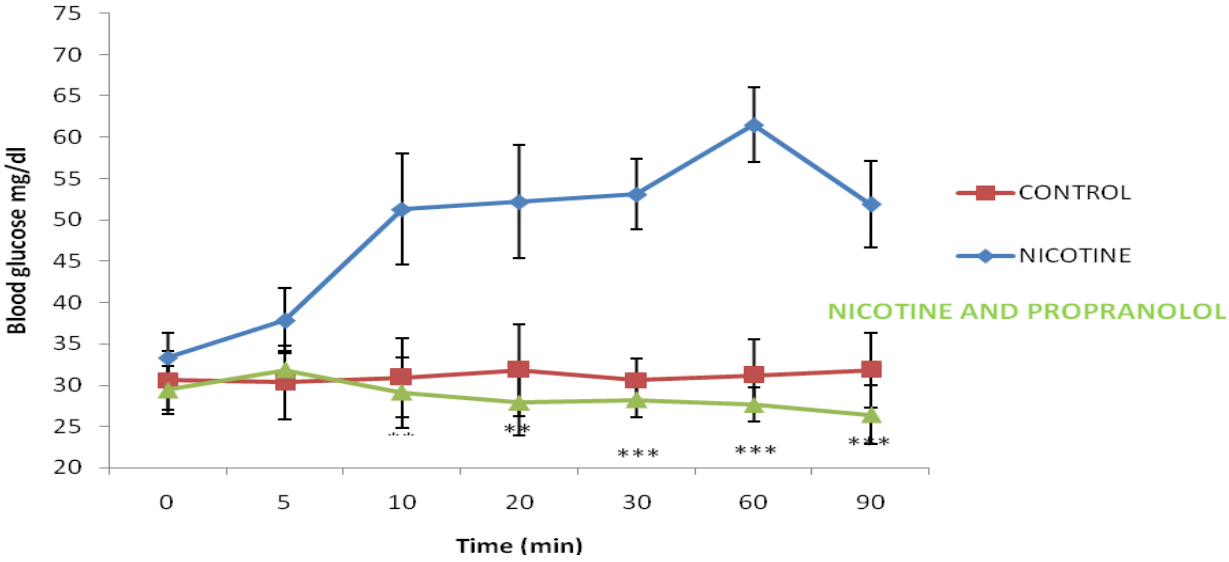

Figure 4. The effects of nicotine (50 µg/kg) on blood glucose levels in untreated versus propranolol- treated (0.5 mg/kg) toads. Propranolol (0.5 mg/kg) abolished the increase in nicotine- induced hyperglycemia.This was followed by decline in blood glucose levels in the remaining post-injection observation period. Each data point represents mean ± S.E.M. Asterisks (*) indicate values that are significantly different (*P ≤ 0.05), (**p≤0.01) and (***p≤0.001) from the nicotine (untreated group).

glucose levels induced by nicotine injection (Figures 3 to 6) while propranolol pre-treatment abolished the increases in glucose levels caused by nicotine injection. The glucose levels fell below basal level throughout post-injection period. A combination of both blockers completely abolished nicotine-induced hyperglycaemia in toad compared with the untreated toads.

DISCUSSION

The findings of the present study in which nicotine infusion caused a rise in blood glucose level of *B. regularis* is consistent with its known pharmacological effect on blood glucose (Oyebola et al., 2009). Since amphibian saline had no effect on blood glucose, the increase in blood glucose

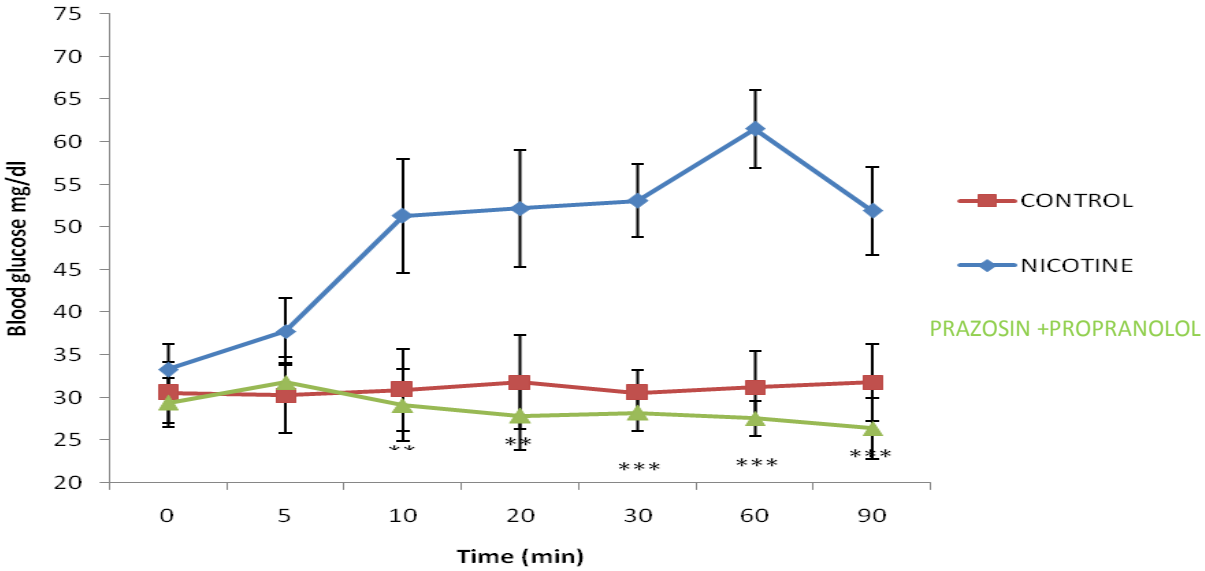

Figure 5. The effects of nicotine (50 µg/kg) on blood glucose levels in untreated and in toads treated with both prazosin (0.2 mg/kg) and propranolol (0.5 mg/kg). Combination of both blockers completely abolished nicotine hyperglycaemia in *Bufo regularis.* Each data point represents mean ± S.E.M. Asterisk (*) indicate values that are significantly different (*P ≤ 0.05), (**p≤0.01) and (***p≤0.001) from the nicotine (untreated) group. N=7 for each observation.

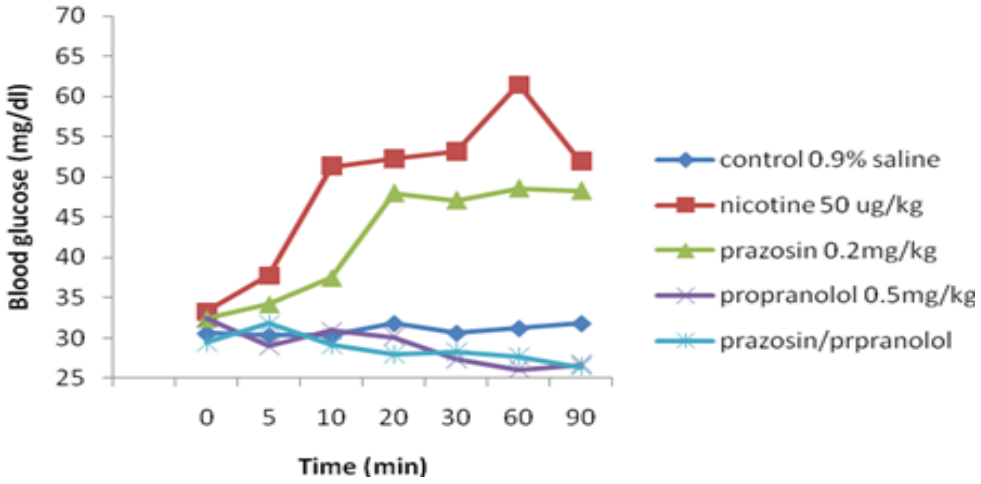

Figure 6. The effects of 0.7% amphibian saline, nicotine (50 µg/kg), prazosin treated (0.2 mg/kg), propranolol treated (0.5 mg/kg) and combination of both prazosin (0.2 mg/kg) and propranolol (0.5 mg/kg) treated toads on glucose levels. The points are mean ± S.E.M. N=7 for each observation.

Table 1. Liver and muscle glycogen content (Mg glycogen/100 g fresh liver and muscle; mean ± S.E.M) in toads infused with 0.7% saline and nicotine (50 µg/kg).

Treatment (1 h)	Liver glycogen	Muscle glycogen
Control 0.7% saline	111.62±47.98	42.31±4.99
Nicotine (50 µg/kg)	7.35±0.87***	5.02±1.04***

Asterisk(*) indicates significantly different values (***P<0.001). n=6 for each infusion.

level in nicotine-injected group could not be due to the stress of nicotine injection. Previous studies in dogs (Tsujimoto et al., 1965; Grayson and Oyebola, 1985) and cats (Milton, 1966) showed that nicotine injection induces hyperglycaemia indirectly through adrenaline release from the adrenal medulla.The hyperglycemia observed during nicotine injection results from an increase in glucose production. The results of the present study in which nicotine caused significant reduction in liver and muscle

glycogen levels suggests that both hepatic and muscle glycogen must have contributed to glucose production which results in a rise in glucose levels following administration of nicotine. This finding agrees with previous reports that nicotine rapidly increases blood glucose by mobilizing hepatic and muscle glycogen stores by adrenergic actions (Tsujimoto et al., 1965; Mlton, 1966; Benowitz, 1986; Molimard, 2013). Additionally, we report that the onset of glycaemic response to nicotine was gradual and the blood glucose levels continued to increase reaching peak levels 60 min post-injection. The sustained nicotine-induced hyperglycaemia was similar to what was previously reported in rats (Oyebola and Alada, 1993) and rabbits (Oyebola et al., 2009). This may suggest similar trends in glucose metabolism in rabbits, rats and toads following glycaemic response to nicotine.

The results of the present study in which prazosin an alpha adrenergic blocker caused profound decrease in nicotine - induced hyperglycemia in *B. regularis* suggested the role of α-adrenergic receptors in nicotine hyperglycaemia. This was consistent with the observations in dogs (Grayson and Oyebola, 1985), rabbits (Oyebola et al., 2009) but contrasts to the findings in rats (Oyebola and Alada, 1993). The studies in dogs (Grayson and Oyebola, 1985) and rabbits (Oyebola et al., 2009) showed that prazosin abolished nicotine-induced hyperglycaemia whereas prazosin merely attenuated nicotine hyperglycaemia in rats (Oyebola and Alada, 1993).

The abolition of nicotine hyperglycemia by propranolol indicated that the ability of nicotine to cause a rise in blood glucose level was mediated through the beta adrenergic receptors. This observation agrees with the studies in dogs (Grayson and Oyebola, 1985), rats (Oyebola and Alada, 1993) and in rabbits (Oyebola et al., 2009). Since beta receptors are present in the skeletal muscles (Arnold and Selbens, 1968; Hendler and Sherwin, 1984) some amount of the glucose released after nicotine administration could have been produced from lactate in the skeletal muscle.

However, the complete abolition of nicotine hyperglycaemia by combination of prazosin and propranolol appears to confirm the involvement of both alpha and beta adrenoceptors in mediating nicotine induced hyperglycaemia in the toad. This finding agrees with the observation in dogs (Grayson and Oyebola, 1985), and rabbits (Oyebola et al., 2009), but contrasts the study report in rats (Oyebola and Alada, 1993). The differences in observations may be due to species variation with respect to the receptors involved in nicotine-induced hyperglycaemia in different animals.

In conclusion, the above results suggest that both alpha and beta adrenergic receptors play roles in nicotine-induced hyperglycaemia in the common African toad *B. regularis*.

Conflict of Interests

The author(s) have not declared any conflict of interests.

REFERENCES

Al-Jibouri LM, Furman BL, Parratt JR (1980). Blockade of adrenaline-induced hyperglycaemia in the anaesthetized cat by continuous infusion of phentolamine and propranolol. Br. J. Pharmacol. 68: 461-466.

Arnold A, Selbens WH (1968). Activation of catecholamines on rats muscle glycogenolytic β2-receptor. Experiment 24:1010-1011.

Benowitz NL (1986). Clinical pharmacology of nicotine. Annu. Rev. Med. 37:21-32.

Benowitz NL (1988). Drug therapy, Pharmacologic aspects of cigarette smoking and nicotine addiction. N. Engl. J. Med. 319: 1318-1330.

Grayson J, Oyebola DDO (1985). Effect of nicotine on blood flow, oxygen consumption and glucose uptake in canine small intestine. Br. J. Pharmacol. 85: 797-804.

Hendler RG, Sherwin RS (1984). Epinephrine-stimulated glucose production is not diminished by starvation: Evidence for an effect on gluconeogenesis. J. Clin. Endocrin. Meta. 58:1014-1021.

Hosseini E (2011). The effect of nicotine on the serum level of insulin in adult male wistar rats. J. Cell Anim. Biol. 5 (10): 215-218.

Jermyn MA (1975). Increasing the sensitivity of the anthrone method for carbohydrate. Anal. Biochem. 68: 322-335.

Matta SG, Balfour DJ, Benowitz NL et al (2007). Guidelines on nicotine dose selection for in vivo research. Psycopharmacology 190 (3): 269-319.

Milton AS (1966). Effects of nicotine on blood glucose levels and plasma non-esterified fatty acid levels in the intact and adrenalectiomised cat. Br. J. Pharmacol. 26: 256-263.

Molimard R (2013). Personal Communication to French High Health Authority retrieved from www.form indep.org on December 26, 2013.

Oyebola DD, Alada AR (1993) Effects of adrenergic receptor blockers on adrenaline and nicotine- induced hyperglycaemia in the rat. Afr. J. Med. Med. Sci. 22(4): 13-18.

Oyebola DDO, Idolor GO,Taiwo EO, Alada ARA, Owoeye O, Isehunwa GO (2009). Effect of nicotine on glucose uptake in the rabbit small intestine. Afr. J. Med. Med. Sci.38: 119-130.

Seifter S, Dayton S, Novic B, Muntwryler E (1950). The estimation of glycogen with anthrone reagent. Arch. Biochem. 25: 191-199.

Trinder P (1969). Determination of blood glucose using 4-amino phenzone as oxygen acceptor. J. Clin. Pathol. 22:158-161.

Tsujimoto A, Tanino S, Kurogochi Y (1965). Effect of nicotine on serum potassium and blood glucose. Jpn. J. Pharmacol.15: 416-422.

academicJournals

Vol. 13(30), pp. 3107-3113, 23 July, 2014
DOI: 10.5897/AJB2012.2941
Article Number: 089108B46228
ISSN 1684-5315

http://www.academicjournals.org/AJB

African Journal of Biotechnology

Full Length Research Paper

Composition and antioxidant and antifungal activities of the essential oil from *Lippia gracilis* Schauer

Caroline da S. Franco[1], Alcy F. Ribeiro[2], Natale C. C. Carvalho[3], Odair S. Monteiro[3], Joyce Kelly R. da Silva[4], Eloisa Helena A. Andrade[2] and José Guilherme S. Maia[1,5]*

[1]Programa de Pós-Graduação em Ciências Farmacêuticas, Universidade Federal do Pará, 66075-900 Belém, PA, Brazil.
[2]Programa de Pós-Graduação em Química, Universidade Federal do Pará, 66075-900 Belém, PA, Brazil.
[3]Programa de Pós-Graduação em Química, Universidade Federal do Maranhão, 65080-040 São Luis, MA, Brazil.
[4]Programa de Pós-Graduação em Biotecnologia, Universidade Federal do Pará, 66075-900 Belém, PA, Brazil.
[5]Programa de Pós-Graduação em Recursos Naturais da Amazônia, Universidade Federal do Oeste do Pará, 68010-110 Santarém, PA, Brazil.

Received 30 November, 2012; Accepted 3 July, 2014

In this study, the oil constituents of *Lippia gracilis* were identified by gas chromatography (GC) and gas chromatography-mass spectrometry (GC-MS). The antioxidant and antifungal activities were also evaluated. The leaf oil showed a yield of 3.7% and its main constituents were thymol (70.3%), *p*-cymene (9.2%), thymol methyl ether (5.4%) and *p*-methoxythymol (2.7%). The thin stem oil showed a yield of 0.4% and its major components were thymol (70.1%), thymol methyl ether (4.4%), *p*-methoxythymol (4.0%), *p*-cymene (3.8%), α-humulene (2.4%) and (*E*)-caryophyllene (2.1%). The aromatic monoterpenes found in the oils showed an average of 88%. The scavenging activity of the 1,1-diphenyl-2-picrylhydrazyl radical (DPPH) for the leaf oil, expressed as half maximal effective concentration (EC_{50}), was 35.7±3.3 µg/ml, indicating high antioxidant activity. The evaluation of fungicide activity for the leaf oil, using direct bioautography, showed also a significant value for lethal concentration (LC_{50} 5.0 µg/ml) against *Cladosporium sphaerospermum* and *C. cladosporioides* fungi.

Key words: Essential oil composition, thymol and carvacrol, DPPH radical scavenging and bioautography

INTRODUCTION

Lippia (Verbenaceae) comprises nearly 200 species of herbs, shrubs and small trees spread wide in South and Central America and Tropical Africa. *Lippia gracilis* Schauer [syn. *Acantholippia trifida* (Gay) Moldenke] is an aromatic shrub up to 1.5 m in height, known popularly as "vereda" or "alecrim-de-tabuleiro", growing wild in areas of savannas of North and Northeast Brazil. Its aerial parts are used to treat gastrointestinal, respiratory and cutaneous infections (Albuquerque et al., 2006).

L. gracilis occurring in Northeast Brazil have shown

*Corresponding author. E-mail: gmaia@ufpa.br. Tel: + 55 91 81467067. Fax: + 55 91 32353043.

variation in the composition of its volatile constituents. The oil produced in Ceará state showed thymol (30.6%), carvacrol (11.8%) and *p*-cymene (10.7%) as main compounds (Lemos et al., 1992). In the oil obtained at Piauí state, the major components were carvacrol (47.7%), *p*-cymene (19.2%), methylthymol (6.2%) and thymol (4.8%) (Matos et al., 1999). The oil analyzed in Sergipe state was dominated by thymol (24.0%), *p*-cymene (15.9%), methylthymol (11.7%) and γ-terpinene (10.9%) (Teles et al., 2010). Previously, the oil of *L. gracilis* showed antibacterial (Mota et al., 2009) activities against *Staphylococcus aureus* and *Biomphalaria glabrata*, respectively, molluscicidal activities (Teles et al., 2010), and its methanolic extract showed antinociceptive effect in mice (Guimarães et al., 2012).

The genus *Lippia* is well-known for its aromatic properties, and more than 50 of its essential oils have been reported (Terblanché and Kornelius, 1996; Pascual et al., 2001). The main volatile constituents frequently found in the oils of *Lippia* species are thymol, carvacrol, *p*-cymene methylthymol, methylcarvacrol, γ-terpinene, 1,8-cineole and (*E*)-caryophyllene. Many *Lippia* species has shown variation in their oil composition, producing various chemical types as occur in *Lippia alba* (Matos et al., 1996; Zoghbi et al., 1998; Atti-Serafini et al., 2002), *Lippia lupulina* (Zoghbi et al., 2001), *Lippia glandulosa* (Maia et al., 2005), *Lippia origanoides* (Morais et al., 1972; Oliveira et al., 2007; Stashenko et al., 2008; Silva et al., 2009) and *Lippia grandis* (Silva et al., 1973; Maia et al., 2003; Damasceno et al., 2011).

Lately, there has been a growing interest in the search for spices, aromatic and medicinal plants as sources of natural antioxidants. The antioxidant capacity of these plants is associated with the activity of the free radical scavenging enzymes and the contents of antioxidant substances, usually phenol compounds. The use of essential oils as functional ingredients in foods, drinks, toiletries and cosmetics has become increasingly valuable also because of concern about potentially harmful synthetic additives. The oils and extracts, being biologically active natural compounds, have been proposed for the control of certain diseases and the prevention of lipid peroxidative damage implicated in various pathological disorders, such as atherosclerosis, Alzheimer`s disease, carcinogenesis and aging processes (Ruberto and Baratta, 2000; Mimica-Durik et al., 2004).

The aim of this study was to analyze the oil composition of leaves and thin stems of *L. gracilis* that occur in the eastern Brazilian Amazon, as well as to evaluate their antioxidant and antifungal and activities.

MATERIALS AND METHODS

Plant material

The specimen *L. gracilis* Schauer was collected in the locality of São Félix de Balsas, Maranhão state, Brazil, February 2011. The plant was identified and deposited (MG 200187) in the Herbarium of Museu Paraense Emílio Goeldi, Belém city, Pará state, Brazil.

Plant processing

The leaves and thin stems were air-dried separately, ground and subjected to hydrodistillation (100 g, 3 h), using a Clevenger-type apparatus. The oils were dried over anhydrous sodium sulfate, and their percentage contents were calculated on basis of the plant dry weight. The moisture content of the samples were calculated after the phase separation in a Dean-Stark trap (5 g, 30 min), using toluene.

Oil-composition analysis

The analysis of the oils were carry out on a THERMO DSQ II GC-MS instrument, under the following conditions: fused-silica capillary column DB-5ms (30 m x 0.25 mm, 0.25 μm film thickness); programmed temperature, 60-240°C (3°C/min); injector temperature, 250°C; carrier gas was helium, adjusted to a linear velocity of 32 cm/s (measured at 100°C); injection type, splitless (2 μL of a 1:1000 hexane solution); split flow was adjusted to yield a 20:1 ratio; septum sweep was a constant 10 ml/min; EIMS electron energy, 70 eV; temperature of ion source and connection parts, 200°C. The quantitative data regarding the volatile constituents were obtained by peak-area normalization using a FOCUS GC/FID operated under conditions similar to those in GC-MS, except for the carrier gas, which was nitrogen. The retention index was calculated for all the volatiles constituents using an *n*-alkane homologous series.

DPPH radical scavenging assay

A stock solution of 1,1-diphenyl-2-picrylhydrazyl (DPPH) radical (0.5 mM) in methanol (MeOH), was prepared. The solution was diluted in MeOH (60 μM approx.) measuring an initial absorbance of 0.62±0.02 in 517 nm at room temperature. The reaction mixture was composed by 1950 μL of DPPH solution and 50 μL of the samples diluted in different methanol portions. For each sample, a methanol blank was also measured. The absorbance was measured in the reaction starting (time zero), each 5 min during the first 20 min and then at constant intervals of 10 min up to constant absorbance value. The concentration of antioxidant required for 50% scavenging of DPPH radicals (EC_{50}) was determined by linear regression using Windows/Excel. All experiments were in triplicate. Butylated hydroxyanisole (BHA) and 6-hydroxy-2,5,7,8-tetramethylchroman-2-carboxylic acid (Trolox) were used as standard antioxidants. The radical scavenging activity of each sample was calculated by the DPPH inhibition percentage according to the equation IP_{DPPH} =100 (A - B) / A (where A and B are the blank and sample absorbance values in the end reaction). The radical scavenging activity, expressed as milligrams of Trolox equivalent per gram of each sample, was also calculated by means of the equation TE = (A – B)/(A – C) x 25/1000 x 250.29/1000 x 1000/10 x D (where A, B and C are the blank, sample and Trolox absorbance values in the end reaction, and D is the dilution factor) (Silva et al., 2007; Silva et al., 2011).

Antifungal bioassay

About 10 μL of the oil solutions (corresponding to 100, 50, 25, 10, 5, 1, 0.5 and 0.1 μg) were applied to pre-coated thin layer chromatographic (TLC) plates, which were developed with *n*- hexane/ethyl

acetate (8:2) and dried for complete removal of solvents. The chromatograms were sprayed with a spore suspension of the fungi *Cladosporium sphaerospermum* and *C. cladosporioides*, in glucose and salt solution and incubated for 48 h in darkness in a moistened chamber at 22°C. Clear inhibition zones appeared against a dark background indicating the minimum amount of the essential oils required. Miconazole was used as the positive control. *C. sphaerospermum* (Penzig) SPC 491 and *C. cladosporioides* (Fresen) de Vries SPC 140 have been maintained at the Laboratory of Engineering of Natural Products, Federal University of Pará, Belém city, Pará State, Brazil (Silva et al., 2011).

Statistical analysis

Samples were assayed in triplicate, and the results are shown as means ± standard deviation. Analysis of variance was conducted, and the differences between variables were tested for significance by one-way ANOVA with Tukey's post test using Minitab, version 14. Differences at $p < 0.05$ were considered statistically significant. The relationship between variables was determined by simple regression analysis.

RESULTS AND DISCUSSION

Oil-composition

The leaves and thin stems of *L. gracilis* provided oil yields of 3.7 and 0.4%, respectively, and their volatile constituents were analyzed by gas chromatography (GC) and gas chromatography-mass spectrometry (GC-MS). Individual components were identified by comparison of both mass spectra and GC-retention data with authentic compounds, which were previously analyzed and stored in the data system, or existing in commercial libraries and cited in the literature (Adams, 2007; NIST, 2005).

In total, 49 components were identified in the oils from leaves and thin stems of *L. gracilis*, comprising 99.5% of the total composition, which is listed in Table 1. Aromatic monoterpenes were the most representative class in the oils, ranging from 84.4 to 91.0%. Aliphatic monoterpenes and sesquiterpenes (hydrocarbons and oxygenated) are represented secondarily in the oils, the first varying from 4.6 to 5.2%, and the last from 3.6 to 9.4%. With a percentage above 2%, the main compounds found in the leaf oil of *L. gracilis* were thymol (73.5%), *p*-cymene (9.2%), thymol methyl ether (5.4%) and *p*-methoxythymol (2.7%) while in the thin stem oil were thymol (70.1%), thymol methyl ether (4.4%), *p*-methoxythymol (4.0%), *p*-cymene (3.8%), α-humulene (2.4%) and (*E*)-caryophyllene (2.1%).

In preliminary analysis, the oil of *L. gracilis* showed the chemical types thymol plus *p*-cymene and carvacrol plus *p*-cymene (Lemos et al., 1992; Matos et al., 1999; Teles et al., 2010). Based on the analysis of this new specimen of *L. gracilis*, we can assume that it is the chemical type thymol plus p-cymene, but with an occurrence in North Brazil. In previous works was observed that *Lippia* oils from the Brazilian Amazon showed significant amounts of thymol, carvacrol, *p*-cymene, 1,8-cineole, γ-terpinene, (*E*)-caryophyllene, citral, carvone and terpinen-4-ol (Zoghbi et al., 1998; Zoghbi et al., 2001; Maia et al., 2005; Morais et al., 1972; Silva et al., 2009; Damasceno et al., 2011). This way, one must consider that these chemical types of *L. gracilis* may result from the polymorphism of the plant, taking into account, mainly, the season time and site collection.

Thymol, carvacrol and *p*-cymene co-occur also as chief constituents in some traditional oils, such as *Monarda punctata* L., *Satureja hortensis* L. and *Thymus vulgaris* L. (Guenther, 1952; Scora, 1967). Also, it is no coincidence that co-occurs in the oil of L. gracilis the same aromatic monoterpenes, thymol, carvacrol and p-cymene. All these compounds are derived from the same biosynthetic plant process, where γ-terpinene, the cyclohexadiene constituent that occur also in the oil, is considered the initiator (Poulose and Croteau, 1978a,b). Figure 1 shows the predicted biosynthetic pathway of these aromatic monoterpenes, which on average comprises for approximately 88% of the oil composition.

Antioxidant activity

Antioxidants interact with the DPPH through the transfer of electrons or donation of hydrogen neutralizing its character of free radical (Silva et al., 2007). The leaves oil of *L. gracilis* was able to scavenging the DPPH radical, displaying a high dose-response (r^2=0.85). The half maximal effective concentration (EC_{50}) was 35.7±3.3 µg/ml, calculated by linear regression, ($p<0.05$), a significant value compared to Trolox (4.5±0.1 µg/ml), which was used as standard antioxidant. EC_{50} values lower than 30 µg/ml indicates high potential for radical scavenging (Ramos et al., 2003). This means that the *L. gracilis* oil showed a significant antioxidant potential for radical free scavenging (Figure 2).

Antifungal activity

The fungicide activity resulted from evaluation of direct bioautography using TLC, after the nebulization of fungal spores (Figure 3). The leaf oil of *L. gracilis*, tested against the *Cladosporium sphaerospermum* and *C. cladosporioides* fungi, showed a minimum inhibitory concentration (MIC) of 5.0 µg/ml. Miconazole, at the maximum concentration of 0.5 µg/ml, was used as positive control, meaning that the leaf oil showed antifungal activity comparable to standard compound.

Conclusion

The essential oil of *L. gracilis* collected in the locality of

Table 1. Constituents identified in the oils of *Lippia gracilis*.

Constituent	RI	Leave (%)	Thin stem (%)
α-Pinene	934	0.4	
Myrcene	990	1.7	0.6
α-Terpinene	1014	0.4	0.2
p-Cymene	1025	9.2	3.8
1,8-Cineole	1032	0.4	0.2
γ-Terpinene	1056	1.0	0.8
cis-Sabinene hydrate	1067		0.1
p-Cymenene	1090	0.2	0.3
Linalool	1095	0.2	0.5
allo-Ocimene	1128		0.1
cis-Limonene oxide	1132		0.1
Borneol	1165		0.5
Umbellulone	1169	0.3	0.1
Terpinen-4-ol	1174	0.6	0.8
p-Cymen-8-ol	1181		0.2
α-Terpineol	1187	0.2	0.4
Methyl salicylate	1192		0.3
Shisofuran	1198		0.2
Thymol methyl ether	1233	5.4	4.4
Thymol	1290	73.5	70.1
p-Cymen-7-ol	1291		0.1
Carvacrol	1297		1.5
Eugenol	1357		0.1
α-Copaene	1376	0.3	0.8
β-Elemene	1390		0.1
(*E*)-Caryophyllene	1416	0.9	2.1
2,5-Dimethoxy-*p*-cymene	1425		0.1
trans-α-Bergamotene	1433	0.1	0.2
α-Guaiene	1439		0.1
α-Humulene	1455	1.4	2.4
allo-Aromadendrene	1461		0.1
cis-Cadina-1(6),4-diene	1462		0.2
Dodecanol	1470		0.1
p-Methoxythymol	1475	2.7	4.0
α-Selinene	1498	0.1	0.1
α-Muurolene	1501	0.1	0.2
β-Bisabolene	1506		0.1
γ-Cadinene	1513		0.1
δ-Cadinene	1523	0.3	0.8
α-Calacorene	1546		0.1
(*E*)-Nerolidol	1563		0.1
Spathulenol	1577		0.2
Caryophyllene oxide	1582	0.2	0.6
Globulol	1584		0.1
Humulene epoxide II	1609		0.6
Dillapiole	1621		0.3
1-*epi*-Cubenol	1629		0.1
epi-α-Cadinol	1639	0.2	0.1
α-Cadinol	1654		0.1

Table 1. Contd.

Aromatic monoterpenes	91.0	84.4
Aliphatic monoterpenes	5.2	4.6
Sesquiterpenes (hydrocarbons and oxigenated)	3.6	9.4
Other		0.8
Total	99.8	99.2

RI = Retention time on DB-5ms column

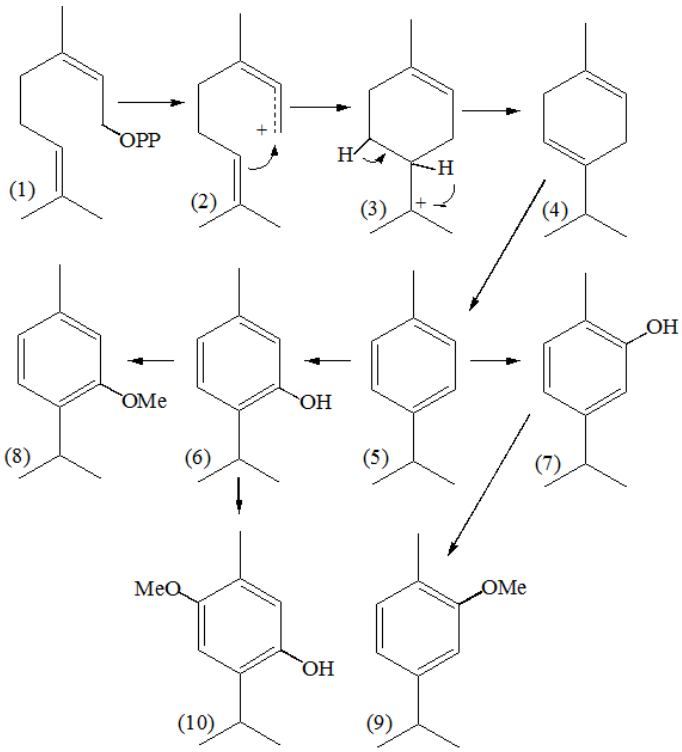

(1) neryl pyrophosphate
(2), (3) intermediate carbocations
(4) y-terpinene
(5) *p*- cynene
(6) thymol
(7) carvacrol
(8) thymol methyl ether
(9) carvacrol methyl ether
(10) *p*-methoxythymol

Figure 1. Proposed biosynthetic pathway for the aromatic monoterpenes occurring in the oil of *Lippia gracilis*.

São Félix de Balsas, Maranhão state, Brazil, showed a composition where the aromatic monoterpenes, thymol, *p*-cymene, thymol methyl ether and *p*-methoxythymol were the main constituents. It was characterized as the chemical type thymol + *p*-cymene. The values obtained for the antioxidant capacity assay (DPPH inhibition), and antifungal test (direct bioautography) showed significant biological properties for the oil at the concentrations tested in this experiment.

Conflict of Interests

The author(s) have not declared any conflict of interests.

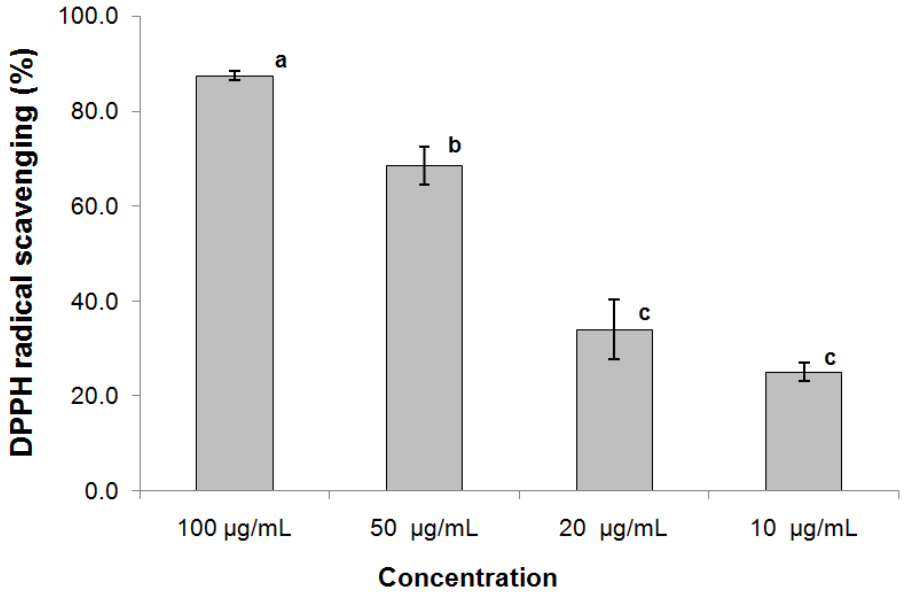

Figure 2. DPPH radical scavenging activity results for essential oil from *L. gracilic*. Error bars show the variation of three determinations in terms of SD. [abc]Values with the same letter are not statistically different at the $p < 0.05$ level (Tukey's test).

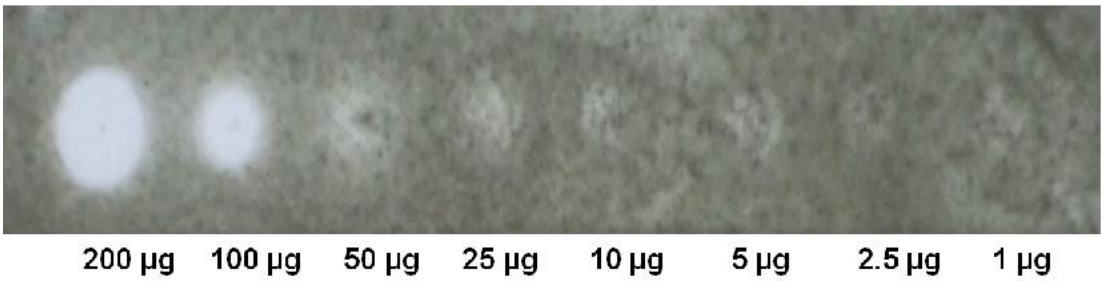

Figure 3. Bioautogram of *L. gracilic* essential oil. TLC plates sprayed with *Cladosporium sphareospermum* and *Cladosporium cladosporioides* culture (identical results). White areas indicate inhibition fungal growth.

ACKNOWLEDGEMENTS

The authors are grateful to CNPq/BIONORTE Program and FAPESPA/PA for their financial support.

REFERENCES

Adams RP (2007). Identification of Essential Oil Components by Gas Chromatography/Mass Spectrometry, 4th ed. Carol Stream, IL, USA: Allured Publishing Corporation.

Albuquerque CC, Camara TR, Mariano RLR, Willadino L. Júnior CM, Ulisses C (2006). Antimicrobial action of the essential oil of *Lippia gracilis* Schauer. Braz. Arch. Biol. Technol. 49: 527-535.

Atti-Serafini L, Pansera MR, Santos AC, Rossato M, Puletti GF, Rota LD, Paroul N, Moyna P (2002). Variation in essential oil yield and composition of *Lippia alba* (Mill. N. E. Br.) grown in southern Brazil. Rev. Bras. Plant. Med. 4: 72-74.

Damasceno EIT, Silva JKR, Andrade EHA, Sousa PJC, Maia JGS (2011). Antioxidant capacity and larvicidal activity of essential oil and extracts from *Lippia grandis*. Rev. Bras. Farmacogn. 21: 78-85.

Guenther E (1952). The essential oils, v. 2. New York, USA: Van Nostrand.

Guimarães AG, Gomes SVF, Moraes VRS, Nogueira PCL, Ferreira AG, Blank AF, Santos ADC, Viana MD, Silva GH, Quintans Júnior LJ (2012). Phytochemical characterization and antinociceptive effect of *Lippia gracilis* Schauer. J. Nat. Med. 66: 428-434.

Lemos TLG, Monte EJQ, Alencar JW, Craveiro AA, Barbosa RCSB, Lima EO (1992). Chemical composition and antimicrobial activity of essential oils from Brazilian plants. Fitoterapia 63: 266-268.

Maia JGS, Silva MHL, Andrade EHA, Carreira LMM (2005). Essential oil variation in *Lippia glandulosa* Schauer. J. Essent. Oil Res. 17: 676-680.

Maia JGS, Taveira FSN, Andrade EHA, Silva MHL, Zoghbi MGB (2003) Essential oils of *Lippia grandis* Schau. Flavour Fragr. J. 18: 417-420.

Matos FJA, Machado MIL, Craveiro AA, Alencar JW (1996). Essential oil composition of two chemotypes of *L. alba* grown in Northeast Brazil. J. Essent. Oil Res. 8: 695-698.

Matos FJA, Machado MIL, Craveiro AA, Alencar JW, Silva MGV (1999). Medicinal plants of northeast Brazil containing thymol and carvacrol - *Lippia sidoides* Cham. and *L. gracillis* H. B. K (Verbenaceae). J. Essent. Oil Res. 11: 666-668.

Mimica-Durik N, Bozin B, Sokovic M, Simin N (2004). Antimicrobial and antioxidant activities of *Melissa officinalis* L. (Lamiaceae) essential oil. J. Agric. Food Chem. 52: 2485-2489.

Morais AA, Mourão JC, Gottlieb OR, Silva ML, Marx MC, Maia JGS, Magalhães MT (1972). Óleos essenciais da Amazônia contendo timol. Acta Amaz. 2: 45-46.

Mota Neto R, Matos FJA, Andrade VS, de Melo MCN, Carvalho CBM, Guimarães SB, Pessoa ODL, Silva SL, Vasconcelos PRL (2009). The essential oil from *Lippia gracilis* Schauer, Verbenaceae, in diabetic rats. Rev. Bras. Farmacogn. 20: 261-266.

NIST/EPA/HIH Mass Spectral Library (2005). Nist Mass Spectral Search Program (NIST 05, Version 2.0d). Gaithersburg, USA: The NIST Mass Spectrometry Data Center.

Oliveira DR, Leitão GG, Bizzo HR, Lopes D, Alviano DS, Alviano CS, Leitão SG (2007). Chemical and antimicrobial analyses of essential oil of *Lippia origanoides* H.B.K. Food Chem. 101: 236-240.

Pascual ME, Slowing K, Carretero E, Sánchez Mata D, Villar A (2001). *Lippia*: traditional uses, chemistry and pharmacology: a review. J. Ethnopharmacol. 76: 201-214.

Poulose AJ, Croteau R (1978a). Biosynthesis of aromatic monoterpenes. Arch. Biochem. Biophys. 187: 307-314.

Poulose AJ, Croteau R (1978b). γ-Terpinene synthetase: A key enzyme in the biosynthesis of aromatic monoterpenes. Arch. Biochem. Biophys. 191: 400-411.

Ramos A, Visozo A, Piloto J, Garcia A, Rodriguez CA, Rivero R (2003). Screening of antimutagenicity via antioxidant activity in Cuban medicinal plants. J. Ethnopharmacol. 87: 241-246.

Ruberto G, Baratta MT (2000). Antioxidant activity of selected essential oil components in two lipid model systems. Food Chem. 69: 167-174.

Scora RW (1967). Study of the essential leaf oils of the genus *Monarda* (Labiatae). Amer. J. Bot. 54: 446-452.

Silva JKR, Andrade EHA, Kato MJ, Carreira LMM, Guimarães EF, Maia JGS (2011). Antioxidant capacity and larvicidal and antifungal activeties of essential and extracts oils from *Piper krukoffii*. Nat. Prod. Commun. 6: 1361-1366.

Silva JKR, Sousa PJC, Andrade EHA, Maia JGS (2007). Antioxidant capacity and cytotoxicity of essential oil and methanol extract of *Aniba canelilla* (HBK) Mez. J. Agric. Food Chem. 55: 9422-9426.

Silva ML, Maia JGS, Mourão JC, Pedreira G., Marx MC, Gottlieb OR, Magalhães MT (1973). Óleos essenciais da Amazônia. VI. Acta Amaz. 3: 41-42.

Silva NA, Silva JKR, Andrade EHA, Carreira LMM, Sousa PJC, Maia JGS (2009). Essential oil composition and antioxidant capacity of *Lippia schomburgkiana* Schauer. Nat. Prod. Commun. 4: 1281-1286.

Stashenko E, Ruiz C, Munoz A, Castaneda M, Martinez J (2008). Composition and antioxidant activity of essential oils of *Lippia origanoides* H. B. K. grown in Colombia. Nat. Prod. Commun. 3: 563-566.

Teles TV, Bonfim RR, Alves PB, Blank AF, Jesus HCR, Quintans-Jr LJ, Serafini MR, Bonjardim LR, Araújo ADS (2010). Composition and evaluation of the lethality of *Lippia gracilis* essential oil to adults of *Biomphalaria glabrata* and larvae of *Artemia salina*. Afr. J. Biotechnol. 9: 8800-8804.

Terblanché FC, Kornelius G (1996). Essential oil constituents of the genus *Lippia* (Verbenaceae) – A literature review. J. Essent. Oil Res. 8: 471-485.

Zoghbi MGB, Andrade EHA, Santos AS, Silva MHL, Maia JGS (1998). Essential oils of *Lippia alba* (Mill.) N. E. Br. growing wild in the Brazilian Amazon. Flavour Fragr. J. 13: 47-48.

Zoghbi MGB, Andrade EHA, Silva MHL, Maia JGS (2001). Volatile constituents of *Lippia lupulina* Cham. Flavour Fragr. J. 17: 29-31.

academicJournals

Vol. 13(30), pp. 3114-3121, 23 July, 2014
DOI: 10.5897/AJB2014.13805
Article Number: F2A591B46229
ISSN 1684-5315

http://www.academicjournals.org/AJB

African Journal of Biotechnology

Case Study

Thermodynamics, thermoeconomic and economic analysis of sugarcane biomass use for electricity production: A case study

Rafael Delapria Dias dos Santos[1], Samuel Nelson Melegari de Souza[3], Willian Cézar Nadaletti[2]*, Reinaldo Aparecido Bariccatti[3] and Paulo Belli Filho[2]

[1]UEL - State University of Londrina. P. O Box 6001. CEP. 86051-990 – Londrina. Paraná. Brazil.
[2]UFSC - Federal University of Santa Catarina, CTC Trindade – CEP. 88040-900 – Florianópolis. Santa Catarina. Brazil.
[3]UNIOESTE - Western Paraná State University , Rua Universitária. 2069. CEP. 85.819-130 Bairro Faculdade. Cascavel. Paraná. Brazil.

Received 19 March, 2014; Accepted 4 July, 2014

This work allows the thermodynamics, thermoeconomic and economic analysis of the cogeneration system of an industrial plant. Two settings were studied: the current that produces electricity only for its own, and secondary, a plant working at high pressure and high temperature using extraction steam turbines to drive an electricity generator and produce 32 MW and a backpressure turbine capable of producing 12 MW. In this case, a high investment is necessary and therefore, a considerable amount of energy sales. The thermodynamic analyses allow the evaluation of some performance indices. The thermoeconomic analysis proposes the distribution of costs based on thermodynamic concepts, enabling the evaluation of reflection of the investment costs and fuel in the cost of products (steam and electricity). The economic analysis acts as a deciding factor for acceptance or project rejection.

Key words: Cogeneration, economic, thermodynamics, thermoeconomic.

INTRODUCTION

With regards to electricity generation, it was observed as a more centralized world electric system during the last century mainly, due to the structure and transmission of power over long distances. However, factors such as the rise in the cost of electricity related environmental policies the recession of production in industrialized countries and the oil crisis, accelerated the reformulation process in industry and sparked the need for change. The quest for improvement in the Brazilian energy system became more evident in 2001 due to the blackout. To Baer (2003), this blackout was due to the drought that occurred three years before it decreased the level of reservoirs and the lack of government planning. According to the author, electricity consumption increased by 5% from 1980 to 2000, while the capacity increased by 4%. As a result of this crisis, the research around the

*Corresponding author. E-mail: williancezarnadaletti@gmail.com. Tel: +55 4599278808.

CHP became the fastest growing and generating a process of priority and decentralization character, which has encouraged the search for other sources of energy. To Rezac and Matghalchi (2004), the introduction of a “clean” cheap available energy has the ability to promote governments, improve the economy of poor countries, provide basic sanitation and increase the health benefits, as well as reducing the amount of pollutants entering our atmosphere in the form of greenhouse gases coming from human activities.

According to Dantas (2010), cogeneration is a process in which a primary energy source feeds an apparatus or heat engine and through a combustion reaction it accomplishes the conversion of chemical energy of the fuel into mechanical shaft. The same is converted into electricity in the electric generators. Therefore, the thermal energy from the hot combustion gases can be used directly or converted into another form of useful energy such as steam. This scenario created by the need for development and use of new energy sources is largely favorable to the use of biomass for electricity generation. When derived from sugarcane, biomass is made up of high levels of lignocellulosic materials, which are great producers of thermal and electrical energy (Oliveira et al., 2009). However, despite the discussion of cogeneration for sale of electricity in Brazil has begun many years ago. The results achieved so far are not very significant. Among the many reasons that contribute to the current framework included, the institutional barriers still existing in the country, the culture and conservatism prevailing in the electricity sector, the importance and extent of hydropower potential, lack political definitions with a view enabling other options for expansion and due to low investment in this type of energy.

According to Mizutani (2013), if all the plants of this sector in Brazil produced electricity from biomass, there would be 1.5 times more energy than the Itaipu hydroelectric plant is capable of generating. The use of waste from sugarcane represents, therefore, a possible viability of expanding the capacity of electricity generation from a technology already available with low investment in research (Walter, 1994). Within this context, the use of biomass from sugarcane for energy purposes contributes to the energy supply in periods of drought and energy crisis, besides acting as a source of energy that does not harm the environment.

In this bias, the development of this research allows the modeling and simulation of thermodynamic, thermoeconomic and economic analysis of the cogeneration system of industrial plant in a sugarcane mill. Two settings are analyzed; the current that produces electricity only for own consumption (with its plant already amortized) and a plant working at high pressure and high temperature with extraction-steam turbine capable of driving an electricity generator to producing 32 MW and a backpressure turbine capable of producing 12 MW. Thus, we analyzed the feasibility of implementing a thermoelectric plant.

MATERIALS AND METHODS

Elements of energy analysis

The solution to the problem addressed in this article involves the basic principles: The first and second law of thermodynamics. Whereas, the control volumes are steady, neglecting the kinetic and potential energies we can write the first law as follows (Borgnakke et al., 2009):

$$\dot{Q}_{v.c.} - \dot{W}_{v.c.} + \sum \dot{m}_e \, . \, h_e - \sum \dot{m}_s \, . \, h_s = 0 \qquad 1$$

Where, $\dot{Q}_{v.c.}$ is rate of heat transfer in the control volume (kW); $\dot{W}_{v.c.}$ is rate power for the control volume (kW); $\dot{m}_e$ and $\dot{m}_s$ is mass flows entering and leaving the control volume, respectively (kg/s); h_e and h_s is specific enthalpy at the inlet and outlet of the control volume, respectively (kJ/kg).

The first law of thermodynamics defined the property of internal energy which led to the definition of enthalpy and allowed to analyze the processes within a system in a quantitative way. The second law of thermodynamics defines the property of entropy which allows the realization of a quantitative and qualitative analysis of the processes. This refers to the quality of energy and direction of energy flow taking as postulate the claim that the heat will flow from the highest to the lowest temperature with no heat flow if these variables are of equal value. In this principle it is also verified that there is no reversible natural process, that is, each process involves the degradation of energy resources then being irreversible (Borgnakke et al., 2009).

Almeida (2005), states that the analysis of the first law does not account for the quality of the energy lost or where the irreversibility occur. The combination of the first and the second law may establish the energy balance and calculate the irreversibility in the processes. For processes in continuous operation the irreversibility generated can be given by:

$$\dot{I}_{v.c.} = \sum \dot{Q}_{v.c.} \cdot \left(1 - \frac{T_0}{T_{v.c.}}\right) - \sum \dot{W}_{v.c.} + \sum \dot{m}_e \, . \, ex_e - \sum \dot{m}_s \, . \, ex_s \qquad 2$$

Where, $\dot{I}_{v.c.}$ is irreversibility rate in the control volume (kW); T_0 is reference temperature (K); $T_{v.c.}$ is surface temperature of the control volume (K); ex_e and ex_s is specific entropy at the inlet and outlet of the control volume, respectively (kJ/kg.K).

Elements of exergy analysis

Rant (1956) was the one who proposed the word exergy to replace various terms of similar meanings employed in different countries, useful energy (France), availability (USA) and work capacity (Germany). This author also proposed the word anergy which is the part of the non-utilized energy or better: Energy = Exergy + Anergy. Energy therefore, is all that can be tapped (exergy) added to that which is not useful (anergy). In other words, energy is that which can be converted into heat and/or work. However, to calculate the exergy is necessary to define the reference state in order to have a basis on which values are to be adopted. For Szargut et al. (1988) exergy is the amount of work obtained when a mass is brought to a state of thermodynamic equilibrium with the common components of the environment. According to the author, the total exergy a given flow or fluid can be subdivided into potential, kinetic, chemical and physical exergy. In a cogeneration system disregarded the kinetic and potential exergies, so the flow energy of a fluid is given only by the sum of physical and chemical exergies.

$$ex_{tot} = \underbrace{\frac{(h - h_0) - T_0(s - s_0)}{I}}_{} + \underbrace{\frac{\sum(\mu_i - \mu_{0,i})x_i}{II}}_{} \qquad 3$$

Where, T_0 is reference temperature; $\mu_{0.i}$ is refers to the element's reference chemical potential($T_0.P_0$); μ_i is element's chemical potential in the mixture($T_0.P_0$); x_i is the component fraction in the mixture. The dead state or reference environment is indicated by the subscript "0". The reversible work will be maximum when $s_s = s_0$ e $h_s = h_0$.

Making use of the idea of an environment that represents the real physical world, the standard conditions of temperature and pressure will be used as reference environment (STP). T_0=298.15K and P_0=101.325 kPa.

Performance indices of cogeneration systems

Ensinas (2008) mentions that generation plants of conventional power and cogeneration systems have different conceptions. Plants of power generation (usually electricity) seek to have maximum efficiency, while cogeneration projects is require to meet the demands of heat and power. Since both products have their advantages and needs according to the production, the calculation of electrical efficiency has become a performance criterion suitable for use. The goal of using performance indices to evaluate the cogeneration systems as a whole, clarifying the differences among them, particularly with respect to the application of methods based on the first and second laws of thermodynamics. The cost effectiveness of a cogeneration system is directly related to the amount of electricity that a system is able to produce for a given amount of heat used in the process (Barreda del Campo, 1999).

$$\mathrm{RPC} = \frac{\dot{W}}{\dot{Q}_U} \quad (4)$$

Another important parameter is the ratio electric power generated and the amount of crushed cane.

$$R_{pot\_elet\ /cana\_moi} = \frac{\dot{W}_{elet}}{3.6.\dot{m}_{cana\_moi}} \quad (5)$$

Where, $\dot{m}_{cana\_moi}$ is amount of cane crushed (kg/s); $\dot{Q}_U$ is useful heat (kW).

Other measures could be used such as the energy use factor, the overall efficiency, the rate of energy saving, energy to be saved and rate of power generation. However, as the same amount of bagasse is not consumed in both case, it is not possible to compare them effectively.

Thermoeconomic elements

The thermoeconomics is a methodology developed based on the concepts of exergy for analysis of thermal systems. For the dissemination of thermoeconomic analysis, is necessary to perform an Exergy analysis followed by an economic analysis. This methodology has a main objective to assign costs to an energy carrier (Jaramillo, 2011). This article uses the exergoeconomic methodology that makes use of the allocation of average costs of equipment being able to determine the cost of products to provide a means of allocating costs and act as a base for making operating decisions. This methodology elaborated by Reistad and Gaggioli (1980) for the exergoeconomic methodology, when formulated for a balance of cost individually in each k-component system. It follows that the sum of rates of all input exergetic flows over the price due to the capital investment and operating costs and maintaining each k-component is equal to the sum of cost rates associated with all the exergetic flows out of the system.

$$\sum_e c_e(\dot{m}_e.ex_e)_k + (c_Q.\dot{Q})_k + \dot{Z}_k = \sum_s c_s(\dot{m}_s.ex_s)_k + (c_W.\dot{W})_k \quad (6)$$

Where, c is average flow cost per time unit in the component k (R$/s);

Economic elements

The use of economic analysis as investment decision aims primarily at assisting and evaluating one or more alternatives to determine the more attractive means of action from quantitative methods. This type of analysis when used as a form of aid in the purchase or expansion of an enterprise should present decisive results for acceptance or rejection of the proposal analyzed. According to Gitman (1984) the best techniques for capital investment make use of the time factor in the future value of money and consider the cash flow over the project life. The VAL method explicitly demonstrates the actual net profit that the investor should receive over the project life. It is obtained by subtracting the initial investment in a project from the present value of the cash flows discounted at a rate equal to the cost of company capital, that is, it determines the total net value of the investment discounted to the Minimum Rate of Attractiveness (TMA) on zero date. The MRA is an interest rate that represents the minimum that an investor intends to gain when there is investment.

$$\mathrm{VAL} = \frac{\mathrm{BEN}}{(1+j^*)^N} - \mathrm{CTI} \quad (7)$$

The equation to describe the VAL is used as criterion of "acceptance" or "rejection" of a given project. If the VAL value is greater than zero, the project can be accepted because the cash inflow is greater than the cash outflow. In the case of VAL be equal to zero, the investment is irrelevant since the inflow is equal to the outflow. Otherwise it must be rejected.

Method of solution

The equations can be solved by using any suitable calculation tool for this purpose. However, the ESS® software (Engineering Equation Solver) developed by Klein and Alvarado (1995) was used, which allows determination of thermodynamic properties such as the enthalpy and entropy in a simple and efficient way without the need to use thermodynamic tables.

CASE STUDY

Case 1: Current

The data cited in Table 1 refer to the production of sugarcane in the 2012/2013 harvest a plant of sugarcane industry located within the Paraná. The company works on two boilers of 21 kgf/cm^2 and only with backpressure turbines. The generator turbo is used only for internal power consumption of the establishment (administrative, kitchen, rooms in general) and not for driving the mills, hoods, fans and pumps as shown in Figure 1.

Case 2: Suggested

In case 2, studied the hypothetical configuration which has one or more modern steam plant with more efficient equipment, all electrified, aimed at expanding the case 1. The boiler proposed produces 200 t/h steam at 66 kg/cm^2 and 530°C. 140 t/hr of this steam is consumed by the extraction steam turbine coupled to a generator of 32 MW. An extraction of 100 t/h of steam is performed

Table 1. Data on grinding, consumption and production of bagasse in the 2012/2013 harvest.

Parameter	Value	Unit
Total cane crushed	1.970.165	t
Harvest period	282	Days
Days effective crop	231	Days
Daily Grind	8.520	t/day
Grinding time	355	t/h
Fiber content of the cane	12.5	%
Fiber content of bagasse	47.4	%
Flow of bagasse in the boiler 1	34.6	t/h
Flow of bagasse in the boiler 2	37.3	t/h
Flow bagasse in boilers	71.9	t/h
Stream full bagasse produced	92.45	t/h
Flow residual bagasse	20.55	t/h

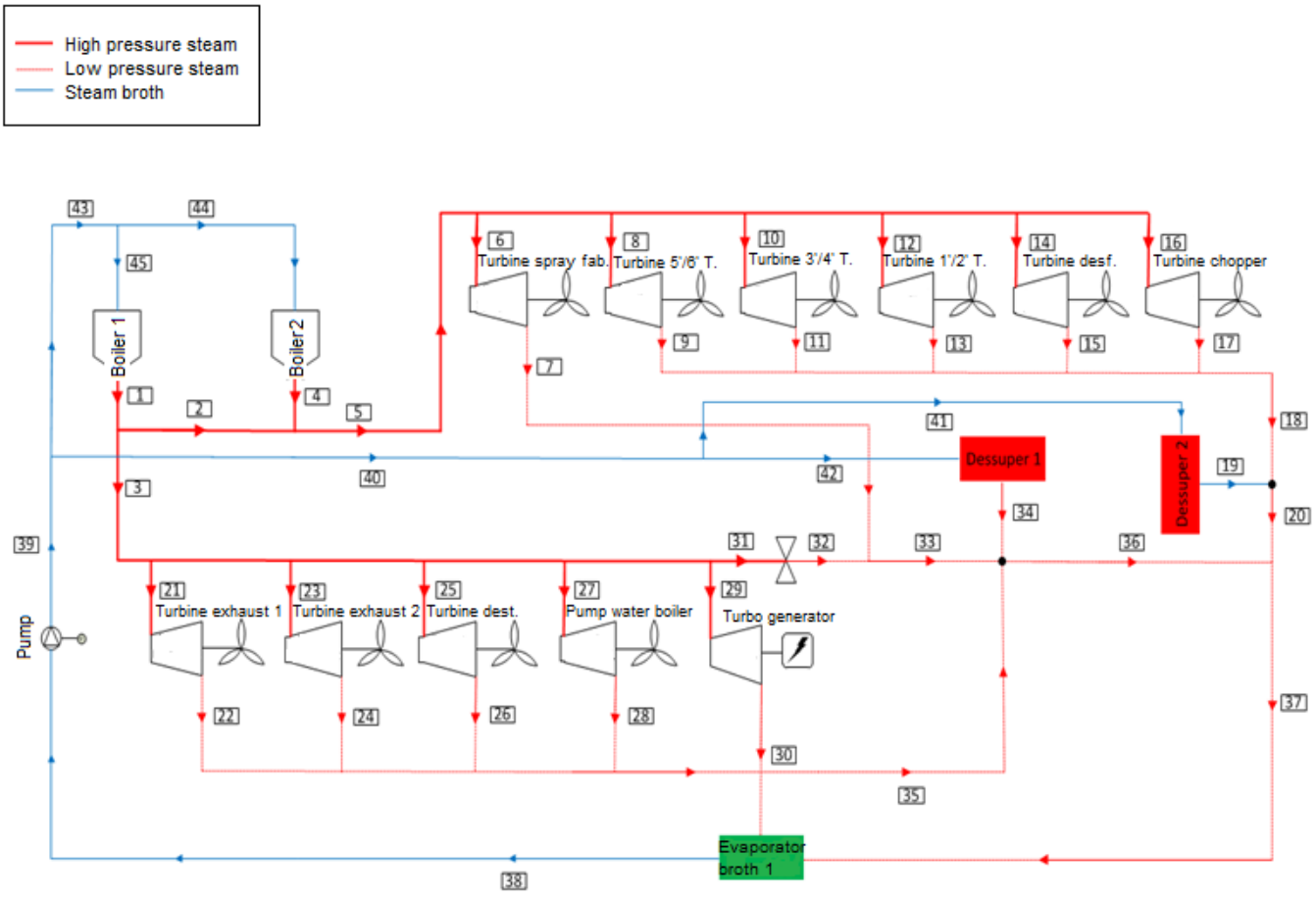

Figure 1. Current plant under analysis.

at a pressure of 245 kPa for the evaporation process of the broth and the remaining steam continues to expand until the pressure of 8 kPa and then condensed. The rest of the steam produced 60 t/h is consumed by a backpressure turbine and capable of generating 12 MW. In this case, the steam is discharged at a pressure of 245 kPa also designed to meet the steam demand in the industrial process as shown in Figure 2. The boiler 2 can be used in exceptional cases as it is already amortized (same boiler of Case 1). However, only the boiler 1 will be use for simulation. According to suppliers, this new boiler would have efficiency of 2.165 kgV/kgB.

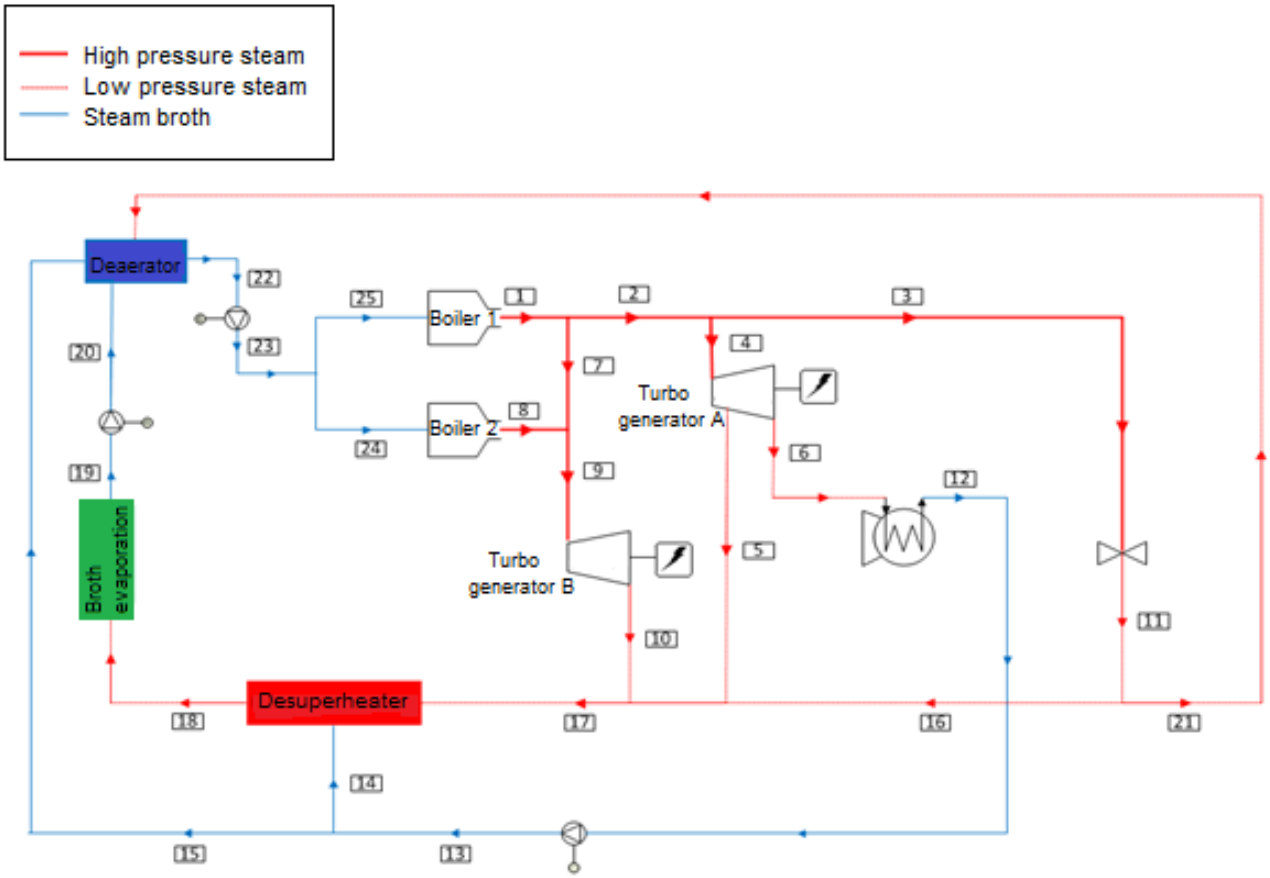

Figure 2. Plant suggested.

Table 2. Bagasse consumption of the crop.

Parameter	Value	Unit
Flow of bagasse in the boiler 1	92.45	t/h
Flow of bagasse in the boiler 2	0	t/h
Flow bagasse in boilers	92.45	t/h
Flow full bagasse produced	92.45	t/h
Flow residual bagasse	0	t/h

The milling data are considered as the same in Table 1 with the difference that the boiler 1 consumes the entire bagasse production according to Table 2. Table 3 shows the power generated or consumed by each device in each case analyzed.

RESULTS AND DISCUSSION

For simulations it was used as a value of 7736 kJ/kg for the LCV (Lower Calorific Value) of bagasse and for the value of its exergy was adopted 10.170 kJ/kg.

Thermodynamic results

The current plan – Case 1 needs 10859.7 kW to meet its demand. Undoubtedly, this demand would be lower due to the higher efficiency of its generators. Table 4 shows the performance indices for two cases.

Thermoeconomic results

The annual cost of equipment with amortization was calculated taking into account a depreciation period of 20 years. The interest rate of 12% was considered. The value of R$ 15/t was taken as reference which is the price adopted for the bagasse sale between the plants at harvest season. Figure 3 shows the cost of electricity produced depending on the bagasse cost. It is found that the cost of electricity generated is R$ 88.02/MWh and R$107.5/MWh for the current and suggested case respectively. Macedo et al., (2004) estimate that the rate of production of bagasse can reach 280 kg per tonne of cane crushed with 50% moisture content and lower calorific value of about 7500 kJ/kg. Figure 4 represents the cost of electricity produced and the cost of process steam depending on the bagasse cost for the current and suggested case. It is observed in this case that the cost of process steam is R$ 20.73/t and R$ 10.76/t for the current and suggested case respectively.

Table 3. The power generated or consumed by each device in each case analyzed.

Parameters/case 1	Case 1 (kW)	Parameters/case 2	Case 1 (kW)
Cop Chopper 8	1.500		
Shredder	1.500		
1 ° and 2 ° Suits Milling	1.120		
3 ° and 4 ° Suits Milling	1.120		
5 ° and 6 ° Suits Milling	1.120		
Turbo Pump Water Boiler	326.7	Turbo Generator A	31.807
Turbo Pump Distiller	200	Turbo Generator B	11.850
Turbo Spray	676	**TOTAL**	**43.657**
Exhaust 01	161		
Exhaust 02	184		
Turbo Generator	2.952		
TOTAL	**10.859.7**		

Table 4. Performance rates.

Cases / parameters	RPC	$R_{pot\_elet/cana\_moi}$
Current	0.0888	39.88
Suggested	0.3421	124.7

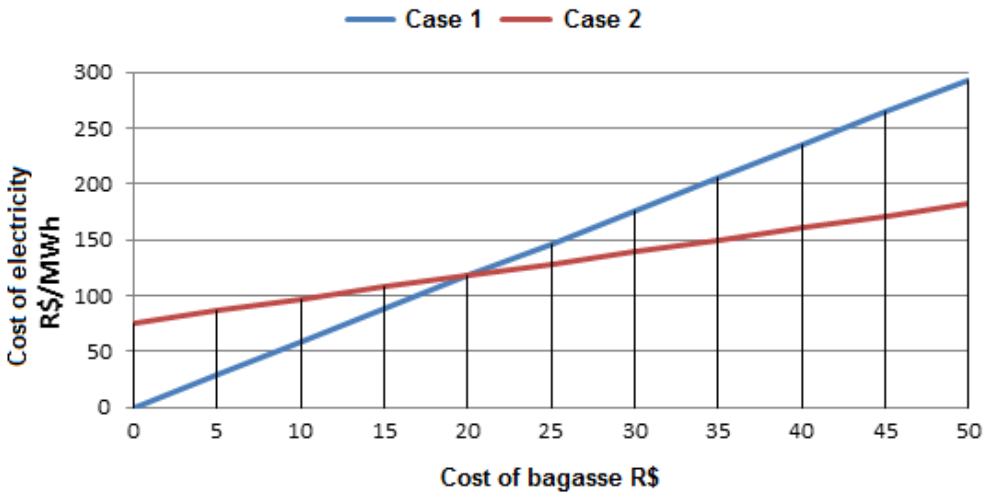

Figure 3. Electricity cost x bagasse cost.

Economic results

The plant of Case 1 is already amortized, therefore, it will only performed the economic analysis of case 2. The internal power consumption will be considered the same 10859.7 kW, thus the excess electricity is 32796.3 kW. The bagasse cost will be considered R$15/t and the total cost of deployment will be R$ 78.4 million, accounting that 40% of the investment refers to the installation, labor, maintenance among others. Table 5 shows the economic indicators related to industrial plant suggested. The plant begins to have return of investment setting the selling price of electricity in R$ 165.22/MWh for a rate of investment return of 12%. Figure 5 shows how cash flow would behave for the case supposed from the sale of electricity at a price of 160, 170, R$ 180/MWh.

This work corroborates with Dantas (2009), in their work with energy generation from bagasse, concluded increased attractiveness for investments in this segment providing positive results to investors. Pellegrini and

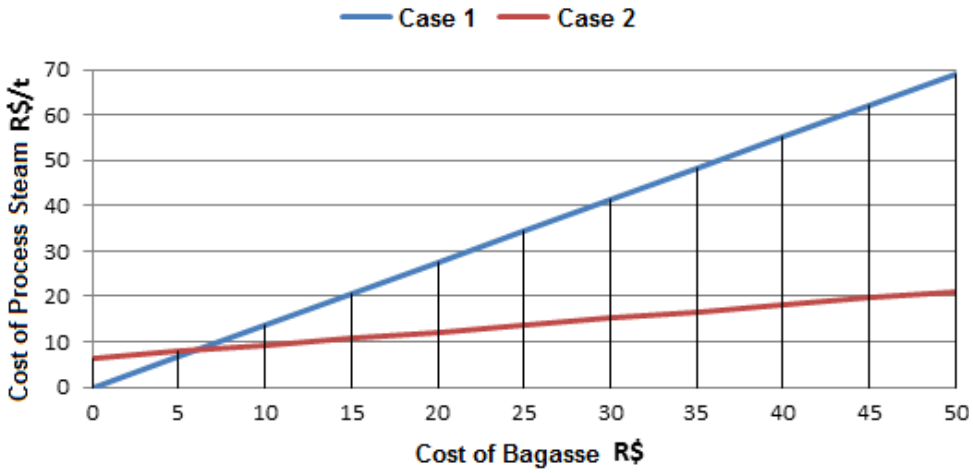

Figure 4. Cost of steam process x bagasse cost.

Table 5. Economic indices concerning the second plant.

Sale price	NPV (R$)	ITR (Years)	IRR
R$ 160/MWh	-R$ 7.096.824.58	0	10.5328%
R$ 170/MWh	R$ 6.484.732.64	15.53919388	13.3029%
R$ 180/MWh	R$ 20.066.289.86	11.03723914	15.9417%

Net present value (NPV), Internal Time of return (ITR), Internal Rate of Return (IRR).

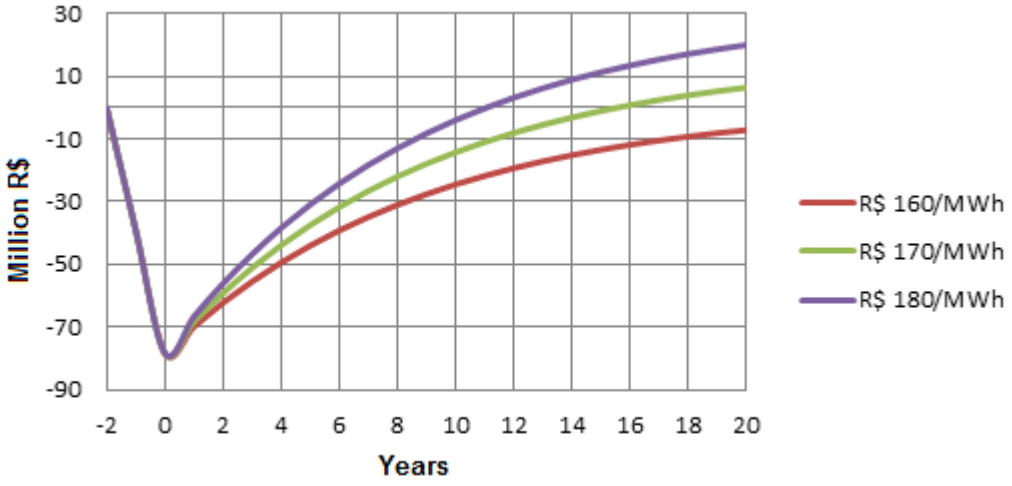

Figure 5. Cash flow for the supposed case.

Oliveira (2011) show the study about production of sugar, ethanol and electricity, that the generation of excess electricity improves the exergo-environmental performance of the mill as a whole. Nadaletti et al. (2014) comments that the use of another energetic plants, like canola (Brassica napus L. var. oleifera Moench.) in large production in Brazil, can be a alternative to agroenergetic purposes.

Conclusions

The thermodynamic analysis of plants demonstrated that the uses of an extraction-steam turbine can double the amount of energy produced by the plant. There is also highest amount of electricity produced compared to thermal energy through the performance indices. Considering the amount of R$ 15/t it is observed in the thermoecono-

mic and economic analyses that the deployment of a modern and efficient plant will not significantly increase the cost of process steam and investment becomes attractive only when the selling price of energy reaches R$ 165.22 MWh being unfeasible to lower values. An alternative would be to reduce the cost of bagasse for the same amount of electricity produced, thus the project would be accepted with a lower selling price of energy. The difficulties inhibiting the development of this segment are not related to the feasibility of developing or deploying a new industrial plant. Since, we consider that it is largely feasible, the expansion and production of electricity at a sale price are less than other energy sources and yes the lack of a clear policy of inclusion of this segment is in the national energy and power matrix.

Conflict of Interests

The author(s) have not declared any conflict of interests.

ACKNOWLEDGEMENTS

The authors thank the Coordination of Improvement of Higher Education Personnel - CAPES for research funding and UNIOESTE/UEL.

REFERENCES

Almeida EM (2005). Análise exergética para recuperação de perdas energéticas de uma central termelétrica com cogeração num complexo petroquímico. 140 f. Dissertação (Mestrado em Engenharia Química) – UFBA – Universidade Federal de Bahia. Salvador.

Baer W (2003). A Economia brasileira. 2nd ed. São Paulo: Nobel.

Barreda del Campo ER (1999). Avaliação termoeconômica do sistema de cogeração da Usina Vale do Rosário. 310 f. Dissertação (Doutorado em Engenharia Mecânica) – UNICAMP – Universidade Estadual de Campinas. Campinas.

Borgnakke C, Wylen GJV, Sonntag RE (2009). Fundamentos da Termodinâmica. 7nd ed. Edgard Blucher.

Dantas DN (2010). Uso da biomassa da cana-de-açúcar para geração de energia elétrica: análise energética. exergética e ambiental de sistemas de cogeração em sucroalcooleiras do interior paulista. Mestrado – Escola de Engenharia de São Carlos. São Carlos.

Dantas Filho PL (2009). Análise de custos na geração de energia com bagaço de cana-de-açúcar: um estudo de caso em quatro usinas de São Paulo. 175 f. Dissertação (Mestrado em Energia) – USP – Universidade de São Paulo.

Ensinas AV (2008). Integração térmica e otimização termoeconômica aplicadas ao processo industrial de produção de açúcar e etanol a partir da cana-de-açúcar. 229 f. Dissertação (Doutorado em Engenharia Mecânica) – UNICAMP – Universidade Estadual de Campinas. Campinas.

Gitman JL (1984). Princípios da administração financeira. São Paulo: Harper & Row.

Jaramillo JCB (2011). Otimização exergoeconômica de sistema tetracombinado de trigeração. 240 f. Dissertação (Doutorado em Engenharia Mecânica) – USP - Universidade de São Paulo. São Paulo.

Klein SA, Alvarado FL (1995). EES – Engineering Equation Solver. F-Chart Software. Middleton. WI.

Macedo IC, Leal MRLV, Silva JEAR (2004). Balanço das emissões de gases de efeito estufa na produção e no uso do etanol no Brasil. São Paulo: Secretaria do Meio Ambiente.

Mizutani P (2013). Supply and Demand for Ethanol. March 29. Interview by Sergio Waib presenter and program editor Giro Business.

Nadaletti WC, Baricatti RA, Santos RF, Souza SNM, Siqueira JAC, Antonelli J, Cremonez P, Rossi, E, Mari, A (2014). Response of canola (Brassica napus L. var. oleifera Moench.) to the use of biofertilizer from swine farming at different groundwater levels. J. Food Agric. Environ. 12: 415 – 417.

Oliveira MM, Galinkin M, Libânio JC, Júnior CB (2009). Agroenergia da Biomassa Residual: perspectivas energéticas. econômicas e ambientais. Revista Technopolitik. 2.

Pellegrini LF, Oliveira Junior S (2011). Combined production of sugar, ethanol and electricity: Thermoeconomic and environmental analysis and optimization. Energy 36: 3704–3715.

Rant Z (1956). Exergie. ein neues Wort fur "Technische Arbeitsfahigkeit" (Exergy. a new word for "technical available work"). *Forschung auf dem Gebiete des Ingenieurwesens*. 22: 36–7.

Reistad GM, Gaggioli RA (1980). Thermodynamics: Second Law Analysis. ACS Series 122:143-60.

Rezac P, Metghalchi H (2004). A Brief Note on the Historical Evolution and Present State of Exergy Analysis. Int. J. Exergy. 1(1):426 –7.

Szargut J, Morris DR, Steward FR (1998). Exergy analysis of thermal. chemical. and metallurgical processes. New York: Hemisphere Publishing Co.

Walter ACS (1994). Viabilidade e perspectivas da cogeração e geração termelétrica no setor sucro-alcooleiro. 1994. 287 f. Dissertação (Doutorado em Planejamento Energético) – UNICAMP – Universidade Estadual de Campinas. Campinas.

African Journal of Biotechnology

Related Journals Published by Academic Journals

- *Biotechnology and Molecular Biology Reviews*
- *African Journal of Microbiology Research*
- *African Journal of Biochemistry Research*
- *African Journal of Environmental Science and Technology*
- *African Journal of Food Science*
- *African Journal of Plant Science*
- *Journal of Bioinformatics and Sequence Analysis*
- *International Journal of Biodiversity and Conservation*

academicJournals